

**AN INVESTIGATION OF THE CILIARY
PROTEIN *PKHD1* IN CYST DEVELOPMENT IN
LIVER DISEASE: CLUES TO THE
PATHOGENESIS OF BILIARY ATRESIA**

BY

SARAH ALEXANDRA BLAIR-REID

A Thesis Presented to the College of Medical and Dental Sciences
The University of Birmingham
For the Degree of Doctor of Philosophy

Centre for Liver Research
School of Immunity and Infection
College of Medical and Dental Sciences
University of Birmingham
2010

ABSTRACT

Biliary atresia is a common form of paediatric liver disease, with progressive, inflammatory obliteration of the biliary tree, leading to liver failure early in life. Mutations in *PKHD1*, encoding the ciliary protein fibrocystin, are associated with autosomal recessive polycystic kidney disease (ARPKD), a ciliopathy with clinical features that resemble biliary atresia. The hepatic developmental defects detectable in a significant number of infants with ARPKD are thought to be caused by dysfunction in the structure and function of primary cilia. The pathogenetic mechanism of both disorders is thought to be dysregulation of epithelial cell growth and tubulomorphogenesis. Preliminary investigations uncovered an association of *PKHD1* sequence variants in a subset of biliary atresia patients with renal cysts, promoting further investigation to determine the functional role of fibrocystin in epithelial cells from renal and biliary tubules. Immunohistochemical studies, using a monoclonal antibody raised against wildtype fibrocystin, showed that it localises specifically to intrahepatic bile ducts. Absence of fibrocystin staining in end-stage liver tissue reflects ongoing damage to the intrahepatic biliary tree, rather than a phenomenon specific to biliary atresia. Studies utilising the *Pkhd1*^{del2/del2} mouse model of ARPKD revealed 17 β -estradiol sensitive centrosomal overduplication underlies the dysregulation of epithelial cell growth in renal tubules, however this does not appear to be in synergy with *Pkhd1* knockdown. Therefore, it remains uncertain whether sequence variants of *PKHD1* are associated with biliary atresia.

DEDICATED TO:

My mother

ACKNOWLEDGMENTS

Thanks must first go to the Children's Liver Disease Foundation, for providing the funding that allowed this project to go ahead. Importantly, thanks must also go to all the patients, and their families, who consented use of tissue for scientific study. Without their co-operation, research of this kind could not advance.

I would like to personally thank my primary supervisor, Dr. Simon C. Afford, for his help and guidance throughout my PhD. I would also like to thank my secondary supervisor, Professor Deirdre Kelly, for her help in the procurement of patient DNA, and also for supporting my year spent in the USA.

Special thanks goes to Dr Christopher Ward, and Dr Peter Harris, at the Mayo Clinic, for the extraordinary opportunity of working in their lab, and allowing me access to their resources. Thanks must also go to Professor Stefan Hubscher, for his independent contribution to the evaluation of the immunohistochemical studies. I would also like to thank Carla Lloyd, Dr Jane Hartley, and Dr Rachel Brown, of the Birmingham Children's Hospital, for their help in obtaining and assessing paediatric tissue for the immunohistochemical studies. I would also like to personally acknowledge Dr Gary M, Reynolds for all his help with technical advice, and support.

A huge thank you must go to the people who provided significant technical support during the course of my PhD. Dr Esther Maina, for all her help and advice with setting up and optimising real-time PCR. Dr John Woollard, for going out of his way to help me set up and optimise primary murine cell culture, and teaching me the ropes. Cynthia Hommerding, and Jason Bakeberg, for assisting me with the animal work carried out at the Mayo Clinic. Norma Gregory, for ensuring all general lab solutions and consumables were available for use.

I would also like to acknowledge the following core service, and technical support staff, who provided the services, and technical advice that supported this project. The theatre, and clinical staff at the liver units of The Queen Elizabeth Hospital, and the Birmingham Children's Hospital. The TACMA, and pathology department personnel at the Mayo Clinic. Members of the La Russo lab at the Mayo Clinic, and members of the Birmingham Centre for Liver Research labs.

I would also like to personally thank those people who provided me with the moral support I needed to get me through this project, my friends: Hannah Ivison, Andrea G. Cogal, Dr Luca Manganelli, York Aarbodem, Cynthia Hommerding, Jason Bakeberg, and Mark Consugar.

TABLE OF CONTENTS

LIST OF TABLES	VII
LIST OF APPENDED TABLES	VIII
LIST OF FIGURES	VIII
LIST OF APPENDED FIGURES	X
CHAPTER 1 INTRODUCTION.....	1
1.1 BILIARY ATRESIA	1
1.2 MICROSTRUCTURE AND DEVELOPMENT OF THE BILIARY TRACT	15
1.3 CHOLANGIOCYTES AND THE CHOLANGIOPATHIES.....	25
1.3.1 <i>Cholangiocytes in health</i>	30
1.3.2 <i>Cholangiocyte function in liver disease</i>	32
1.4 THE CILIOPATHIES.....	38
1.4.1 <i>An overview of the cilium</i>	41
1.4.2 <i>Pathogenetic mechanisms relevant to the ciliopathies</i>	50
1.5 AUTOSOMAL RECESSIVE POLYCYSTIC KIDNEY DISEASE AND <i>PKHD1</i>	78
1.5.1 <i>Expression features of PKHD1</i>	86
1.5.2 <i>Functional insights</i>	87
1.6 UNRAVELLING THE PATHOGENESIS OF BILIARY ATRESIA: INSIGHTS PROVIDED BY ANIMAL MODELS	92
1.6.1 <i>THE PKHD1^{DEL2/DEL2} ARPKD MOUSE MODEL</i>	98
1.7 INTRODUCTION SUMMARY	107
1.8 HYPOTHESIS	109
1.8.1 <i>Project Aims</i>	110
CHAPTER 2 EXPERIMENTAL APPROACHES	112
2.1 IMMUNOHISTOCHEMISTRY	112
2.2 <i>IN VITRO</i> CELL CULTURE	114
CHAPTER 3 MATERIALS AND METHODS	123
3.1 MUTATIONAL SCREENING	123
3.1.1 <i>Subjects</i>	123
3.1.2 <i>Methods</i>	125
3.1.3 <i>Statistical analysis</i>	126
3.2 IMMUNOHISTOCHEMISTRY IN HUMAN TISSUE.....	126
3.2.1 <i>Cohort</i>	127
3.2.2 <i>Cases</i>	127
3.2.3 <i>Methods</i>	128
3.2.4 <i>Optimisations</i>	130
3.2.5 <i>Analysis</i>	132
3.2.6 <i>Liver disease cohort studies</i>	132
3.3 HUMAN <i>IN VITRO</i> CELL CULTURE.....	134
3.3.1 <i>Culture and optimisation of the human embryonic kidney (HEK 293) cell line</i>	134
3.3.2 <i>Biliary epithelial cell isolation and culture</i>	137
3.4 MURINE EXPERIMENTATION AND <i>IN VITRO</i> CELL CULTURE	140
3.4.1 <i>Immunofluorescent immunohistochemistry</i>	140
3.4.2 <i>Isolation and culture of primary mouse proximal tubular cells</i>	143
3.4.3 <i>Data analysis</i>	147

CHAPTER 4 MUTATIONAL SCREENING OF <i>PKHD1</i> IN A COHORT OF BILIARY ATRESIA PATIENTS WITH ASSOCIATED RENAL CYST FORMATION	149
4.1 INTRODUCTION	149
4.2 AIM	149
4.3 RESULTS	150
4.3.1 <i>Association of renal cysts in transplant patients with BA</i>	150
4.3.2 <i>Clinical evaluation</i>	150
4.4 CONCLUSIONS	157
4.5 DISCUSSION	158
CHAPTER 5 INCREASED ACETYLATION OF α-TUBULIN AND DECREASED EXPRESSION OF FIBROCYSTIN ARE SENSITIVE MARKERS OF CELLULAR DAMAGE AND ACTIVATION IN INFLAMMATORY LIVER DISEASE	162
5.1 INTRODUCTION	162
5.2 AIMS	163
5.3 RESULTS	163
5.3.1 <i>Evaluation of fibrocystin immunostaining achieved with different fixatives on frozen tissue</i>	163
5.3.2 <i>Optimisation of monoclonal antibodies for immunohistochemical study</i>	168
5.3.3 <i>Increased levels of acetylated α-tubulin and decreased levels of fibrocystin expression are detected in a cohort of various adult liver diseases</i>	177
5.3.4 <i>Immunofluorescence analysis of primary ciliary expression in HEK293 cells: time-course evaluation</i>	187
5.3.5 <i>Immunofluorescence analysis of primary ciliary expression in primary BEC: substratum, ECM, and time-course evaluation</i>	188
5.4 CONCLUSIONS	191
5.5 DISCUSSION	192
CHAPTER 6 KNOCKDOWN OF <i>PKHD1</i> DOES NOT INCREASE OESTROGEN DRIVEN CENTROSOMAL AMPLIFICATION IN PRIMARY MURINE PROXIMAL TUBULE EPITHELIAL CELLS	200
6.1 INTRODUCTION	200
6.2 AIMS	201
6.3 RESULTS AND ANALYSIS	202
6.3.1 <i>Treatment of primary murine proximal tubular epithelial cells in vitro drives centrosomal overduplication</i>	202
6.3.2 <i>Susceptibility of primary murine proximal tubular epithelial cells to E2 driven centrosomal overduplication is age dependent</i>	231
6.3.3 <i>Knockdown of fibrocystin in primary proximal tubular epithelial cells has no effect on 17 β-estradiol driven centrosomal overduplication</i>	243
6.3.4 <i>At what age do 'star-burst' primary cilia occur in <i>Pkhd2</i>^{Del2/Del2} animals?</i>	251
6.4 CONCLUSIONS AND DISCUSSION.....	255
6.4.1 <i>Centrosomal amplification in primary murine proximal tubule epithelial cells shows positive correlation to increasing levels of 17 β-estradiol in vitro</i>	255
6.4.2 <i>Severity of centrosomal amplification and the associated nuclear dysmorphia increases with increasing levels of 17 β-estradiol</i>	257
6.4.3 <i>PTC from older mice display increased susceptibility to E2 induced centrosomal overduplication</i>	262
6.4.4 <i>Fibrocystin knockdown does not result in increased frequency or severity of centrosomal amplification in primary murine PTCs</i>	263

6.4.5 The age at which 'star-burst' cilia and associated centrosomal amplification occurs in the PTs of <i>Del2</i> animals is not apparent upon examination of tissue from one and four month old animals	265
CHAPTER 7 DISCUSSION AND CONCLUSIONS	267
CHAPTER 8 FUTURE DIRECTIONS	287
APPENDIX 1	297
APPENDIX 2	301
APPENDIX 3	305
One month old wildtype B6 mice: raw data.....	305
One month old <i>del2</i> B6 mice: raw data	306
Three month old wildtype B6 mice: raw data.....	307
Three month old <i>del2</i> B6 mice: raw data	308
Six month old wildtype B6 mice: raw data.....	309
Six month old <i>del2</i> B6 mice: raw data.....	310
Nine month old wildtype B6 mice: raw data.....	311
Nine month old <i>del2</i> B6 mice: raw data	312

LIST OF TABLES

TABLE 1.1 Two clinical forms of biliary atresia	5
TABLE 1.2 Potential mechanisms involved in the pathogenesis of biliary atresia	6
TABLE 1.3 Regulation of cholangiocyte proliferation	36
TABLE 1.4 Autosomal recessive polycystic kidney disease.....	81
TABLE 3.1 Table showing the clinical relationship between transplant status, renal cyst natural history, and changes in renal function	124
TABLE 3.2 Frozen tissue section fixative panel.....	130
TABLE 3.3 Primary antibody titrations.....	131
TABLE 5.1 Fibrocystin antibody titration on FFPE human liver tissue sections.....	176
TABLE 5.2 Expression levels of fibrocystin in various structures within human liver tissue sections	180
TABLE 5.3 Fibrocystin immunohistochemical staining data analysis	180
TABLE 5.4 Expression levels of acetylated α -tubulin in a number of structures within human liver tissue sections	187
TABLE 5.5 Summary of BEC substratum and ECM ciliary expression optimisations.....	191
TABLE 6.1 Cell count data analysis for one-month-old wt males	204
TABLE 6.2 Cell count data analysis for one-month-old wt females.....	204
TABLE 6.3 Cell count data analysis for one-month-old wt males Vs. females.....	205
TABLE 6.4 Cell count data analysis for one-month-old <i>Del2</i> males	207
TABLE 6.5 Cell count data analysis for one-month-old <i>Del2</i> females.....	207
TABLE 6.6 Cell count data analysis for one-month-old <i>Del2</i> males Vs. females.....	208
TABLE 6.7 Cell count data analysis for three-month-old wt males.....	210
TABLE 6.8 Cell count data analysis for three-month-old wt females	210
TABLE 6.9 Cell count data analysis for three-month-old wt males Vs. females	211
TABLE 6.10 Cell count data analysis for three-month-old <i>Del2</i> males	213
TABLE 6.11 Cell count data analysis for three-month-old <i>Del2</i> females.....	213
TABLE 6.12 Cell count data analysis for three-month-old <i>Del2</i> males Vs. females.....	214
TABLE 6.13 Cell count data analysis for six-month-old wt males.....	216
TABLE 6.14 Cell count data analysis for six-month-old wt females.....	216
TABLE 6.15 Cell count data analysis for six-month-old wt males Vs. females	217
TABLE 6.16 Cell count data analysis for six-month-old <i>Del2</i> males.....	219
TABLE 6.17 Cell count data analysis for six-month-old <i>Del2</i> females	219

TABLE 6.18 Cell count data analysis for six-month-old <i>Del2</i> males Vs. females	220
TABLE 6.19 Cell count data analysis for nine-month-old wt males	222
TABLE 6.20 Cell count data analysis for nine-month-old wt females	222
TABLE 6.21 Cell count data analysis for nine-month-old wt males Vs. females	223
TABLE 6.22 Cell count data analysis for nine-month-old <i>Del2</i> males	225
TABLE 6.23 Cell count data analysis for nine-month-old <i>Del2</i> females	225
TABLE 6.24 Cell count data analysis for nine-month-old <i>Del2</i> males Vs. females	226
TABLE 6.25 Cell count data analysis for one-month-old versus three-month-old wt males	233
TABLE 6.26 Cell count data analysis for one-month-old versus three-month-old wt females	233
TABLE 6.27 Cell count data analysis for one-month-old versus three-month-old <i>Del2</i> males	235
TABLE 6.28 Cell count data analysis for one-month-old versus three-month-old <i>Del2</i> females	235
TABLE 6.29 Cell count data analysis for one-month-old versus six-month-old wt males	237
TABLE 6.30 Cell count data analysis for one-month-old versus six-month-old wt females	237
TABLE 6.31 Cell count data analysis for one-month-old versus six-month-old <i>Del2</i> males	239
TABLE 6.32 Cell count data analysis for one-month-old versus six-month-old <i>Del2</i> females	239
TABLE 6.33 Cell count data analysis for one-month-old versus nine-month-old wt males	241
TABLE 6.34 Cell count data analysis for one-month-old versus nine-month-old wt females	241
TABLE 6.35 Cell count data analysis for one-month-old versus nine-month-old <i>Del2</i> males	243
TABLE 6.36 Cell count data analysis for one-month-old versus nine-month-old <i>Del2</i> females	243
TABLE 6.37 Cell count data analysis for one-month-old wt versus one-month-old <i>Del2</i> males	245
TABLE 6.38 Cell count data analysis for one-month-old wt versus one-month-old <i>Del2</i> females	245
TABLE 6.39 Cell count data analysis for three-month-old wt versus three-month-old <i>Del2</i> males	247
TABLE 6.40 Cell count data analysis for three-month-old wt versus three-month-old <i>Del2</i> females	247
TABLE 6.41 Cell count data analysis for six-month-old wt versus six-month-old <i>Del2</i> males	249
TABLE 6.42 Cell count data analysis for six-month-old wt versus six-month-old <i>Del2</i> females	249
TABLE 6.43 Cell count data analysis for nine-month-old wt versus nine-month-old <i>Del2</i> males	251
TABLE 6.44 Cell count data analysis for nine-month-old wt versus nine-month-old <i>Del2</i> females	251
TABLE 6.45 Proposed classification of centrosome abnormalities in tumour cells. Taken from [Duensing, 2005]	261

LIST OF APPENDED TABLES

TABLE 1.1 Disorders associated with the ductal plate malformation. Modified from [Knisely, 2003]	297
--	-----

LIST OF FIGURES

FIGURE 1.1 Histology of liver and bile ducts in biliary atresia	13
FIGURE 1.2 The human biliary system	16
FIGURE 1.3 Blood supply of the extrahepatic and intrahepatic biliary system	17
FIGURE 1.4 Hepatic portal tract	18
FIGURE 1.5 Morphogenesis of the intrahepatic biliary system	21
FIGURE 1.6 Ductal plate malformation	23
FIGURE 1.7 Biliary tree, cholangiocytes and ductal bile formation	27
FIGURE 1.8 Normal human bile duct morphology	29
FIGURE 1.9 Theoretical scheme for paracrine communications between cholangiocytes and non-epithelial cells in the liver	31
FIGURE 1.10 Cystoproteins are proteins of genes that are mutated in cystic kidney diseases of humans, mice, or zebrafish	40
FIGURE 1.11 Ciliary categories	47
FIGURE 1.12 Representative time sequence of primary cilia bending in response to fluid shear	54
FIGURE 1.13 The intracellular Ca^{2+} increase induced by bending of the primary cilium in MDCK cells	55
FIGURE 1.14 Classic morphogen accumulation model for nodal flow sensing	61

FIGURE 1.15 Human laterality disorders and current models for establishing left-right asymmetry	63
FIGURE 1.16 Flow-based model of Wnt regulation in the kidney.....	73
FIGURE 1.17 Noncanonical Wnt signalling and tubular morphogenesis	75
FIGURE 1.18 Model of fibrocystin	83
FIGURE 1.19 Sections of <i>inv</i> mouse liver tissue stained with DBA histochemistry	96
FIGURE 1.20 A schematic diagram of the knockout construct used to produce the <i>Pkhd1^{del2/del2}</i> mouse model of ARPKD	99
FIGURE 1.21 Gross appearance of <i>Pkhd1^{del2/del2}</i> liver from Mallory trichrome stained sections.....	100
FIGURE 1.22 <i>Pkhd1^{del2/del2}</i> kidney sections stained with H&E.....	101
FIGURE 1.23 Primary cilia in bile duct and proximal tubule by SEM and fluorescent histochemistry	103
FIGURE 3.1 Experimental layout of culture slides	146
FIGURE 4.1 Patient 10 liver biopsy.....	151
FIGURE 4.2 Renal cyst ultrasound.....	152
FIGURE 4.3 Mutational analysis of <i>PKHD1</i>	154
FIGURE 4.4 Mutational analysis of <i>PKHD1</i>	156
FIGURE 5.1 Sections of snap frozen normal human liver tissue stained using DAB immunohistochemistry	165
FIGURE 5.2 Immunohistochemical fixative panel performed on sections of snap frozen normal human liver tissue	166
FIGURE 5.3 Acetone fixed sections of snap frozen normal human liver tissue.....	167
FIGURE 5.4 Acetylated α -tubulin antibody titrations on sections of formalin-fixed paraffin embedded human liver stained using DAB immunohistochemistry	169
FIGURE 5.5A Fibrocystin antibody (clone 5a) titration on sections of formalin-fixed paraffin embedded human liver tissue stained using DAB immunohistochemistry	171
FIGURE 5.5B Fibrocystin antibody (clone 11) titration on sections of formalin-fixed paraffin embedded human liver tissue stained using DAB immunohistochemistry	172
FIGURE 5.5C Fibrocystin antibody (clone 14) titration on sections of formalin-fixed paraffin embedded human liver tissue stained using DAB immunohistochemistry	173
FIGURE 5.5D Fibrocystin antibody (clone 18) titration on sections of formalin-fixed paraffin embedded human liver tissue stained using DAB immunohistochemistry	174
FIGURE 5.5E Fibrocystin antibody (clone 19) titration on sections of formalin-fixed paraffin embedded human liver tissue stained using DAB immunohistochemistry	175
FIGURE 5.6 Fibrocystin expression on sections of formalin-fixed paraffin-embedded adult human end-stage liver disease tissue stained using DAB immunohistochemistry	178
FIGURE 5.7 Fibrocystin expression on sections of formalin-fixed paraffin embedded human biliary atresia liver tissue	179
FIGURE 5.8 Fibrocystin cohort staining count data: total percentage of positive ducts	181
FIGURE 5.9 Fibrocystin cohort staining count data: intra-specimen mean percentage of positive ducts	182
FIGURE 5.10 Section of end-stage autoimmune hepatitis human liver tissue displaying periseptal ductular reactivity	184
FIGURE 5.11 Acetylated α -tubulin expression on sections of formalin-fixed paraffin-embedded human end-stage liver disease tissue stained using DAB immunohistochemistry	185
FIGURE 5.12 Acetylated α -tubulin expression on sections of formalin-fixed paraffin-embedded human biliary atresia liver tissue	186
FIGURE 5.13 Representative images of a primary cilium observed on an isolated cell from 100% confluent HEK293 cells grown on gelatine coated glass coverslips	189
FIGURE 5.14 Representative images of a primary cilium observed on an isolated cell from sub-confluent BEC grown on gelatine coated glass coverslips	190
FIGURE 6.1 One-month-old wt: Mean percentage of primary proximal tubular cells displaying centrosomal overduplication	204
FIGURE 6.2 One-month-old <i>Del2</i> : Mean percentage of primary proximal tubular cells displaying centrosomal overduplication	207
FIGURE 6.3 Three-month-old wt: Mean percentage of primary proximal tubular cells displaying centrosomal overduplication	210
FIGURE 6.4 Three-month-old <i>Del2</i> : Mean percentage of primary proximal tubular cells displaying centrosomal overduplication	213

FIGURE 6.5 Six-month-old wt: Mean percentage of primary proximal tubular cells displaying centrosomal overduplication	216
FIGURE 6.6 Six-month-old <i>Del2</i> : Mean percentage of primary proximal tubular cells displaying centrosomal overduplication	219
FIGURE 6.7 Nine-month-old wt: Mean percentage of primary proximal tubular cells displaying centrosomal overduplication	222
FIGURE 6.8 Nine-month-old <i>Del2</i> : Mean percentage of primary proximal tubular cells displaying centrosomal overduplication	225
FIGURE 6.9 Immunofluorescence staining of 17 β -estradiol treated primary proximal tubular epithelial cells isolated from wildtype mice	229
FIGURE 6.10 Immunofluorescence staining of 17 β -estradiol treated primary proximal tubular epithelial cells isolated from <i>Del2</i> mice	230
FIGURE 6.11 One-month-old Vs three-month-old wt: comparison of centrosomal amplification in 17 β -estradiol treated primary proximal tubular epithelial cells	232
FIGURE 6.12 One-month-old Vs three-month-old <i>Del2</i> : comparison of centrosomal amplification in 17 β -estradiol treated primary proximal tubular epithelial cells	234
FIGURE 6.13 One-month-old Vs six-month-old wt: comparison of centrosomal amplification in 17 β -estradiol treated primary proximal tubular epithelial cells.....	236
FIGURE 6.14 One-month-old Vs six-month-old <i>Del2</i> : comparison of centrosomal amplification in 17 β -estradiol treated primary proximal tubular epithelial cells	238
FIGURE 6.15 One-month-old Vs nine-month-old wt: comparison of centrosomal amplification in 17 β -estradiol treated primary proximal tubular epithelial cells.....	240
FIGURE 6.16 One-month-old Vs nine-month-old <i>Del2</i> : comparison of centrosomal amplification in 17 β -estradiol treated primary proximal tubular epithelial cells	242
FIGURE 6.17 Age-matched comparison of the mean percentage of primary proximal tubular epithelial cells displaying centrosomal amplification from one-month-old wt and <i>Del2</i> animals	244
FIGURE 6.18 Age-matched comparison of the mean percentage of primary proximal tubular epithelial cells displaying centrosomal amplification from three-month-old wt and <i>Del2</i> animals.....	246
FIGURE 6.19 Age-matched comparison of the mean percentage of primary proximal tubular epithelial cells displaying centrosomal amplification from six-month-old wt and <i>Del2</i> animals	248
FIGURE 6.20 Age-matched comparison of the mean percentage of primary proximal tubular epithelial cells displaying centrosomal amplification from nine-month-old wt and <i>Del2</i> animals.....	250
FIGURE 6.21 Fluorescent immunohistochemistry of wt and <i>Pkhd1</i> ^{<i>Del2/Del2</i>} kidney tissue sections	253
FIGURE 6.22 Fluorescent immunohistochemistry of wt and <i>Pkhd1</i> ^{<i>Del2/Del2</i>} liver tissue sections	254

LIST OF APPENDED FIGURES

FIGURE 3.1 One-month-old wt: Scatter plot of mean percentage of cells with >2 centrosomes.....	305
FIGURE 3.2 One-month-old <i>Del2</i> : Scatter plot of mean percentage of cells with >2 centrosomes	306
FIGURE 3.3 Three-month-old wt: Scatter plot of mean percentage of cells with >2 centrosomes.....	307
FIGURE 3.4 Three-month-old <i>Del2</i> : Scatter plot of mean percentage of cells with >2 centrosomes	308
FIGURE 3.5 Six-month-old wt: Scatter plot of mean percentage of cells with >2 centrosomes	309
FIGURE 3.6 Six-month-old <i>Del2</i> : Scatter plot of mean percentage of cells with >2 centrosomes	310
FIGURE 3.7 Nine-month-old wt: Scatter plot of mean percentage of cells with >2 centrosomes	311
FIGURE 3.8 Nine-month-old <i>Del2</i> : Scatter plot of mean percentage of cells with >2 centrosomes	312

LIST OF BOXES

BOX 1 Ciliary subcompartments.....	42
------------------------------------	----

ABBREVIATIONS

2D-PAGE	Two-dimensional polyacrylamide gel electrophoresis
3D	3-dimensional
ADPKD	Autosomal dominant polycystic kidney disease
AF	Alexa Fluor
AIH	Autoimmune hepatitis
ALD	Alcoholic liver disease
ALTER	Agitated low-temperature epitope retrieval
AP1	Activator protein 1 transcription factor
APC	Anaphase promoting complex
ARPKD	Autosomal recessive polycystic kidney disease
B6	(Black 6) C57L/6J mouse strain
BA	Biliary atresia
BASM	Biliary atresia splenic malformation syndrome
BBS	Bardet-Biedl syndrome
BCH	Birmingham children's hospital
BCHLU	Birmingham children's hospital liver unit
BCLR	University of Birmingham centre for liver research
BDL	Bile duct ligated
BEC(s)	Biliary epithelial cell(s)
BSA	Bovine serum antigen
Ca ²⁺	Calcium ion
CAML	Calcium modulating cyclophilin ligand
cAMP	Cyclic adenosine monophosphate
CBC	Ciliary-basal body-centrosomal complex
CD(s)	Collecting duct(s)
cDNA	Complementary DNA
<i>CFC1</i>	Cryptic gene
cGMP	Cyclic guanosine monophosphate
CHF	Congenital hepatic fibrosis
CMV	Cytomegalovirus
CNI	Calcineurin inhibitors
DAB	Diaminobenzidine
DAPI	4'-6-diamidion-2-phenylindole
DBA	Dolicus biflorus agglutinin
ddH ₂ O	Double distilled water
<i>Del2</i>	<i>Pkhd1^{del2/del2}</i> mouse model of ARPKD
DHPLC	Denaturing high-performance liquid chromatography
DMEM	Dulbecco's Modified Eagle's Medium
DNA	Deoxyribonucleic acid
DNase	Deoxyribonuclease
dNTPs	Deoxyribonucleotide triphosphates
DPM	Ductal plate malformation
DS	Dissection solution
dsDNA	Double-stranded DNA

dsRNA	Double-stranded RNA
Dvl	Dishevelled
ϵ	Epsilon
E2	17 β -estradiol
EBV	Epstein-Barr Virus
ECM	Extracellular matrix
EDTA	Ethylene diaminetetracetic acid
EGF	Epidermal growth factor
EHBA	Extrahepatic biliary atresia
EHBD(s)	Extrahepatic bile duct(s)
ELV	Exosome-like vesicle
EMT	Endothelial-mesenchymal transformation
ER	(O)estrogen receptor
ERK	Extracellular signal-related kinase
FACS	Fluorescent-activated cell sorting
FAK	Focal adhesion kinase
FBS	Foetal bovine serum
FCS	Foetal calf serum
FFPE	Formalin-fixed paraffin-embedded
FITC	Fluorescein isothiocyanate
GAPDH	Glyceraldehyde-3-phosphate dehydrogenase
gDNA	Genomic DNA
GFR	Glomerular filtration rate
GPS	Glutamine-Penicillin-Streptomycin
H&E	Haematoxylin and eosin
HATs	Histone acetyltransferase
HBSS	Hank's buffered salt solution
HCC	Hepatic cholangiocarcinoma
HCV	Hepatitis C virus
HDAC6	Histone deacetylase 6
HEA125	Human epithelial antigen
HEK293	Human embryonic kidney cell line
HEPES	4-(2-hydroxyethyl)-1-piperazineethanesulfonic acid
HFN	Human fibronectin
HGF	Hepatic growth factor
HLA	Human leukocyte antigen
HNF6	Hepatic nuclear factor 6
HPE	Hepatic portoenterostomy
HRFC	Hepato-renal fibrocystic
HRP	Horse radish peroxidase
HSC	Hepatic stellate cell
HTP	High-throughput
IBDU(s)	Intrahepatic bile duct unit(s)
ICAM-1	Intercellular adhesion molecule 1
ID2	Inhibitor of DNA binding 2
IFN- γ	Interferon - γ (gamma)
IFT	Intraflagellar transport

IgG	Immunoglobulin sub-type G
IHBD(s)	Intrahepatic bile duct(s)
IL	Interleukin
IMCD	Inner medullary collecting duct
INVS	Inversin protein
JAK	Janus kinase
LTA	Lotus tetragonolobus agglutinin
MAP(s)	Microtubule associated protein(s)
MDCK	Madin Darby canine kidney (cell line)
MgCl ₂	Magnesium chloride
MHC	Major histocompatibility complex
mIMCD3	Murine inner medullary collecting duct 3 (cell line)
MKS	Meckel-Gruber syndrome
mRNA	Messenger RNA
MT(s)	Microtubule(s)
MTOC	Microtubule organising centre
MVB(s)	Multi-vesicular body(s)
NGS	Normal goat serum
NL	Normal liver
NLS	Nuclear localisation signal
NPHP	Nephronophthisis
NVP(s)	Nodal vesicular parcel(s)
OD	Optical density
ORF	Open reading frame
orpk	Oak ridge polycystic kidney (mouse model)
PBC	Primary biliary cirrhosis
PBS	Phosphate buffered saline
PC-1	Polycystin 1 protein
PC-2	Polycystin 2 protein
PCD	Primary ciliary dyskinesia
PCK	Polycystic kidney
PCLD	Polycystic liver disease
PCM	Pericentriolar material
PCNA	Proliferating cell nuclear antigen
PCP	Planar cell polarity
PCR	Polymerase chain reaction
PDL	Poly-d-lysine
PGK	Phosphoglycerate kinase
PKA	Protein kinase A
PKC	Protein kinase C
PKD	Polycystic kidney disease
<i>PKD1</i>	Polycystic kidney disease 1 gene
<i>PKD2</i>	Polycystic kidney disease 2 gene
<i>PKHD1</i>	Polycystic kidney and hepatic disease 1 gene
PLL	Poly-l-lysine
PSC	Primary sclerosing cholangitis
PT(s)	Proximal tubule(s)

PTC(s)	Proximal tubular cell(s)
PTFE	Polytetrafluoroethylene
PtK ₁	Female Rat Kangaroo Kidney Epithelial (cell line)
PVP	Peribiliary vascular plexus
qRT-PCR	Quantitative real-time PCR
RIP	Regulated intramembrane proteolysis
RISC	RNA induced silencing complex
RNA	Ribonucleic acid
RNAi	RNA interference
RNase	Ribonuclease
rRNA	Ribosomal RNA
RRV	Rhesus rotavirus
RT-PCR	Reverse transcription polymerase chain reaction
SEM	Scanning electron microscopy
siRNA	Small interfering ribonucleic acid
<i>Sirt2</i>	Sirtuin 2 gene
STAT	Signal transducer and activator of transcription
T ₃	3-iodo-thyronine
TACMA	Tissue and cell molecular analysis
TBS	Tris buffered saline
TCF	T-cell transcription factor
Texas-red	Sulphorhodamine 101 acid chloride
Th1	Type 1 helper T cell
Th2	Type 2 helper T cell
TM	Transmembrane
T _m	Melting temperature
TNF- α	Tumour necrosis factor α (alpha)
TPN	Total parenteral nutrition
VIP	Vasoactive intestinal peptide
wt	Wildtype
<i>ZIC3</i>	Zinc finger protein of cerebellum 3 gene
α 1AT	Alpha-1-antitrypsin
α 1ATdef.	Alpha-1-antitrypsin deficiency

CHAPTER 1 INTRODUCTION

1.1 BILIARY ATRESIA

Extrahepatic biliary atresia (EHBA) is an idiopathic congenital obliterative ductular cholangiopathy. It results from a progressive localized inflammatory and fibrosclerosing destruction of the extrahepatic bile ducts (EHBDs) accompanied by a characteristic intrahepatic portal lesion. The resulting obstruction to bile flow leads to cholestasis, progressive fibrosis and ultimately cirrhosis [Balistreri et al., 1996]. As fibrotic obliteration may involve the entire extrahepatic biliary system or any part of the system, with concomitant injury and fibrosis of intrahepatic bile ducts (IHBDs), consequently the term extrahepatic has been dropped from the name of this disorder in recent years [Sokol et al., 2003] and will therefore be referred to only as biliary atresia (BA) throughout this thesis.

Despite being relatively rare, BA is the most common cholestatic disorder in neonates [Sokol et al., 2003]. Approximate incidence figures are available from France (1 in 19,500 live births), the UK and Eire (1 in 16,700 live births), the USA and Sweden (1 in 14,000 live births) and Asian countries (1 in 18,000 live births) [Chardot et al., 1999; Fischler et al., 2002; McKiernan et al., 2000; Yoon et al., 1997], with large studies reporting a 1.4:1 female:male predominance [Lipsett et al., 1997]. The overall clinical presentation is of persisting jaundice from the second day of life. Other features include hypopigmented or noticeably acholic (white or gray) stools, dark urine, failure to thrive, and hepatosplenomegaly [Kelly and Davenport, 2007; Sokol et al., 2003]. Most infants with BA are full term with a

normal birth weight [Kelly and Davenport, 2007]. However, upon careful anthropometric evaluation it has been stated that infants with BA have significantly decreased body fat stores and lean body mass. The added mass of an enlarged liver and spleen, and the occasional finding of subclinical ascites may account for the appearance of a well-nourished infant (i.e. a relatively normal birth weight) [Sokol and Stall, 1990].

Attempts to characterise BA on the basis of differential phenotypes have led to the description of anatomical and clinical subtypes. Three broad anatomical forms based on the patency of the hepatic bile duct and the extent of biliary damage are recognised [Lipsett et al., 1997]. Type I affects the common bile duct and proximal cystic biliary duct; type II affects the common hepatic duct; and type III, which is the most common, affects the entire extrahepatic biliary tree. Each of the anatomical subtypes presents a unique surgical challenge. Type I BA referred to as “correctable” is characterised by a patent hepatic duct, up to the porta hepatis, without duodenal communication, and may allow for a direct extrahepatic biliary duct-intestinal anastomosis. This “correctable” subtype is less frequent compared with types II and III, accounting for only 10% to 15% of BA patients. No lumen is available for bile duct-intestinal anastomosis in types II and III, referred to as “uncorrectable”. However, in the late 1950s, Dr Morio Kasai reported the presence of patent microscopic biliary channels at the porta hepatis in young infants with “uncorrectable” BA. Exposure of these remnants by radical excision to the jejunum allows the microscopic biliary structures to drain bile into the intestinal conduit, thus relieving the obstruction to bile flow [Kobayashi and Stringer, 2003; Lipsett et al., 1997]. The Kasai hepatic portoenterostomy (HPE) operation is now accepted as the standard operation for the condition [Kobayashi and Stringer, 2003]. However, with

the HPE procedure many factors can affect the success of the surgery [Balistreri et al., 1996]. If diagnosed in the first 2-3 months of life, HPE can restore bile flow from the liver into the intestinal tract in 30% to 80% of patients [Ohi, 2000; Schweizer, 1986; Sokol et al., 2003]. Even if the outcome of surgery is an initial success, progressive inflammation and fibrosis of IHBDs develops to varying degrees in all patients. Consequently, 70% to 80% of BA patients will eventually require liver transplantation, approximately half in the first two years of life [Chardot et al., 1999; Karrer and Bensard, 2000; Karrer et al., 1996]. Approximately another third of patients with BA will require transplantation by their teens, and the rest will live with some degree of liver disease [Balistreri et al., 1996]. Hence, BA remains the foremost indication for liver transplantation in infants and children, accounting for almost 50% of all paediatric liver transplants [Mack and Sokol, 2005; Whittington and Balistreri, 1991]. The natural history of BA without medical or surgical management is reasonably well documented. In the absence of orthotopic liver transplantation, patients with BA are subject to progressive and rapid development of end-stage liver disease due to the persistent intrahepatic inflammatory process. Therefore, survival beyond 24 or 36 months of age is very unusual [Adelman, 1978; Hays and Synder, 1963; Karrer et al., 1990; Karrer et al., 1996; Kelly and Davenport, 2007].

The concept of two distinct clinical forms of BA was described by Desmet [1992a] and Schweizer [1986], (Table 1.1). The embryonal or foetal type occurs in approximately 35% of patients, characterised by early onset cholestasis, absence of a jaundice-free period after physiological jaundice, and absence of bile duct remnants in the hepatoduodenal ligament. Stereotypical coexisting congenital anomalies of laterality complicate this foetal type in 10-

20% of cases [Lipsett et al., 1997]. Coincidental congenital anomalies could include intestinal malrotation, asplenia or polysplenia, portal vein anomalies (preduodenal, absence, cavernous transformation), *situs inversus* (complete), *situs ambiguus* (partial), congenital heart defects, annular pancreas, Kartagener's syndrome, duodenal, oesophageal, or jejunal atresia, polycystic kidneys, and cleft palate [Carmi et al., 1993; Silveira et al., 1991; Tanano et al., 1999]. In particular, polysplenia syndrome (polysplenia, midline liver, interrupted inferior vena cava, *situs inversus*, preduodenal portal vein, and malrotation of the intestine) is present to some degree in 8% to 12% of all children with BA [M. Davenport et al., 1993; Karrer et al., 1991]. The perinatal or acquired form of BA is more common and represents 80% to 90% of cases. In contrast to the foetal form, the perinatal type of BA usually presents with cholestatic jaundice between one and two months of age, such that a jaundice-free interval may even be present between physiological jaundice and onset of cholestasis. Perinatal BA is not associated with congenital abnormalities, and remnants of bile duct structures can typically be seen in histological sections of the hepatoduodenal ligament [Bassett and Murray, 2008; Lipsett et al., 1997; Sokol et al., 2003].

TABLE 1.1 Two clinical forms of biliary atresia

EMBRYONIC OR FOETAL TYPE (35%)
<ol style="list-style-type: none">1. Early onset of neonatal cholestasis2. No jaundice-free period after physiological jaundice3. No bile duct remnants in hepatoduodenal ligament4. Associated congenital anomalies (10-20% of cases)
PERINATAL TYPE (65%)
<ol style="list-style-type: none">1. “Later onset” of neonatal cholestasis2. Jaundice-free interval may be present after physiological jaundice3. Remnants of bile duct structures found in hepatoduodenal ligament4. No associated congenital anomalies

NOTE. According to Schweizer [1986] and Desmet [1992a]

The cause of BA is not known. Our understanding of the aetiology and pathogenesis of liver and bile duct injury in patients has remained essentially unchanged until recent years. Multiple theories regarding the pathogenesis of BA differ in the proposed primary mechanism of injury, but they are often similar in their dependence on secondary or coexisting factors. Currently, BA is believed to be a common phenotypic response of the neonatal liver and bile ducts to a variety of prenatal insults (viral, metabolic, vascular) that perturbs the normal development or maturation of the biliary tree that occurs during a specific period (perinatally to up to three months of age) amid the milieu of genetic or immunologic susceptibilities to this disease. Currently, research efforts designed to address the pathogenesis of BA are centred on five major mechanisms that have been proposed in the literature (Table 1.2).

TABLE 1.2 Potential mechanisms involved in the pathogenesis of biliary atresia

MECHANISM	SUPPORTING DATA
1. Defect in morphogenesis	<p>Coexistence of non-hepatic embryologic abnormalities</p> <p>Abnormal remodelling of the “ductal plate”</p> <p>HGF (c-met oncogene, adhesion molecules, differentiation of biliary epithelial cells)</p> <p>Mutations in hepatic developmental genes (<i>HNF6, Jagged1</i>)</p> <p>Mutations in laterality genes (<i>CFC1, ZIC3</i>) in patients with biliary atresia and laterality defects</p> <p>Epigenetic factors: overexpression of regulatory genes in children with the embryonic form of biliary atresia</p> <p><i>Inv</i> mouse: model of biliary obstruction and <i>situs inversus</i></p>
2. Defect in prenatal circulation	Intrauterine devascularisation results in abnormal extrahepatic bile ducts
3. Immunologic dysregulation	<p>Altered class I and II major histocompatibility complex expression</p> <p>Increased expression of intracellular adhesion molecules: ICAM-1</p> <p>Increased frequency of the HLA-B12, B8 or DR3 alleles</p> <p>Hepatic profile displaying a predominant Th1-like phenotype</p> <p>Prevention of inflammatory obstruction of bile ducts in IFN-γ deficient mice</p>
4. Viral infection	<p>CMV, reovirus, rotavirus, retrovirus, human papilloma virus, and other viral agents detected in infants with biliary atresia</p> <p>Biliary obstruction in newborn mice infected with rotavirus</p>
5. Environmental toxin exposure	<p>Time-space clustering of cases</p> <p>Phytotoxin or mycotoxin in Australian lambs</p>

NOTE: Adapted from Balistreri [1996] and Bezerra [2006]

It has been suggested by many that the trigger for the inflammatory cascade may be a hepatotropic viral infection [Bassett and Murray, 2008]. Several reports of time-space clustering of cases tends to support an infectious aetiology [Danks and Bodian, 1963; Strickland and Shannon, 1982]. A hepatotropic viral infection may lead to an initial bile duct injury that triggers a persistent immune mediated sclerosing process and results in obstruction of EHBDs [Leifeld et al., 2001]. There have been many hypotheses and studies to identify the aetiological virus. Potential candidates have included Epstein-Barr virus (EBV) [Fjaer et al., 2005; Kobayashi and Stringer, 2003], cytomegalovirus (CMV) [Domati-Saad et al., 2000; Fischler et al., 1998], human herpes virus [Domati-Saad et al., 2000], human papilloma virus [Drut et al., 1998], group C rotavirus [Riepenhoff-Talty et al., 1996], and reovirus type 3 [Steele et al., 1995; Tyler et al., 1998]. However, these suggestive results have been largely inconsistent and underpowered, with many other studies having disputed the role of these viruses in the pathogenesis of BA. However the main criticism of the hypothesis, of a viral infection as the primary trigger for BA, is the inability to document the presence of any virus in many patients with the disease [Bassett and Murray, 2008; Rauschenfels et al., 2009]. Although congenital infections with CMV, EBV, or rubella virus have been found occasionally, the presence of these common agents may be coincidental [Balistreri, 1985; Hays and Kimura, 1980; Howard, 1983; Landing, 1974; Smith et al., 1991].

The exposure of pregnant women to hepatotoxic substances has been considered in studies on the pathogenesis of BA. Time and space clustering of cases has led to the proposal that an environmental toxin could be involved in its pathogenesis [Perlmutter and Shepherd, 2002]. Currently, other than infectious agents, no environmental agent has been clearly associated

with BA in humans. The possible toxic and inflammatory effects of bile that has extravasated through the injured bile duct epithelial layer into the submucosa of the damaged EHBDs could also be considered as a secondary factor in the pathogenesis of BA [Balistreri et al., 1996; Sokol et al., 2003].

Vascular insults during foetal hepatobiliary development have also been implicated in the pathogenesis of BA. Studies by Ho *et al* [1993] identified thickened, tortuous and dilated arteries in the biliary remnants of infants with BA. These observations were taken as evidence for an arteriopathy accompanying the disorder, however the causative or consequential nature of these lesions remains unclear [Balistreri et al., 1996; Sokol et al., 2003]. However, this pathologic mechanism in BA does not appear to be a current research priority.

An abnormality in the immune and/or inflammatory response as a pathologic mechanism in BA is a plausible theory. The presence of lymphocytic infiltration in the portal tracts in liver biopsy specimens of infants with BA suggests a primary inflammatory process leading to bile duct obstruction. The role of the immune system in bile duct injury in BA is poorly understood, but does appear to be highly complex. Several studies have investigated whether bile duct epithelial cells are susceptible to immune/inflammatory attack because of abnormal expression of human leukocyte antigen (HLA) or intercellular adhesion molecules on their surface [Dillon et al., 1994; Seidman et al., 1991].

The progressive nature of BA, despite initial reestablishment of bile flow with HPE, suggests that a persistent autoimmune attack directed at bile ducts may play a role [Schreiber and Kleinman, 1993; Sokol and Mack, 2001]. BA shares features with several autoimmune diseases, such as female predominance, apparent triggering by viral infection, and aberrant major histocompatibility complex (MHC) expression in bile duct epithelium. Consequently, it has been proposed that tissue injury in patients with BA may represent an autoimmune-mediated process. It is possible that the initiator of bile duct injury is a cholangiotropic virus, leading to the exposure of altered self-cholangiocyte epithelial antigens or previously sequestered self-cholangiocyte antigens that would then be recognized as “non-self” and elicit a persistent autoimmune-mediated bile duct injury [Eagar et al., 2001; Sokol and Mack, 2001]. To date, there have been no studies addressing the frequency of other autoimmune diseases in BA patients or in other family members. Interestingly, children with BA who undergo liver transplantation have a 2.5% risk of developing *de novo* autoimmune hepatitis after transplantation, perhaps indicating a genetic predisposition to autoimmune disease [Hernandez et al., 2001; Kerkar et al., 1998].

Another proposed theory as to the pathogenesis of BA, of specific relevance to this project, is the hypothesis that there could be a genetic component resulting in defective morphogenesis of the biliary tree. Generally, BA is not considered to be an inherited disorder, for example HLA-identical twins discordant for the disease have been described, and recurrence of BA within the same family is exceedingly rare [Gunasekaran et al., 1992; Hyams et al., 1985; Smith et al., 1991]. However, the presence of congenital non-hepatic malformations in the subset of infants with the embryonic (syndromic) form of BA points to a potential role of

genetic defects that result in defective embryogenesis and asymmetric left-right determination of visceral organs [Carmi et al., 1993]. The initial animal model that suggested the class of genes involved in axis determination was that of a recessive insertional mutation in the proximal region of mouse chromosome 4 or complete deletion of the *inversin* (*inv*) gene in the mouse. The *inv* mouse model, with laterality defects in abdominal organ placement, also included anomalous development of the hepatobiliary system, and extrahepatic biliary obstruction [Mazziotti et al., 1999; Yokoyama et al., 1993]. Therefore, the human *INV* gene, mapped by Schön and colleagues [2002] was examined in 64 patients with heterotaxia. No mutations were found in seven patients with BA and various congenital laterality defects, making it unlikely that the *INV* gene is responsible for the majority of embryonic cases of BA. Perhaps more subtle alterations in the human *inversin* orthologue accounts for some of the cases of BA without other *situs* anomalies, especially if it is true that the action of *inversin* has specific effects on morphogenesis of the biliary duct system [Perlmutter and Shepherd, 2002]. Interestingly, recessive mutations in *INV* are responsible for infantile nephronophthisis type 2, a disease in which abnormal biliary development with or without *situs inversus* has been described [Otto et al., 2003]. Furthermore, *inversin* the protein encoded by the *INV* gene was found to interact with *nephrocystin*, the gene mutated in nephronophthisis type 1. Both *inversin* and *nephrocystin* are located in the primary cilia of renal tubular cells [Otto et al., 2003]. Thus, gene products with localisation to the mechanosensory primary cilium of renal tubular cells and cholangiocytes may produce aberrant biliary development with predominance of ductal plate malformation (DPM) [Mack and Sokol, 2005]. Further supportive evidence for such gene products is the subset of patients with BA who display the DPM on liver biopsy [Low et al., 2001]. It remains to be seen whether mutations or

polymorphisms in genes that code for proteins regulating functions of the primary cilia, will play a role in the pathogenesis of BA. One of the primary aims in this project is to try to shed some light on this possible mechanism of pathogenesis.

More than thirty other mammalian proteins have now been described that are involved in establishment of right-left patterning during embryogenesis, although few have been examined in BA. The *CFC1* gene, encoding the human cryptic protein, is associated with familial and sporadic cases of laterality defects. In 2008 Davit-Spraul et al. [2008] identified a mutation in the *CFC1* gene in five of ten patients with biliary atresia splenic malformation syndrome (BASM). A loss-of-function mutation identified in the *CFC1* gene in patients with heterotaxy and BA provides yet further evidence supporting the potential role of laterality genes in contributing to the phenotypic determination of BA [Bamford et al., 2000; Jacquemin et al., 2002]. Therefore, in the case of *CFC1*, it can be concluded that mutations are probably not responsible for the development of BA, but may represent a genetic predisposition requiring secondary genetic or environmental factors to produce the BA phenotype [Davit-Spraul et al., 2008]. Other human genes that determine laterality, such as *ZIC3* have been shown to be associated with human *situs* defects and BA [Ware et al., 2004]. It is certain however further investigations of such genes will be required in the coming years to help clarify whether inherited or somatic, mutations or deletions are responsible for individual cases of BA.

Tied into the hypothesis that BA has a possible genetic component, is the proposed pathogenic mechanism of defective morphogenesis of the extrahepatic biliary tract. This hypothesis is also supported by the coexistence of anomalies of visceral organ symmetry in the syndromic form of the disease, especially when considered together with the evidence of DPM in infants with BA [Low et al., 2001]. Abnormal remodelling of the ductal plate leads to the DPM that is present in congenital hepatic fibrosis (CHF) and other bile duct dysplasias. Polymorphisms in *HNF6*, *HNF1-β*, *JAGGED1*, *PKHD1* or other related genes that regulate remodelling of the ductal plate [Clotman et al., 2002; Clotman et al., 2003; Coffinier et al., 2002] could act as susceptibility factors or modifier genes necessary, but not sufficient, for the development of BA. The roles of *JAGGED1*, which is expressed in ductal plate epithelia [Kohsaka et al., 2002], and *HNF6*, a nuclear transcription factor expressed in the developing EHBD and gall bladder [Clotman et al., 2002], are being studied in patients with BA.

Irrespective of the cause, the histopathologic appearance of liver biopsy samples from patients with BA appear the same [C.E. Tan et al., 1994a]. Histologically BA is characterised by portal tract fibrosis, widening of portal tracts with infiltration of inflammatory cells, portal oedema, intrahepatic cholestasis, canalicular and cellular bile stasis, presence of bile plugs in portal tract bile ducts, ductular proliferation, and hepatic giant cell transformation observable under light microscopy, and degenerate biliary ductular cells containing bile pigment and the loss of bile canalicular microvilli seen under electron microscopy [Park et al., 1996] (Fig. 1.1). The portal tract fibrosis varies from portal expansion to cirrhosis.

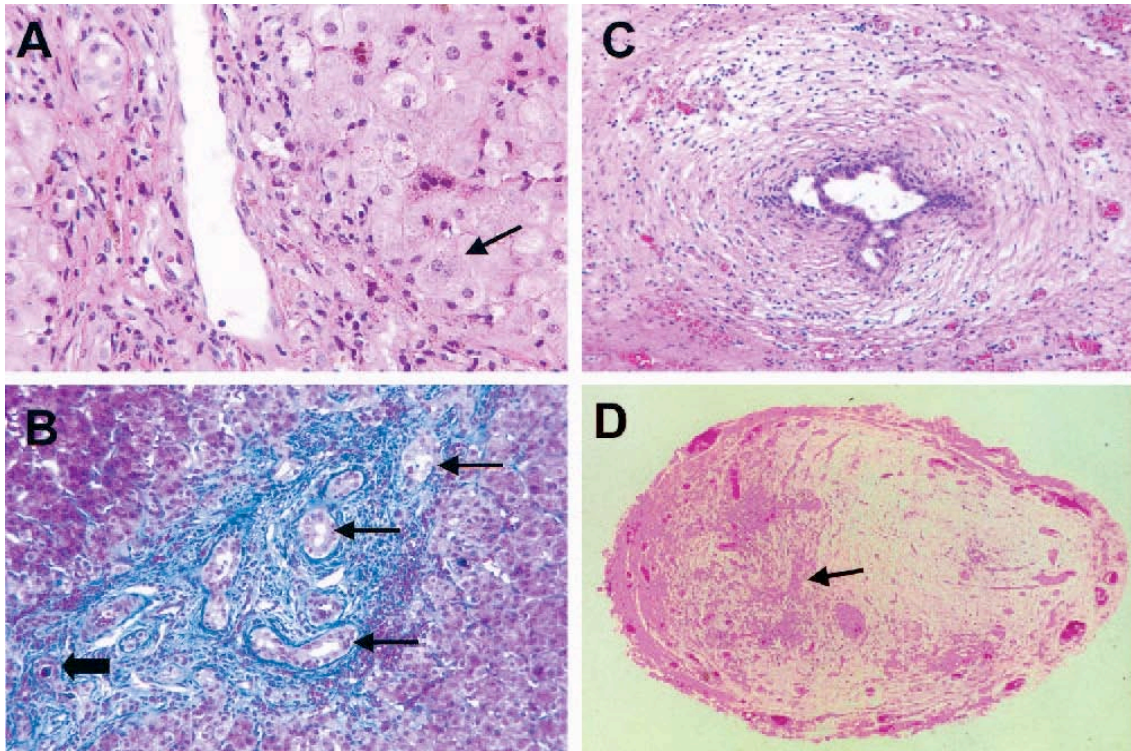


FIGURE 1.1 Histology of liver and bile ducts in biliary atresia. (A) Hepatocellular and canalicular cholestasis, swollen hepatocytes, multinucleated giant cells (arrow), and portal tract inflammation (hematoxylin and eosin, x400). (B) Expanded portal tracts with increased fibrosis, bile duct proliferation (line arrows), and bile plug in portal tract bile duct (block arrow) Trichrome, x250). (C) Proximal common hepatic duct, and increased concentric sclerosis (hematoxylin and eosin, x100). (D) Remnant of common bile duct with absent lumen (arrow) and concentric sclerosis (hematoxylin and eosin, x40). Taken from [Sokol et al., 2003].

Comparisons of the histological features of the livers from infants suffering from BA with and without congenital anomalies show no difference. There are no statistically significant differences in the presence or absence of DPM, bile duct injury/destruction, degree of giant cell transformation, or fibrosis [M. Davenport et al., 2006]. It is important to note that the liver histology in patients with alpha-1-antitrypsin (α_1 AT) deficiency, occasionally in those with Alagille's syndrome [Deutsch et al., 2001], cystic fibrosis, and total parenteral nutrition (TPN)-related cholestasis, can resemble all the features of BA. Infants with chromosomal anomalies (e.g. trisomy 18) and BA have been reported [Carmi et al., 1993; Silveira et al., 1991], associated with unusual anomalies, such as diaphragmatic hernia [D-Y. Zhang et al., 2004a], and oesophageal atresia [Pameijer et al., 2000]. Other genetic diseases, such as cat-eye syndrome (trisomy or tetrasomy 22qter q11), have also been noted [Schinzel et al., 1981]. This evidence supports the recent observations suggesting that BA is not a single disease entity, but rather a phenotype of several underlying specific disorders to which the infant liver responds in a stereotypic manner by a complex and dynamic series of processes, including inflammation, bile duct proliferation, apoptosis, and fibrogenesis [Perlmutter and Shepherd, 2002]. Furthermore, these multiple different insults and potentially divergent mechanisms may be occurring not only simultaneously but also both antenatally and perinatally. There are an abundance of studies implicating different primary triggers for the biliary tract obstruction underlying BA, suggesting that the pathogenesis is multifactorial. Thus genetic, inflammatory, and infectious factors likely all play a role, but the timing and characterisation of the interplay between these factors remains unclear.

1.2 MICROSTRUCTURE AND DEVELOPMENT OF THE BILIARY TRACT

Understanding the development of the biliary system and its cell types is crucial to interpreting the proposed aetiopathologic mechanisms of BA. The biliary tract is an excretory system with two secretory units: hepatocytes and biliary epithelial cells (BEC), including the peribiliary glands. This tract drains bile, produced by the hepatocytes, from the liver to the duodenum. The biliary tract is grossly divided into the intra- and extrahepatic biliary tract according to their anatomical locations relative to the liver. The extrahepatic biliary tract is grossly divided into the common hepatic duct, common bile duct, cystic duct, and gallbladder (Fig. 1.2). The intrahepatic biliary tract is grossly defined as the biliary tract proximal to the hepatic duct, it is subdivided into the right and left hepatic ducts, segmental ducts, area ducts, and their finer branches such as septal and interlobular bile ducts and bile ductules. The right and left hepatic, segmental and area ducts, and their finer branches are collectively termed the “intrahepatic large bile ducts”. These are grossly recognisable and characterised by association with intrahepatic peribiliary glands. By contrast, the septal and interlobular bile ducts and bile ductules, which are only identifiable under light microscopy are generally called “small bile ducts” or “peripheral bile ducts”, and are not associated with peribiliary glands. On liver wedge biopsies, these small bile ducts can be studied, whereas on needle biopsies only interlobular bile ducts and ductules are present for histological examination [Nakanuma et al., 1997]. The glandular elements of the biliary tract are usually not visible on wedge or needle liver biopsy specimens, and are of no interest to this study.

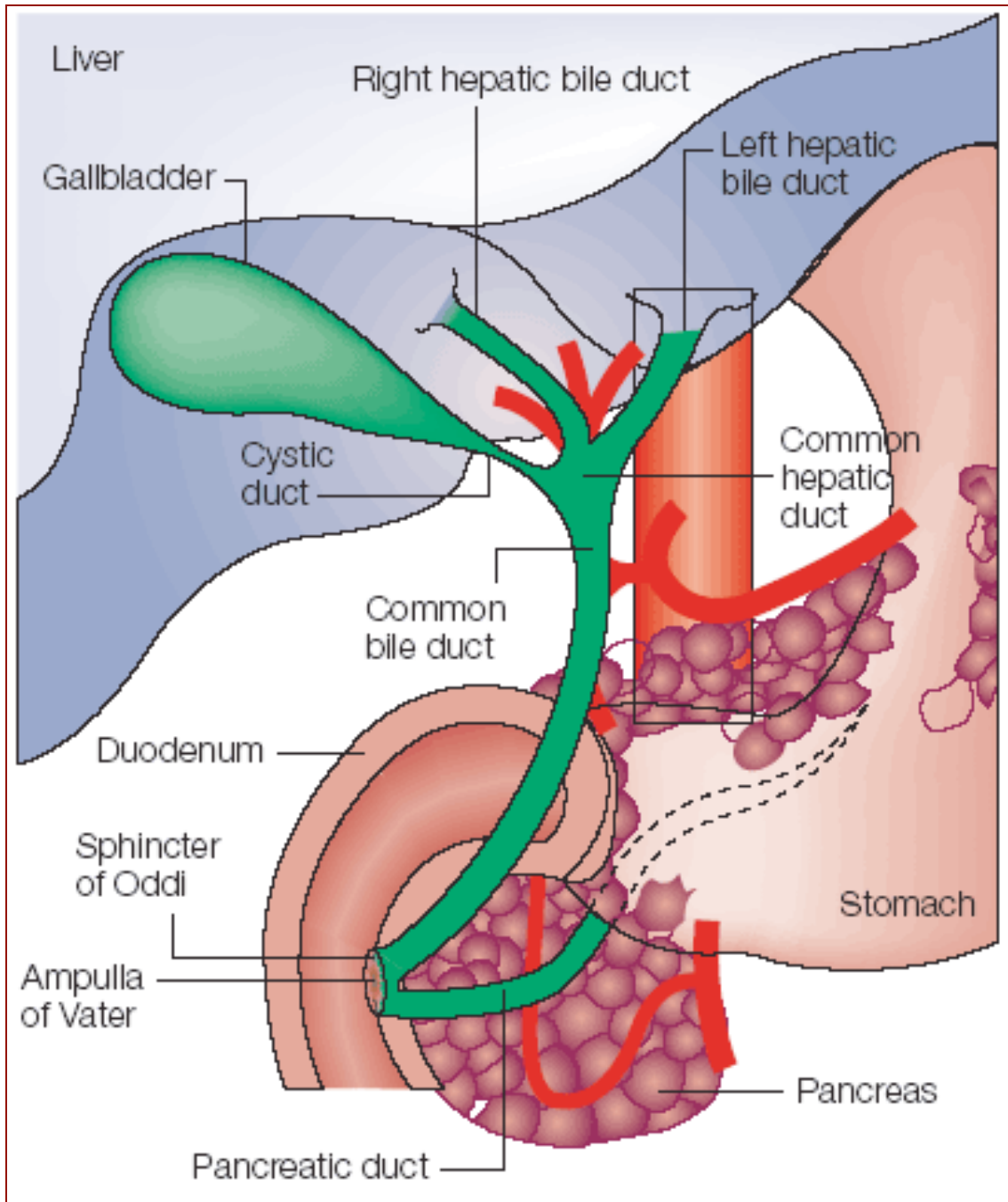


FIGURE 1.2 The human biliary system. Bile is secreted from each lobe of the liver through the right and left hepatic ducts, which join to form the common hepatic duct. The latter meets the cystic duct from the gallbladder to form the common bile duct. After reaching the gallbladder, bile is concentrated and re-enters the common bile duct through the cystic duct, which usually enters the duodenum after combining with the pancreatic duct to form the ampulla of Vater. The ampullary opening into the duodenum is controlled through the muscular sphincter of Oddi. [Wistuba and Gazdar, 2004].

The intrahepatic and extrahepatic biliary tract is supplied and nourished by a network of fine vessels called the peribiliary vascular (or capillary) plexus (PVP). The hepatic arterial branches supply blood to this plexus, and the PVP drains into the sinusoids through “radicular portal veins” or communicate with portal venous branches through internal roots (Fig 1.3).

Within the liver, the three anatomical elements, bile ducts, portal venous, and hepatic arterial branches, run parallel to each other in the portal connective tissue, termed the portal tract (Fig. 1.4). There are usually one or two bile ducts in each portal tract, with the bile duct and hepatic arterial branch running parallel in the same portal tract being roughly of equal size (Fig. 1.4). Bile ductules are not associated with or accompanied by hepatic arterial branches.

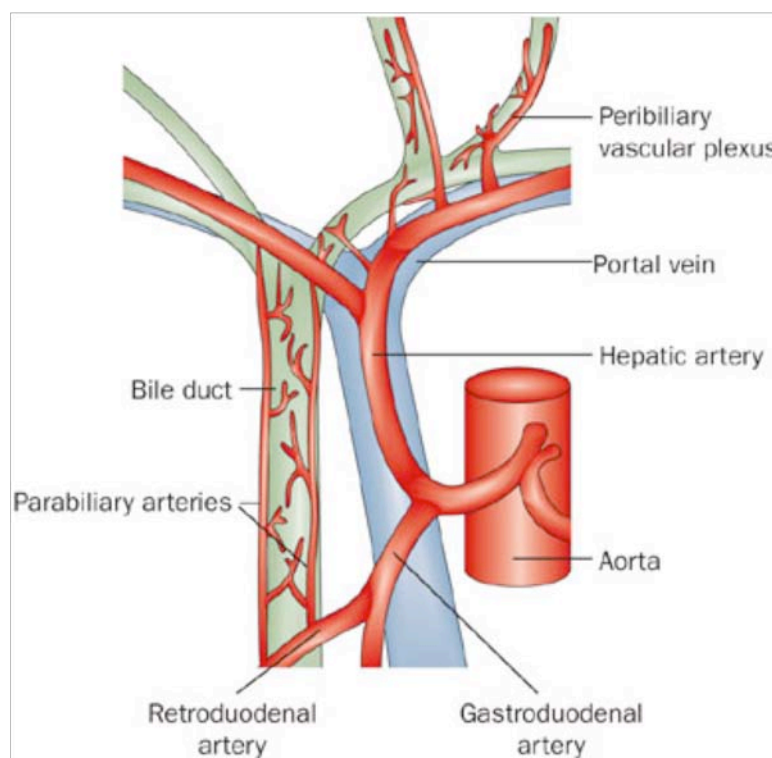


FIGURE 1.3 Blood supply of the extrahepatic and intrahepatic biliary system. The common bile duct is vascularised by the parabiliary arteries, which run adjacent to the bile duct. The majority of their blood is supplied via the inferior retroduodenal artery, while the right hepatic artery supplies a minor portion. By contrast, the intrahepatic bile ducts are supplied by a rich, nonaxial network of small arteries that are solely derived from the right and left hepatic arteries, known as the peribiliary vascular plexus. [Ruemmele et al., 2009].

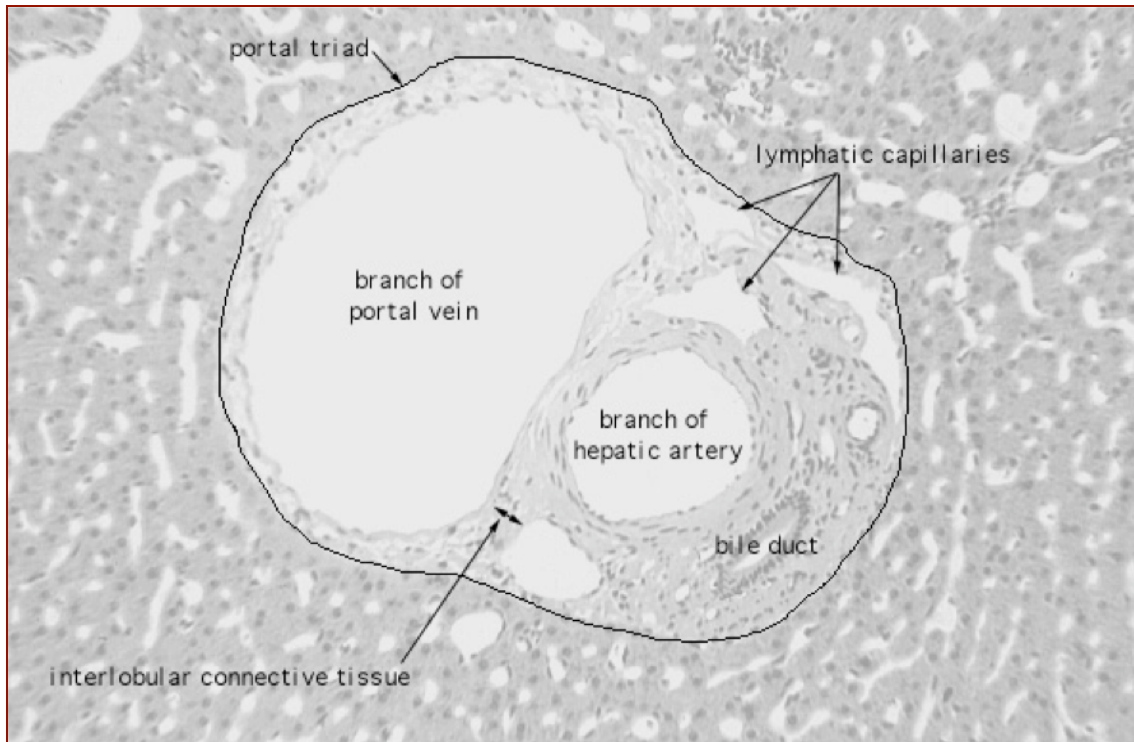


FIGURE 1.4 Hepatic portal tract. Consisting of branches of a portal vein, hepatic artery, bile duct, and lymphatic vessels. These four vessels lie within a network of connective tissue, and are surrounded on all sides by hepatocytes. The ring of hepatocytes abutting the connective tissue of the tract is called the limiting plate. [Hansen, 2001].

The development of the hepatic biliary system in humans begins at the third post-ovulation week. The distal foregut (duodenum) endodermal epithelium gives rise to a ventral outgrowth known as the liver primordium [Lipsett et al., 1997; Sergi et al., 2000]. The liver primordium, a collection of rapidly proliferating liver precursor cells, forms the hepatic diverticulum. As the hepatic diverticulum grows towards and penetrates the adjacent mesodermal tissue (the septum transversum), the hepatic diverticulum separates from the distal foregut [Lipsett et al., 1997]. Two parts emerge: the pars hepatica (cranial), which gives rise to the liver, common hepatic duct and the IHBDs; and the pars cystica (caudal), from which the gallbladder, cystic duct and extrahepatic biliary tree originate [Lipsett et al., 1997].

The development of the intrahepatic biliary system begins around the eighth week of gestation and proceeds centrifugally from the porta hepatis to the periphery. This process may not be completed at birth, and the intrahepatic biliary tract completes its maturation during the first years of life [Strazzabosco et al., 2005]. Histologically, three stages in the development of the intrahepatic biliary tree can be distinguished. In the first step, occurring during the period from 6 to 9 weeks of gestation, a subset of periportal hepatoblasts (progenitor cells), in contact with the mesenchyme surrounding a portal vein branch, switch their phenotype and begin to strongly express biliary specific cytokeratins. These cells are located at the site where ducts form, and are therefore considered as biliary precursor cells. At that stage, hepatoblasts expressing much lower levels of the same cytokeratins are also found throughout the parenchyma (Fig. 1.5) [Lemaigre, 2003]. In the next step, the biliary precursor cells form a continuous single-layered ring around the portal mesenchyme (ductal plate stage) [Nakanuma et al., 1997]. The ductal plate, which is composed of small flat epithelial cells, is recognised at 7 weeks [Lemaigre, 2003; Nakanuma et al., 1997]. Over the

following weeks a second layer of cells duplicates the ductal plate over some segments of its perimeter (double-layered ductal plate) (Fig. 1.5). At around ten weeks of gestation, the ductal plate enters a phase of profound remodelling. During this phase, the ductal plate is in the process of forming immature tubules; focal dilatations appear between the two cell layers, giving rise to immature tubules (Fig. 1.5) [Lemaigre, 2003; Nakanuma et al., 1997]. A few of these dilated primitive intrahepatic biliary structures migrate towards the centre of the portal tract (peripheral tubular or ductular structures) and become incorporated into the mesenchyme of the nascent portal space (migratory stage) [Sergi et al., 2000; Strazzabosco et al., 2005]. The part of the ductal plate not involved in the formation of the ducts progressively regresses and is gradually deleted by apoptosis [Strazzabosco et al., 2005]. At 30 weeks of gestation, the migratory BEC are almost completely transformed into tubules and, concurrently, the ductal plate at the hepatic hilum disappears by 25 weeks of gestation [Nakanuma et al., 1997].

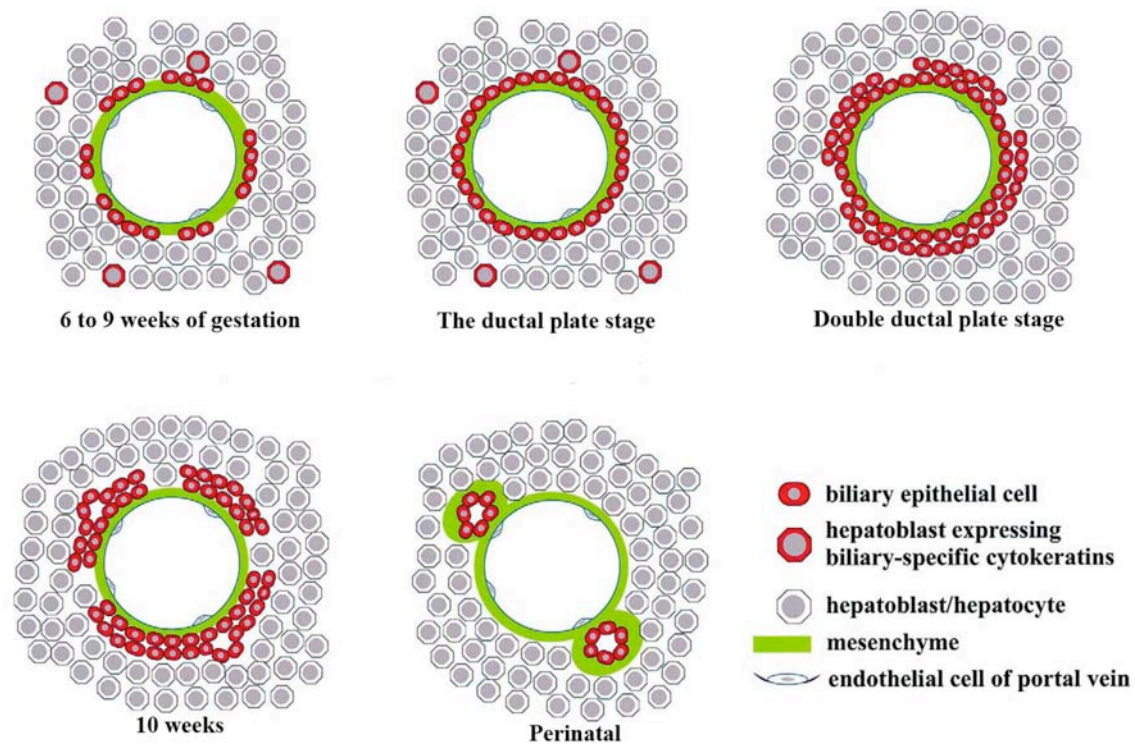


FIGURE 1.5 Morphogenesis of the intrahepatic biliary system. At 6 to 9 weeks of gestation, the biliary precursor cells, which express biliary-specific cytokeratins, are located close to the portal mesenchyme, and some hepatoblasts expressing low levels of biliary specific cytokeratins are found throughout the parenchyma. By week 7, the biliary precursor cells form a continuous single-layered ring called the ductal plate. Over the following weeks the ductal plate becomes partly bilayered. At around 10 weeks of gestation, focal dilatations appear between the two cell layers. These dilatations give rise to the bile ducts, while the rest of the ductal plate progressively regresses. Around birth, the ducts become incorporated into the portal mesenchyme. Adapted from [Lemaigre, 2003].

The timing of IHBD morphogenesis described above corresponds to that of the most advanced biliary structures found near the hilum. The development of small bile ducts (peripheral bile duct development), which proceeds from deep within and moves towards the periphery of the liver, is essentially similar to that of the large IHBDs with three identifiable stages. This development occurs later than that of large IHBDs. In the period from 15 to 19 weeks of gestation, the development of small (peripheral) bile ducts is at the stage of the ductal plate. From 20 weeks of gestation, remodelling of the ductal plate involving biliary cell migration into the mesenchyme occurs and bile duct formation, which begins at 27 weeks of gestation, is completed by 35 weeks of gestation [Nakanuma et al., 1997]. The ductal plate at the peripheral portion of the liver becomes unrecognisable by two weeks after birth [Terada and Nakanuma, 1994]. The EHBDs develop from the caudal part of the hepatic diverticulum. The biliary epithelium lining the EHBDs is continuous at its caudal end with the duodenal epithelium and at the cranial end with the proliferating precursor liver cells. The caudal segment develops into the gallbladder, part of the cystic duct, and the common bile duct. The extrahepatic segments of the right and left hepatic ducts, which are recognisable from 12 weeks of gestation are continuous with the common hepatic duct, and part of the diverticulum [Nakanuma et al., 1997].

Impaired remodelling or persistence of the ductal plate during foetal and postnatal development (DPM) (Fig. 1.6) [Desmet, 1992a] is pathogenetically related to a number of developmental diseases termed the cholangiopathies. The presence of ductal plate remnants, von Meyenburg complexes (excessive bile ducts or ductules with variable degrees of ectasia), biliary cysts, and in some cases intense fibrosis are the pathologic features of this group of

diseases [Desmet, 1992a]. Among them, BA, the autosomal dominant polycystic kidney disease with liver involvement, the polycystic liver disease with renal involvement, and the hepatorenal fibrocystic diseases (autosomal recessive polycystic kidney disease, Caroli's disease, and CHF), all possess distinct features from a genetic, pathophysiologic, and clinical point of view (Appendix 1, Table 1.1) [Strazzabosco et al., 2005]. However, just how a defect in the ductal plate could lead to the phenotypic features shared by the cholangiopathies, and particularly BA, is not intuitively obvious.

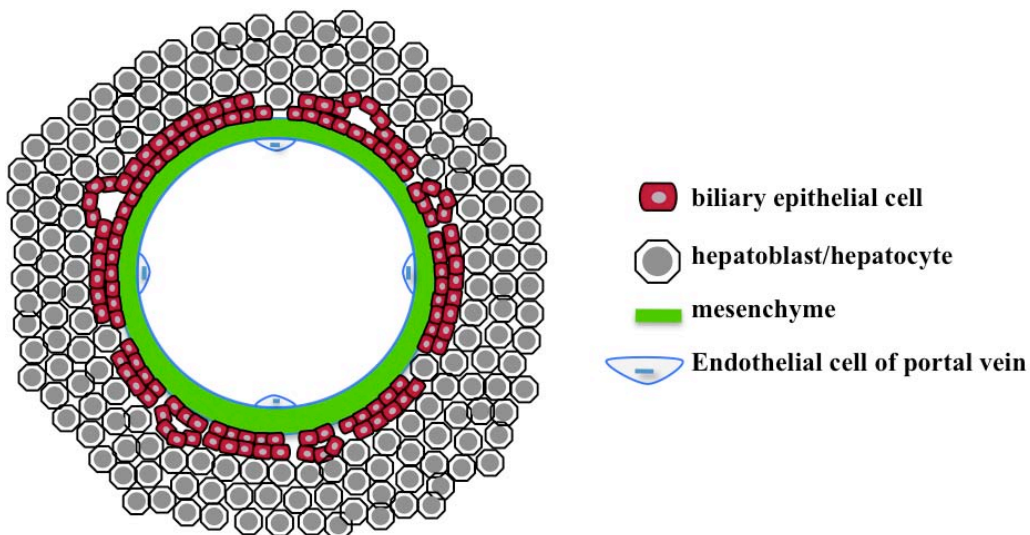


FIGURE 1.6 Ductal plate malformation. Any interruption in the remodelling of the ductal plate can result in the persistence of embryonic duct structures, termed the ductal plate malformation. The ductal plate (red biliary epithelial cells) is in the form of either an interrupted circle or peripheral tubular structures. The ductal plate malformation is a characteristic manifestation of a number of congenital fibrocystic syndromes that are inherited in an autosomal recessive manner. The ductal plate malformation can also result in subsequent liver damage, and inflammation can induce the formation of fibrosis, and in some cases, cirrhosis.

It is well known that bile begins to flow at about twelve weeks, so that the union of the extrahepatic segments of the right and left hepatic ducts with the common hepatic duct, and part of the cystic duct should be completed before twelve weeks of gestation [Nakanuma et al., 1997; C.E.L. Tan and Moscoso, 1994b]. Two groups have demonstrated the presence of extravasated bile in the bile ducts of patients with BA, they proposed that this originated from breaks in the biliary mucosa at the porta hepatis [Park et al., 1996; C.E. Tan and Moscoso, 1994a]. The hypothesis drawn on these findings is that there is a vulnerable stage of human biliary development between 11 and 13 weeks of gestation, when failure of remodelling of the ductal plate structures could lead to disturbances in the normal development of the mesenchymal cuff that surrounds the hepatic hilar bile ducts. Alternatively, connections of the hepatic ducts with the EHBDs could be perturbed; either of these alterations could potentially cause hilar bile ducts to rupture at the initiation of bile flow. Extravasated bile, with its detergent properties, in adjacent periductal tissues would then lead to protracting secondary obliteration and obstruction of more distal EHBDs [Sokol et al., 2003]. First described by Rolleston and Hayne in 1901, this hypothetical mechanism for ductular damage was termed “descending cholangitis” [Rolleston and Hayne, 1901].

It is the very complex nature of BA that makes it challenging to uncover the possible aetiopathologic mechanisms that could result in this phenotype. However, as with many other complex diseases it is the study of less complex genetic and inherited diseases with common clinical features that can help increase our understanding of the disease process. In the case of BA, the group of diseases termed the cholangiopathies may provide insight into its pathogenesis.

1.3 CHOLANGIOCYTES AND THE CHOLANGIOPATHIES

Chronic cholestatic liver diseases which target the biliary system at any site along the intrahepatic and extrahepatic bile ducts represent a large group of potentially evolutive congenital and acquired liver disorders affecting both the adult and paediatric populations. These diseases are collectively called “cholangiopathies” to recognise that cholangiocytes are the primary cell target in the pathogenetic sequence [Strazzabosco et al., 2005]. Cholangiopathies are liver diseases resulting from a failure in cholangiocyte function or from the reaction of cholangiocytes to acute or chronic liver damage. The spectrum of cholangiopathies ranges from genetically transmitted developmental diseases arising from an abnormal bile duct biology, such as cystic fibrosis, Alagille syndrome, and fibropolycystic liver diseases; to conditions in which the biliary epithelium is damaged by disordered immunity, infectious agents, ischemia, toxic compounds, or by an extrahepatic obstruction to bile efflux [Strazzabosco et al., 2005]. However, there are those that remain idiopathic in their cause, and despite their obvious heterogeneity, cholangiopathies share a number of basic pathogenetic mechanisms. The cholangiopathies are typically characterised by coexistence of cholangiocyte growth and apoptosis, inflammation, and fibrosis, differentially targeting the biliary epithelium with heterogeneous proliferative and apoptotic responses of different sized ducts [Alpini et al., 2001; Strazzabosco et al., 2005]. Therefore, to gain a greater understanding of these disorders significant effort has been devoted to understanding the normal physiology of cholangiocytes and their pathophysiology in diseased states. To aid the unravelling of the complexity of BA a basic understanding of cholangiocyte function is vital, and so follows.

Two kinds of epithelial cell, hepatocytes and cholangiocytes, are present in the liver [Alpini et al., 2001], with BEC accounting for 3-5% of the hepatic cell population [Roberts et al., 1997]. While hepatocytes initially secrete bile into the bile canaliculi, cholangiocytes in addition to funnelling bile into the intestine are also actively involved in bile-secretory processes and in liver regenerative/repairative processes [Nathanson and Boyer, 1991; Strazzabosco, 1997]. Cholangiocytes possess both absorptive and secretory properties, modifying bile of canalicular origin by a series of coordinated, spontaneous, and hormone/peptide regulated secretion/reabsorption of water and electrolytes before it reaches the intestine. In humans, around 40% of total bile production is of ductal origin [Alpini et al., 2001; Kanno et al., 2001; Strazzabosco et al., 2005]. Such secretory functions are mainly performed by cholangiocytes lining the interlobular and major ducts, which express the appropriate ion transporters and hormone receptors in polarised domains of the plasma membrane (Fig. 1.7) [Strazzabosco, 1997].

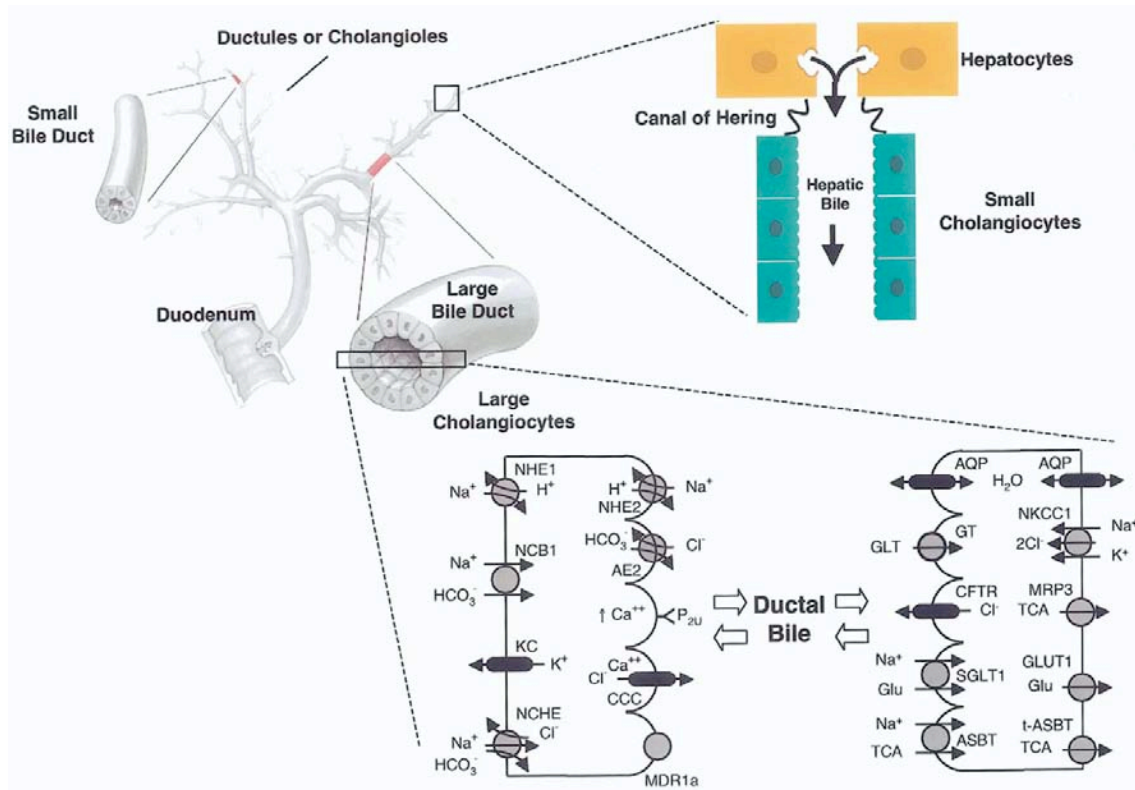


FIGURE 1.7 Biliary tree, cholangiocytes and ductal bile formation. Bile is originated by hepatocytes (i.e., primary or hepatic bile) and is subsequently delivered into bile ducts. The canals of Hering provide the continuum between the hepatocyte canaliculus and the ductules or cholangiocytes ($<15\ \mu\text{m}$), the small size bile ducts ($15\ \mu\text{m}$ to $300\ \mu\text{m}$), and the large bile ducts ($300\ \mu\text{m}$ to $800\ \mu\text{m}$) in which hepatic bile is modified by large size cholangiocytes (i.e., ductal bile). Active biliary epithelial transport of electrolytes and solutes occurs mainly in large bile ducts and determines the vectorial water movement (i.e., absorption or secretion) across cholangiocytes, thus altering ductal bile composition and flow. To achieve this notable task, biliary epithelia express an array of flux molecules located on their apical (i.e., luminal) and/or basolateral plasma membrane domains. The periductular capillary plexus (not shown) located under the basolateral cholangiocyte domain facilitates the communication of bile ducts with the systemic circulation (i.e., the cholehepatic shunt). NHE1 or SLC9A, Na^+/H^+ exchanger; NCB1 or SLC4A4, $\text{Na}^+/\text{HCO}_3^-$ cotransporter; KC, K^+ channel; NCHE, Na^+ -dependent, $\text{Cl}^-/\text{HCO}_3^-$ exchanger; NHE2 or SLC9A2, Na^+/H^+ exchanger-2; AE2 or SLC4A2, $\text{Cl}^-/\text{HCO}_3^-$ exchanger; P2U, purinergic receptors; CCC, Ca^{2+} -activated Cl^- channel; MDR1a or ABCB1, multidrug resistance protein 1a; AQP, aquaporins (i.e., water channels); GT, glutamate transporter; CFTR or ABCC7, cystic fibrosis transmembrane conductance regulator; SGLT1 or SLC5A1, Na^+ -dependent glucose cotransporter-1; ASBT or SLC10A2, apical Na^+ -dependent bile acid cotransporter; NKCC1 or SLC12A2, $\text{Na}^+/\text{K}^+/\text{2Cl}^-$ cotransporter; MRP3 or cMOAT2, or ABCC3, multidrug resistance protein 3; GLUT1 or SLC2A1, facilitated glucose transporter-1; t-ASBT, truncated ASBT; GLUT, glutathione; Glu, glucose; TCA, taurocholate. Adapted from [Lazaridis et al., 2004].

Other biological properties such as plasticity (the ability to undergo limited phenotypic change), reactivity (the ability to participate in the inflammatory reaction to liver damage), and the ability to behave as liver progenitor cells appears to be restricted to the smaller bile duct branches [Strazzabosco et al., 2005]. This functional heterogeneity of cholangiocytes is also accompanied by a morphological diversity. Under light microscopy small ductules are lined by small cuboidal cells, whereas in larger bile ducts cholangiocytes become progressively larger and more columnar in shape, ranging from 6 to 15 μm in height (Fig. 1.8 A & B) [Roberts et al., 1997]. Ultrastructurally no difference exists among cholangiocytes lining small or large bile ducts [Alpini et al., 1988]. Cholangiocytes lining a typical bile duct show apical and basolateral domains easily distinguished by features such as apically oriented vesicles and tight junctions and numerous apical microvilli (Fig. 1.8 C & D) [Roberts et al., 1997]. Cholangiocytes also have primary cilia extending from the apical plasma membrane into the ductal lumen [Bogert and LaRusso, 2007]. Studies have confirmed a mechano-sensory function of cholangiocyte cilia linking ductal bile flow to intracellular signalling via Ca^{2+} and cAMP, and will be discussed in later chapters.

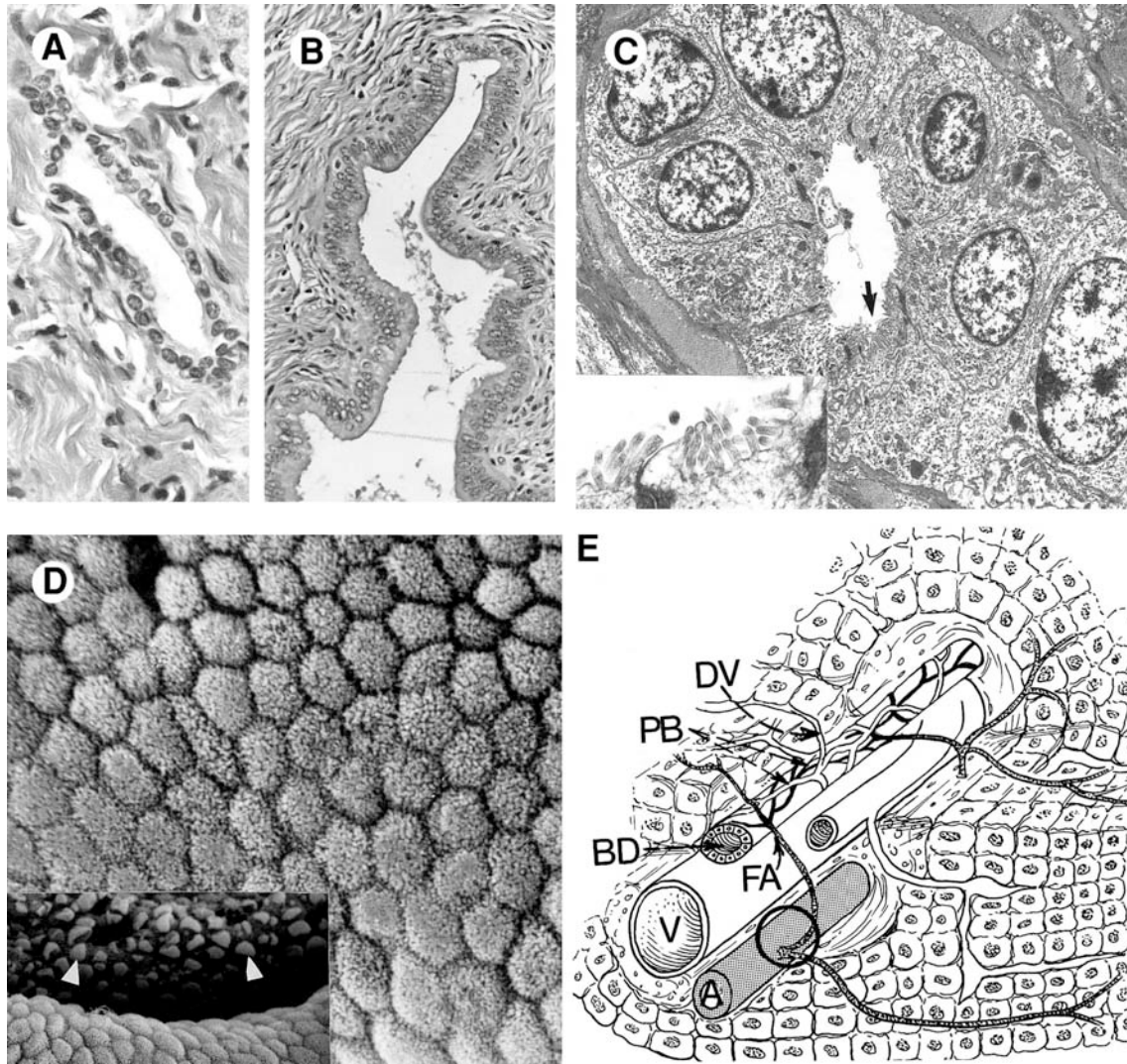


FIGURE 1.8 Normal human bile duct morphology. (A) Interlobular bile duct lined by cuboidal cholangiocytes. The accompanying hepatic artery (a) and portal vein (v) radicles are not visible in this particular frame (H&E). (B) Septal bile ducts lined by columnar cholangiocytes (H&E). These ducts are fed by two or more interlobular bile ducts as is shown in (A). Note that in both frames the ducts appear empty. (C) Transmission electron micrograph of interlobular bile duct. Note microvilli in the lumen of the duct (arrow). (Inset) Close-up view of microvilli. (D) Scanning electron micrograph of cholangiocytes lining the common bile duct. Each cell is delineated by a groove. Note the uniformly distributed microvilli on the surface of each cholangiocyte. (Inset) View into a choledochal lacuna showing mucus secretion (arrowheads) by cholangiocytes. (E) Schematic drawing of the peribiliary vascular plexus (PBVP). DV, drainage vein for PBVP; FA, feeder artery for peribiliary vascular plexus; PB, portal branch (original magnification: A, 400x; B, 100x; C, 1400x; inset, 6300x; D, 3000x; and inset, 700x). [Ludwig et al., 1989].

1.3.1 Cholangiocytes in health

In terms of bile production, the function of cholangiocytes is finely tuned to that of hepatocytes. The biliary epithelium is thus the site of rapid hormone-mediated regulation of the fluidity and alkalinity of the primary canalicular bile secreted by the hepatocytes. The net amount of fluid and bicarbonate secreted is determined by integration of pro-secretory (secretin, glucagon, VIP, acetylcholine, bombesin) and anti-secretory signals (somatostatin, insulin, gastrin, endothelin 1) [Strazzabosco et al., 2005]. The secretory functions of the biliary epithelium are also regulated paracrinally via molecules (such as bile salts, glutathione, and purigenic nucleotides) secreted by hepatocytes into the canalicular bile, and delivered to receptors and transporters located on the apical aspect of cholangiocytes [Strazzabosco, 1997]. The biliary epithelium is also involved in the reabsorption of biliary constituents, such as glucose and glutathione and in the cholehepatic circulation of bile salts [Strazzabosco et al., 2005]. In addition, bile acids can stimulate proliferation of BEC [Alpini et al., 1997; Barone et al., 2004]. On the other hand, the overflow of bile acids, as found in BA [Park et al., 1996; C.E. Tan and Moscoso, 1994a], may alter the epithelial barrier function and cause portal inflammation [Fickert et al., 2004].

Finally, cholangiocytes synthesise and secrete a number of cytokines, chemokines, growth factors, and angiogenetic factors, that likely enable the bile duct epithelium to communicate extensively with other liver cells, including hepatocytes, endothelial cells, hepatic stellate cells, portal fibroblasts, and inflammatory cells (Fig. 1.9) [Strazzabosco et al., 2000].

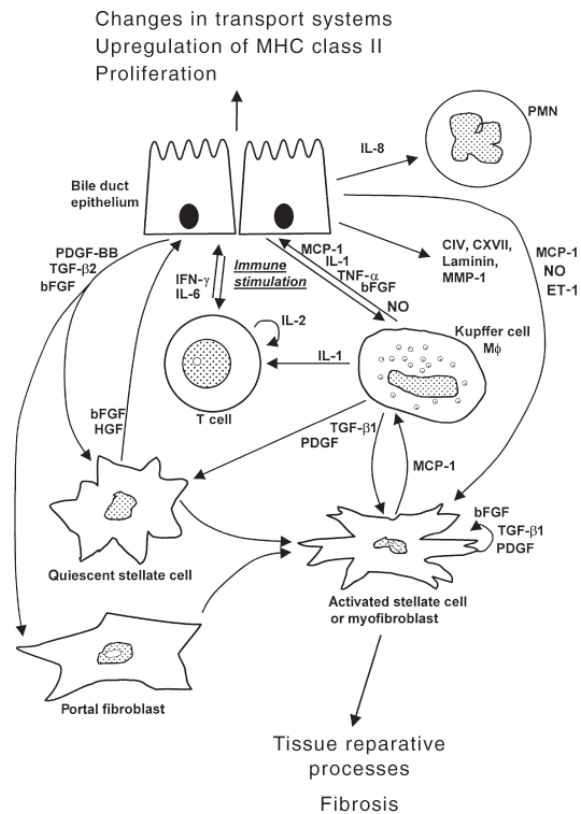


FIGURE 1.9 Theoretical scheme for paracrine communications between cholangiocytes and non-epithelial cells in the liver. Cholangiocytes synthesize and secrete a number of peptides and mediators that are likely to enable the biliary epithelium to communicate extensively with other liver cells, such as hepatic stellate cells, portal fibroblasts and inflammatory cells, by stimulating the fibrogenic response. However, peptides and mediators, either released in the portal spaces by immune cells, macrophages (M ϕ) and mesenchymal cells or produced by the epithelium itself, may have profound effects on epithelial cell function, inducing expression of molecules of MHC class II antigen expression or affecting transport properties. MCP-1, monocyte chemotactic protein-1; NO, nitric oxide; ET-1, endothelin-1; FGF, fibroblast growth factor; TGF- β 1, transforming growth factor- β 1; PDGF, platelet-derived growth factor; HGF, hepatocyte growth factor, IFN- γ , interferon-gamma; CIV, collagen IV; CXVII: collagen XVII; IL, interleukin; TNF- α , tumour necrosis factor- α ; MMP-1, matrix metalloproteinase-1; PMN, polymorphonuclear cell. Modified and adapted from Strazzabosco et al [2000].

1.3.2 Cholangiocyte function in liver disease

A derangement in the physiological processes outlined above constitutes the pathophysiological basis for cholangiopathies. From a pathophysiological perspective, common to all cholangiopathies is the coexistence of cholangiocyte death (lytic and apoptotic), cholangiolar proliferation, various degrees of portal inflammation and fibrosis, and qualitative/quantitative changes in bile production (cholestasis) [Strazzabosco et al., 2000]. These basic disease mechanisms are present, albeit to a different extent, in all kinds of cholangiopathies. Cytokines and other proinflammatory mediators released in close proximity to the biliary epithelium contribute to these processes through (a) stimulation of cholangiocyte apoptotic and proliferative responses [Sakamoto et al., 1999]; (b) activation of fibrogenic processes [Friedman, 1999]; (c) induction of damage to the peribiliary circulation, and (d) induction of histocompatibility antigen expression transport function [Strazzabosco et al., 2000].

1.3.2.1 Inflammation

Most cholangiopathies are associated with significant amounts of inflammatory infiltrates into the portal space [Strazzabosco et al., 2005]. Current views of the pathogenesis of cholangiopathies implicate the instrumental role of inflammatory mediators, cytokines and chemokines in determining most of the pathophysiological changes occurring in the biliary epithelium, from proliferation to apoptosis, cytotoxicity, cholestasis, fibrosis, and inflammation-related carcinogenesis [Marra, 2002; Spirli et al., 2003]. For example the inflammatory mediators TNF- α , IL-2, IL-4, IL-5, IL-6, and INF- γ , released into the portal

spaces by immune cells, macrophages, or mesenchymal cells have profound effects on epithelial cell function [Ayres et al., 1993; Vos et al., 1997].

However, beyond being a target for inflammatory mediators, cholangiocytes actively contribute to liver inflammation and the ensuing reparative/fibrogenic processes by secreting proinflammatory and chemotactic cytokines, and growth factors [Lazaridis et al., 2004; Strazzabosco et al., 2000]. Interestingly, these factors are not produced by normal epithelium, but by “reactive cholangiocytes”. Reactive cholangiocytes are not present in “normal livers”, but their presence is common in many forms of liver injury, especially the cholangiopathies [Strazzabosco et al., 2005]. The presence of an increased number of cholangioles (i.e. the smallest of bile ducts) at the periphery of portal spaces and parenchymal areas marked by the presence of an inflammatory infiltrate are commonly seen in many forms of liver injury and is called the “ductular reaction” [Lazaridis et al., 2004; Strazzabosco et al., 2005]. These newly formed bile ducts are composed of reactive cholangiocytes, which have abandoned their differentiated secretory epithelial phenotype. These so-called “reactive” cholangiocytes express adhesion molecules that are transiently present during ontogenesis, turn on antiapoptotic genes, and acquire the ability to produce proinflammatory and chemotactic mediators. Thus, activated cholangiocytes are likely to play an important role, not only in liver damage, but also in the progression of liver damage in chronic cholestatic syndromes [Strazzabosco et al., 2000]. As discussed below, the inflammatory reaction is central to most manifestations of the cholangiopathies, from cholestasis, fibrosis, and proliferation, to ductopenia.

1.3.2.2 Apoptosis

Ductopenia (i.e. a decrease in the number of bile ducts per portal tract) is the end result of most cholangiopathies. With the progressive disappearance of bile ducts in conjunction with portal fibrosis accounting for the majority of complications seen in cholangiopathies. Ductopenia results from a continuous immune-mediated assault to the biliary epithelium, from the combination of alloimmune and ischemic damage, or from genetic changes in mechanisms signalling lateral specification [Lazaridis et al., 2004; Strazzabosco et al., 2005]. The exact mechanisms by which cholangiocytes die are not well known, but may be due to lytic or apoptotic cell death [Alpini et al., 2002b].

Cholangiocyte apoptosis does occur physiologically and has a role in ontogenesis during ductal plate regression, as previously described [Strazzabosco et al., 2005]. Apoptotic mechanisms also contribute to tissue regression after induced biliary hyperplasia (e.g. disappearance of proliferating ducts following the relief of biliary obstruction) [Bhathal and Gall, 1985]. It is currently believed, that under normal homeostatic conditions there is a balance between apoptosis of senescent and damaged/abnormal cholangiocytes, and the proliferation of new cholangiocytes [Lazaridis et al., 2004]. In light of this, ductopenia could be considered to result primarily from excessive apoptosis that dominates over cholangiocyte proliferation [Celli and Que, 1998]. However, this remains a difficult question to address, because apoptosis is a transient phenomenon and apoptotic cells may be eliminated by shedding into the bile duct lumen [Strazzabosco et al., 2000].

1.3.2.3 Proliferation

Cholangiocytes maintain latent mitotic capabilities throughout adult life, and actively proliferate following a number of liver injuries resulting in what is referred to as “ductular reaction” [Strazzabosco et al., 2000]. Proliferation of cholangiocytes and subsequent distortion of the biliary tree architecture is an important step in the development of chronic liver damage, as ductular reaction is considered to be the pacemaker of portal fibrosis [Desmet et al., 1995; Lazaridis et al., 2004]. In the early stages of many cholangiopathies, destruction of interlobular bile ducts is associated with a vigorous proliferation of bile ductules in a variety of patterns at the periphery of portal spaces. Elucidation of the mechanisms responsible for cholangiocyte proliferation has been the subject of extensive investigation [Alvaro et al., 2000b; Melero et al., 2002]. In general, any stimuli increasing intracellular cAMP content facilitates cholangiolar proliferation [Alvaro et al., 2000b]. A number of growth factors, such as epidermal growth factor (EGF), hepatocyte growth factor (HGF), and 3-iodo-thyronine (T₃) have been shown to stimulate cholangiocyte growth *in vitro* (Table 1.3) [Lazaridis et al., 2004; Matsumoto et al., 1994]. The list of stimulators of cholangiocyte proliferation also includes some bile salts [Alpini et al., 2002a], cytokines such as IL-6 [Yokomuro et al., 2000], and hormones such as oestrogens (Table 1.3) [Alvaro et al., 2002a; Alvaro et al., 2000a]. The ability of oestrogens to stimulate cholangiocyte proliferation has many important pathophysiologic implications for a number of cholangiopathies from PBC and primary sclerosing cholangitis (PSC), to liver cyst growth in autosomal dominant polycystic kidney disease (ADPKD) [Alvaro et al., 2002b; Chapman, 2003].

TABLE 1.3 Regulation of cholangiocyte proliferation

	STIMULATION	INHIBITION
Cytokines/growth factors	IL-1 α , IL-6 α , TNF- α , EGF, HGF, IGF-1	TGF- β 1, TGF- β 2
Hormones/neuropeptides	Oestrogens, Ach, PTHrP	Somatostatin, Gastrin
Bile salts	LCA, TLCA, TCA	UDCA, TUDCA

IL=interleukin; TGF=transforming growth factor; TNF=tumour necrosis factor; EGF=epidermal growth factor; HGF=hepatocyte growth factor; IGF=insulin-like growth factor; ACh=acetylcholine; PTHrP=parathyroid hormone-related peptide; LCA=lithocholate; TLCA=tauroolithocholate; TCA=taurocholate; UDCA=ursodeoxycholate; TUDCA=tauroursodeoxycholate. Table taken from Alvaro et al [2000b].

1.3.2.4 Portal fibrosis

A complex interplay of signals between reactive cholangiocytes, inflammatory cells, mesenchymal cells and extracellular matrix components, polypeptide growth factors, cytokines, and other soluble mediators regulates portal fibrosis. Progressive disappearance of bile ducts, in conjunction with extensive portal fibrosis, contributes to most of the pathophysiologic implications of cholangiopathies. Fibrogenesis is a dynamic process that depends on the extent and duration of cholangiocyte damage. Several lines of evidence indicate that reactive cholangiocytes play an important role in initiating and modulating the response of a multiplicity of mesenchymal cells, as well as hepatic stellate cells (HSCs), the main connective tissue producing cells in the liver. During tissue repair HSCs undergo activation from a quiescent to a highly proliferative myofibroblastic phenotype resulting in increased synthesis of collagen types I and III [Lazaridis et al., 2004; Pinzani et al., 1998].

These mechanisms have mostly been studied in experimental models of obstructive cholestasis (such as ligation of the common bile duct in rat) [Alpini et al., 1998]. Indeed, chronic obstructive cholangiopathies are characterised by rapid appearance of an important portal fibrosis, as in BA [Perlmutter and Shepherd, 2002]. However, it remains unclear whether the changing epithelial phenotype directly induces an alteration of the mesenchymal cells or if the changes in the extracellular matrix induces the phenotypic shift in the biliary epithelium [Strazzabosco et al., 2000].

1.3.2.5 Cholestasis

Consistent with the role of cholangiocytes in bile production, cholestasis is a prominent clinical manifestation in cholangiopathies. Most frequently, cholestasis is the effect of immune-mediated toxic, or inflammatory damage to the biliary epithelium resulting in fibro-inflammatory obliteration of bile ducts. In other cases, cholangiocyte cholestasis may originate from an impaired fluid secretion caused by mutations in transport proteins, or by inflammatory mediators as the primary event that exposes the biliary epithelium to further damage [Strazzabosco et al., 2005]. Extrahepatic obstructions to bile outflow, as in BA, induces the retention of biliary constituents and triggers important pathophysiologic changes in cholangiocytes that promote the rapid appearance of significant liver fibrosis [Strazzabosco et al., 2000]. Retention of bile salts is another mechanism able to cause dramatic changes in biliary epithelial barrier function, also able to promote hepatocyte apoptosis and necrosis resulting in hepatocellular cholestasis [Lazaridis et al., 2004; Trauner et al., 1998].

1.3.2.6 Altered development

A number of cholangiopathies are caused by an altered development of the biliary tree. The common pathological features of this group of diseases are the presence of ductal plate remnants, von Meyenburg complexes, biliary cysts, and in some cases intense fibrosis. Disorders characterised by abnormalities of the biliary tree that can be interpreted as sequelae of persistence of the ductal plate beyond embryonic and foetal life are not limited to the cholangiopathies. Classed together as the DPM [Desmet, 1992a; Desmet, 1992b; 1998], at least ten heritable disorders, some of which are defined only phenotypically are recognised (Appendix 1, Table 1.1). As seen in the cholangiopathies, they include circumferentially disposed bile ducts at the margin of the portal tract (that is, not separated from hepatocytes by connective tissue), increased numbers of bile duct profiles with connective contours, ectasia of bile duct lumina, and lack of bile ducts or portal venules within portal tracts. It must be noted, not all features are present in every disorder, nor need to be present in every portal tract [Knisely, 2003].

1.4 THE CILIOPATHIES

Cystic diseases of the liver and kidney are a clinically important and genetically diverse group of disorders that share in common altered regulation of tubular morphology. Among them can be listed the hepatorenal fibrocystic syndromes, and disorders associated with altered development of the ductal plate (Appendix 1, Table 1.1). The hepatorenal fibrocystic (HRFC) syndromes are a heterogeneous group of severe monogenic conditions that may be detected before birth. Commonly presenting in the neonatal and paediatric age, HRFC syndromes consistently include developmental abnormalities mostly involving the liver and

kidneys. The changes include the proliferation and dilatation of epithelial ducts in these tissues with abnormal deposition of extracellular matrix. Included within this group of syndromes are autosomal recessive polycystic kidney disease, nephronophthisis (NPHP), Meckel-Gruber syndrome (MKS), Bardet-Biedl syndrome (BBS), and Jeune asphyxiating thoracic dystrophy. Despite their clinical and pathological heterogeneity, the fact that these disorders result in a similar outcome – dilated tubules or cysts – led to the naïve assumption that the gene defect in each of these disorders must somehow disrupt a common pathway [Watnick and Germino, 2003]. However, the observation that many of the genes responsible for various cystic diseases encode proteins that localise to subcellular compartments including focal adhesions, adherens junctions, cilia, basal bodies, centrosomes, and the mitotic spindle has resulted in many hypotheses on the mechanisms of cystogenesis based upon these subcellular localisations. Among them are (i) the mechanosensory hypothesis of renal cilia function, (ii) participation in signalling at focal adhesions and adherens junctions, (iii) a role in the maintenance of planar cell polarity (PCP) within the noncanonical Wnt signalling pathway, and (iv) a role in centrosome-related functions of cell cycle regulation [Hildebrandt and Zhou, 2007]. The ciliary hypothesis has however evolved as the unifying concept of cystogenesis and revolutionised studies into the pathogenesis of many apparently unrelated genetic disorders. The “ciliary/centrosome” hypothesis of renal cystic disease and related disorders states that virtually all proteins that are mutated in renal cystic disease in humans, mice, or zebrafish (“cystoproteins”) are part of a functional module, as defined by their subcellular localisations to primary cilia, basal bodies, or centrosomes [Igarashi and Somlo, 2003; Watnick and Germino, 2003]. This applies to polycystin-1 and -2;

fibrocystin/polyductin; nephrocystin-1, -2 (inversin), -3, -4, and, -5; Bardet-Biedl associated proteins; cystin; polaris; ALMS1; and many others (Fig. 1.10) [Hildebrandt and Zhou, 2007].

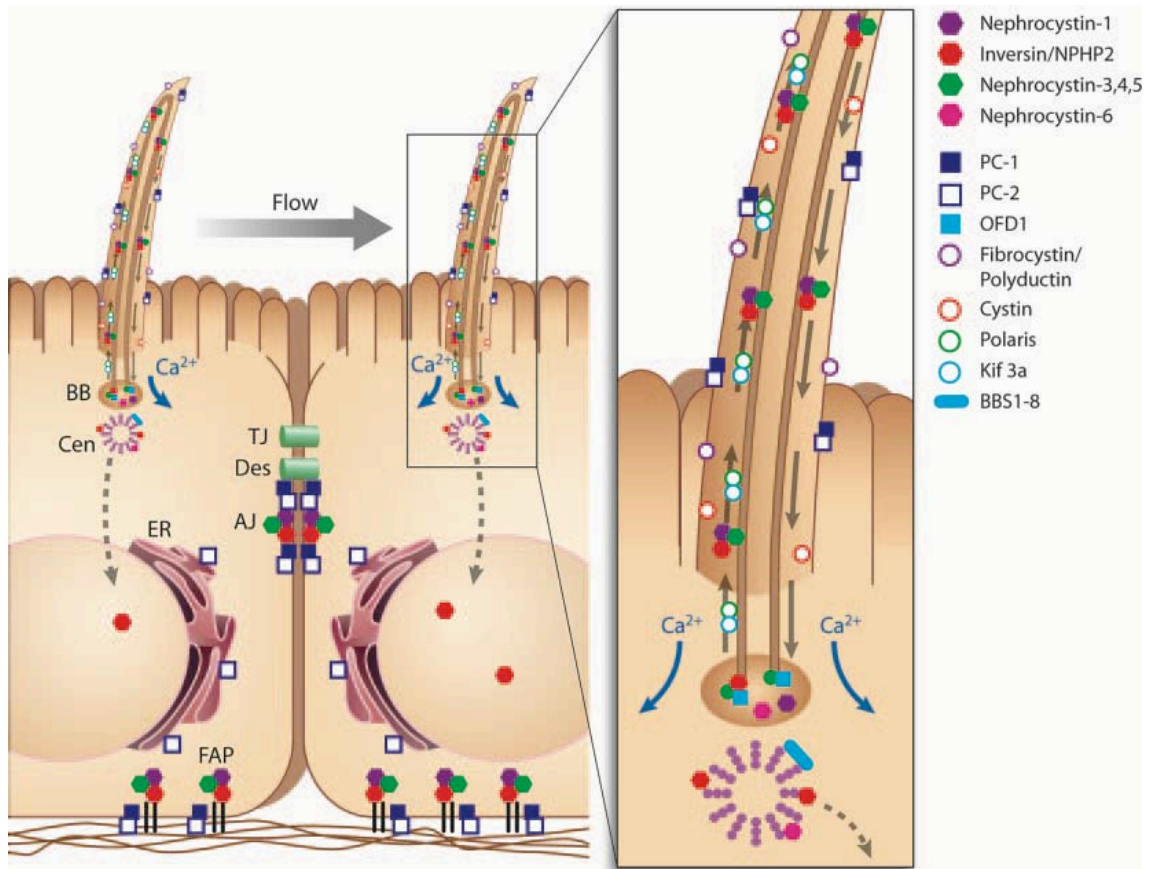


FIGURE 1.10 Cystoproteins are proteins of genes that are mutated in cystic kidney diseases of humans, mice, or zebrafish. They share the common feature of expression in primary cilia, basal bodies, or centrosomes. Depending on cell-cycle stage, some cystoproteins localise to adherens junctions or focal adhesions. Many cystoproteins have been localised to more than one intracellular domain. AJ, adherens junction; BB, basal body; Cen, centriole; ER, endoplasmic reticulum; FAP, focal adhesion plaque; TJ, tight junction; PC-1, polycystin-1; PC-2, polycystin-2. Taken from Hildebrandt and Zhou [2007].

Disorders caused by mutations in genes encoding ‘cystoproteins’ are collectively termed “ciliopathies”. Ciliopathies can either involve single organs or can occur as multisystemic disorders with phenotypically variable and overlapping disease manifestations [Fliegauf et al., 2007]. A non-exhaustive list of ‘classical’ ciliopathies includes polycystic kidney disease (PKD), retinal degeneration, laterality defects, chronic respiratory problems, *situs inversus*, hydrocephalus, and infertility. More recently, the discovery of other syndromes such as BBS and MKS, has extended the list of cilia related phenotypes to include obesity, diabetes, liver fibrosis, hypertension, heart malformations, sensory deficits (anosmia, hearing impairment), skeletal, neurological and developmental anomalies [Inglis et al., 2006].

To appreciate how a single organelle, and its associated proteins can result in such a vast array of phenotypes, a basic understanding of this fascinating structure is invaluable.

1.4.1 An overview of the cilium

Cilia are ancient, evolutionarily conserved microtubule-based hair-like organelles that typically project from the apical surface of almost all cell types in the human body [Badano et al., 2006; Fliegauf et al., 2007]. Although these highly conserved structures are found across a broad range of species, a nearly ubiquitous appearance is observed only in vertebrates [Fliegauf et al., 2007]. Cilia can be structurally divided into subcompartments that include a basal body, transition zone, axoneme, matrix, ciliary membrane, and the ciliary tip (Box 1).

Box 1 Ciliary subcompartments

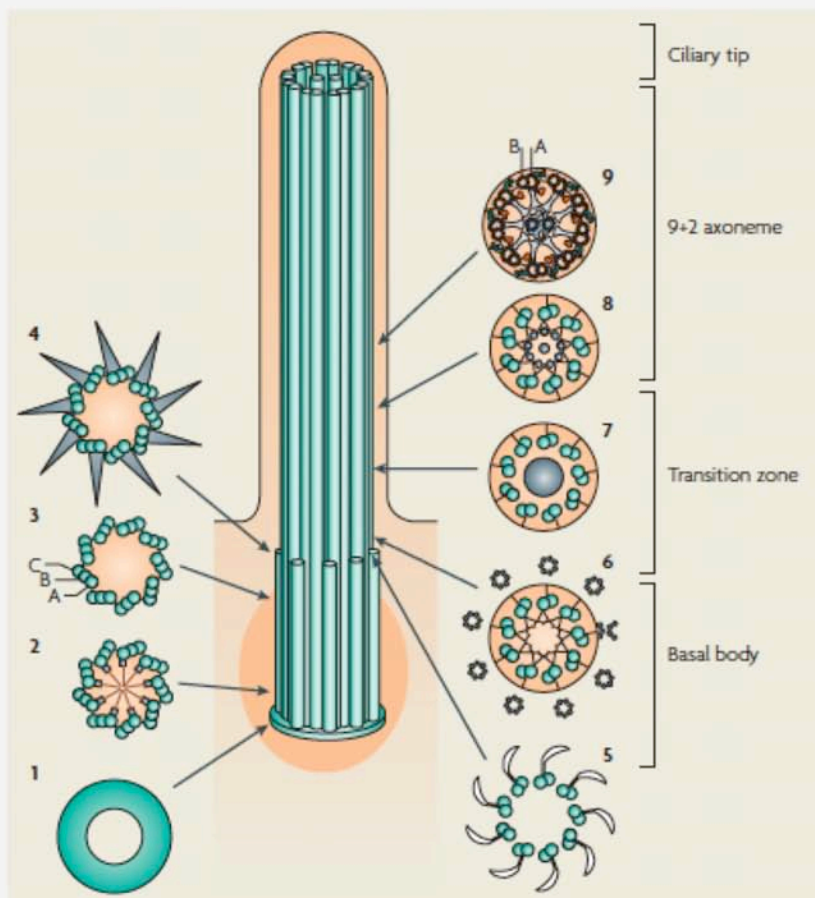
The **ciliary tip** harbours the microtubule plus (+) ends (from which axonemes grow) and the switch between the anterograde (kinesin) and retrograde (dynein) intraflagellar transport (IFT) motors. It contains signalling molecules and can undergo morphological changes in response to signalling processes.

The **axoneme** (part 9) is the structural core of a cilium (without a membrane or soluble material). Its peripheral microtubule doublets, comprising an A- and a B-tubule, are continuous with the microtubules at the transition zone. The doublets are connected by nexin links and are held in place by radial spokes that extend into the axonemal centre. In motile cilia, inner and outer dynein arms are attached to the A-tubules and mediate ciliary bending by reversibly binding to the neighbouring B-tubule. A sheath surrounds the central microtubule pair. The radial spoke-central pair is involved in beat regulation.

The **transition zone** (parts 5-8) converts the triplet microtubular structure of the basal body into the axonemal doublet structure. Proximal transition fibres (parts 4 and 5) connect each microtubule doublet (without dynein arms) to the membrane and mark the compartment border at which IFT proteins accumulate. The distal part contains stellate fibre arrays (parts 6 and 8) and an amorphous disk structure (part 7) and gives rise to the central microtubules in 9+2 axonemes. The transition zone might contain a gate that controls access to the ciliary compartment.

The **basal body** (parts 1-4) of each cilium is a specialized centriole (9x3 microtubular structure; the tubules of one triplet are depicted as A, B, and C in part 3) embedded in pericentriolar material (dark orange) with a proximal amorphous disc (part 1), a cartwheel structure (part 2), a middle piece that lacks appendages (part 3) and transition fibres at the distal end (part 4). In most quiescent cells, the centrioles move to the apical plasma membrane and the mother centriole functions as the microtubule-organising centre to nucleate the axonemal microtubules. The daughter centriole remains perpendicular to the mother centriole. In multiciliated cells, centriolar replication is required first.

The **ciliary membrane** is continuous with the plasma membrane but contains specific signalling molecules that are essential for the function of cilia as antennae. IFT rafts move between the ciliary membrane and the peripheral microtubules and carry membrane anchors. [Fliegauf et al., 2007]



The basal body (Box 1) is a specialised centriole that serves as the foundation upon which the cilium is constructed. Consisting of nine sets of helically arrayed tubulin-based triplet microtubules (MTs) (9x3 structure), this hollow cylinder lies embedded within pericentriolar material. In most quiescent cells, the two centrioles that together constitute the centrosome move to the apical plasma membrane, and the mother (inherited) centriole functions as the microtubule organising centre (MTOC) to nucleate the axonemal MTs. The daughter (newly synthesised) centriole remains perpendicular to the mother centriole [Fliegauf et al., 2007].

The transition zone (Box 1) refers to the junction of the basal body and the ciliary axoneme, where the triplet microtubular structure of the basal body converts into the characteristic doublet microtubular structure of the axoneme. Demarcated by Y-shaped transition fibres connecting each MT doublet to the ciliary membrane. The transition zone is proposed to contain a ciliary-pore complex that marks the compartment border at which access, import and export of cilia-specific proteins from the cytoplasmic compartment to the ciliary compartment, is controlled [Fliegauf and Omran, 2006].

The axoneme (Box 1) is the underlying structural scaffold of the cilium, comprised of a cylindrical array of nine peripheral MT doublets nucleated directly by the MTs found in the basal body. In 9+2 cilia, the nine doublet MTs surround a central pair of singlet MTs; 9+0 cilia lack this central pair of MTs. Protein complexes known as radial spokes run inwards from the outer doublets to interact with the central pair, when present. Inner and outer

dynein motors that power ciliary movement are attached to the outer doublets in a precise geometry that allows them to generate a bending force [Marshall and Nonaka, 2006].

Another component is the matrix, the fluid phase between the axoneme and the membrane that contains the intraflagellar transport machinery necessary to assemble and maintain cilia, as well as axonemal subunits being transported by this machinery. The matrix may also contain factors involved in signal transduction via second messenger systems [Marshall and Nonaka, 2006].

The ciliary membrane, although continuous with the cell membrane, is both structurally and functionally distinct [Eley et al., 2005]. Containing many receptors and channels that are essential for the function of cilia as sensory antennae.

The ciliary tip complex (Box 1) harbours the MT plus ends, which are bound to the ciliary membrane by capping structures. The tip of the cilium is thought to also contain a set of unique proteins related to intraflagellar transport (IFT) function, as many IFT-related processes are restricted to the cilium tip, and the switch between the anterograde (kinesin) and retrograde (dynein) IFT motors [Fliegauf et al., 2007; Sloboda, 2005].

1.4.1.1 Constructing the cilium

In contrast to other cell organelles, cilia are only assembled when cells exit the cell cycle from mitosis into a stationary or quiescent and/or differentiated state. Formation of most cilia begins when the basal body docks to the plasma membrane and serves as the template for MT nucleation and axoneme assembly. The axoneme and the surrounding ciliary membrane projects out of the cell body, elongates and forms a compartment, the boundary of which is marked by the transition fibres, in a process referred to as compartmentalised ciliogenesis [Fliegauf and Omran, 2006]. The ciliary axoneme elongates by adding new material at the distal tip [K. A. Johnson and Rosenbaum, 1992; Rosenbaum and Child, 1967], this assembly at the tip does not cease when the cilium reaches its final length, but continues to occur. The fixed length is maintained by continuous turnover at the tip [Marshall and Rosenbaum, 2001; Stephens, 1997]. Because the cilium lacks ribosomes, all proteins required for axoneme assembly, maintenance, and function must be transported from their site of synthesis in the cell body [Marshall and Nonaka, 2006]. This is achieved by the targeting of these specific proteins to the basal body area where pre-assembly of axonemal substructures (such as outer dynein arms) occurs [Fowkes and Mitchell, 1998]. The transport of proteins and multiprotein precursors across the ciliary compartment border and along the length of the axoneme to their functional site is dependent on IFT, the bidirectional movement of particles along the ciliary axoneme on raft-like transport structures [Rosenbaum and Witman, 2002].

Because cilia are devoid of protein synthesis, IFT is thought to be the sole mechanism of protein transportation to the axoneme for, cilia assembly, maintenance and function. Recent studies at the Mayo clinic [Hogan et al., 2009] have however uncovered a possible additional

mechanism for the delivery of proteins to the ciliary axoneme involving the multivesicular body (MVB) sorting pathway. Urinary exosomes are thought to be end products of the MVB-sorting pathway in which membrane proteins are uniquely packaged into intraluminal vesicles within the MVB, some of which are secreted as exosomes when MVBs fuse with the apical plasma membrane [Hyams et al., 1985]. MVBs and exosomes are thought to have a role in left/right axis determination in the embryonic node, released from the floor of the node and swept by nodal flow to the left side where they interact with the “picket-fence” immotile cilia [Tanaka et al., 2005]. This unifies the disparate localisation of many proteins implicated in ciliopathies, those not having a ciliary or centrosomal localisation. Thus, raising the possibility of a novel form of “urocrine” and perhaps “bilocrine” signalling, fostering IFT independent communication along the length of the nephron/biliary tree [Hogan et al., 2009].

1.4.1.2 Classification of cilia

Cilia can either be motile or immotile. Based on whether the axoneme has a 9+0 or a 9+2 structure, cilia have previously been referred to as primary cilia (immotile monocilia) or motile cilia, respectively [Fliegauf and Omran, 2006]. However, owing to numerous exceptions to this definition, the distinction of cilia into four subtypes is more appropriate, although at least eight categories of cilia or cilia-derived organelles exist in the human body upon more stringent categorisation (Fig. 1.11) [Afzelius, 2004]. All of which have been associated with human disease [Fliegauf et al., 2007].

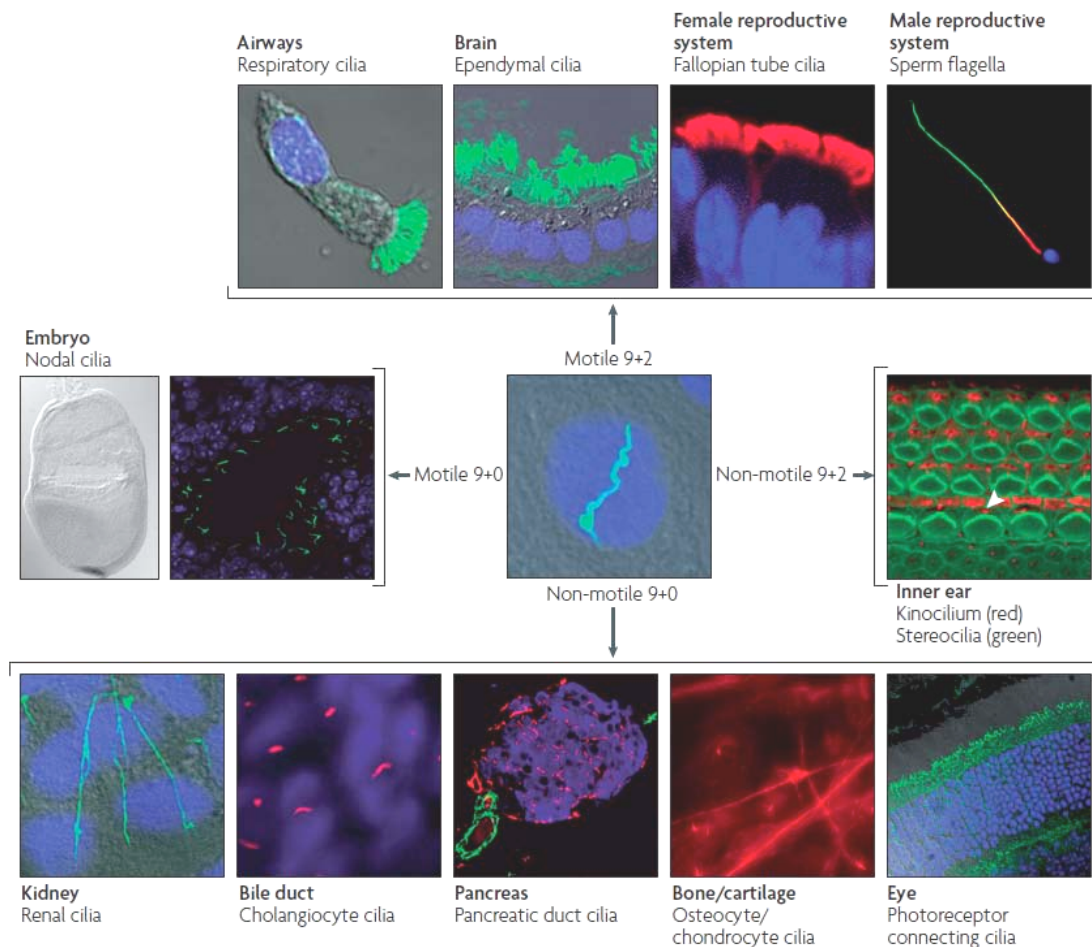


FIGURE 1.11 Ciliary categories. A monociliated cell is shown in the centre. Motile monocilia (9+0 axoneme, middle left panels) are found at the embryonic node and generate the nodal flow that is essential for determination of left-right body asymmetry. Multiple motile cilia (9+2 axonemal structure, top panels) that transport extracellular fluid along the epithelial surface are located on respiratory epithelial cells, brain ependymal cells and epithelial cells lining the fallopian tubes. The sperm flagellum (top right panel; co-stained with antibodies against the dynein heavy chain DNAH5, red) represents a specialised, elongated motile cilium (9+2) that confers motility. Non-motile monocilia (9+0, bottom panels) extend from the surface of most quiescent cells of the body and sense environmental signals such as fluid flow and/or fluid composition. Well-known examples are the monocilia of the tubular epithelia of the kidney, and the epithelia of the bile duct and pancreatic ducts. The chondrocyte and osteocyte monocilia probably function to sense the amount of strain on bones. The connecting cilia of photoreceptor cells are specialised non-motile cilia (9+0) that connect the inner and outer segments. Non-motile 9+2 cilia (middle right panel) are found in the inner ear (kinocilium, red, arrowhead; stereocilia, green). Besides the four cilia types shown, there might be a high variability of the axonemal structures within vertebrates. In all panels, axonemes were stained (red or green) by indirect immunofluorescence using an antibody against the cilia-specific acetylated α -tubulin isoform. Nuclei were stained using Hoechst or 4',6-diamidino-2-phenylindole (DAPI). Figure taken from [Fliegauf et al., 2007]

Histologically, motile 9+2 cilia have been the most studied of all cilia. Normally concentrated on the cell surface in large bundles that consist of 200-300 individual organelles (multiple cilia), motile cilia beat in an orchestrated wave like fashion. And are involved in fluid and cell movement such as mucociliary clearance in the lung, cerebrospinal fluid movement in the brain, and ovum and sperm transport along the respective reproductive tracts [J. R. Davenport and Yoder, 2005]. The primary or immotile 9+0 cilium is generally considered to be immotile because it lacks the central microtubule pairs, radial spokes, and the dynein apparatus needed to generate force. When visualised by video microscopy, the cilium shows only Brownian movements, i.e. small fast movements induced by thermal energy. An exception to the lack of motility of the 9+0 cilium is the specialised motile 9+0 primary cilium, the nodal cilium in the blastocyst, which does have radial spokes and dynein arms but lacks the central pair of MTs [Praetorius and Spring, 2005]. Instead of beating from side to side as does the motile 9+2 cilia, nodal cilia exhibit a characteristic propeller-like movement that is responsible for the nodal flow crucial for the development of left-right sidedness in the developing embryo [Nonaka et al., 1998].

1.4.1.3 The primary cilium

The primary cilium is a solitary, nearly ubiquitous organelle in vertebrates [Pazour and Witman, 2003]. It has been found on most vertebrate cells that have been carefully examined; epithelial cells such as the kidney tubule, the bile duct, the endocrine pancreas, and the thyroid but also on nonepithelial cells such as chondrocytes, fibroblasts, smooth muscle cells, neurons, and Schwann cells (Fig. 1.11) [Satir and Christensen, 2007]. The most important exceptions are cells of myeloid and lymphoid origin, and the intercalated cells of the kidney

collecting duct [Praetorius and Spring, 2005; Wheatley, 1995]. The near ubiquity of cilia in human tissues and through eukaryotic biodiversity suggests that they must perform important functions that have been subject to evolutionary selection [Marshall and Nonaka, 2006]. However, in spite of this near ubiquity, the function(s) of vertebrate primary cilia are very poorly understood. Since the discovery of these organelles in 1898 [Zimmerman, 1898], three major hypotheses for their function have been put forward. The first is that they are merely vestigial organelles inherited from an evolutionary ancestor whose cells had motile cilia, and that they now have no purpose [Sorokin, 1962]. However, the enormously complicated structure, and complexity of its protein composition, which has been shown to comprise of roughly 250 distinct proteins, argues against this hypothesis. It would not be evolutionarily or biologically efficient to invest such high-energy expenditure into a vestigial organelle. A second hypothesis is that they are involved in controlling the cell cycle [Tucker et al., 1979a]. Primary cilia are intimately connected to the same centrioles that serve to organise the mitotic spindle. Furthermore, although not required for a cell cycle the presence of the primary cilia is coordinated with the cell cycle [Pazour and Witman, 2003; Tucker et al., 1979a]. The third hypothesis implies cilia are sensory organelles [Poole et al., 1985; Wheatley et al., 1996]. This hypothesis is based on the fact that cilia are clearly used as sensory organelles in lower eukaryotes, and that the sensory structures of the vertebrate visual and olfactory systems are modified cilia. This is a hypothesis that is not incompatible with a role in cell cycle control [Pazour and Witman, 2003].

This poses the question: why use a cilium as a sensory organelle? A surprisingly large number of receptor proteins are localised mainly within cilia. Clearly, cells benefit by projecting a

sensory compartment like a probe into the surrounding fluid. It is a well-known principle of fluid mechanics that any fluid immediately adjacent to a surface, such as the cell membrane, will be immobile and thus poorly mixed even when the surrounding media is flowing by the surface. Moreover, many cells are encrusted with a glycocalyx that extends beyond the reach of a membrane-embedded receptor, thus producing a microenvironment around the receptors that differs from the true chemical environment of the media [Marshall and Nonaka, 2006]. Cells may therefore obtain a more accurate reading of chemical composition and fluid velocity by extending receptors away from the cell surface. The high flexural rigidity of the axoneme makes the primary cilium an ideal choice for such a whisker-like probe [Marshall and Nonaka, 2006].

Another rationale for the evolutionary use of primary cilia for sensing may be signal processing. The high surface to volume ratio of the cilium makes it an ideal compartment for signal transduction by second messenger generation. A relatively small number of active receptors on the surface would produce an extremely high concentration of second messengers in the ciliary matrix, compared with the same number of receptors acting in the much more voluminous cytoplasm [Marshall and Nonaka, 2006].

1.4.2 Pathogenetic mechanisms relevant to the ciliopathies

While the existence of primary cilia has been known for more than a century, the interest of biomedical scientists in these organelles has increased only recently, providing the experimental evidence to support the hypothesis that primary cilia have an important sensory

role. Three critical observations have been made in only the last six years: (i) that primary cilia in the node of gastrulation-stage embryos are essential for the determination of left-right asymmetry of the body [Marshall and Nonaka, 2006; McGrath et al., 2003]; (ii) that the two most frequent lethal genetic disorders (i.e. ADPKD and ARPKD), both characterised by progressive cyst development in the kidney, liver, and pancreas, are cilia-related diseases [T. V. Masyuk et al., 2004a; Tahvanainen et al., 2005]; and (iii) that Bardet-Biedl syndrome (patients with this syndrome have kidney failure, lose their eyesight, are obese, and develop diabetes) is a ciliary-related disease caused by mutations in genes that determine ciliary structure and functions [Pan et al., 2005; Vogel, 2005]. It has therefore become apparent that primary cilia are functionally important organelles that are involved in both normal developmental and pathologic processes. Primary cilia themselves may have a different composition or ultrastructure in different cell types thus potentially accounting for the array of phenotypes representing the ciliopathies when ciliary structures are mutated. The most relevant established and emerging functions of the single, immotile primary cilia in relation to this project are described below, along with their potential pathophysiological role in the “classical” ciliopathies.

1.4.2.1 The renal phenotype of ciliary dysfunction

In considering a role for the primary cilia in the renal cystic phenotype, the exact nature of a cyst must be considered. It is now well accepted that cell proliferation is an essential component of cyst formation; however, it is not clear what drives this proliferation. It seems likely that for fully functional patent tubules to form, renal tubules need to undergo a highly regulated morphologic structuring that coordinates tubular elongation with tubular

expansion. It is therefore a certainty that there is an ideal diameter for the tubule to perform optimally, and that this is a regulated process in the developing and adult kidney, perhaps allowing the tubule to adapt to varying luminal flow rates and pressure gradients. If the cues for regulating tubular diameter are lost by mutation, the tubule may begin to lose morphology, transforming into a cyst. It is theoretically acceptable that cystic epithelial cells do not dedifferentiate completely; instead they lose their sense of being a tubule and revert to what is essentially an epithelial sheet at first. It has therefore been speculated that the primary cilia functions to measure luminal flow rates, or a lack thereof, and thus regulate tubule diameter by generating signals that the cells interpret as morphologic cues.

The concept that defective cilia are the principal cause of PKD, originated with the discovery that the causative gene mutated in the Oak Ridge polycystic kidney (orpk) ARPKD mouse model, encoding polaris, is homologous to an IFT gene essential for ciliary assembly in *Chlamydomonas*, IFT88 [Pazour et al., 2000]. IFT mutant *Tg737^{orpk}* mice develop progressive kidney and pancreatic cysts as well as abnormalities involving the hepatic bile ducts [Cano et al., 2004; Q. Zhang et al., 2005]. Indeed, scanning electron microscopy of the kidneys revealed that the renal epithelia was unable to assemble normal primary cilia [Pazour et al., 2000]. Taken together, this strongly suggested that ciliary dysfunction affects the morphogenesis and integrity of kidney, liver, and pancreas. All three organs contain similar functional units, tubular systems that transport urine, bile fluid, or pancreatic secretions respectively; monocilia extend into the lumen of each. A clear interpretation from these studies is that mechanotransduction via the primary cilium is necessary for continued normal

function, and cellular differentiation of the tubule epithelium, and that loss of the cilium leads to abnormal function, abnormal cell division, and PKD.

Interestingly, many mutations that cause PKD are not found in genes that encode IFT proteins or the molecular motors involved in constructing the cilium. In humans, all cases of ADPKD are caused by mutations in *PKD1* and *PKD2*, which encode integral membrane proteins polycystin-1 (PC-1) and polycystin-2 (PC-2), respectively [Nauli et al., 2003]. PC-1 and PC-2 are known to heterodimerise and normally also localise to the primary cilium of human renal epithelial cells [Hanaoka et al., 2008; A. I. Masyuk et al., 2006]. PC-1, a cell surface receptor activates a G-protein signalling pathway, which in turn, modulates the functions of the calcium-permeable cation channel PC-2 [Nauli et al., 2003].

1.4.2.2 The mechanosensory hypothesis

In 1997, Bowser and co-workers [Schwartz et al., 1997] provided the evidence that the structural properties of the primary cilium were appropriate for the detection of a range of bending forces present in renal tubule lumen. Using a cultured renal cell line (PtK₁) they showed that the primary cilium of these cultured cells was able to bend when the cells were superfused to flow rates comparable to those seen in renal tubules (Fig. 1.12).

In 2001, Praetorius and Spring [2001], devised an elegant experimental procedure to test whether bending of the cilium itself was able to produce an intracellular response. Using the

Madin Darby canine kidney (MDCK) cell line and a suction pipette to bend the cilium to avoid disturbing putative cell membrane flow sensors they were able to show bending of the cilium causes a substantial increase in intracellular calcium levels (Fig. 1.13). They were also able to show that the calcium signal was able to spread as a wave from intracellular calcium stores from the perturbed cell to its neighbours by diffusion of a second messenger through gap junctions. Pointing towards flow sensing as a coordinated event within the tissue, such as the renal tubule lumen, rather than an isolated phenomenon in a single cell. The flow response observed was also proven by Praetorius and Spring [2002] to be absolutely dependent on the presence of a primary cilium, because immature cells that do not present a primary cilium or cells from which the cilium was removed by chloral hydrate treatment did not respond to increasing flow rates by increasing their intracellular calcium levels [Praetorius and Spring, 2002].

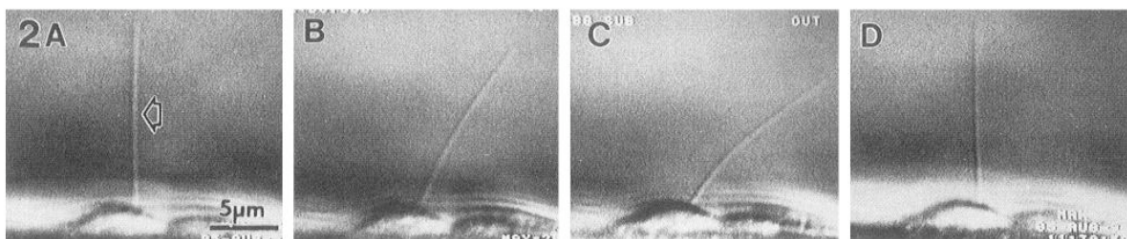


FIGURE 1.12 Representative time sequence of primary cilia bending in response to fluid shear. Under conditions of zero flow primary cilia of the rat kangaroo kidney epithelial cells were perpendicular and straight (A). Upon exposure to low levels of shear, the cilia passively bent in the direction of flow (B). As flow increased, the degree of cilium bending increased considerably (C). When flow stopped, the cilia returned to their original, straight, perpendicular position (D). [Schwartz et al., 1997].

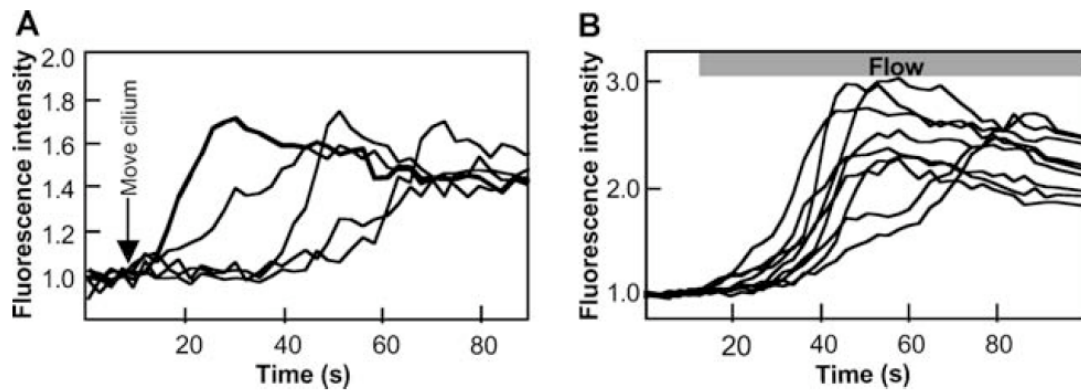


FIGURE 1.13 The intracellular Ca^{2+} increase induced by bending of the primary cilium in MDCK cells. (A) Bending of a single primary cilium with a micropipette. The pipette was positioned $\sim 4\mu\text{m}$ above the apical membrane and the primary cilium was bent toward the micropipette (arrow) by application of negative pressure in the pipette. The MDCK cells were grown to confluency on cover slips and loaded with the fluorescent probe fluo-4. (B) Bending primary cilia by flow. The traces represent increments of the intracellular Ca^{2+} concentration after changing the perfusate flow rate from 0 to $8\ \mu\text{l/s}$. [Praetorius and Spring, 2001].

Evidence connecting primary ciliary mechanosensation and PKD was provided by Nauli et al [2004]. They found epithelial cells isolated from the kidney of transgenic mice that lack functional PC-1 formed cilia but did not produce a Ca^{2+} influx in response to physiological fluid flow. Blocking antibodies directed against PC-2 similarly abolished the flow response in wildtype cells. They concluded that their data suggested that PC-1 and PC-2 contribute to fluid-flow sensation by the primary cilium in renal epithelium and that they both function in the same mechanotransduction pathway [Nauli et al., 2003]. Defects due to mutant polycystin proteins might generate false signals that indicate a “lack of flow” and might result in a compensatory growth of the tubular cells and subsequent cyst formation [Fliegauf et al., 2007].

Interestingly, studies have shown that cessation of flow in kidney tubules of adult mice induces a proteolytic cleavage resulting in a cytoplasmic fragment of PC-1. This is followed by translocation of the fragment to the nucleus where it directly initiates signalling processes that regulate branching morphogenesis of kidney tubule cells, suggesting that the protein is involved in early embryonic development of the nephron or in maintenance of its normal tubular structure [Nickel et al., 2002]. Such a pathway could regulate cellular proliferation; it is also likely that polycystin-mediated, flow-regulated calcium signalling also influences other epithelial properties within the tubule lumen, such as ion and/or fluid movement across the epithelium altering the composition of the luminal contents [Pan et al., 2005]. Additionally, considering the mechanisms involved in the NVP model, it is also feasible that molecules within the fluid flow might activate chemosensory or receptor-based signalling events to induce the subsequent intracellular calcium-release response. Hence, chemical as well as mechanical fluid-flow sensing might provide morphogenic cues that regulate tubule diameters [Fliegauf et al., 2007]. However, the physiological consequences of ciliary mechanosensory and chemosensory dependent calcium signalling in the functioning of the normal renal epithelium remains to be fully uncovered.

1.4.2.3 Hepatic disease in association with ciliary dysfunction

Hepatic disease is one of the most common extrarenal features of the ciliopathies. The hepatic involvement varies from cystic disease to fibrosis, with a combination of both present in some disorders. The severity of hepatic involvement can also vary from serious impact on a patient's quality of life whilst retaining normal liver function, to a significant impairment in liver morphology and function becoming a major cause of morbidity and mortality.

Development of cysts in the liver originally from the bile ducts is the most frequent extrarenal manifestation in both ADPKD (75% of patients) and ARPKD [Everson et al., 2004; Tahvanainen et al., 2005]. Liver involvement in ADPKD is characterised by altered remodelling of the embryonic ductal plate with presence of biliary cysts and aberrant portal vasculature [Bogert and LaRusso, 2007]. In stark contrast, ARPKD is invariably associated with biliary dysgenesis, a DPM characterised by aberrant IHBDs and portal fibrosis. Gross cystic dilatation of the bile ducts is unusual except in the 6 to 12% of patients with Caroli's disease [Igarashi and Somlo, 2003; Zerres et al., 1996]. In those who survive the renal disease, hepatic lesions become progressively more severe with age, and polycystic liver then becomes the major cause of morbidity and mortality [Everson et al., 2004; Tahvanainen et al., 2005].

Cholangiocytes have primary cilia extending from the apical membrane into the ductal lumen, heterogeneous in length along the biliary tree axis (i.e. longer in large vs. small ducts) [Huang et al., 2006]. Currently, nothing is known about the physiologic and pathophysiologic functions of primary cilia in cholangiocytes, the cells from which the liver cysts originate, as a potential result of an increased cholangiocyte proliferation and abnormal fluid secretion. In contrast, considerable information has been generated within the last few years regarding the physiologic functions of primary cilia in renal epithelia providing an invaluable insight into the possible roles of cholangiocyte primary cilia in health and disease. In light of these findings, Masyuk et al proposed that cholangiocyte primary cilia might function as a mechanosensor that monitors and transmits luminal bile flow stimuli into integrated intracellular calcium and cAMP signalling, as shown in renal tubules.

The mechanosensory function of cholangiocyte cilia was addressed directly by using microperfused rat intrahepatic bile duct units (IBDUs) allowing controlled manipulation of luminal fluid flow rates, detection of both intracellular calcium and cAMP levels, and effective utilisation of gene silencing by small interfering RNA (siRNA) [A. I. Masyuk et al., 2006]. In microperfused IBDUs, luminal fluid flow induced an increase in intracellular calcium and caused suppression of the forskolin-stimulated cAMP increase. In contrast, the fluid flow induced changes in intracellular calcium levels and cAMP levels were significantly reduced or abolished when cilia were chemically removed. Furthermore, they were able to show that changes in intracellular calcium levels and cAMP are dependent on extracellular calcium, and expression of PC-1 and PC-2, as the changes were also abolished upon removal of extracellular calcium, and when PC-1 and PC-2 were individually down-regulated by siRNA [A. I. Masyuk et al., 2006]. Collectively, these data support the concept that cholangiocyte cilia function as sensory organelles that transmit luminal fluid flow stimuli into integrated intracellular calcium and cAMP signalling, as in the renal tubules, monitoring changes in bile flow within IHDs and adjusting cholangiocyte functional response (i.e. ductal bile secretion) to such changes.

Moreover, recent data from Masyuk et al [T. V. Masyuk et al., 2004a; 2004b] have revealed a strong connection between cholangiocyte cilia and hepatic cystogenesis. Specifically, in an animal model of ARPKD, the PCK rat, cilia are functionally and structurally abnormal; in contrast to normal, they are shorter, have bulbous extensions on the axonemal membrane, and do not express fibrocystin, the protein mutated in ARPKD [2004a; T. V. Masyuk et al., 2004b]. Therefore, it is feasible that defects in cholangiocyte primary cilia may result in the

hepatic phenotypes observed in the ciliopathies. However, as is the case for renal tubule primary cilia, the precise mechanisms of a mechanosensory function of cholangiocyte cilia and the physiologic and pathophysiologic implications remain to be fully characterised.

1.4.2.4 Lateralisation defects in association with ciliary dysfunction

Abnormalities of left-right body patterning (or *situs*) is the third most likely relevant feature predicted to be a characteristic of disorders with ciliary involvement [Badano et al., 2006]. Determination of left-right axis is a precocious embryonic event. During embryonic development in vertebrates, the earliest organ lateralisation process is the looping of the heart tube to the right side. This phenomenon represents only part of the lateralisation that corresponds to the asymmetric positioning of all internal organs along the left-right axis [Schön et al., 2002]. For example, the normal arrangement of asymmetrical organs (*situs solitus*) is characterised by the major lobe of the liver lying on the right side of the abdomen, whereas the spleen and the stomach are on the left side. All phenotypic anomalies resulting from disruption of the normal lateralisation process are collectively referred to as the lateralisation defects [Schön et al., 2002].

Evidence to support a role for primary cilia in lateralisation defects is the infantile form of nephronophthisis (NPHP2). Infantile NPHP with and without *situs inversus* is caused by mutations in the gene encoding the protein inversin (*INVS*). Inversin has been shown to interact and co-localise with nephrocystin-1 and β -tubulin, which constitute the MT axoneme of primary cilia [Otto et al., 2003], not motile cilia [Pan et al., 2005]. In particular,

inversin/NPHP2 function is not implicated in ciliary assembly or motility, but in signalling mechanisms of PCP [Pan et al., 2005]. Thus, the co-localisation to primary cilia of nephrocystin-1, inversin, and β -tubulin provide a functional link between primary cilia function and left-right axis determination in humans [Pan et al., 2005].

1.4.2.5 Nodal hypothesis

In early development of mammalian embryos a small triangular indentation, termed the “node”, forms transiently [Pazour and Witman, 2003]. Involved in the development of normal left-right asymmetry the node possess a specific cluster of primary cilia that play a crucial role in body axis determination [Nauli and Zhou, 2004]. Although these so-called intermediate primary cilia structurally show a “9+0” microtubule arrangement [Takeda et al., 1999], careful observations showed that they also possess radial spokes and dynein arms, and are motile [Nonaka et al., 1998; Takeda et al., 1999]. Nodal cilia exhibit a characteristic clockwise twirling movement, generating a leftward flow of fluid across the node [Nonaka et al., 1998].

However, directional information of nodal flow must be converted to asymmetric gene expressions. Theoretically, there are three independent questions in this process. One is whether the information is chemically or mechanically sensed. Another is whether the sensor is localised on the cilia or other non-ciliary cell membranes. Finally, if the information is sensed on the cilia, are the necessary receptors situated on the nodal cilia themselves or on the non-motile sensory primary cilia [Marshall and Nonaka, 2006]?

The earliest model hypothesised that the nodal flow creates a gradient of a putative morphogen across the left-right axis of the node (Fig. 1.14), and that this gradient is responsible for the development of normal left-right asymmetry [Nonaka et al., 1998; Okada et al., 1999]. However, in a study carried out by Nonaka et al [2002], where superimposed flow from left to right over wt mouse embryos *in vitro* could reverse left-right asymmetry argues against that. The relatively large volumes of fluid pumped over the nodes to achieve this makes it difficult to envision a gradient of a morphogen developing under such experimental conditions [Pazour and Witman, 2003].

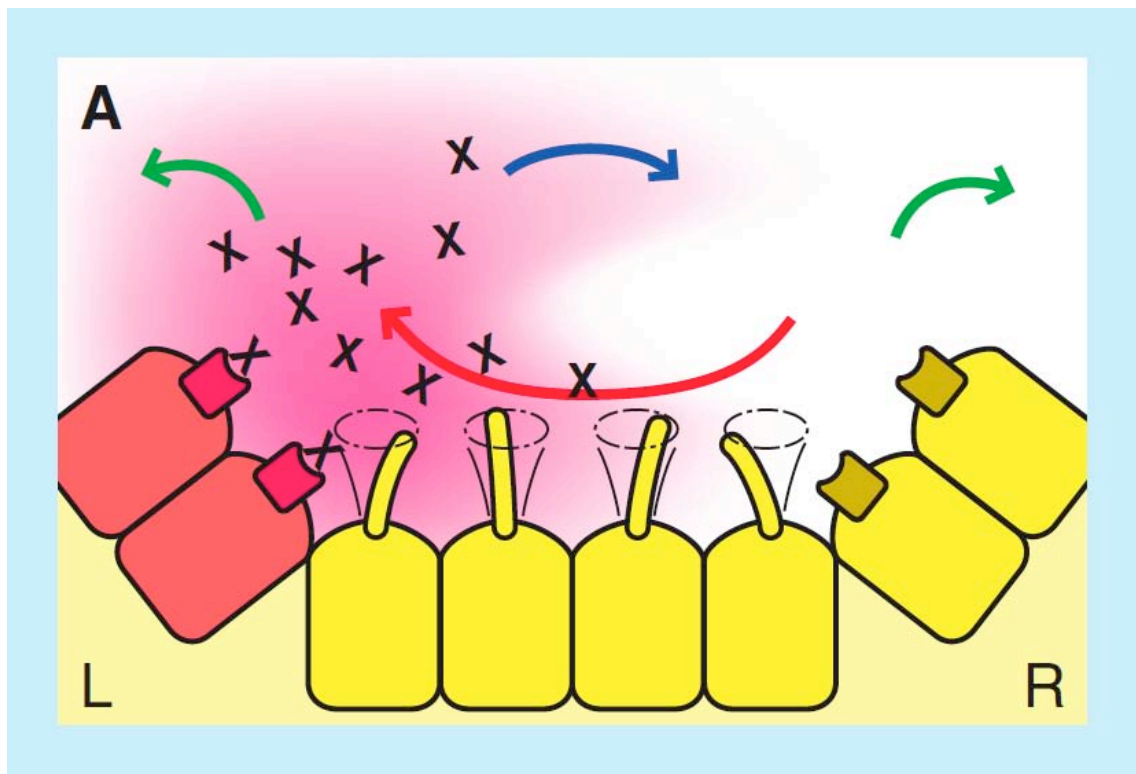


FIGURE 1.14 Classic morphogen accumulation model for nodal flow sensing. A secreted molecule (X) makes a concentration gradient by leftward flow (red arrow). Okada et al estimated the molecular weight of X to be 15-50 kDa considering effects of diffusion (green arrows) and returning flow (blue arrow). Taken from [Marshall and Nonaka, 2006].

An alternative hypothesis was proposed by Brueckner and colleagues [McGrath et al., 2003; Tabin and Vogan, 2003]; the “two cilia model” in which mechanical stress of the flow is sensed by a population of non-motile cilia at the periphery of the node (Fig. 1.15c), and in response generate a morphogenetic signal within the cell. This model encompasses a functional role for the non-motile primary cilium in the determination of lateralisation providing a possible explanation for the presence of *situs inversus* in disorders caused by mutations in genes not encoding proteins involved in ciliary structure or IFT.

Currently nodal flow hypotheses cannot efficiently explain the complex laterality defects that are observed in humans and mice with inborn ciliary defects (Fig. 1.15a) [Fliegauf et al., 2007]. Partial laterality defects such as *situs abdominalis* and *situs thoracalis* indicate that reversal of left-right body asymmetry can independently occur along the anterior-posterior axis (corresponding to the upper and lower part of the human body) and is controlled by the nodal cilia function [Fliegauf et al., 2007]. It has been postulated that functional differences of the anterior and posterior part of the node, distinct signalling molecules for determining upper-lower body asymmetry and/or a temporal difference of left-right determination might explain partial laterality defects as seen in some cases of syndromic BA [Carmi et al., 1993].

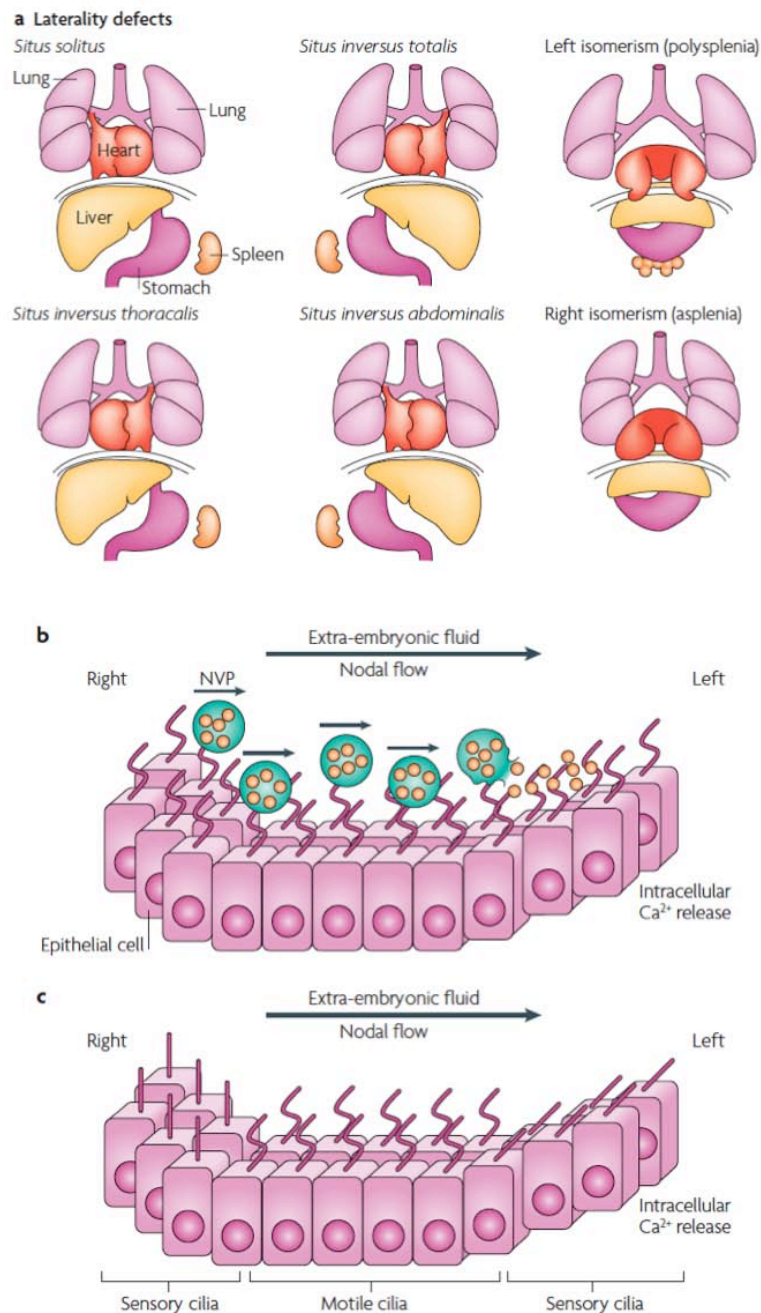


FIGURE 1.15 Human laterality disorders and current models for establishing left-right asymmetry. (a) Schematic illustration of normal left-right body asymmetry (*situs solitus*) and five laterality defects that affect the lungs, heart, liver, stomach and spleen. By their vigorous circular movements, motile monocilia at the embryonic node generate a leftward flow of extra-embryonic fluid (nodal flow). (b) The nodal vesicular parcel (NVP) model predicts that vesicles filled with morphogens (such as sonic hedgehog and retinoic acid) are secreted from the right side of the embryonic node and transported to the left side by nodal flow, where they are smashed open by force. The released contents probably bind to specific transmembrane receptors in the axonemal membrane of the cilia on the left side. The consequent initiation of left-sided intracellular Ca²⁺ release induces downstream signalling events that break bilaterality. In this model, the flow of extra-embryonic fluid is not detected by cilia-based mechanosensation. (c) In the two-cilia model, non-sensing motile cilia in the centre of the node create a leftward nodal flow that is mechanically sensed through passive bending of non-motile sensory cilia at the periphery of the node. Bending of the cilia on the left side leads to a left-sided release of Ca²⁺ that initiates the establishment of body asymmetry. Taken from [Fliegeauf et al., 2007].

1.4.2.6 Cilia and the cell cycle

As previously touched upon, a balance between hyperproliferation and apoptosis may play an important role in the pathogenesis of cystic kidney diseases. For example, whereas in PKD kidneys are grossly enlarged, in NPHP and BBS kidney size remains normal and cysts grow at the expense of normal tissue [Hildebrandt and Zhou, 2007]. This hypothesis could also be applied to the liver in these disorders, in PKD the liver shows significant cystic enlargement [Everson et al., 2004; Tahvanainen et al., 2005], whereas NPHP and BBS are associated with hepatic fibrosis [Boichis et al., 1973; Pagon et al., 1982]. It is therefore speculated that hyperproliferation may be the predominant mechanism in PKD-like diseases [A. C. Ong and Harris, 2005], whereas apoptosis is predominant in diseases of the NPHP and BBS group. Thus, defects in cell-cycle regulation may be ultimately responsible for the derangement of the balance between cellular proliferation and apoptosis in the ciliopathies.

The cilium is nucleated from the elder centriole of the centrosome, the basal body. Given the complex involvement of the centrosome in cell-cycle control, it is likely that the cilia may also play a role in cell cycle control. Supportive of this possible role, the expression of cilia in most mammalian cells is coordinated with the cell cycle. The presence of a cilium is associated with the establishment of polarity and differentiation of the cell; ciliated cell lines grown *in vitro* often grow a primary cilium as they approach confluence, and most ciliated cells are probably in the stationary or G₀ phase of the cell cycle [Avidor-Reiss et al., 2004]. In many cells, entry into mitosis is preceded by ciliary resorption. Following the absorption, the basal body converts back into a centriole. After centriole duplication, the two centrosomes (i.e. four centrioles) form the poles of the spindle apparatus. Shortly after mitosis, the centrosome

containing two centrioles migrates towards the apical membrane, where the elder centriole gives rise to the basal body, providing the base for the ciliary axoneme [Quarmby and Parker, 2005; Wheatley et al., 1996]. If cilia provide information that serves to retain cells in their functioning differentiated G₀ state, then defects in this pathway are predicted to cause proliferative disorders: cystic diseases, and fibrosis of various types. Multiple signalling pathways are localised to cilia in mammalian cells, and some proteins have been shown to act both in the cilium and in cell cycle regulation [Quarmby and Parker, 2005]. It is interesting to consider that if cilia are indeed sending signals that regulate cell cycle progression; by physical necessity these signals must pass near or through the centrosome. Proteomic analyses of centrosomes reveal that apart from structural components, several kinases and phosphatases involved in cell cycle progression and cytokinesis localise to the centrosome [Anderson et al., 2003; Hinchcliffe et al., 1999]. The cell cycle is an important aspect of cystoprotein biology that might help in the understanding of how ciliary defects can result in the extensive pleiotropy seen in the ciliopathies at a molecular level, as cystoproteins change their subcellular localisation according to the cell-cycle stage [Hildebrandt and Otto, 2005; Mollet et al., 2005].

In support of a role for primary cilia in cell cycle regulation, it has been observed that when cholangiocyte cell lines derived from the *Tg737^{orp/k}* mouse were transfected with the wildtype *Tg737* gene, they proliferated at a slower rate than those transfected by a control vector alone [Richards et al., 1997]. As it is known the IFT-particle protein *Tg737* is involved in primary cilia assembly, it is reasonable to conclude that the difference in the rates of cellular

proliferation in these cells reflected the presence or absence, respectively, of a functional primary cilium [Pazour et al., 2000; Pazour and Witman, 2003].

The polycystins have been reported to participate in a confusing plethora of signalling pathways. PC-2 regulates cell proliferation and differentiation by directly interacting with and influencing the nuclear translocation of ID2 (inhibitor of DNA binding-2). Overexpressing PC-2 blocks cell-cycle progression through PC-1 dependent upregulation of the cyclin-dependent kinase inhibitor p21 [X. Li et al., 2005]. Overexpression of PC-1 directly activates signalling through Janus Kinase (JAK)-signal transducer and activator of transcription (STAT) to regulate the cell cycle [Bhunia et al., 2002]. Furthermore, the cytoplasmic C-terminal of PC-1 undergoes proteolytic cleavage in response to fluid flow, enters the nucleus and directly initiates signalling processes (such as Wnt and the activating protein-1 (AP1) mediated pathways) that are modulated by PC-2. As the transcription factor AP1 is involved in various processes, including proliferation, transformation, and apoptosis, this provides further evidence that ciliary mechanosensation in tubular regulation might be directly linked to cell-cycle regulation [Chauvet et al., 2004].

1.4.2.7 Centrosomes

Named for its location near the centre of the cell, the centrosome first described by Boveri in the early 1900s can be recognised under a light microscope as a densely staining structure that is adjacent to the eukaryotic nucleus, and comprises two centrioles that are surrounded by an amorphous, proteinaceous matrix termed the pericentriolar material (PCM) [Badano et al.,

2005]. In addition to its already established role in cilia assembly, the centrosome serves as the MTOC in interphase cells, is important for organising the mitotic spindle during mitosis, and organises regulatory aspects of cell physiology.

The MTOC activity of the centrosome includes the nucleation and organisation of those MTs that form the interphase cytoplasmic microtubular array and the mitotic spindle, as well as cilia. However, recent data indicate that centrosomes are not essential for spindle assembly in mammalian cells, suggesting that most, if not all, cells can assemble spindles by non-centrosomal pathways [Hinchcliffe and Sluder, 2001; Khodjakov et al., 2000]. However, given its complexity and conservation, the centrosome must perform essential functions as otherwise it would have been eliminated during evolution by random mutations.

Positioning of the spindle within cells is important for several fundamental processes, including, accurate segregation of chromosomes, asymmetric distribution of cell-fate determinants during development, normal and asymmetric cell divisions, and defining the plane of cytokinesis. Thus centrosome-mediated spindle assembly could provide a redundant pathway to ensure that centrosomes are inherited during each cell division so they can complete other essential cellular functions [Doxsey, 2001]. One such role emerging from studies into centrosome function is in defining cell polarity. One very interesting aspect of acentrosomal spindles is the lack of astral MTs (MTs that link centrosomes to the cell cortex). Astral MTs are important for the correct positioning of the spindle during mitosis, and for the establishment of the spindle axis [Rieder et al., 2001]. Thus, the centrosome seems to be

involved in either establishing or maintaining cell polarity, which relies on the directionality of MTs (which are inherently polar structures) [Badano et al., 2005]. As the centrosome represents a cellular organelle shared by the mitotic-spindle and cilia, it is tempting to speculate that cilia-sensed signals integrate into cellular programs that provide a vectorial cue for the positioning of the centrosome after mitosis and thus cellular polarity [Badano et al., 2005]. Mutations in genes affecting the structure and/or function of cilia may result in impairment of the organelles to sense and transduce signals relating to cellular orientation onto the centrosome, perhaps explaining in part, the observation that almost all cell types affected in the ciliopathies are polarised.

Another area of centrosome biology of relevance to the ciliopathies is the role of centrosomes in generating genetic instability [Doxsey, 2001]. Much like chromosomes, centrosomes duplicate precisely once every cell cycle. The fidelity and timing of centrosome duplication is essential for ensuring that this process is effectively coupled to other events, such as cell-cycle progression and DNA replication [Hinchcliffe and Sluder, 2001]. Uncoupling of these events can lead to excess centrosomes that can organise multipolar spindles or single centrosomes with associated monopolar spindles [Doxsey, 2001]. As centrosomes act dominantly when present in somatic cells, abnormal centrosome numbers contribute to spindle abnormalities, chromosome misregulation and genetic instability, either alone or in combination with alterations in other cellular pathways [Doxsey, 2001; Heald et al., 1997]. The observation of a high frequency of chromosome anomalies and genetic aberrations in the cystic cells from patients with ADPKD [Gogusev et al., 2003], prompted investigation into the mechanisms underlying this observation. Increased centrosome numbers and centrosome defects have

been observed and analysed in most aggressive tumours, in some low-grade tumours, and pre-cancerous lesions [Marx, 2001; Pihan et al., 2001]. Although there is no correlation between ADPKD and renal carcinoma, various observations liken ADPKD to a benign neoplasia [Brasier and Henske, 1997; Harris and Watson, 1997]. Cystic cells are hyperproliferative, display abnormal expression of cell adhesion molecules, and show resistance to anoikis [Battini et al., 2006; Roitbak et al., 2004]. Recent studies have established that amplification of centrosomes, as well as formation of micronuclei and defects in DNA segregation, leads to genetic instability [Burtey et al., 2008; Fukasawa, 2005]. It is therefore speculated that this may either cause the cell to die, or survive a cycle through asymmetric division with the generation of viable, yet aneuploid cells in which cell death may ensue as a consequence of extensive loss of genetic material. However, while mitotic catastrophe does occur within such cell populations, the observed disappearance of remarkable polyploidism over time suggests that cells are able to converge genomically towards a chromosomal composition adaptive to growth [Battini et al., 2008]. Thus, renal and hepatic phenotypes observed in the ciliopathies, cysts and fibrosis could be explained by chromosomal instability, with a balance between the rates of apoptosis and adaptive growth.

Recently, the loss of oriented cell division consequent to alteration of mitotic spindle orientation has been suggested as an early mechanism of the cystogenic process in a mouse model of PKD [Fischer et al., 2006]. Therefore it is also conceivable centrosomal amplification may play a role in cystogenesis and fibrosis by causing the loss of normal mitotic orientation when multiple centrosomes are present [Burtey et al., 2008].

1.4.2.8 Primary cilia in tubulomorphogenesis, and planar cell polarity

Tubulogenesis involves many cellular processes, including differentiation, polarisation, shape change, proteolysis, growth, mitosis, death, motility, adhesion, signalling, ion fluxes, cytoskeletal organisation and membrane trafficking [Zegers et al., 2003]. Although each of these processes has been well studied, less is known about the complete temporal-spatial picture of how things are coordinated, and especially how the behaviours of many individual cells are linked together to form patent functional tubules. Tubulogenesis is the most complex of several classically described alterations in epithelial tissue architecture, including convergent extension, epiboly, sheet closure, and epithelial-mesenchymal transition, and may share some features with these other types of morphogenic movement [Zegers et al., 2003].

Tubular epithelial cells are polarised along their apical-basal axis, allowing specialisation of function of their apical and basolateral surfaces [Drubin and Nelson, 1996; Shulman and St Johnston, 1999]. Cues for polarisation along the axis are derived from direct contacts with other cells and the substratum [Müller, 2000]. Many epithelia such as those lining tubules are also polarised along an axis orthogonal to the apical-basal axis, resulting in asymmetry within the plane of the epithelium (referred to as PCP) [Shulman et al., 1998; Shulman and St Johnston, 1999]. Polarisation along this axis requires signals to reach across vast expanses of cells [Axelrod and McNeill, 2002].

It is clear that the function of the tubular cells of the nephron and biliary system require a precisely defined structure not only at the single cell level but also at the tissue level.

Therefore, one of the main developmental challenges of the kidney and liver is to assemble a perfect architecture of the nephron and biliary system. Morphogenesis involves coordinated proliferation, differentiation, and spatial distribution of cells, notably the massive proliferation lengthens tubules without substantial increase in their diameter. Studies by Fischer et al [2006] were able to demonstrate that lengthening of renal tubules is associated with mitotic orientation of cells along the tubule axis, demonstrating intrinsic planar cell polarisation. Their study also demonstrated that mitotic orientations are significantly distorted in rodent polycystic kidney models [Fischer et al., 2006]. Thus, it was suggested that oriented cell division dictates the maintenance of constant tubule diameter during tubular lengthening, and that defects in this process trigger abnormal tubule growth and formation.

Oriented cell division is the result of a correctly positioned spindle axis. A number of studies in different model organisms have placed the spindle axis orientation under the control of the PCP pathway, also known as the non-canonical Wnt pathway [Klein and Mlodzik, 2005; Simons and Walz, 2006]. Wnt signalling regulates a diverse set of developmental processes [Logan and Nusse, 2004; Veeman et al., 2003]. In vertebrates, processes requiring precise PCP signalling include; regulation of convergent extension movements during embryo gastrulation, body hair orientation and skin development, neural tube closure, as well as the organisation of the stereocilia bundles of the inner ear epithelium [Simons and Walz, 2006]. The central elements of the Wnt signalling pathway include a family of ligands and receptors that together regulate activity of the cytoplasmic protein dishevelled (Dvl). The Wnt pathway then branches into two pathways, the β -catenin dependent (canonical) and the β -catenin independent (non-canonical). During early kidney development, canonical Wnt

signalling is necessary for the induction of metanephric mesenchyme and cell proliferation in branching morphogenesis [Perantoni, 2003]. At later developmental stages however the non-canonical Wnt pathway is required for oriented cell division to allow proper elongation of the renal tubules.

Several groups have been able to show that a number of cystoproteins may be directly involved in switching between the canonical and non-canonical Wnt Pathways [Guo et al., 2004; Schwarz-Romond et al., 2002; Simons et al., 2005]. Most convincingly Simons et al [2005] were able to show that fluid flow detected by primary cilia regulates a crucial inversin-dependent switch between Wnt signalling pathways during renal development. On the basis of these findings, Simons et al [2005] propose a model in which urinary flow terminates canonical Wnt signalling to facilitate β -catenin-independent Wnt pathways, perhaps to endow tubular epithelial cells with the spatial information important to maintain the genetically determined tubular geometry (Fig.1.16).

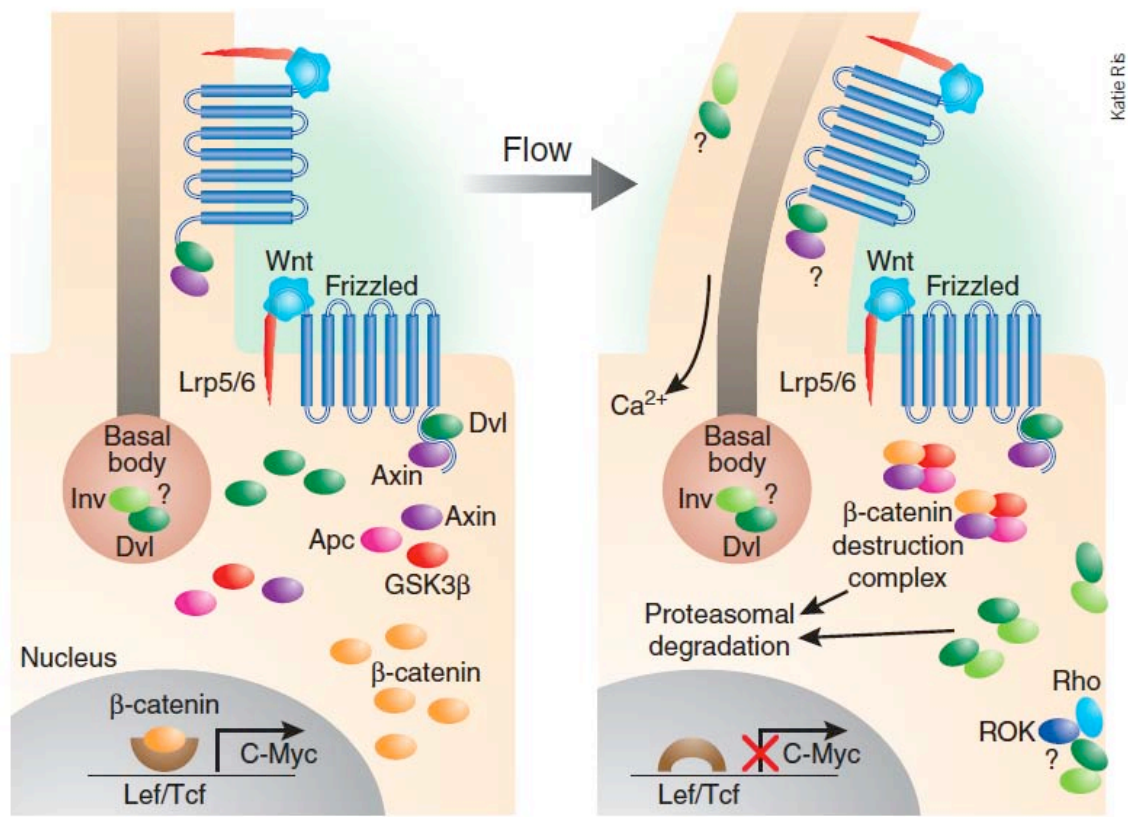


FIGURE 1.16 Flow-based model of Wnt regulation in the kidney. In the model proposed by Simons et al. [2005], Wnt signalling occurs primarily through β -catenin-dependent pathways in the absence of flow. Ligand binding by the Frizzled-LRP complex results in inactivation of the β -catenin destruction complex, increased cytoplasmic and nuclear β -catenin levels, and upregulation of effector gene expression (left). Stimulation of the primary cilium by flow is postulated to result in increased expression of inversin (Inv), which then reduces levels of cytoplasmic dishevelled (Dvl) by increasing its proteasomal degradation. This process is thought to switch off the canonical pathway by allowing reassembly and activation of the β -catenin destruction complex. Inversin might also enhance trafficking of Dvl to the plasma membrane, where it could activate noncanonical Wnt pathway components. The question marks indicate uncertainty as to whether the inversin-Dvl or Frizzled-LRP complexes are present in the primary cilia-basal body-centrosomal complex. Taken from [Germino, 2005].

According to this model, any process that impairs this switch would result in compromised canonical Wnt signalling and abnormal tubulomorphogenesis (Fig. 1.17). Interestingly, urine and bile production begins remarkably early in embryogenesis. Long before fluid and electrolyte balance is required for homeostasis [Nakanuma et al., 1997; Simons and Walz, 2006]. It is therefore tempting to speculate that urine and bile flow terminates canonical Wnt signalling. Given that primary cilia are now believed to function as mechanosensors to flow [Praetorius and Spring, 2001], this model provides a mechanistic link between the primary cilia-basal body-centrosomal (CBC) complex and a pathway regulating tubular morphology.

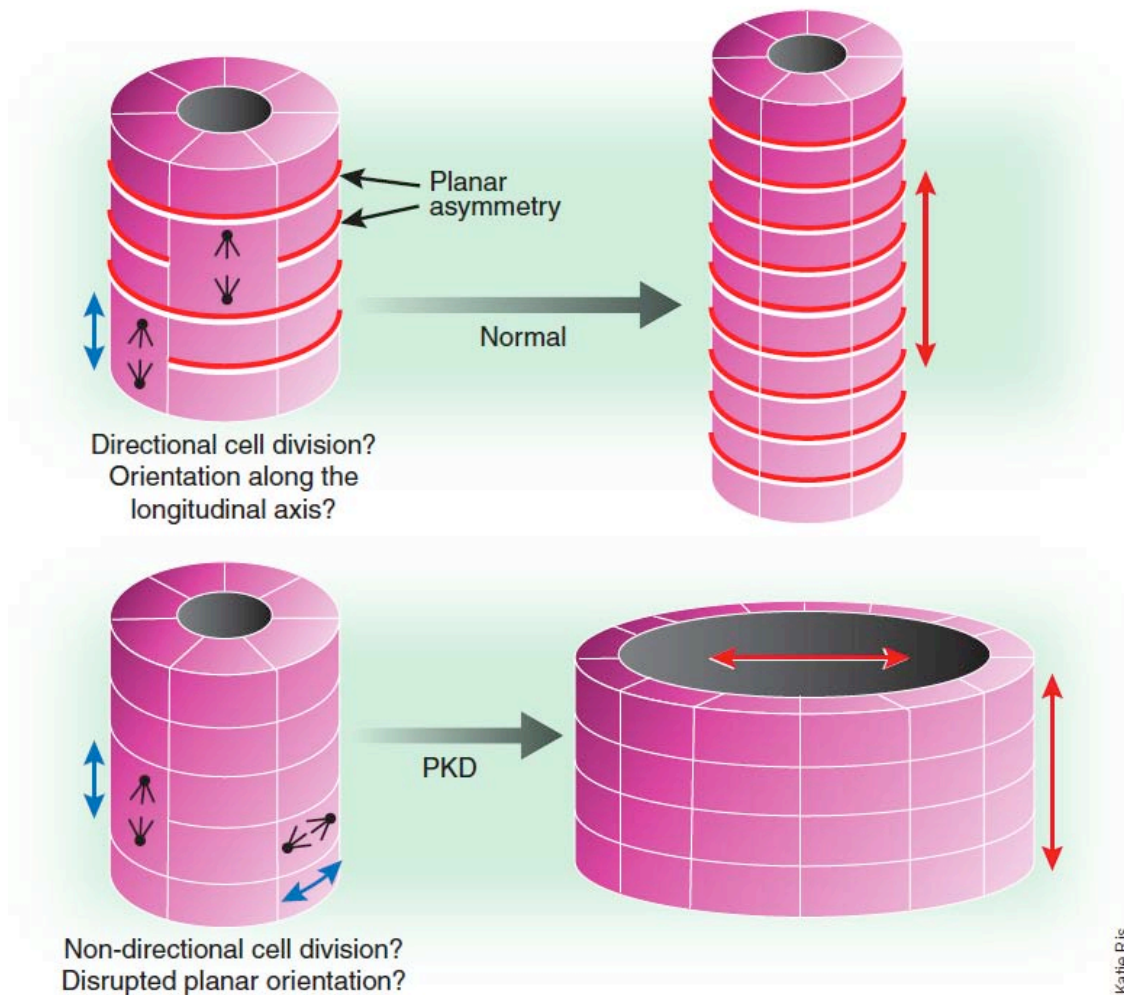


FIGURE 1.17 Noncanonical Wnt signalling and tubular morphogenesis. Proper apical-basolateral polarity is essential for normal solute and water transport, and tubular epithelial cells must also be correctly oriented with respect to the longitudinal axis of the tubule. This is especially true during renal and biliary development when newly formed tubules undergo progressive lengthening. The default structure that would result from disruption of this planar orientation is predicted to be a dilated tubule or cyst. Noncanonical Wnt signalling regulates a number of processes that could help orient cells properly along the longitudinal axis. Tubular flow could be one of these signals that provide information about cellular orientation. Adapted from [Germino, 2005].

Taken together, these findings and this model support the emerging link between PCP and the CBC complex. The monocilium appears to provide the spatial cues (by sensing tubular fluid flow, for example) to position the centrosome and the mitotic spindle before the next cell division [Benzing and Walz, 2006]. Defective cilia function or PCP signalling might cause the tubular epithelial cells to lose spatial orientation and apical-basolateral polarity, to proliferate abnormally and to form defective tubules [Fliegauf et al., 2007].

Although Wnts are known to play a role in PCP and hepatic development, another developmental pathway shown to interact with Wnt signalling in organogenesis is the Notch pathway. Experimental studies in mutant mice and zebrafish, and human genetic studies have shown that Notch signalling is required for biliary tree development during ductal plate remodelling [Flynn et al., 2004; Kodama et al., 2004]. Notch signalling seems to control hepatoblast and mature hepatocyte transdifferentiation into cholangiocytes, by altering the expression of liver-enriched transcription factors [Nishikawa et al., 2005; Tanimizu and Miyajima, 2004]. Interestingly, changes in Jagged1 and Notch expression have been reported also in the course of chronic liver diseases [Nijjar et al., 2001]. Most notably, mutations in Jagged1, a notch Ligand, have been shown to result in the cholangiopathy Alagille syndrome. Alagille syndrome (OMIM #118450) is a pleiotropic developmental disorder characterised by neonatal jaundice and impaired differentiation of IHBDs [Alagille et al., 1987; Emerick et al., 1999]. Much like syndromic BA, features including congenital heart defects, and kidney abnormalities also accompany Alagille syndrome [Bassett and Murray, 2008; Krantz et al., 1997].

The notch-signalling pathway plays an important role in cell-to-cell communication and cell fate determination in a wide range of organisms [Gridley, 1997; Hadchouel, 1992], and has been shown to have a role during tubulogenesis [McCright et al., 2001; 2002]. Notch signalling leads to amplification and consolidation of molecular differences between neighbouring cells, apparently via various mechanisms depending on the cellular context and integration with other factors [Artavanis-Tsakonas et al., 1999]. Studies in *Drosophila* indicate an interplay between Frizzled and Dvl, of the Wnt pathway, and Notch, indicating that polarity is established through local comparisons between cells, and explains how a signal from one position (for example, a proximally located cell relative to bile flow) could be interpreted by distal cells in the tubule.

Importantly, the hypothesis that the renal cystic disease phenotype of the ciliopathies, and possibly their accompanying features is linked to the maintenance of PCP seems plausible for multiple reasons: (i) it would reconcile previous functional hypotheses, because focal adhesions, adherens junctions, cilia, centrosomes, basal bodies, and regulation of the cell cycle all play a pivotal role in the regulation and maintenance of PCP [Keller, 2002]; (ii) because PCP plays an important role in developmental morphogenesis, tubulogenesis, and also in the regeneration of differentiated tissue, a defect in PCP may explain both the occurrence of cysts during organogenesis in certain ciliopathies and degenerative cystogenesis and fibrosis as it occurs in NPHP, and (iii) the mechanism of convergent extension, which may be central to renal and hepatic tubular morphology, was shown to be disturbed in many ciliopathies with a renal cystic phenotype [Ross et al., 2005].

Thus, when all the above evidence is considered the possibility of CBC dysfunction, as a pathogenetic mechanism in BA cannot be dismissed. The interaction of multiple developmental pathways shown to be important in hepatic development and tubulogenesis, two of which are clearly linked to primary cilia mechanosensation, provides evidence of a relationship between hepatic development and tubulomorphogenesis, PCP, and the CBC complex.

1.5 AUTOSOMAL RECESSIVE POLYCYSTIC KIDNEY DISEASE AND *PKHD1*

Despite the evidence presented here so far, it is still unclear how mutations in a cystoprotein could contribute to the syndromic BA phenotype. To clarify this link the notable features of syndromic BA must be considered in relation to the other ciliopathies. Like many of the other cholangiopathies BA displays an assortment of associated abnormalities that have been proven to be caused by mutations in cystoproteins, and abnormalities in PCP and the CBC complex. These features include the occasional association of renal cysts in patients with BA (unpublished observation) [Franchi-Abella et al., 2007], anomalies of *situs* determination, and evidence of DPM in a number of infants with BA [Strazzabosco et al., 2005]. The compelling overlap of the clinical features of syndromic BA with the ciliopathies suggests a common aetiology.

Of the many disorders classified as both cholangiopathy and ciliopathy, fewer also display DPM; these include ADPKD, ARPKD, Caroli's disease, and CHF [J. R. Davenport and Yoder, 2005; Strazzabosco et al., 2005]. However, of these four ARPKD stands out in

relation to BA for several specific reasons. Autosomal recessive polycystic kidney disease is one of the most important paediatric nephropathies associated with significant neonatal mortality and childhood morbidity [Guay-Woodford, 1996; MacRae Dell and Avner, 2001; Zerres et al., 1998b]. Estimates of the disease prevalence vary widely, with a proposed incidence of 1:20,000 to 1:40,000 [Guay-Woodford, 1996; Guay-Woodford and Desmond, 2003; Zerres et al., 1998b].

The renal cystic disease typically begins *in utero* and manifests as fusiform dilatation of the collecting ducts (CDs) that radiate from the medulla to the cortex [Blyth and Ockenden, 1971]. During foetal development, cysts also appear transiently in proximal tubules (PTs) [Nakanishi et al., 2000]. This results in a typical neonatal presentation of bilaterally enlarged, echogenic kidneys [Harris and Rossetti, 2004]. However, the clinical spectrum is highly variable, ARPKD can present as perinatal, neonatal, infantile, or juvenile – onset disease [Blyth and Ockenden, 1971]. This variability in the age of onset is due to variable expression of mutations within the same gene, as well as the effects of modifier genes and environmental factors, rather than mutations of different genes [Guay-Woodford et al., 1995; Kaplan et al., 1988]. ARPKD is also characterised by liver disease, which is detectable in approximately 45% of infants and is often a major feature in older patients [Onuchic et al., 2002; Roy et al., 1997]. The liver disease in ARPKD is primarily manifest by two major types of pathophysiology; biliary disease and portal hypertension, due to biliary dysgenesis and portal tract fibrosis [D'Agata et al., 1994; Shneider and Magid, 2005]. The hepatic histopathology of ARPKD is characterised by DPM [Desmet, 1992a], portal spaces enlarged by portal fibrosis, and proliferation of biliary ducts, which can become dilated. Abnormal multiple bile

ductules can lose connection with the biliary system and dilate to form large cysts [Sherlock and Dooley, 1997]. When larger biliary ducts are also dilated, the disorder is called Caroli's disease [Menezes and Onuchic, 2006]. In some cases, cholestasis leads to a gradual replacement of the immature ducts by fibrosis, resulting in a condition known as hepatic fibrosis. Thus, patients with ARPKD tend to present with CHF and Caroli's disease, known as Caroli's syndrome [C. A. Johnson et al., 2003].

There is a remarkable parallelism in the type and evolution of both the renal and hepatic lesions of ARPKD, illustrated in table 1.4. The renal lesion consists of a fusiform dilatation of the CDs and the hepatic lesions of DPM of the interlobular bile ducts. Atrophy of tubules and ducts occurs in BA. It appears that the early lesions of ARPKD, in the kidneys and in the liver can be conceived as a malformation, i.e. a disturbance in normal development. Both fusiform ectasia of the CDs in the kidney and DPM in the liver seem to result from a faulty epithelial-mesenchymal inductive interaction [Desmet, 1992b]. In ARPKD, both tubular systems seem to be subject to a slowly progressive, destructive process of epithelial involution, resulting in the disappearance of increasing numbers of patent tubules (both renal and hepatic) and associated with increasing amounts of interstitial fibrosis. Thus, the morphological similarities of the destructive cholangiopathy caused by CHF in ARPKD and the basic disease process of BA may suggest shared aetiology and pathogenesis [Desmet, 1992b].

TABLE 1.4 Autosomal recessive polycystic kidney disease

	Hepatic lesions	Renal lesions
Early stage	Ductal plate malformation of interlobular ducts ('cystic' form of cholangiodysplastic pseudo-cirrhosis)	Fusiform dilation of collecting ducts (+ tubules) (<i>Neonatal form of ARPKD</i>)
Progression	'Destructive cholangiopathy'	Destructive tubulopathy
	(<i>Rapid variant: 'early severe EHBDA'</i>)	(<i>Rapid variant: 'nephronophthisis'</i>)
Later stage	CHF (non-cystic form of cholangiodysplastic pseudo-cirrhosis)	Renal cysts, tubular atrophy, interstitial fibrosis (later infantile and juvenile form of ARPKD)
	(<i>Biliary cirrhosis + liver fibrosis</i>)	(<i>Renal failure</i>)
CHF = congenital hepatic fibrosis; EHBDA = extrahepatic bile duct atresia; ARPKD = autosomal recessive polycystic kidney disease		

Taken from [Desmet, 1992b]

All typical forms of ARPKD are caused by mutations in a single gene *PKHD1* (polycystic kidney and hepatic disease 1) [Menezes and Onuchic, 2006]. *PKHD1* was cloned and sequenced in 2002 independently by three different groups. Identification of *PKHD1* as the gene defective in ARPKD was dependent upon the analysis of patients with ARPKD and a relevant rat model of the disease, the *pck* rat [Onuchic et al., 2002; Ward et al., 2002; Xiong et al., 2002]. While Xiong et al. [2002] also identified and mapped the mouse orthologue (*Pkhd1*) on mouse chromosome 1. Taken together, the work of these three groups provided evidence that the gene responsible for ARPKD had been identified.

PKHD1 is a very large and complex gene consisting of at least 86 exons extending over approximately 472kb of genomic DNA [Onuchic et al., 2002; Ward et al., 2002]. The gene undergoes a complex pattern of alternative splicing to generate a large number of mRNA transcripts ranging in size from 8.5kb to 13kb [Igarashi and Somlo, 2003; Onuchic et al.,

2002]. These predicted translation products are novel proteins that share homology to a superfamily of proteins involved in the regulation of cell proliferation, and cellular adhesion and repulsion. The longest transcript in humans is 16,235bp encoded by 67 exons, spanning a genomic region of approximately 472kb [Ward et al., 2002]. The open reading frame starting within exon 2 is 12,222bp, and is predicted to encode a protein of 4,074 amino acids [Onuchic et al., 2002; Ward et al., 2002; Xiong et al., 2002]. The encoded protein, designated fibrocystin/polyductin, is a large protein with a calculated unglycosylated molecular mass of 447kDa. Fibrocystin is predicted to be a highly glycosylated, novel single transmembrane protein with a 192 amino acid intracellular carboxyl-terminus, and a very large extracellular amino-terminus, with a total molecular mass greater than 500kDa (Fig. 1.18) [Kaimori et al., 2007; Ward et al., 2002].

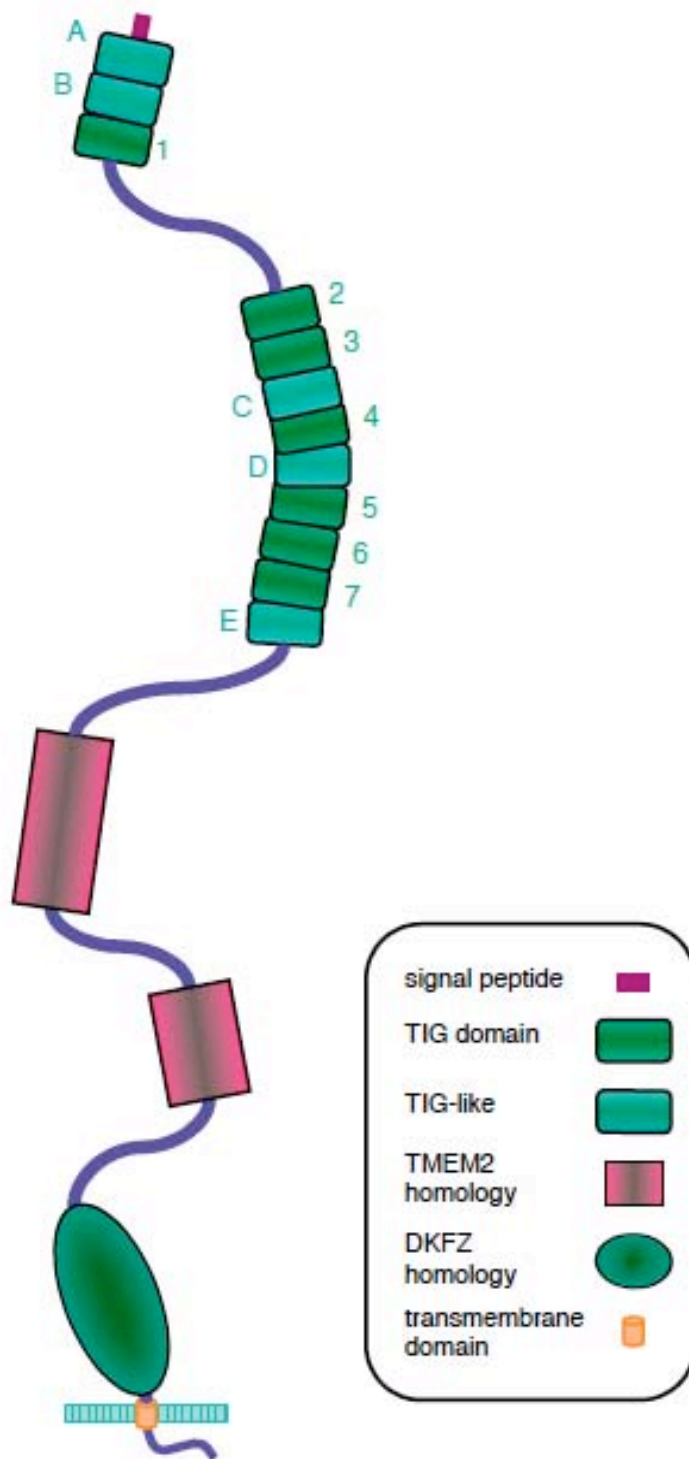


FIGURE 1.18 Model of fibrocystin. Structure of the fibrocystin protein showing conserved domains and regions of homology with other proteins. Taken from [Ward et al., 2002]

Although the overall predicted structure of the protein is new, it contains significant homologies to several other proteins, which may provide a clue to its function. The extracellular domain contains 6-8 of the recognised TIG/IPT domains (Fig. 1.18), immunoglobulin like folds that have been identified in cell surface receptors, such as the HGF receptor and plexins, as well as in the Rel family of transcription factors [Igarashi and Somlo, 2003; Ward et al., 2002]. Between the TIG/IPT domains and the transmembrane domain, there are between nine and ten PbH1 repeats, found in polysaccharidases and are essential for enzyme function forming both the ligand-binding and catalytic sites necessary for degradation of cell-wall polysaccharides [Onuchic et al., 2002]. The predicted external region is also predicted to contain a single arginine-glycine-aspartate (RGD) domain. This motif is found in fibronectin and numerous other proteins, where it has been shown to play a role in cell adhesion. Three putative cAMP/cGMP-dependent protein kinase phosphorylation sites have been identified within the cytoplasmic carboxyl terminus [Onuchic et al., 2002]. In addition, there are potential phosphorylation sites for Protein kinase A (PKA), and protein kinase C (PKC) in the C-terminal tail that are conserved in mouse [Ward et al., 2002]. Significant homologies are present for two expressed sequences *TMEM2*, and *PKHD1L*. However, the sequence homology to *TMEM2* or *PKHD1L* also provides little insight into structure or the biological role of fibrocystin, as the role of these proteins is also unknown [Hogan et al., 2003].

Analysis of the N-terminal region of fibrocystin showed the presence of a hydrophobic signal peptide [Ward et al., 2002]. The C-terminal cytoplasmic domain has also been found to harbour a nuclear localisation signal (NLS) [Hiesberger et al., 2006]. However, despite the

identification of these multiple domains shared by a multitude of protein families the function of fibrocystin remains elusive. While containing domains from many full and part characterised protein super-families, fibrocystin also lacks key structural elements of these protein classes, suggesting that its mechanism of action will differ from that observed in the other classes.

It is notable that mouse fibrocystin presents the same general domain structure as the human product. In fact, these proteins share 73% identity over their complete length, though there are segments with considerably higher (87%) and lower (40%) identity values [Nagasawa et al., 2002], this level of evolutionary conservation suggests fibrocystin to be of functional importance.

As previously mentioned, the *PKHDI* gene encodes a complex and extensive array of splice variants [Onuchic et al., 2002]. Although it is presently unknown how many of the transcripts are actually translated into protein, the complicated pattern of splicing has been shown to be conserved in the mouse orthologue, indicating a functional role for this property [Nagasawa et al., 2002]. In the event that various mRNAs are translated, it could mean that this single gene might encode numerous distinct polypeptides differing in size and amino acid sequence, that are predicted to fall into two broad categories [Bergmann et al., 2004; Onuchic et al., 2002]. One group, which includes the longest continuous open reading frame (ORF), but which may also include molecules lacking some middle domains, has a single transmembrane (TM) element and are likely to be associated with the plasma membrane.

The other group lacks the TM domain and, thus, its members may be secreted [Bergmann et al., 2004].

When taken all together, the structural features of the deduced protein and the human ARPKD phenotype, fibrocystin might be involved in cellular adhesion, repulsion, and proliferation. In addition, the domain and structural analyses suggest that the potential *PKHD1* products may be involved in intercellular signalling and function as receptors, ligands, and/or membrane-associated enzymes [Bergmann et al., 2004].

1.5.1 Expression features of *PKHD1*

The tissue expression profile of *PKHD1* by northern blot analyses suggests that the gene is predominantly expressed in the kidney, consistent with the observed phenotype in ARPKD. Strong staining is observed in human adult kidney, with moderate expression in foetal kidney [Menezes et al., 2004; Ward et al., 2002]. Much lower transcript expression is detected in whole adult and foetal liver [Onuchic et al., 2002]. The human foetal expression pattern of *PKHD1* is consistent with both the observation that renal and hepatic abnormalities develop *in utero* and the hypothesis that disease pathogenesis involves a defect in terminal epithelial differentiation [Calvet, 1993]. Continued expression of *PKHD1* in adult human tissue suggests an additional undefined role for fibrocystin in mature, terminally differentiated organs [Onuchic et al., 2002]. *PKHD1* expression slightly greater than that observed in the liver is also reported in the pancreas, although in this organ it may be an underappreciated manifestation [Lu et al., 1997; Wu et al., 1998]. Additionally, loss of protein expression in

the kidney and liver samples taken from ARPKD patients has also been shown [Ward et al., 2003].

Several studies to determine the localisation of fibrocystin at the subcellular level have shown fibrocystin to be expressed in the primary cilia and basal body in renal epithelial cells and cholangiocytes [Menezes et al., 2004; Wang et al., 2004]. Providing further evidence to support the cystoprotein hypothesis of defects in tubulomorphogenesis. Fibrocystin has also been shown to localise to the apical membrane and cytoplasm of epithelial cells lining the CDs in human tissue stained for the protein [Ward et al., 2003]. Cytoplasmic staining is also reported in inner medullary collecting duct (IMCD) and MDCK cell lines grown in culture [Menezes et al., 2004; Ward et al., 2003]. This may reflect protein that is being processed for ciliary and/or plasma membrane localisation, or recycling from the surface of the cell, as is the case for the ADPKD associated protein PC-1 [Ward et al., 2003]. However, this also raises the possibility of multiple functional roles for fibrocystin, and thus by extension, the generation of pathologies differing to ARPKD involving disruptions in other subcellular domains.

1.5.2 Functional insights

Although the exact function of fibrocystin remains elusive, efforts remain ongoing to uncover its role in health and disease pathogenesis. Studies have uncovered a number of interesting observations, all providing clues to the exact function(s) of this protein. Multiple studies do confirm a ciliary role for fibrocystin. The simple fact that the protein structure is conserved in

Chlamydomonas but not in nonciliated organisms such as *Saccharomyces* and *Arabidopsis* is consistent with a ciliary function [Pazour, 2004]. This was further confirmed when Masyuk et al [2003], were able to show the cholangiocyte cilia of the pck rat were abnormal with bulbous extensions and diminished length, and were devoid of fibrocystin. They further supported this finding by silencing *Pkhd1* in cholangiocytes of normal isolated IBUs, this resulted in significant shortening of cilia, and reduced fibrocystin ciliary expression to an undetectable level. This is yet further supported by the work of Mai et al [2005], who were able to show that stable knockdown of *Pkhd1* in IMCD cells in culture resulted in aberrant ciliogenesis, suggesting that fibrocystin plays a role in this event. However, the mechanism by which this occurs is not clear. Fibrocystin is not a known subunit of the IFT particle. Interestingly, an ARPKD mouse model with an exon 40 deletion of *Pkhd1* which causes distinct liver cysts, does not show any ciliary abnormality in cholangiocytes, suggesting that a lack of fully functional fibrocystin may not affect normal ciliogenesis *in vivo* [Moser et al., 2005].

Indeed, extra-ciliary roles for fibrocystin have also been suggested. In the same study where Mai et al [2005] demonstrated silencing of *Pkhd1* results in aberrant ciliogenesis, they also discovered that the down-regulation of *Pkhd1* also resulted in: (i) inhibition of tubulomorphogenesis; (ii) impairment of cell-cell interactions and inducement of spontaneous cell scattering; (iii) disorganisation of the actin cytoskeleton and induction of endothelial-mesenchymal transformation (EMT); (iv) reduction of integrin-dependent adhesion; (v) increased apoptosis and decreased cell proliferation; and (vi) decreased extracellular signal-regulated kinase (ERK) and focal adhesion kinase (FAK) activation [Mai

et al., 2005]. Implicating fibrocystin in a complex network of cellular polarity, cell-cell/matrix contact, cell cycle control, and ciliary/cytoskeleton assembly, all of which is vital for normal tubule formation.

Studies are now beginning to uncover features of the protein fibrocystin that may explain the diversity of cellular alterations observed by Mai et al [2005]. In order to better understand the function of fibrocystin, Nagano et al [2005] utilised the yeast two-hybrid system to identify proteins that interact with the intracellular C-terminus of fibrocystin. From the screening they identified calcium modulating cyclophilin ligand (CAML), a protein involved in calcium signalling by regulating cytosolic calcium pools with an intracellular distribution that is similar to that of PC-2 [Feng et al., 2002; Tovey et al., 2000]. The study was able to show that these two proteins co-localise in cilia, the basal body, and the plasma membrane in cells from the distal nephron, bile ducts, and pancreatic ducts, and that expression constructs of the two proteins co-immunoprecipitate from mammalian cells. Thus supporting the possibility that fibrocystin may participate in calcium signalling like PC-1 and PC-2 [Nagano et al., 2005]. Further evidence for a role in calcium signalling came from studies by Hiesberger et al [2006]. In their study Hiesberger and colleagues were able to show that fibrocystin undergoes a calcium-dependent proteolysis, similar to that of PC-1. While they found fibrocystin undergoes several proteolytic cleavages within the predicted ectodomain, at least one was found to occur within the cytoplasmic portion. This cleavage generates a C-terminal intracellular fragment that was found to harbour a NLS and translocates to the nucleus [Hiesberger et al., 2006]. It was also determined that this cleavage event is regulated by activation of PKC and release of intracellular calcium, in what they suggest is a cilia-

dependent event, much like that of PC-1. Similar to other proteins that are subjected to regulated proteolysis, only a small fraction of fibrocystin was found to be cleaved. In particular, the pattern of proteolytic cleavage observed (close proximity to the transmembrane fragment) resembles regulated intramembrane proteolysis (RIP) of other type 1 membrane proteins. Nuclear signalling of cytoplasmic fragments generated by RIP is most extensively described for Notch, the pathway involved in PCP and bile duct development, as previously discussed [Flynn et al., 2004; Kodama et al., 2004; Landman and Kim, 2004; Lorent et al., 2004].

Evidence to further support the importance of calcium in the function of fibrocystin is the observation that fibrocystin can be found in the same complex as the calcium channel PC-2, suggesting these two proteins may function in a common molecular pathway [Kim et al., 2008; Wang et al., 2007]. Kim et al [2008] found that the C-terminus of fibrocystin and the N-terminus of PC-2 interact, and that a lack of fibrocystin reduced PC-2 expression, but not *vice versa*, suggesting that PC-2 may function immediately downstream of fibrocystin *in vivo*. PC-2 channel activities were also found to be dysregulated in cultured renal epithelial cells derived from *Pkhd1* mutant mice. Furthermore, Wang et al [2007] determined that the extracellular domains of fibrocystin may be responsible for the flow induced cellular calcium response. Thus, the work of these groups suggests that both cystoproteins function, at least in some part, in a common mechanotransduction pathway.

Hogan et al [2009] proposed that fibrocystin acts as a bi-directional signalling molecule with the ectodomain acting as a ‘urocrine’ and perhaps ‘bilocrine’ signalling molecule fostering communication along the length of the nephron/biliary tree [Hogan et al., 2009; Kaimori et al., 2007]. Hogan et al observed an accumulation of PC-1 positive exosome-like vesicles around renal cilia in *Pkhd1* knockdown mice and ARPKD patients [Hogan et al., 2009]. Upon further examination, they were able to determine these vesicles resembled the exosomes thought to be the end product of the MVB-sorting pathway. The MVB-sorting pathway involves the unique packaging of membrane proteins into intraluminal vesicles within multi-vesicular bodies, some of which are secreted as exosomes when MVBs fuse with the apical plasma membrane. The unique way in which these vesicles are formed results in the ectodomain of the packaged proteins to be facing outwards into the lumen upon release. MVBs and exosomes have been shown to have a role in left/right axis determination in the embryonic node. The observation of PC-1 rich exosome-like vesicles and of abnormal exosome-like vesicle (ELV) accumulation in fibrocystin-deficient mice led the group to examine whether these vesicles have a functional role in the urinary and biliary systems analogous to NVPs in the node, and if fibrocystin plays a role in their interactions with the primary ciliary axoneme. Using a plethora of techniques they were able to produce results suggesting that urinary ELVs interact with the primary cilia *in vivo*, analogous to the ‘smashing’ events described by Tanaka et al [2005]. From these results and observations they postulated that because fibrocystin contains multiple domains similar to those involved in host invasion (PA14 and PBH domains [de Groot and Klis, 2008; Onuchic et al., 2002; Rigden et al., 2004]), it is possible that this molecule behaves as an invasin and the accumulation of ELVs on the ciliary axoneme in fibrocystin (*Pkhd1*) deficient mice may

represent a failure of the invasion process, with fibrocystin itself not being responsible for the initial adhesion event [Hogan et al., 2009].

Not only do all the mentioned studies and observations unify the apparently disparate and transitory localisations of fibrocystin and its cleaved products, they also raise the possibility of fibrocystin being a highly complex bi-directional signalling molecule, fostering communication along the length of the biliary tree that is vital to its development. It is for these reasons fibrocystin and its encoding gene *PKHD1* are candidates in the pathogenesis of the complex disorder BA, especially as a definite function remains elusive.

1.6 UNRAVELLING THE PATHOGENESIS OF BILIARY ATRESIA: INSIGHTS PROVIDED BY ANIMAL MODELS

There is no ideal animal model of BA, and this has slowed understanding of its pathogenesis. During the past forty years, several groups have tried to create an animal model of EHBA, but failed to simulate the real pattern of liver damage [Bangaru et al., 1980; Papadimitriou, 1968; P. A. Phillips et al., 1969; Schmeling et al., 1991; G. A. Wilson et al., 1994]. Basic research in animal models of EHBA has often showed fibrosing inflammation of the bile ducts, but without complete and definitive atresia [Bangaru et al., 1980; Parashar et al., 1992]. This could only be obtained by direct manipulation either by injection of chemically defined substances into the gall bladder [Schmeling et al., 1991], or by operative intervention [Spitz, 1980]. In this way, the expected consequences of mechanically caused cholestasis were seen, but without simulating the clinical entity of BA [Petersen et al., 1997a]. In 1993, Riepenhoff-

Talty et al [1993] observed a temporary biliary obstruction after rota virus inoculation in newborn mice, similar to BA. This was the initial step in the development of the first animal model for BA. Consecutive studies confirmed these observations, and focused on the immunological aspect [Petersen et al., 1997b].

In brief, the intraperitoneal inoculation of newborn Balb/c mice in the first 24 hours of life with rhesus rotavirus (RRV) group A leads to a generalised jaundice, acholic stools, and bilirubinemia by the end of the first week of life. Progressive inflammation and obstruction of the EHBD is observed by two weeks of age, resembling human BA [Czech-Schmidt et al., 2001; Riepenhoff-Talty et al., 1993]. The histological appearance of the liver and biliary tree in late stages of biliary obstruction shows similarity with the histological features of BA, although no definitive atresia of the common bile duct is described in this model [Petersen et al., 1997a]. Analysis of the EHBDs before and after onset of jaundice shows inflammation and oedema of the duct wall, progression to sloughing of the biliary epithelium, closure of the duct lumen by inflammatory cells and other cellular debris, and finally concentric fibrosis of the EHBDs. These processes result in a segmental or continuous obstruction of the extrahepatic lumen [Bezerra, 2006]. The intrahepatic changes are as those described in the EHBDs, including reactive necrosis and proliferation of the small bile ducts [Petersen et al., 1997a].

This infectious model does comply with two conditions to qualify it as a model for BA. Firstly, the changes in the EHBDs develop progressively without direct manipulation, and the atresia is irreversible. Secondly, all described observations occur in an infection model, and

varying changes can be observed in different mice simultaneously [Petersen et al., 1997a]. However, despite all these findings, the evidence in humans remains inconclusive [Petersen et al., 1997a; Petersen et al., 1997b; Riepenhoff-Talty et al., 1993]. The similarity between the immune response seen in human BA and the rota virus-simulated animal model, does however demonstrate the potential for use of this model as a powerful tool to hopefully further elucidate the pathogenesis of BA [Bassett and Murray, 2008].

A transgenic mouse strain currently under investigation as a possible experimental model for BA is the *inv* mouse, created by insertional mutagenesis. Yokoyama et al [1993] first reported the *inv* transgenic mouse in 1993, when they described *situs inversus* and severe jaundice in homozygous mutants, carrying partial deletion of the *inversin* gene. Anomalies included mirror-image left-right inversions of stomach, spleen, and liver. Some had asplenia, preduodenal portal vein, intestinal malrotation, and dextrocardia in various combinations [Shimadera et al., 2007]. *Inv* mice became progressively jaundiced soon after birth, had cystic changes in their kidneys, grew poorly, and rarely lived beyond one week of age [Yokoyama et al., 1993]. Detailed morphological studies of the hepatobiliary system in the *inv/inv* mouse to determine the aetiology of the jaundice identified a defect in the patency of the extrahepatic ductular system. The results from several groups show that these mice have cholestasis with conjugated hyperbilirubinemia, failure to excrete technetium-labelled mebrofenin from the liver into the small intestine, lack of continuity between the extrahepatic biliary tree and the small intestine as demonstrated by Trypan blue cholangiography, and a liver histologic picture indicative of extrahepatic biliary obstruction with the presence of microscopic EHBD remnants [Perlmutter and Shepherd, 2002; Shimadera et al., 2007].

One of the most interesting characteristics of the *inv* mouse is the histology of the liver (Fig. 1.19). There is very little, if any, hepatocellular injury, inflammation, or necrosis within the hepatic parenchyma or portal tracts, but a marked abnormality in the IHBDs and ductules. Instead, persistence of the biliary plate is associated with marked BEC proliferation as defined by a marked increase in lectin-positive epithelial cells surrounding the portal vein and/or portal mesenchyme, corresponding to an arrest on ductal plate maturation (Fig 1.19) [Perlmutter and Shepherd, 2002]. With respect to the EHBDs the histology appears to vary widely between studies. A marked lack of evidence of ischemia or inflammation is consistent between independent studies in the *inv* mouse, however other observations differ significantly. While some groups describe a fully patent common bile duct and normal extrahepatic duct anatomy, others show distant anatomic variations in the extrahepatic biliary system such as anatomic and cystic changes [Mazziotti et al., 1999; Shimadera et al., 2007]. Thus, a number of characteristics of the *inv* mouse are identical to those of human infants with BA and *situs inversus*. There is a similar spectrum of *situs* anomalies. There is conjugated hyperbilirubinemia and progressive cholestasis. There is marked IHBD proliferation in the ductal plate region identical to the DPM that has been described in infants with the prenatal form of BA [Desmet, 1992a]. Furthermore, there is functional obstruction to bile flow as demonstrated by biliary scintigraphic and Trypan blue cholangiographic analyses [Mazziotti et al., 1999]. However, the feasibility of using the *inv* transgenic mouse as an experimental model to elucidate the pathophysiology of BA is still questionable.

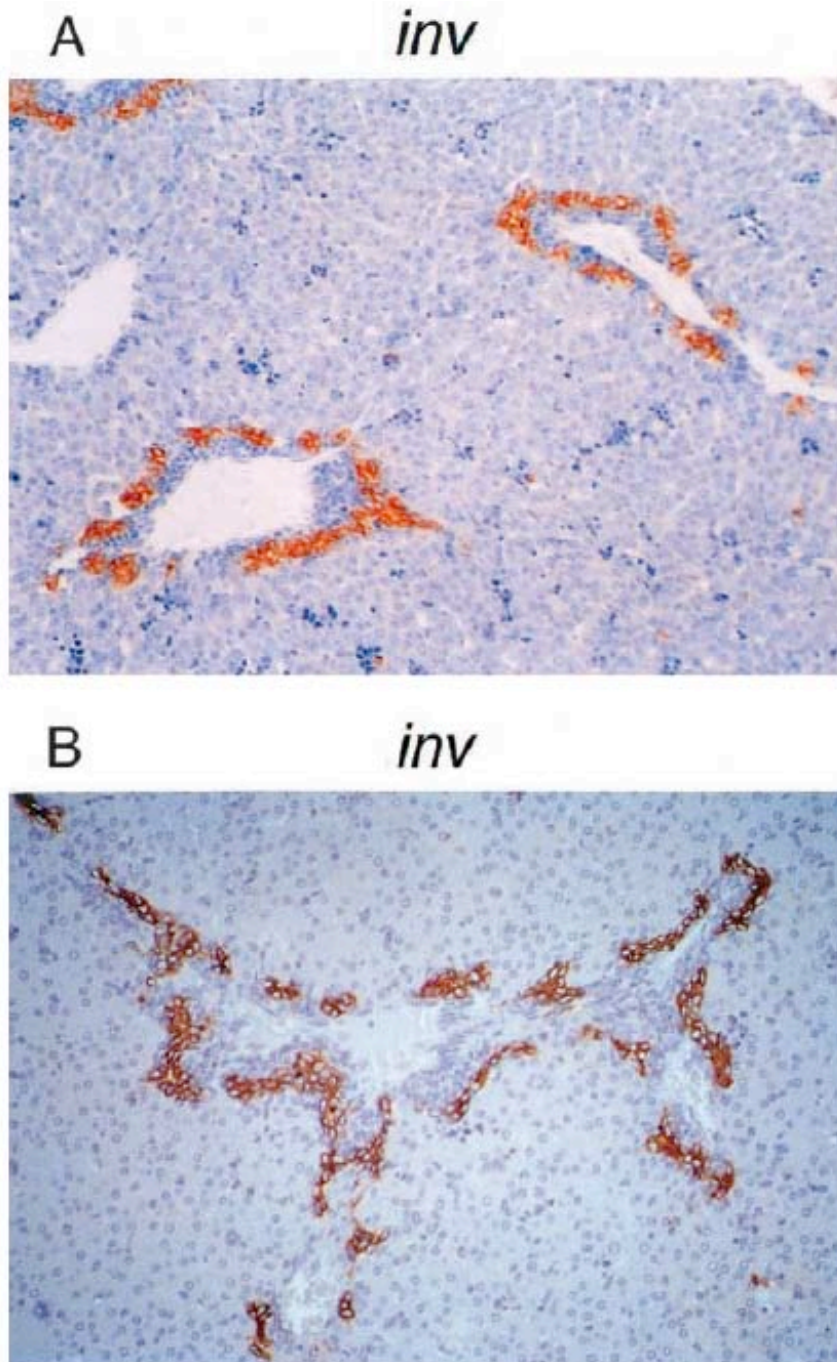


FIGURE 1.19 Sections of *inv* mouse liver tissue stained with DBA histochemistry. This method results in a brown reaction product exclusively in biliary epithelial cells. The stained sections show intense proliferation of biliary epithelial cells around (A) portal vein radicles, and (B) portal vein mesenchyme, but no lumina are formed and thus there are no ducts or ductules. There is no evidence of hepatocellular injury or inflammation. DBA = *Dolichus biflorus* agglutinin. Taken from [Perlmutter and Shepherd, 2002].

The use of other animal models displaying biliary abnormalities similar to those characteristic to BA may still provide clues to its pathogenesis. Such animal models include the pck rat [Lager et al., 2001; T. V. Masyuk et al., 2004a], the cpk mouse [Hou et al., 2002], the HNF-6-KO mouse [Clotman et al., 2003], the HNF-1 β -KO mouse, the *Pkhd1ex40* mouse [Moser et al., 2005], and the *Pkhd1^{del2/del2}* mouse [Woollard et al., 2007]. Despite the diversity between these models, they are all able to aid in understanding the genetic modulation of bile duct pathology.

The *Pkhd1ex40* mouse developed by Moser et al [2005] represents a model of cystic biliary dysgenesis in ARPKD. Generated by targeted mutation of *Pkhd1*, exon-skipping results in expression of a modified *Pkhd1* transcript, resulting in severe malformations of the IHBDs. Detailed histological study of the liver of these mice revealed that they display a severe malformation of the ductal plate with mild duct ectasia. Deterioration in the condition of *Pkhd1ex40* mice occurs soon after birth with progressive bile duct proliferation, and ectasia accompanied by fibrosis of the portal tracts. Further detailed examination of the cholangiocellular ultrastructure revealed that cholangiocytes retained their normal appearance, with no ciliary abnormalities. Interestingly, in contrast to human ARPKD individuals, *Pkhd1ex40* mice develop morphologically and functionally normal kidneys. Thus, the *Pkhd1ex40* mutation mouse highlights the complexity of the role fibrocystin and primary cilia play on biliary tubulomorphogenesis, proving to be a valuable source of information to investigate biliary pathogenesis. Finally, the *Del2* mouse developed by Woollard et al [2007] as a model of ARPKD with biliary duct and PT dilatation, presents yet

another valuable resource in understanding the role of fibrocystin in the development of the renal and biliary tubular system.

1.6.1 THE *PKHD1*^{DEL2/DEL2} ARPKD MOUSE MODEL

Due to the generosity of our collaborators Dr. Peter Harris, and Dr Christopher Ward at the Mayo Clinic (MN, USA), the model studied in this project is the *Pkhd1*^{del2/del2} (*Del2*) mouse, developed by the Harris group to study the disorder ARPKD.

The *Del2* mouse was produced by targeted deletion of the murine *Pkhd1* gene using a LoxP flanked phosphoglycerate kinase (PGK) neomycin cassette system [Wagner et al., 2001] (Fig. 1.20). By targeting the first coding exon of *Pkhd1*, exon 2 which contains the start methionine and the signal peptide of fibrocystin, the resulting homozygous *Del2* mice were viable, fertile, and exhibited hepatic, pancreatic, and renal abnormalities.

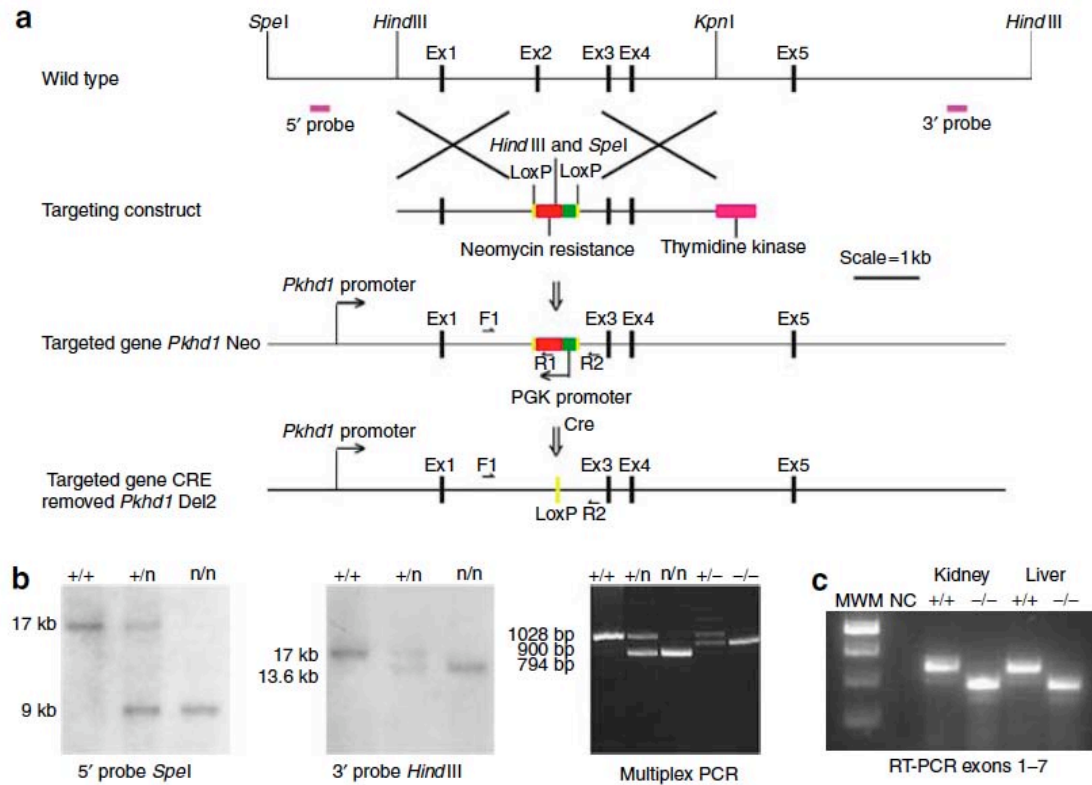


FIGURE 1.20 A schematic diagram of the knockout construct used to produce the *Pkhd1*^{del2/del2} mouse model of ARPKD. (a) The neomycin cassette was positioned in an orientation opposite to the *Pkhd1* promoter, replacing exon2. Exon 2 contains the start methionine and the signal peptide. Two LoxP sites flank the neomycin cassette so that it can be removed by the expression of Cre recombinase. (b) Southern blot analysis shows the expected DNA fragments using the 5' and 3' probes. The left panel shows genomic DNA cut with *Spe*-1 with bands of the expected size 9 and 17 Kb; the middle panel shows genomic DNA cut with *Hind*III with bands of 17 and 13.6 Kb. The right hand panel is a 1.5% agarose gel with PCR products derived from primers F1 and R1/R2. The wt is 1028bp, the LoxP deleted allele is 900bp and the neomycin allele is 794bp. (c) Reverse transcription-PCR data confirming that exon 2 is skipped in both kidney and liver of homozygous mice. Taken with permission from [Woollard et al., 2007].

1.6.1.1 Hepatic phenotype of *Pkhd1*^{del2/del2} mice

Pkhd1^{del2/del2} mice develop fibrocystic disease of the liver. Upon gross inspection, livers are massively enlarged occupying much of the abdominal cavity and are macroscopically cystic (Fig. 1.21a). The biliary disease starts at one month of age with the development of tortuous bile ducts and enlargement of the portal triads. This progresses with age, at three months (Fig. 1.21c) and nine months (Fig. 1.21e), but portal fibrosis and cystogenesis become more prominent so that by twelve to fifteen months the liver is very cystic and fibrotic (Fig. 1.21f-g). At early stages, bile duct proliferation is evident in the portal areas with primitive tortuous bile ducts and reactive stroma (Fig. 1.21b-d).

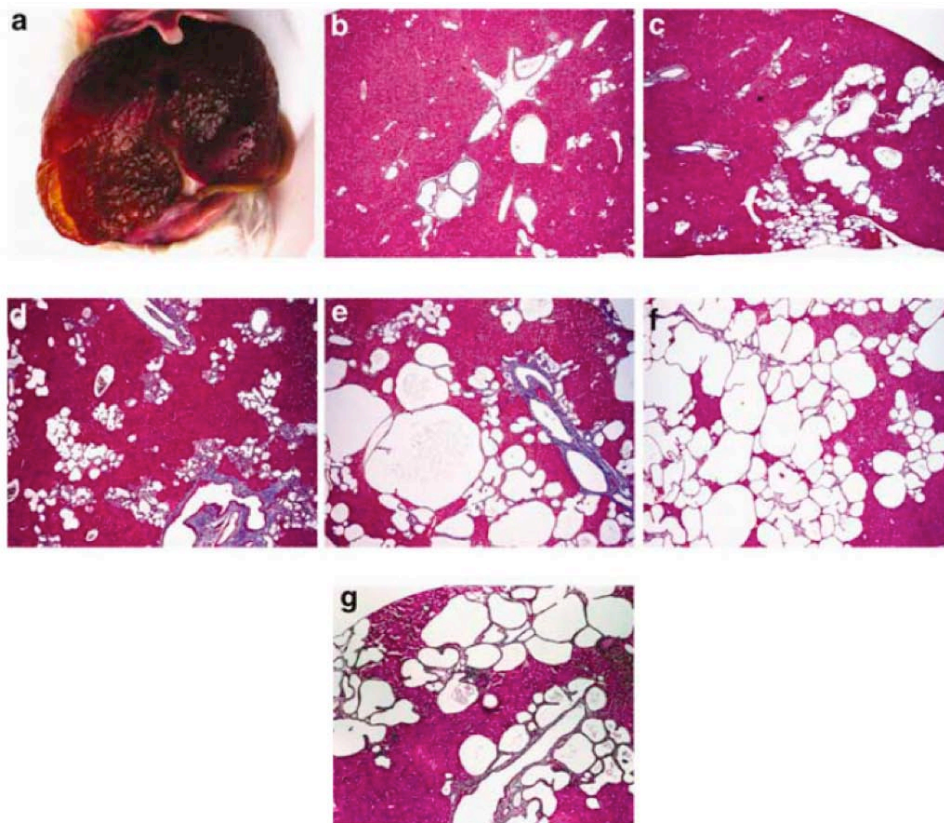


FIGURE 1.21 Gross appearance of *Pkhd1*^{del2/del2} liver from Mallory trichrome stained sections. (a) Gross appearance of 11 months outbred *Pkhd1*^{del2/del2} liver. (b-g) Sections stained with Mallory trichrome, (b) 1, (c) 3, (d) 6, (e) 9, (f) 12, (g) 15 months. The livers become more cystic and fibrotic with age. Original magnification of (b-g) is x10. Taken with permission from [Woollard et al., 2007].

1.6.1.2 Renal phenotype of *Pkhd1*^{del2/del2} mice

The kidneys of *Del2* mice appear normal until approximately nine months of age, when outbred females begin to develop cystic dilatation of the PTs (Fig. 1.22d-f). Outbred male kidneys remain unaffected up to eighteen months of age (Fig. 1.22a-c). Interestingly, female outbred animals exhibit an increase in PT diameter between nine and twelve months in both the wt and *Del2* animals. Woollard et al [2007] also reported that the increase in wt PT diameter is small yet significant, whereas the increase in the *Del2* PT is much greater. Inbred females display PT dilatation from three months of age on both BALBc/J and C57BL/6J backgrounds.

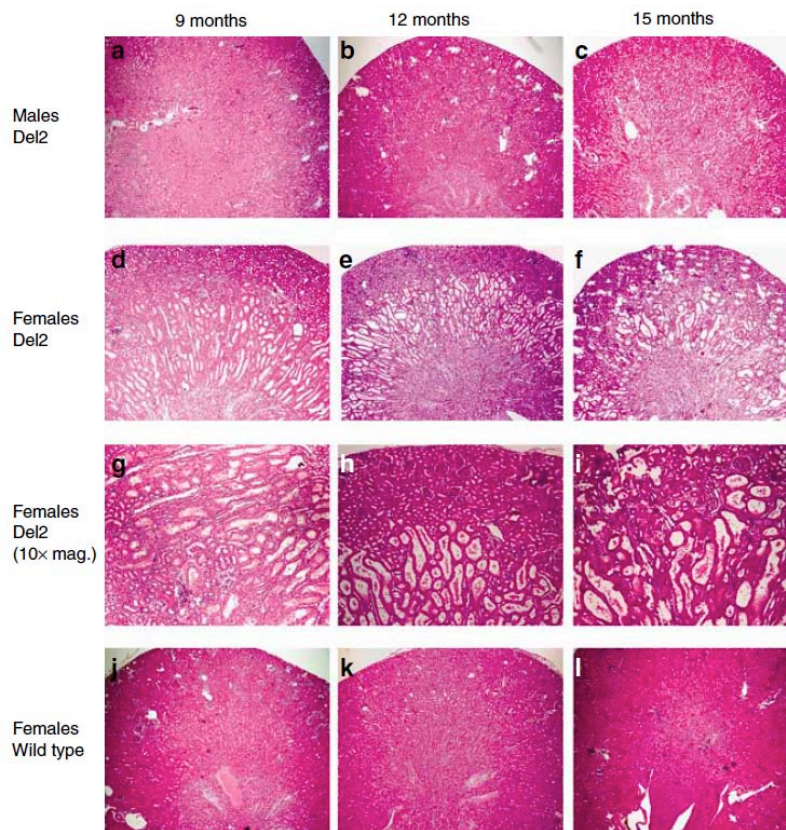


FIGURE 1.22 *Pkhd1*^{del2/del2} kidney sections stained with H&E. Kidneys from *Pkhd1*^{del2/del2} male mice at ages (a) 9, (b) 12, and (c) 15 months, respectively (original magnification x4). (d, e, and f) Kidneys from *Pkhd1*^{del2/del2} female mice at ages (d) 9, (e) 12, and (f) 15 months, respectively (original magnification x4). (g, h, and i) are high power views of the same female kidneys (original magnification x10). (j, k and l) Low-power views of wildtype female kidneys at (j) 9, (k) 12, and (l) 15 months, respectively (original magnification x4). Taken with permission from [Woollard et al., 2007].

1.6.1.3 Ciliary phenotype of $Pkhd1^{del2/del2}$ mice

There are conflicting reports about the ciliary morphology in animal models of ARPKD [T. V. Masyuk et al., 2003; Moser et al., 2005]. Using scanning electron microscopy (SEM) and fluorescent histochemistry, Woollard et al [2007] were able to show that the primary cilia in the affected biliary tree of *Del2* mice were significantly shorter versus wt cilia length (Fig. 1.23). Cilia were found to be misshapen, and surrounded by multiple small vesicular structures (Fig. 1.23f). In the kidneys of nine-month-old *Del2* animals, vesicular structures were observed surrounding the primary cilia. Most interestingly, cilia appeared as branched clumps. In animals with advanced cystic disease, the cilia from cyst lining epithelial cells were found to be stunted and highly branched or 'star-burst' in form (Fig. 1.23 d and h).

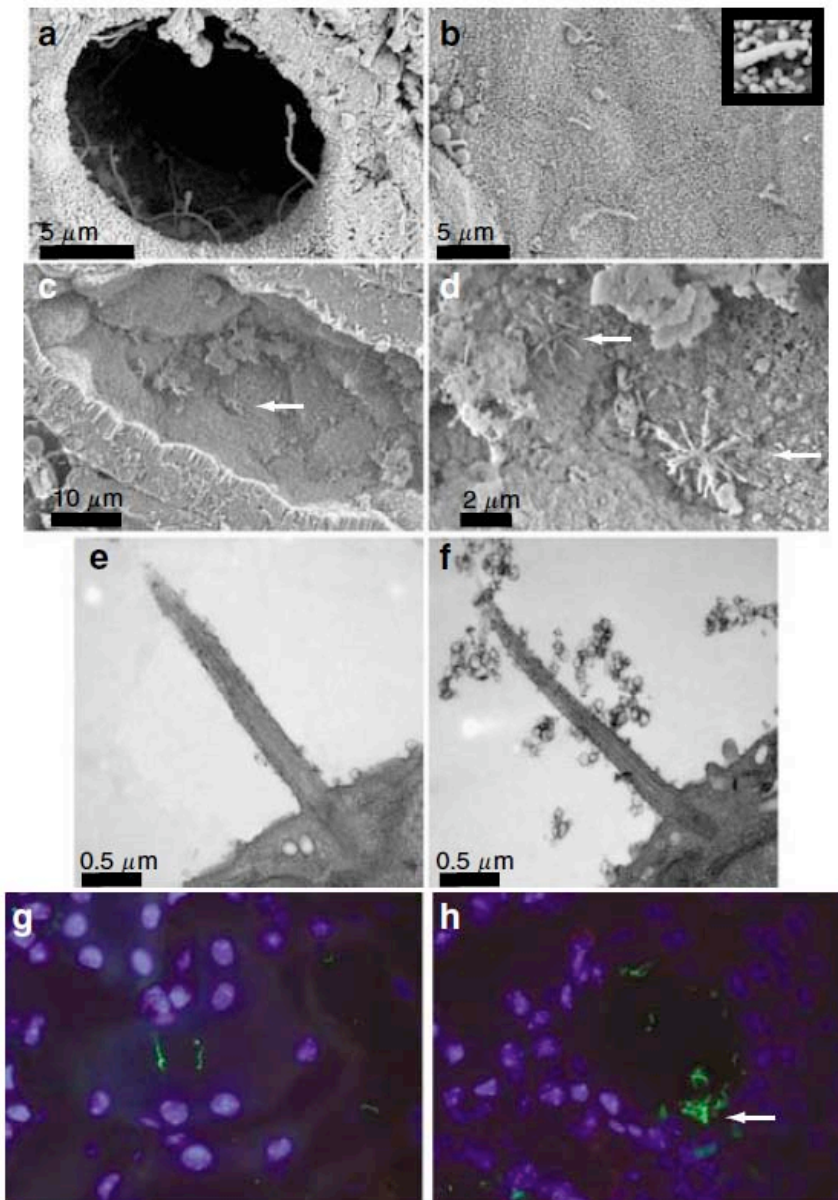


FIGURE 1.23 Primary cilia in bile duct and proximal tubule by SEM and fluorescent histochemistry. (a) A normal bile duct with normal cilia from a wt animal 3 months of age. (b) Three month biliary tree from a *Pkhd1*^{del2/del2} animal showing shorter and malformed cilia, see inset. (c and d) In the PT, brush border is still visible in these early dilatations (9 month *Pkhd1*^{del2/del2} animals) but appear disorganised. The cilia at this early stage are ‘starburst’ (arrows in c and d). This implies gross cilial dysfunction in these animals. Inset shows a branched primary cilium. (e and f) TEM of wt biliary cilia (e) and *Pkhd2*^{del2/del2} biliary cilia (f) note the small vesicular structures around the cilium. (g and h) Staining of PT cilia by anti-acetylated α -tubulin (green) and nuclei by DAPI (blue) in the wt (g) and *Pkhd1*^{del2/del2} (h). Note the ‘starburst’, highly branched cilia in (h) (arrow). (g-h, Original magnification x40). Taken with permission from [Woollard et al., 2007].

In summary, the *Del2* mouse model of ARPKD develops both cystic liver and pancreatic disease regardless of gender. The PT dilatation in the kidney is seen in the female mouse relatively late in the animals' life, nine months on an outbred background, and around three months in the inbred lines.

An interesting aspect of this animal model is that the renal disease is restricted to the female whilst the male appears to be protected [Woollard et al., 2007]. The difference in renal disease between the sexes could be due to sexual dimorphism in the S3 segment of the PT, as is evident from the restricted PT dilatation in wt females as they age. This difference in morphology is thought to be due to the differential effects of androgens, and more specifically could be driven by oestrogen.

The effects of oestrogen on classical endocrine target organs, such as the female reproductive tract, mammary gland, ovary, and neuroendocrine system have been thoroughly studied. However, knowledge of the effects of oestrogen in non-classical endocrine organ systems such as cardiovascular, immune, gastrointestinal, renal, and hepatic, is now starting to become more appreciated [Korach and Wintermantel, 2007].

Knowledge of the renal cortex as an oestrogen-sensitive target organ is long-standing [De Vries et al., 1972; J. A. Johnson et al., 1970; Kochakian, 1947], as demonstrated by (i) the presence of a specific oestrogen receptor, (ii) the observed increase in oestrogen receptor levels

after prolonged oestrogen treatment, (iii) an increased progesterone receptor level following oestrogen treatment, and (iv) stimulated growth of proximal tubular cells *in vitro* [Han et al., 1999; J. J. Li and Li, 1987; J. J. Li et al., 1974; Oberley et al., 1989].

Oestrogen receptors (ERs) are expressed in both hepatocytes and cholangiocytes, where oestrogen may play a role in the process of growth, regeneration, and proliferation *in vitro* and *in vivo* [Alvaro et al., 2002a; Alvaro et al., 2002b; Desmet et al., 1998]. After partial hepatectomy, for example, ER expression in hepatocytes increases together with their translocation to the nucleus, where they induce DNA synthesis and allow restoration of normal liver mass [Blum and Cannon, 1998; Eagon et al., 1996]. The characteristic selective proliferation of residual bile ducts to compensate for the disappearance of bile ducts in response to damage typical of cholestatic liver disease has also been shown to be associated with a marked increase in the expression of ER, and enhanced estradiol serum levels [Alvaro et al., 2002a; Alvaro et al., 2002b; Desmet et al., 1998]. In fact, oestrogens have also been proven to reduce cholestasis induced cholangiocyte apoptosis [Svegliati-Baroni et al., 2006].

Oestrogens are also involved in liver growth in the neonate, and long-term administration for pharmacological purposes in adults induces enlargement of liver mass [Alvaro et al., 2000a; Eagon et al., 1985]. Several studies have addressed the relationship between ER expression, oestrogen metabolism, and biliary secretion, and the development and course of chronic liver diseases [Eagon et al., 1985]. Currently there is much evidence supporting the role of oestrogen in proliferative disorders such as neoplasias and cystogenesis. Studies in ADPKD

patients have reported a female predominance in the risk of developing chronic hepatic involvement and cysts, with a reported female prevalence of 58% to 75%, compared to a 42% to 62% prevalence in males [Gabow et al., 1990].

However, the mechanistic involvement of oestrogen in the aetiology and pathogenesis of such disorders has only recently started to be investigated. Chromosomal instability and centrosomal anomalies are observed in cystic cells from patients with ADPKD. Studies by Li et al [2004] concluded that oestrogen is causally linked via the ER to overexpression of the centrosome kinase Aurora A and γ -tubulin, centrosomal amplification, chromosomal instability, and aneuploidy.

To summarise, simulated models enable a greater understanding of the clinical aspects of the disease process, and provide insight into the immunological aspects of BA. However, as these models are created by physical/viral manipulation they cannot provide clues towards a definitive genetic cause. However, this does not mean something cannot be gained from the study of animal models displaying similar pathologies. Any insight into the pathogenesis of various aspects of BA can only serve to draw research closer to determining the cause(s) of this complex disorder.

1.7 INTRODUCTION SUMMARY

BA is an idiopathic disorder of infants in which there is localised progressive obliteration or discontinuity of the extrahepatic biliary system at any point between the porta hepatis and the duodenum, accompanied by a characteristic intrahepatic lesion. Incidence figures vary widely, with an estimated worldwide incidence of 1 in 8,000 to 12,000 live births [Balistreri et al., 1996]. At present, there is no specific therapy for BA; restoration of bile flow by HPE within the early stages of the disease can prove successful in up to 60% of cases. However, it is not curative and 70-80% of children will still require a liver transplant despite undergoing HPE, making BA the main indication for paediatric liver transplantation.

BA occurs in two clinical forms: a) the more common perinatal or non-syndromic type, and b) the foetal (embryonic) or syndromic type. Non-syndromic presentations are characterised by late onset cholestasis and absence of congenital anomalies. In contrast, the embryonic or foetal cases of BA are characterised by early onset cholestasis and are often associated with congenital anomalies.

The cause of BA is not known at present, however several theories as to the underlying pathogenetic mechanisms are under investigation. These include viral infection, immunologic dysregulation, autoimmune mechanisms, vascular lesion/arteriopathy, defective morphogenesis (inherited mutations, somatic mutations, modifier genes), and toxin exposure. Evidence of a polygenic multifactorial basis is supported by a number of early studies describing familial instances of BA [Cunningham and Sybert, 1988], sibships in which two or

more siblings were affected [Krauss, 1964], and discordance for the non-syndromic form of BA in monozygotic twins [Hyams et al., 1985; Strickland et al., 1985].

A number of reports in the literature have described disorders that display clinical features that resemble BA, which are caused by mutations, or perturbations in the expression of certain genes encoding proteins which localise to primary cilia, basal bodies, and/or centrosomes, and have also been shown to be important in tubulomorphogenesis. These notable features include renal cysts [Bassett and Murray, 2008], anomalies of *situs* determination [M. Davenport et al., 1993], and evidence of DPM [Low et al., 2001]; underlining a pathogenetic mechanism possibly linking left-right axis determination, renal and hepatic tubulomorphogenesis, and primary cilia function. The disorders and diseases that display these features in various combinations are those belonging to two large groups, the cholangiopathies, and the ciliopathies. Of the many syndromes and disorders falling within these two large groups a subset of disorders stand out. The hepatorenal fibrocystic syndromes are a group of severe monogenic conditions that present in the neonatal and paediatric age, with consistent developmental abnormalities involving the liver and kidneys associated with other developmental anomalies. Of the known hepatorenal fibrocystic syndromes, ARPKD stands out in relation to BA as it is characterised by significant hepatic involvement in all cases. All cases of ARPKD are caused by mutations in the gene *PKHD1*, encoding the novel protein fibrocystin.

Fibrocystin, a large receptor-like protein is a component of primary cilia in kidney epithelial cells, and biliary and pancreatic duct epithelia. Although the precise function of fibrocystin is unknown, studies have shown it to be important in ciliary function and epithelial tubulomorphogenesis in both the kidney and liver. Thus, *PKHD1* could be a key developmental gene that is expressed during the embryonic development of the biliary system. Loss of expression due to sporadic or germ-line mutations may lead to BA, either directly or via altered susceptibility.

The evident lack of a suitable experimental animal model of BA has hindered understanding the pathogenesis of this complex disorder. However, the existence of mouse models displaying phenotypes similar to those in patients with BA will aid understanding of the disease process and the molecular pathways involved.

1.8 HYPOTHESIS

Specific sequence variants and/or altered expression in a key gene of biliary development that encodes a protein that is a functional component of primary cilia may be associated with cyst development and cellular damage in human liver disease.

1.8.1 Project Aims

The initial aim of this project is to investigate the phenotypic variability of *PKHD1* associated disease in human and animal models. Especially in relation to the cholangiopathy biliary atresia, which shares a number of phenotypic features with ARPKD.

In order to meet this aim the key objectives of this project are as follows:

- 1) Perform an initial mutational screening of *PKHD1* in a small cohort of biliary atresia patients that develop renal cysts to determine if sequence variants in the *PKHD1* gene are associated with the pathogenesis of biliary atresia. The findings of the initial screen will help determine whether it is appropriate to extend the screening to a larger, more stratified cohort.
- 2) Carry out a preliminary series of immunohistochemical and/or immunofluorescence studies in tissue samples from patients with early and end-stage liver disease to determine if expression of fibrocystin is altered.
- 3) Establish an *in vitro* cell culture system using primary biliary epithelial cells, from a range of liver diseases, to determine if there are structural defects in the basal bodies or primary cilia of BEC that display altered fibrocystin expression.
- 4) Investigate the mechanism driving, *PKHD1* associated cyst development in the ARPKD mouse model *Pkhd1^{del2/del2}*, and the phenotypic difference in disease severity and progression in male and female animals.

These objectives were set out to determine the following:

- 1) If sequence variants of *PKHD1* are associated with cases of biliary atresia and renal cysts.
- 2) If altered expression of fibrocystin is a causative factor of human biliary disease, or a consequence of an altered cellular state.
- 3) If the biliary epithelia of patients with early or late stage liver disease have structurally or functionally defective primary cilia.
- 4) If a defect in the sensory function of BEC primary cilia can result in abnormal bile duct structure or function, culminating in their subsequent destruction.
- 5) Characterise the variable phenotypic features of altered *PKHD1* expression.
- 6) If altered expression of *PKHD1* can result in disorders that share select phenotypic features of ARPKD.

CHAPTER 2 EXPERIMENTAL APPROACHES

In order to ensure the aims of this project were met, and the results obtained accurate and of value, several areas of the experimental work had to be optimised.

2.1 IMMUNOHISTOCHEMISTRY

One of the main requirements of an experimental approach to immunohistochemistry is to ensure any staining observed is specific to the protein under investigation, and is not non-specific background. The proteins under investigation in this project, acetylated α -tubulin and fibrocystin, are known to co-localise to the primary cilia. Due to this overlap, it was decided to investigate the localisation and expression levels of these two proteins on separate tissue samples, as trying to determine the specific signal for each protein would introduce a greater margin for error if detection were attempted on a single sample.

The specificity of the antibodies and the recognised epitopes are also of great importance. The experimental work, with regards to acetylated α -tubulin, is based on the use of one commercially available monoclonal antibody, clone 6-11B-1 (Sigma, UK; Cat #T6793), specific to acetylated α -tubulin. The specificity of the antibody was determined by experiments binding antibodies to α -tubulin from various sources that were described by Piperno and Fuller [1985]. The antibody 6-11B-1 does not bind to acetylated lysine alone, but recognises an epitope present only in acetylated α -tubulin, making it a long-standing, well trusted antibody for specific detection of acetylated α -tubulin.

With regard to fibrocystin, a total of five monoclonal antibodies were generously provided by Dr Christopher Ward (Mayo Clinic, USA, MN). Ward et al [2003] generated four monoclonal antibodies to the cytoplasmic tail of the protein (as published) and four to the extracellular N-terminus. Using western analysis and immunohistochemical staining on a panel of normal human, mouse, and rat tissues, as well as tissue from ARPKD patients, this group confirmed specificity of the antibodies to fibrocystin. Of those antibodies tested by the group, four directed against N-terminal epitopes, and one directed against a cytoplasmic epitope were gifted for use in this project.

Appropriate tissue selection is also an important requirement for any immunohistochemical study. The method of tissue preservation can have numerous effects on different types of epitope, whether they are extracellular, cytoplasmic, membrane-bound, cytoskeletal, hydrophobic, or hydrophilic etc. Different fixatives used to preserve different specimen types can either conserve or destroy the antigenic epitope to which a monoclonal antibody is raised. Another important consideration for immunostaining is the type of section to use. Sections available for use in this study included unfixed (frozen) sections, and formalin-fixed paraffin-embedded (FFPE) sections. The choice of section in the project was therefore determined by which type would provide optimal results and allow the desired analysis to be carried out.

Taking all these factors into consideration, appropriate experimental conditions for each of the variables discussed above had to be determined. This included optimisation of the appropriate final working dilutions of the primary antibodies, to ensure they provided

optimal specificity and sensitivity. Assessment of the most suitable section type for both antigens was important; to ensure staining was acceptable for subsequent analysis. Finally, the most suitable fixative, which is dependent upon the type of section, had to be determined.

2.2 *INVITRO* CELL CULTURE

Studies trying to assess mechanisms of cellular pathophysiology often make use of cell culture systems to avoid the complexity of whole organ/animal experiments. Primary cultures are generally preferred above studies on cell lines as the latter often lose important characteristics and/or acquire biochemical/functional properties due to clonal selection and dedifferentiation [Charlton and Simmons, 1993; Cho et al., 2001; Kastner et al., 1993]. Thus, the first requirement of an experimental approach to primary cellular culture is an easy means of isolating the desired cell type whilst causing minimal stress to the cells, which may result in low yields or an altered state of differentiation.

Although the isolation, and culture of primary human cholangiocytes in two-dimensional culture systems is well established at the BCLR [Afford et al., 2001; Auth et al., 2001]. The expression of primary cilia by BEC in culture had not been established prior to initiation of this project. In order to examine protein isolation in primary cilia in single cells, a culture system in which primary BEC uniformly express primary cilia was an obvious requirement.

However, as fresh human tissue that will produce viable cells is a scarce resource, especially normal tissue, a suitable ciliated human cell line also had to be identified in which optimisations could be implemented. Unfortunately a suitable human cholangiocyte cell line is not available commercially, and a suitable cell line that is from tubular epithelium needed to be identified and also optimised to ensure uniform ciliary expression. The human embryonic kidney epithelial cell line, HEK293, was also investigated as a possible ciliated human tubular epithelial cell line.

In contrast to the relative ease of isolating primary BEC from human liver, the isolation and culture of murine primary BEC is very difficult. Whilst the ideal cells to study in terms of BA are BEC, this could not be fulfilled in this case. The isolation and culture of primary human BEC has been a long established practise within the BCLR since first being described by Joplin et al [1989]. In contrast however, the isolation and culture of murine primary BEC is not routinely practised for many reasons. While mouse cholangiocyte cell lines exist, the routine isolation and culture of primary cholangiocytes is not feasible. Although it is possible to isolate and culture primary BEC from murine liver using techniques such as microdissection or enzymatic dissection of the liver [Cho et al., 2001], these methods are very labour intensive and time consuming and yield only a small number of isolated cells. These techniques are less than suitable for routine use, and also expose the cells to oxidative or mechanical aggression that leads to diminished viability. In contrast however, isolation of primary proximal tubular cells (PTCs) from murine kidney, the segment most severely affected in the *Del2* knockout mouse, can be performed routinely. Terryn et al [2007] developed a quick and simple method by which primary cultures of murine PTCs can be

established without aggressive manipulation. Although the method described by Terryn et al for the isolation of murine PTCs will be described in greater detail in the following section (3.4.2), it did require modification to better meet the requirements of this project. The goal of Terryn's group was to establish a culture system that enabled study of both the apical and basolateral surfaces of the cell to enable electrophysiological characterisation [Terryn et al., 2007]. In contrast, the main requirement of this project was an easy and quick means of detection of primary cilia and centrosomes at a resolution that allowed centrosome numbers to be counted. Solid, impermeable cell growth support was most suitable as both structures would be visible without having to resort to confocal microscopy, which is costly and time consuming. Whilst being less than ideal for studying cells in an environment matched as closely as possible to an *in vivo* location, as a conventional long-standing technique it is a reasonable system to use in this case. The quality of immunostaining that can be achieved when using inserts is not optimal due to interference of the filter, which can be observed as a striped aspect on the image. Furthermore, the filter is not flat but an uneven surface, making it difficult to obtain a good focus on all cells of a monolayer. These aspects make filters less suited for immunohistological purposes compared with glass culture slides [Terryn et al., 2007]. Thus the ideal growth matrix used in conjunction with the glass culture slides had to be determined, one that would allow the cells to grow normally to confluence, remain differentiated and polarised, maintain their epithelial organisation, and most importantly produce primary cilia.

Of equal importance to the study of primary cell systems *in vitro* is the constitution of the culture medium used. Despite a detailed description of the medium used by Terryn et al

[2007], extra considerations had to be made due to the alterations made to the culture of the cells for this study, and the experimental conditions to be tested. The most significant alteration to the protocol described by Terryn and colleagues was the use of impermeable glass culture slides rather than permeable collagen-coated polytetrafluoroethylene (PTFE)-filter supports. This drastic change in culture conditions meant it was more than likely slight alterations to the basic composition of the culture medium would be required, thus optimisations of the most basic additive, FBS were carried out to determine the optimum concentration that would support cell growth. Furthermore, as the basis of this study is to determine the effect of oestrogen on centrosome duplication, a number of extra considerations were essential. As a cell culture additive FBS is used because it provides a mixture of nutrients, and growth and differentiation factors essential for normal cellular growth. This also includes steroid hormones, such as oestrogen. Therefore it was important to choose serum with reduced hormone levels that had been assayed to assure treatment efficacy. Using dextran/charcoal treated FBS reduces the levels of hormones and growth factors. This serum has been shown to be effective in reducing steroid levels for utilisation in oestrogen related investigations [Eagon et al., 1996]. Although much attention has been paid to the removal of hormones from sera and to the development of serum-free media for studies on hormone responsive cells in culture, less consideration is given to the possible hormonal activity of other media components [Berthois et al., 1986].

Phenol red is a pH indicator commonly used as an additive to cell culture medium. However, phenol red was found to be a weak oestrogen mimic. Berthois et al [1986] determined that at the concentrations used in tissue culture medium (15-45 μ M), phenol red has a significant

oestrogenic activity causing partial oestrogenic stimulation in oestrogen-responsive cells in culture. Therefore, as this study utilises oestrogen-responsive cells, and is based upon oestrogen-dependent observations all media used for growth of murine PTCs was phenol red free.

In terms of the actual levels of E2 used to treat the cells, levels below, equivalent, and excessive to physiological were used. The basal circulating plasma levels of E2 in young and aged mice are not a commonly studied area, making retrieval of relevant data on which to base these studies difficult. Levels published in readily available sources varied greatly [Dubal et al., 2001; Gong et al., 2003; Leng et al., 2005; Parkening et al., 1978]. Based on the data that could be found concentrations of 25, 75, and 500 pg/ml were used. 25pg/ml representing both lowest physiological levels reported, and also the average concentration found in untreated FBS (Invitrogen). 75pg/ml represents a higher physiological level, while 500pg/ml is excessive for any age of mouse at any stage within the oestrous cycle [Parkening et al., 1978]. The exact treatment of the cells with E2 is detailed in materials and methods section 3.4.2.2.

The development and normal functioning of cells depends on interactions with molecules in their microenvironment. The major classes of molecules that regulate cellular development and function, that need to be considered when performing *in vitro* studies include growth and differentiation factors, cell adhesion molecules, and the components of the extracellular matrix (ECM). The ECM is composed of a number of different macromolecules whose structural integrity and functional composition are important in maintaining normal tissue

architecture. The ECM exerts influences on behaviour (adherence, spreading, differentiation, and migration) and the pattern of gene expression of the cells in contact with it, and is intimately involved in both normal biological function and response to injury [Alberts et al., 1994].

To create a physiologically relevant *in vitro* system that would support normal cell growth and function, the components of the *in vitro* environment had to be considered. The use of ECM components as tissue culture surface matrices permits the development of model systems that closely mimic *in vivo* conditions. Thus, the choice of ECM was an important component to consider when optimising the *in vitro* culture system in this study. The ECM components readily available as pre-coated cellware or for coating culture vessels were gelatine, poly-lysine, collagen type I, and collagen type IV. Collagen, found in most tissues and organs is most plentiful in dermis, tendon and bone, it is an integral part of the framework that holds cells and tissues together, and has been recognised as a useful matrix for improving cell culture. *In vitro* use of collagen can exert effects on the adherence, morphology, growth, migration, and differentiation of a variety of cell types [Kleinman et al., 1987]. Collagen coated cell culture vessels are used not only to promote cell attachment and spreading, but also improves the survival of primary cells in culture [BDBiosciences]. Poly-D-lysine (PDL) and Poly-L-lysine (PLL) are synthetic components that enhance adhesion and protein absorption by altering surface charges on the culture substratum. In addition to promoting cell adhesion, poly-lysine surface treatments support the outgrowth, and improves survival of many types of primary cells in culture. As PDL and PLL are synthetic molecules, they do not stimulate biological activity in the cells cultured on them, and they do not introduce impurities carried by natural

polymers. Used in the culture of a variety of primary cell types poly-lysine applications include: attachment and spreading of a variety of cell types, attachment, support and survival of fastidious cells, and reduced serum culture [BDBiosciences]. Gelatine is a heterogeneous mixture of water-soluble proteins derived from the hydrolysis of collagen. Gelatine is commonly used in the culture of vascular endothelial cells, muscle, embryonic stem cells, and F9 teratocarcinoma cells as an attachment and growth-promoting substrate. Human fibronectin (HFN) is a widely distributed glycoprotein that is used as a substrate to promote attachment of cells through its central-binding domain RGD sequence. HFN is a product of most mesenchymal and epithelial cells, and is present in both the ECM and plasma. The principal function of HFN appears to be in cellular migration during wound healing and development, regulation of cell growth and differentiation and haemostasis/thrombosis. *In vitro* use of fibronectin as a cell support matrix shows that it promotes cell attachment and spreading, rapid expansion of cell populations and improved survival of primary cells in culture [BDBiosciences]. The variety of cell support matrices available meant optimisations were required to determine the ideal support matrix for all of the cell types included within this study.

The temperamental nature of primary BEC to grow well and maintain their differentiated state when in culture meant optimisation was required to determine the best possible support matrix for culture and manipulation of the cells. Of equal importance to the study was the suitability of the culture vessel material, not only for suitability for culture, but also optimal visual clarity for subsequent image analysis. The substrata under consideration were plastic culture slides (Permanox®, nunc), plastic coverslips (Thermanox®, nunc), acid washed glass

coverslips, and untreated glass coverslips. Culture substrata affect the adhesion, morphology, differentiation, and behaviour of various cell types. Glass is often used as a growth surface for cells that will undergo subsequent fluorescent staining since it has superior optical qualities and is naturally charged. Washing of glass coverslips with acid can further improve cell growth by helping cells and matrix molecules adhere more efficiently to the glass. Plastic culture vessels are also of acceptable optical quality. However, as most plastics are hydrophobic, and unsuitable for cell growth they are often treated to generate a charged, hydrophilic surface. Permanox™ plastic slides, and Thermanox™ coverslips are treated for optimal cell culture performance, and are also acceptable for fluorescent applications.

A vital requirement of an experimental approach to primary cilia is an easy means of detection. The tubulin based axoneme of primary cilia means they can be visualised using anti-tubulin antibodies. However, general tubulin staining reveals the whole microtubular cytoskeleton, which is especially dense around the centrosome region in which primary cilia occur, and would obscure visualisation of this organelle. This was of little value until confocal microscopy allowed greatly improved resolution on the narrow optical sections within which a primary cilium would nestle, along with many other positive structures. However, this is a costly and time-consuming method. Thus, this study makes use of the fact that primary cilia in cultured cells can be seen despite the high background of general tubulin staining without resorting to confocal microscopy [P. T. C. Ho and Tucker, 1989; Tucker et al., 1979b], a method which also allows analysis of primary ciliary expression through the cell cycle. The anti-acetylated α -tubulin antibody 6-11B-1 specific for the ϵ -amino group of acetylated lysine residues within α -tubulin stains primary cilia, centrioles, mitotic spindles, midbodies, and

small subsets of cytoplasmic MTs in mammalian cells with little general staining of the cytoplasmic network [Piperno et al., 1987]. This has been corroborated by many other laboratories working on primary cilia, and is now routinely employed for visualisation of this organelle [Wheatley et al., 1996]. It was also vital to ensure cells were at a state where expression of primary cilia was maximal. Within *in vitro* systems the degree of ciliary expression depends on several factors, including the state of cell division, confluency, and differentiation [A. C. M. Ong and Wheatley, 2003]. Therefore it was also important to determine the optimal number of days to maintain the cells in culture to allow for maximal ciliary expression without loss of cells due to competition for nutrients.

CHAPTER 3 MATERIALS AND METHODS

3.1 MUTATIONAL SCREENING

Work carried out in this chapter was done so in collaboration with the Birmingham Children's Hospital Liver Unit (BCHLU), and the Nephrology and Hypertension Group at the Mayo Clinic, MN, USA. Any work done by the collaborators will be highlighted in the appropriate sections. Mutational analysis study design, subjects, samples, sample preparation, sample analysis, and data retrieval was initiated and carried out prior to initiation of this thesis project, and therefore not carried out by myself. Subsequent analysis of data in relation to biliary atresia was carried out independently.

3.1.1 Subjects

Ten children with BA developed renal cysts at a median age of 9.5 years (range 0.25 - 14 years). Nine underwent liver transplantation, with eight presenting cysts post-transplantation. One developed renal cysts and has not required a liver transplant, and another had renal cysts detected prior to transplantation, Table 3.1. The screening of these ten samples was carried out alongside a panel of ARPKD patients, which therefore acted as the control samples. Details of the control samples were not made available for use in this project, except that none presented with BA like features.

TABLE 3.1 Table showing the clinical relationship between transplant status, renal cyst natural history, and changes in renal function. The results highlight that development and change in the size and number of renal cysts are independent of the transplant process, calcineurin inhibitor use, and renal dysfunction, in these cases.

Patient number	Type of biliary atresia	Age at diagnosis of biliary atresia (days)	Age at liver transplant (years)	Age at detection of renal cysts (years)	Natural history of cysts	IS at time of renal dysfunction	cGFR at conversion to MMF	cGFR after 1 year on MMF	Renal cyst relation to dysfunction conversion MMF
1	Perinatal	26	Not transplanted	0.83	0.83 year – multiple cysts bilaterally 5 years – no cysts detected 8 years – single cyst left kidney lower pole No changes to date				
2	Perinatal	28	0.66	14	14 years – 2.3cm cyst left kidney mid pole 15 years – 2 cysts in left kidney and 1.3cm cyst in right kidney 16 years – right increased to 2.1cm, left now septated	Cyclosporin	68	130	Cysts identified after conversion to MMF and increased in size and number since
3	Perinatal	63	4	10	10 years – 4.9cm cyst in left kidney mid pole 15 years – cyst increased to 5.4cm. New cysts in left kidney in upper pole	Cyclosporin	74	92	Cysts identified prior to the conversion to MMF. Number of cysts increased since conversion.
4	Perinatal	49	5	10	10 years – 1.2cm right kidney mid-pole. No changes to date	Cyclosporin	Remains on cyclosporin	N/A	No renal dysfunction and no changes in cyst morphology or number
5	Perinatal	42	0.83	8	8 years – 2 cysts in right upper pole and 1 left upper pole. No changes to date	Tacrolimus	29	14	Cysts identified at time of dysfunction and have not changed since conversion to MMF
6	Perinatal	67	0.66	3	3 years – 1cm cyst left upper pole. No changes to date	Cyclosporin	Remains on cyclosporin		No renal dysfunction, no change in cyst morphology or number
7	Perinatal	21	2.2	0.25	0.25 years – 3mm mid-pole left kidney on CT scan. Undetectable on US scan	Tacrolimus	Remains on tacrolimus		
8	Perinatal	133	0.83	12	12 years – 1cm upper pole right kidney 16 years – cyst not detected since	Tacrolimus	41	71	Cysts detected at time of dysfunction and have not changed since
9	Perinatal	49	0.75	12	12 years – 2 small cysts lower pole left kidney 15 years – several cysts bilaterally in all poles	Tacrolimus	59	81	Cysts detected following conversion to MMF
10	Perinatal	56	1.33	9	9 years – multiple cysts bilaterally 13 years – many more cysts all larger in size 15 years – all cysts developed irregular walls	Tacrolimus	7	41	Cysts detected at the time of dysfunction and have increased in size and number since conversion to MMF

IS – Immunosuppression; cGFR - calculated glomerular filtration rate, calculated using the Schwartz formula (height(cm) x 40/creatinine (µmol/l)); MMF – Mycophenolate mofetil

3.1.2 Methods

All children attending the BCHLU undergo examination of liver and kidneys. Retrospective reviews of all patient records from children diagnosed with BA at this unit, between 1984 to present day were investigated for the presence of renal cysts. The diagnosis of BA was confirmed by histological examination of the obliterated biliary tract at the time of Kasai HPE. Renal cysts were identified during routine patient care with abdominal imaging (either ultrasound or CT scan). Blood samples for DNA extraction were obtained by clinical staff at the BCH liver unit with the full consent of the patients and/or their families, with ethical approval from The South Birmingham Ethics Committee. DNA was extracted from samples at the regional genetics laboratories at Birmingham Women's Hospital prior to initiation of this thesis project.

Once purified, DNA for mutational analysis was sent to the Nephrology and Hypertension labs at the Mayo Clinic, MN, USA, where samples were processed by members of the Harris group. Mutational analysis of the gene *PKHD1* was undertaken using both denaturing high-performance liquid chromatography (DHPLC) and direct sequencing. Possible mutations detected by DHPLC were characterised by direct sequencing and changes compared to previously described mutations and polymorphisms in the ARPKD Mutation Database (www.humgen.rwth-aachen.de). DNA was amplified by standard PCR techniques using exon flanking primers covering the exon and splice sites [Rossetti et al., 2003]. The ABI 3.0 BigDye™ system was used to sequence the exonic and flanking intronic regions and analysed using an ABI3730 DNA analyser. Sequences were screened for variants using the Mutation Surveyor program, and any pedigrees drawn up. Any polymorphisms or mutations found by

the group were then forwarded on to myself for further interpretation in relation to this project. The likely pathogenicity of any changes found was based upon the chemical differences of the substitution [R. Grantham, 1974]; the degree of conservation in mouse, rat and chicken orthologs [Hogan et al., 2003]; and whether the change had previously been described as pathogenic (or as a polymorphism). The conservation of residues was tested by BLAST using the NCBI website (www.ncbi.nlm.nih.gov/BLAST/), and sequences were aligned with the online COBOLT Constraint-based multiple alignment tool (<http://www.ncbi.nlm.nih.gov/tools/cobalt/>).

3.1.3 Statistical analysis

A 2X2 contingency table was used to determine if there was a significant difference in the number of patients with BA that presented with cysts, and the number of patients transplanted for other liver diseases that also presented with cysts. Although the total number of samples was not small, there were however only two groups, and one factor with two outcomes. The Fisher's exact test, and the chi-squared test of association were used to determine if the association between the two groups (patients with BA, and patients without BA), and the two outcomes (cysts and no cysts) was statistically significant.

3.2 IMMUNOHISTOCHEMISTRY IN HUMAN TISSUE

Independent contributors to the analysis conducted in this chapter were: Dr G. M. Reynolds (GMR), Professor S. Hubscher (SH), and Dr S. C. Afford (SCA). All other work conducted in this chapter was done so unaided.

3.2.1 Cohort

The cohort of patients used within this study were chosen to represent a range of disease aetiologies and histological properties in order to determine the effect of multiple disease processes on fibrocytin expression and α -tubulin acetylation. To clarify the classification of these diseases in terms of inflammatory, malignant, cystic etc, a table summarising the characteristic features of each disease can be found in appendix 2, table 2.2.

3.2.2 Cases

Cases were selected from the pathology archive at the University of Birmingham, and the BCH. Age and gender information was available for most patients, however all patient information and identifiers were removed for subsequent analysis.

In total, liver tissue from sixty patients was available for the present study from an array of diseases falling into the following groups; inflammatory, malignant, and cholangiopathic. This included adult polycystic liver disease (PCLD), n=6; primary biliary cirrhosis (PBC), n=5; primary sclerosing cholangitis (PSC), n=5; autoimmune hepatitis (AIH), n=5; hepatitis C virus infection (HCV), n=5; chronic alcoholic liver disease (ALD), n=5; α -1-antitrypsin deficiency (α_1 ATdef.), n=5; biliary atresia (BA), n=11, biopsies taken at Kasai HPE (early-stage) and end-stage; and hepatocellular carcinoma (HCC), n=5. Normal liver (NL) tissue surplus to transplantation requirements was used as a control, n=5. All end-stage tissue was obtained from donors who had consented to the research use of explants.

3.2.3 Methods

3.2.3.1 Paraffin-embedded section preparation: Agitated low-temperature epitope retrieval

Archival haematoxylin and eosin (H&E)-stained slides were examined by an independent pathologist (GMR) to determine suitability of the specimen for inclusion within the study.

Prior to the immunohistochemical assay, 4µm tissue sections were prepared onto commercial, charged microscope slides (SurgiPath, UK) and heated for 1 hour at 65°C before use. Sections were then subjected to agitated low-temperature epitope retrieval (ALTER) using a modified method that has been previously described [Reynolds et al., 2002]. In brief, sections were routinely dewaxed and dehydrated, followed by a wash in tap water. Slides were incubated in 1mmol/l ethylenediaminetetraacetic acid (EDTA), pH8.0 with 0.01% Tween20 on a hot-plate stirrer at 60°C for 16 hours (overnight). Agitation was achieved using a 30x5mm magnetic bar, with the stirrer set at 600rpm.

Sections were washed in tap water and mounted onto a Sequenzer (Shandon, UK). The Sequenzer is a semi-automated staining station, where sections are mounted onto cover plates (as per manufacturers instructions) and all washes and incubations are performed by applying the solutions to the reservoir at the top of the cover plate for ease of processing. As the detection system used was peroxidase based, the sections were incubated with Dako peroxidase blocking reagent (Dako, Cat# S2001) for 10 minutes at room temperature, to suppress non-specific staining due to endogenous peroxidase and pseudoperoxidase activity. After a tris buffered saline (TBS) wash pH7.6, sections were probed with optimally diluted

primary antibody (as indicated in later sections) for 1 hour at room temperature. Slides were washed in TBS, pH7.6 containing 0.01% Tween20.

The detection system used was a universal peroxidase/DAB kit, the DAKO ChemMate™ Envision detection system (DAKO, UK, Cat #K5007). Briefly, this involved a 30-minute incubation with the rabbit/mouse ENV detection reagent; which consists of a dextran backbone to which a large number of horseradish peroxidase (HRP) molecules and goat anti-mouse and goat anti-rabbit secondary antibody molecules have been coupled. Following the final TBS/Tween wash, sections were removed from the Sequenzer and incubated for 5 minutes with the tertiary substrate: a two-component DAB+ chromogen solution, and substrate buffer containing hydrogen peroxide. This produces a crisp brown end product at the site of the target antigen that can easily be visualised using light microscopy. Following a final wash in tap water, sections were counterstained in Mayer's Haematoxylin (SurgiPath, UK), dehydrated, cleared, and mounted with a glass cover-slip in a permanent resin based mounting medium, DPX (SurgiPath, UK).

3.2.3.2 Frozen tissue section preparation

Snap frozen tissue blocks were mounted into 'OCT' cryo-embedding media (Sakura, Japan) before sectioning on a cryostatic microtome. Prior to immunohistochemical assay, 5µm cryostat sections were cut and mounted onto gelatine coated glass microscope slides and allowed to air-dry for 30 minutes. The slides were then placed in fixative for 10 minutes (as in section 3.2.4.1) and air dried before being foil wrapped and stored at -20°C, until needed.

Before staining was carried out, slides were warmed to room temperature in the foil wraps before being removed and post-fixed in acetone for 10 minutes. Once fixed slides were mounted on a Sequenzer (Shandon, UK) and washed in TBS, pH7.6. Endogenous peroxidase activity was then blocked by incubating the sections with Dako ready-to-use peroxidase blocking reagent (Dako, UK, Cat# S2001), for 10 minutes. After washing with TBS, pH7.6, sections were incubated with primary antibody, optimally diluted in TBS for 1 hour, followed by a TBS/Tween wash. Secondary detection was carried out using the Dako ChemMate Envision system as previously described (Section 3.2.3.1). Following a final wash in tap water, sections were counterstained with Mayer's Haematoxylin (SurgiPath, UK), dehydrated in alcohol, cleared in xylene, and finally mounted with a cover-glass in DPX (SurgiPath, UK).

3.2.4 Optimisations

3.2.4.1 *Frozen tissue section fixative panel*

The following panel of liquid fixatives were used to fix frozen sections after cutting, in an attempt to determine which best maintains tissue morphology whilst having the least detrimental affect on epitope availability. A combination of both crosslinking and coagulant fixatives were included (Table 3.2).

TABLE 3.2 Frozen tissue section fixative panel

Coagulant Fixatives	Crosslinking Fixatives
Iced methanol	4% Paraformaldehyde in PBS
Ice cold methanol:acetone (1:1)	Formal saline (formaldehyde, formalin)
Iced ethanol (absolute)	
Acetone	

Each fixative was applied for 10 minutes, before sections were air dried and stored at -20°C. Once required for use, sections from 5 cases of normal human liver were stained using the section preparation method described in section 3.2.3.2. The primary antibodies included within these optimisations were two of the fibrocystin monoclonal antibodies raised to the extracellular region of the protein: clones 11 and 19. Antibody dilutions were also titrated at 1:25, 1:50, 1:100, and 1:200 in order to determine the optimal titre for each antibody if frozen tissue were to be used for the full study. Controls included monoclonal antibody raised against the BEC marker human epithelium antigen (HEA) 125 at a dilution of 1:100; the negative control lacked a primary antibody and was incubated with TBS alone.

3.2.4.2 Primary antibody titrations on paraffin-embedded tissue sections

All antibodies under consideration for use, were titrated to determine which provided the highest levels of specificity and sensitivity on FFPE tissue. The details of each antibody and the titrations used are detailed in table 3.3. The titrations were carried out on normal liver tissue only for fibrocystin, and normal and PBC for acetylated α -tubulin.

TABLE 3.3 Primary antibody titrations

Target antigen	Clone	Stock concentration (mg/ml)	Titration dilutions
Acetylated α -tubulin	6-11B-1	1.6	1:25, 1:50, 1:100, 1:200
Fibrocystin (C-term)	5a	0.5	1:50, 1:100, 1:200, 1:400, 1:800
Fibrocystin (N-term)	11	0.38	1:50, 1:100, 1:200, 1:400, 1:800
Fibrocystin (N-term)	14a	0.57	1:50, 1:100, 1:200, 1:400, 1:800
Fibrocystin (N-term)	18	0.27	1:50, 1:100, 1:200, 1:400, 1:800
Fibrocystin (N-term)	19	0.59	1:50, 1:100, 1:200, 1:400, 1:800

Key: C-term = Carboxyl-terminus; N-term = Amino-terminus

Positive and negative controls consisted of a monoclonal antibody directed against the BEC marker HEA125, and exclusion of primary antibody, respectively. Immunohistochemical staining was carried out as described in section 3.2.3.1.

3.2.5 Analysis

All optimisation immunostaining was evaluated microscopically by a pathologist (GMR) to determine the experimental conditions that produced the cleanest, most specific staining.

3.2.6 Liver disease cohort studies

Once optimal experimental conditions had been determined, the full cohort study was conducted using archival, FFPE tissue. Immunohistochemical staining was carried out as described in section 3.2.3.1. The optimal primary antibody dilutions used were: anti-acetylated α -tubulin (6-11B-1) at 1:200, and anti-fibrocystin (5a) at 1:100. All other conditions, as described in section 3.2.3.1, remained unaltered. Normal human tissue was used as a reference point to assess disease altered expression levels and protein localisation. Negative controls consisted of randomly selected samples from within the study cohort, in which primary antibody was substituted with a mouse monoclonal immunoglobulin G (IgG) antibody for comparison.

3.2.6.1 Immunohistochemical analysis

Three independent investigators evaluated immunostaining microscopically using the Axioskop 40 (Zeiss, UK). Specificity of staining was assessed by a pathologist (GMR), to ensure accurate results. Standard of staining, and quality of specimen morphology was evaluated by a pathologist (SH), who was unaware of the expected pattern of staining. Histologic scoring was performed by one investigator (SCA), and verified by two pathologists independently (GMR and SH). Images were captured using the AxioCam MRc5, and edited using AxioVision software (Zeiss, UK).

The peroxidase immunostaining was analysed at various magnifications using an upright transmission light microscope. A semiquantitative method was used to assess fibrocystin expression in whole ducts, based on the extent and intensity of staining. This included patent ducts, as well as ductules and reactive ductules, based upon all ductular epithelial cells staining consistently. The intensity of staining was graded as follows: -, no visible staining; +, faint staining on cells; ++, moderate staining on most cells; +++ intense staining on cells. A grade of \pm was used to represent questionably weak positive cells in tissue sections. An overall analysis of staining for both fibrocystin and acetylated α -tubulin within the tissue was also performed, taking into account the general histopathology of the specimen and any inflammatory infiltrates.

3.2.6.2 Statistical analysis

Data for fibrocystin was expressed as a percentage of positive 'ducts' from all ducts counted per specimen. Samples with no visible ductal structures detectable at low magnification (x10) received a count of 0%. For statistical analysis, data were expressed both as total percentage positive for each disease group, and mean percentage positive within each specimen type, comparison between groups was calculated using a 1-tailed t-test, with the assumption of unequal variances. Statistical analysis was performed using SPSS software (SPSS Inc., Bologna, Italy). All quoted p-values are one sided and statistical significance relates to results in which the p-value is <0.05.

3.3 HUMAN *IN VITRO* CELL CULTURE

3.3.1 Culture and optimisation of the human embryonic kidney (HEK 293) cell line

3.3.1.1 Chemicals and plasticware

Tissue culture plasticware was obtained from corning. GlutaMAX™ high glucose Dulbecco's modified Eagle's media (DMEM) with phenol red (1x liquid), non-essential amino acids (x100 liquid), foetal calf serum (FCS), penicillin/streptomycin liquid, Trypsin-EDTA solution, 1x phosphate buffered saline (PBS), bovine serum antigen (BSA), and normal goat serum (NGS) were purchased from Invitrogen (Paisley, UK). All other chemicals were purchased from Sigma (Dorset, UK), unless stated otherwise.

3.3.1.2 Cell lines

Human embryonic kidney cell line HEK293 was purchased from ATCC via LGC Promochem (Middlesex, UK). Cells were resuscitated as recommended by the manufacturers instructions.

3.3.1.3 Growth conditions

HEK 293 cells were maintained in GlutaMAX™ DMEM supplemented with 10% FCS, and penicillin (50 Units/ml), streptomycin sulphate (50µg/ml) until 100% confluent.

For plating out, media was aspirated from the cell monolayer and the cells washed with warm PBS. Cells were trypsinised to release them from the flask by a 5-minute trypsin digestion at 37°C. Trypsin was inactivated by the additions of the aspirated media made up with warm PBS. Cells were pelleted by centrifugation at 1000rpm for 5 minutes, and resuspended in the appropriate amount of media needed. Cells to be used for subsequent immunostaining were seeded at high density onto gelatine coated glass coverslips placed in 6-well plates. Once plated, cells were left for 3 days to settle and grow to confluency before immunostaining.

3.3.1.4 Assessment of ciliary expression by immunostaining

Once confluency was reached cells were maintained at 100% confluency for 1, 3, or 5 days, media was changed every 24 hours. After removal of old culture medium, 100% confluent monolayers of HEK293 were washed with PBS before fixation in 4% paraformaldehyde.

After permeabilising with Triton X-100, and quenching with 0.01M glycine in PBS. Cells were blocked in 10% NGS in buffer (1% BSA in 1x PBS) for 30 minutes. After washing in buffer, monolayers were incubated with primary antibody diluted in buffer for 1 hour. After washing monolayers were incubated for 1 hour in the dark with the appropriate fluorophore-conjugated secondaries, optimally diluted in buffer. Monolayers were then washed in PBS before mounting onto a microscope slide using Vectashield® anti-fade mountant with DAPI.

3.3.1.5 Antibodies

Immunostaining for cilia analysis was performed using mouse monoclonal antibodies against acetylated α -tubulin (6-11B-1) (Sigma, UK), and fibrocystin (clone 5a). Fluorophore-conjugated subclass specific secondary immunoglobulin combinations to achieve dual labelling included: fluorescein isothiocyanate (FITC), and sulphorhodamine 101 acid chloride (Texas red/TxRed) conjugated goat anti-mouse antibodies. Negative controls were treated identically to test samples, except with exclusion of primary antibody, secondary antibody, or both primary and secondary.

3.3.1.6 Image capture and analysis

Stained cells were analysed for the presence of primary cilia using the Axioskop upright epifluorescence microscope (Zeiss, UK). Images were captured using the AxioCam MRc5 and AxioVision software (Zeiss, UK).

3.3.2 Biliary epithelial cell isolation and culture

All tissue was obtained with the consent of the patients or their relatives, and approved by the South Birmingham Research Ethics Committee.

3.3.2.1 *Chemicals*

Collagenase type IA, RPMI-1640 medium, DMEM, Ham's F12 nutrient medium, L-Glutamine-Penicillin-Streptomycin (GPS), hydrocortisone, cholera toxin, and triiodo-L-thyronine (T₃) were purchased from Sigma (Dorset, UK). Percoll™ was purchased from GE Healthcare (UK). Mouse anti-human anti-EpCAM (HEA125) antibody was purchased from Progen Biotechnik (Germany). Recombinant human hepatocyte growth factor (HGF), and epithelial growth factor (EGF) were purchased from Peprotech (London, UK). Insulin was acquired from the Queen Elizabeth Hospital pharmacy (Birmingham, UK). Human serum was purchased from HD Supplies (Buckingham, UK). Dynabeads® and TrypLE™ cell dissociation enzyme were purchased from Invitrogen (Paisley, UK). Nylon mesh was purchased from John Stanier & Co. (Manchester, UK). Collagen was made in-house from rat-tails.

3.3.2.2 *Primary cell culture*

Primary BECs were cultured under sterile conditions from collagenase-digested liver tissue from normal livers, and a number of liver diseases using methods modified slightly from that described by [Joplin, 1994].

Briefly, 80-100g of liver tissue was minced with scalpels on a chopping board. Minced liver was digested in 20ml PBS and 5ml sterile filtered collagenase type IA incubated at 37°C for 30 minutes with intermittent agitation. After digestion, the digested liver was sieved through fine nylon mesh (pore size 63 microns), and washed through with PBS to make the final volume up to 160-200ml. The cell suspension was then aliquoted into 8 universals and centrifuged at 2000rpm for 10 minutes. The supernatant was discarded, and the 8 pellets pooled into 4 universals were washed once more with PBS by centrifugation at 2000rpm for a further 10 minutes. This washing procedure was repeated twice more until only one universal remained containing the cell suspension. The cell suspension was then carefully layered onto a 33% and 77% iso-osmotic Percoll™ gradient in 8 conical tubes and centrifuged at 2000rpm for 30 minutes. The interface layer was collected into 4 universals, made up with PBS and washed by centrifugation at 2000rpm for 5 minutes. Washing was repeated twice more, pooling the pellets until a single universal remained. The supernatant was discarded, and the remaining pellet resuspended in 500µl ice-cold RPMI, and incubated with BEC-specific mouse monoclonal antibody to HEA125 for 30 minutes at 37°C with intermittent agitation. Cells were washed once more with 10ml PBS by centrifugation at 2000rpm for 10 minutes. The supernatant was discarded, and the remaining pellet resuspended in 500µl RPMI, with the addition of 10µl sheep anti-mouse IgG1-coated Dynabeads®. The cell and Dynabead suspension was incubated on ice for 30 minutes with constant agitation. BEC were then positively selected by magnetic separation. The cell and Dynabead suspension was placed on a Dynamag™ magnet for 5 minutes. With the tube remaining in the magnet, the supernatant was removed and discarded. The magnetic separation step was repeated once more to wash away non-specific cells and cellular debris. Cells and attached beads were resuspended in 5ml

of BEC culturing media: Ham's F12:DMEM (1:1), heat-inactivated human serum (10% v/v), GPS (1% v/v), EGF (100µg/ml), hydrocortisone (2µg/ml), cholera toxin (1µg/ml), HGF (100µg/ml), T₃ (2nM), and insulin (0.125µg/ml). Cells were left undisturbed for two days to allow the cells to settle and adhere to the flask. After 2 days the medium was removed, and the cells gently washed with warmed PBS to remove detached Dynabeads®. Cells were expanded in 25cm³ tissue culture flasks with regular medium changes until they became a confluent monolayer. For passage and plating out, cells were subjected to a gentle trypsinisation, 5 minutes in TrypLE, followed by neutralisation with PBS containing 10% FCS. In all subsequent experiments cells were used between passages two and four depending on the initial yield of the primary isolate.

3.3.2.3 Ciliary optimisations in cultured BEC

For the ciliary optimisations cells were seeded onto plastic chamber slides, plastic coverslips, acid-washed glass coverslips, or untreated glass coverslips. Each culture substratum was either left uncoated, or coated with gelatine, poly-lysine, or collagen. Cells were cultured in BEC medium with regular media exchanges until 100% confluent. Once cells had reached 100% confluency cells were stained at 1, 3, or 5 days post-confluency.

3.3.2.4 Assessment of ciliary expression by immunostaining

Carried out as previously described in section 3.3.1.4.

3.3.2.5 Antibodies

Details of antibodies used are the same as those in section 3.3.1.5.

3.3.2.6 Image capture and analysis

Carried out as previously described in section 3.3.1.6.

3.4 MURINE EXPERIMENTATION AND *IN VITRO* CELL CULTURE

All animal experiments were conducted under protocols approved by the Mayo Institutional Animal Care and Use Committee (IACUC).

3.4.1 Immunofluorescent immunohistochemistry

Archival tissue from *Del2* mice was available as either snap-frozen tissue blocks or FFPE tissue blocks. In order to cover the desired age range, tissue of both types was used as visualisation of primary cilia in both section types is comparable at a level satisfactory for the initial investigations.

3.4.1.1 Paraffin-embedded section preparation: Citrate buffer antigenic retrieval

Prior to immunostaining, 5 μ m tissue sections of murine kidney and liver were prepared onto commercial charged microscope slides by the Tissue and Cell Molecular Analysis (TACMA) shared resource group at Mayo Clinic (MN, USA). Upon receipt, sections were heated for 1 hour at 65°C before use, to ensure sections would not float free of the slides during processing. Sections were then subjected to antigenic retrieval in citrate buffer. Briefly, slides were deparaffinised in Histo-Clear (National diagnostics, USA; Cat# HS-200) for 10 minutes before rehydration through a series of ethanol washes, 1-2 minutes each at 100%, 90%, 80%, 70%, and 50% ethanol in double distilled water (ddH₂O), before a final wash in PBS. A 10mM solution of unbuffered sodium tricitrate was heated to near boiling in a steamer, and the slides were immersed in this buffer and placed back into the steamer for 40 minutes. Once removed and the liquid allowed to cool to near room temperature, any free aldehydes that might cause autofluorescence were quenched by washing the slides in 0.1M glycine in PBS for 10 minutes. Slides were then washed twice in PBS and incubated with 10mg/ml sodium borohydride in ice-cold Hank's buffered salt solution (HBSS) for 40 minutes to reduce shift bases that can cause autofluorescence. After further washes in PBS, sections were delineated with a hydrophobic barrier pen (DAKO, Cat# S2002) to contain any liquids added to the section, thereby reducing the amount of reagent required. Sections were then subjected to immunofluorescent staining with the desired antibodies (Refer to section 3.4.1.3).

3.4.1.2 Frozen tissue section preparation

Snap frozen tissue blocks of murine liver and kidney were mounted into OCT embedding media (Sakura, Japan) before sectioning on a cryostatic microtome. Prior to

immunohistochemical assay, 5 μ m cryostatic sections were cut and mounted onto commercially available charged glass microscope slides and dried at 60°C for 20 minutes. Once dry, sections were permeabilised by submerging in either PBS or TBS with 0.1% Triton X-100 for 10 minutes. Sections were delineated with a hydrophobic barrier pen (DAKO, Cat# S2002) before immunofluorescent staining with the desired antibodies (Refer to section 3.4.1.3).

3.4.1.3 Immunostaining

Dependent upon the detection molecules used, different buffer systems had to be adopted when staining was conducted. In order to bind to their ligand, lectins require free metal ions such as Mn²⁺, Ca²⁺, and Mg²⁺. However, with PBS this can result in the formation of a calcium phosphate precipitation, therefore TBS was used in place of PBS whenever lectins were used.

Delineated and rehydrated sections were blocked with Image-iT[®] FZ signal enhancer (Invitrogen, Cat# I36933) for 30 minutes to improve the fluorescence signal-to-noise ratio. After a 5-minute wash in PBS or TBS, pH7.4, sections were blocked for a further 30 minutes. Sections to be probed with biotinylated-lectin were blocked in lectin buffer (1mM Mn²⁺, 1mM Ca²⁺, and 1mM Mg²⁺ in TBS, Ph7.4) with 0.2% BSA. Sections to be probed with antibodies were blocked in PBS with 0.2% BSA and 10% NGS. After washing with 0.2% BSA in PBS/lectin buffer, sections were incubated for one hour with primary antibody or biotinylated lectin optimally diluted in buffer (PBS/lectin buffer with 0.2% BSA). After

washing in buffer, sections were then incubated for 30 minutes with optimally diluted Alexa Fluor (AF) conjugated secondary antibodies in the dark. Sections were then washed several times in buffer, then PBS or TBS to wash away any serum proteins before a 1-2 minute incubation with 1 μ g/ml DAPI in PBS or TBS. Following one last wash in PBS or TBS, sections were mounted in Vectashield[®] anti-fade mountant (Vector labs, Cat# H-1000), and sealed with clear nail polish to prevent evaporation of the mounting media.

3.4.1.4 Antibodies

Immunostaining analyses were performed using well-characterised mouse monoclonal antibodies against acetylated α -tubulin (6-11B-1), and γ -tubulin (GTU-88) (Sigma, MO, USA). Biotinylated, PT specific lotus tetragonolobus lectin (LTA), and BEC specific lectin dolichos biflorus (DBA) were used as markers for the target tubular structures. Isotype specific goat anti-mouse secondary antibodies used in various combinations included AF-488 (green), and AF-594 (red) conjugated immunoglobulins, and AF-594, and AF-488 conjugated streptavidin, used in the appropriate combinations to allow for dual staining. Negative controls were included with exclusion of either the primary or secondary antibodies, or exclusion of both to determine basal levels of tissue autofluorescence.

3.4.2 Isolation and culture of primary mouse proximal tubular cells

3.4.2.1 Chemicals

Dulbecco's modified Eagle's/Ham's F12 (DMEM-F12) without phenol red, Hank's balanced salt solution (HBSS) without phenol red (liquid 1x), non-essential amino acids (liquid, 100x),

sodium pyruvate, L-glutamine, 4-(2-hydroxyethyl)-1-piperazineethanesulfonic acid (HEPES), and charcoal-stripped FBS were purchased from Invitrogen (USA). Nylon mesh was obtained from Small Parts Inc. (FL, USA). All other enzymes, hormones, and chemicals were purchased from Sigma (MO, USA). Chamber slides were 8-well (0.72cm²) collagen I coated glass cultureslides (BD Biosciences, USA).

3.4.2.2 Primary cell culture

Primary PTCs were cultured under sterile conditions from collagenase-digested cortical fragments of kidneys isolated from male and female *Del2* and wildtype mice of the C57BL/6 background. Although mice of both the C57BL/6 and BALB/c background were available, there were no significant phenotypic differences between mice from either background. The C57BL/6 background was chosen, as these animals were more abundant and readily available for study.

Renal cortices were micro-dissected visually in ice-cold dissection solution (DS) (HBSS with in mmol/l: 10 glucose, 5 glycine, 1 alanine, 15 HEPES, pH7.4) and sliced into ~1mm wide pieces. The fragments were transferred to sterile filtered collagenase solution (DS with 0.1% wt/vol type-IV collagenase) at 37°C and digested for 30 minutes with intermittent agitation. After digestion, the supernatant was sieved through two nylon sieves (pore size 250µm and 80µm). The long PT fragments (about 100µm in length) remaining on the 80µm sieve were resuspended by flushing the sieve in the reverse direction with warm DS (37°C containing BSA 1% (wt/vol)). The PT fragments present in the BSA solution were centrifuged for 5

minutes at ~170g, washed, and then resuspended into the appropriate amount of culture medium: 1:1 DMEM/F12 without phenol red supplemented with heat inactivated charcoal stripped FBS 10%, HEPES 15mmol/l, L-glutamine 2mmol/l, insulin 5µg/ml, transferrin 5µg/ml, selenium 50nmol/l, sodium pyruvate 0.55mmol/l, 100x nonessential amino acids 10ml/l, dexamethasone 50nmol/l, and Nystatin 10,000 units/l. Different concentrations of FBS ranging from 1% to 10% were trialled. Only at 10% FBS, did cells proliferate readily and maintain an unchanged epithelial morphology. The PT fragments were seeded onto collagen I coated 8-well chamber slides at a density of one mouse (two kidneys) to 12 wells.

Fragments were also seeded onto poly-lysine and fibronectin coated chamber slides, however optimal cell growth and adhesion were achieved only on collagen coated chamber slides. Once seeded, the PT fragments were left unstirred for 48 hours at 37°C, and 95% air, ~5% CO₂ in a standard humidified incubator. After which, culture medium was changed for the first time. For wells to be treated with oestrogen, this first media change included the appropriate concentration of E2 in duplicate (Fig. 3.1). The medium was then replaced every two days. After seven days, cellular outgrowth from the fragments was sub-confluent in control wells (0pg/ml E2), while confluency increased at higher levels of E2. Cilia were expressed across the panel.

Well 1: Control 0pg/ml E2	Well 2: Sub-physiological 25pg/ml E2	Well 3: Physiological 75pg/ml E2	Well 4: Excess to physiological 500pg/ml
Well 5: Control 0pg/ml E2	Well 6: Sub-physiological 25pg/ml E2	Well 7: Physiological 75pg/ml E2	Well 8: Excess to physiological 500pg/ml

Well 9: Control 0pg/ml E2	Well 10: Control 0pg/ml E2		
Well 11: Control 0pg/ml E2	Well 12: Control 0pg/ml E2		

FIGURE 3.1 Experimental layout of culture slides. Schematic diagram of the experimental layout used for 17 β -estradiol (E2) experiments on the primary PTCs. The top slide layout enabled all conditions to be performed in duplicate for each animal, ensuring enough cells were available to count. The lower slide with 4 control (0pg/ml E2) wells were used for antibody controls for each animal, and each time staining was carried out.

3.4.2.3 Immunostaining

Subsequent to removal of old culture medium, 7-day-old monolayers of primary cultured PTCs were washed in PBS before fixation in ice-cold methanol. Following permeabilisation with Triton, cells were blocked with 10% NGS in buffer (0.2% BSA in PBS) for 30 minutes. After washing in buffer, cultures were incubated with primary antibodies optimally diluted in buffer for 1 hour. After washing, cultures were incubated with the appropriate AF-conjugated secondaries, optimally diluted in buffer, for 30 minutes in the dark. Cultures were then washed in successive changes of; buffer, PBS, 1 μ g/ml DAPI in PBS, and finally PBS. Finally, cultures were mounted with a coverglass using Vectashield[®] anti-fade mountant, and sealed with clear nail polish to prevent specimens from drying out.

3.4.2.4 Antibodies

Immunostaining analyses were performed using well-characterised mouse monoclonal antibodies against acetylated α -tubulin (6-11B-1), and γ -tubulin (GTU-88) (Sigma, MO, USA). PTC specific cell adhesion molecule N-cadherin [Nurnberger et al., 2002; Prozialeck et al., 2004] was used as a marker to confirm that the cells being observed were indeed PTCs. Secondary immunoglobulin subclass specific combinations to achieve dual staining included: AF-594, and AF-488 conjugated goat anti-mouse antibodies. Negative controls were treated identically to test samples, except with exclusion of primary antibody, secondary antibody, or both primary and secondary.

3.4.3 Data analysis

All immunostaining of tissue and primary PTCs was analysed using the Nikon Eclipse E600 upright epi-fluorescence microscope, and images were captured using the Nikon DXM1200 digital camera (Nikon, IL, USA). Confocal images were also captured using the Zeiss LSM510 laser-scanning microscope. Data on centrosomal overduplication was collected by counting cells with the normal complement of centrosomes (≤ 2), versus those with centrosomal overduplication (> 2). An average of over 100 cells were counted for every sample and treatment. Values are expressed as the percentage of cells with more than 2 centrosomes from the total number of cells counted. For each experimental condition, counts were taken in multiples (n=3/4 animals) and values expressed as the mean \pm SD. Significance of difference between two means was calculated using a 1-tailed, unpaired t-test, with assumption of unequal variance. Statistical analysis was performed using SPSS software (SPSS

Inc., Bologna, Italy). All quoted p-values are one-sided, and statistical significance related to results for which the p-value is <0.05 .

CHAPTER 4 MUTATIONAL SCREENING OF *PKHD1* IN A COHORT OF BILIARY ATRESIA PATIENTS WITH ASSOCIATED RENAL CYST FORMATION

4.1 INTRODUCTION

Renal cysts are a common feature of the ciliopathies, syndromes characterised by both renal cyst formation and liver disease. The underlying pathogenesis of these conditions is an abnormality of primary ciliary structure and function. ARPKD is a classic ciliopathy characterised by the development of renal and hepatic cysts, and CHF as a result of DPM [Desmet, 1992b], features also of BA [C.E. Tan et al., 1994b]. Mutations in the gene *PKHD1* result in the ciliopathy ARPKD [Rossetti et al., 2003]. The shared clinical features of BA and ARPKD, along with the knowledge that ARPKD is the result of an abnormality in primary cilia, prompted investigation to determine if sequence variants of *PKHD1* could provide a clue to the pathogenesis of BA, or even play a role in the development or susceptibility of BA in patients who also develop renal cysts.

4.2 AIM

Perform an initial mutational screen of *PKHD1* in a small cohort of biliary atresia patients that develop renal cysts, to determine if mutations in this key ciliary gene could contribute to the above phenotype.

4.3 RESULTS

4.3.1 Association of renal cysts in transplant patients with BA

Nine of the 206 (4%) patients with BA who were transplanted at the BCHLU had renal cysts as compared with cyst identification in 9 of 463 (2%) of children with other forms of liver disease. However, statistical analysis using a 2-tailed Fisher's test for a 2X2 contingency table, with the alternative hypothesis that the incidence of cysts will be higher in patients with BA than in other liver diseases, returned a p-value of 0.1188. The same data examined using a χ^2 test of association returned the same conclusion with a value of $\chi^2 = 3.008$, d.f. = 1, p = 0.0829. With the critical figure of statistical significance being represented with a p-value of $p < 0.05$, this signifies that it is unlikely that cysts occur more frequently in patients with BA when compared to patients with other liver diseases. Thus the association of renal cysts in transplant patients with BA is not significantly higher than renal cysts associated with other causes of paediatric liver transplantation.

4.3.2 Clinical evaluation

Histological examination of the biliary remnants at the time of Kasai HPE confirmed the diagnosis of BA in 355 patients (Fig. 4.1). No child had renal cysts identified at the time BA was confirmed as the diagnosis (Table 3.1). 206 patients diagnosed with BA subsequently required liver transplantation (58%).

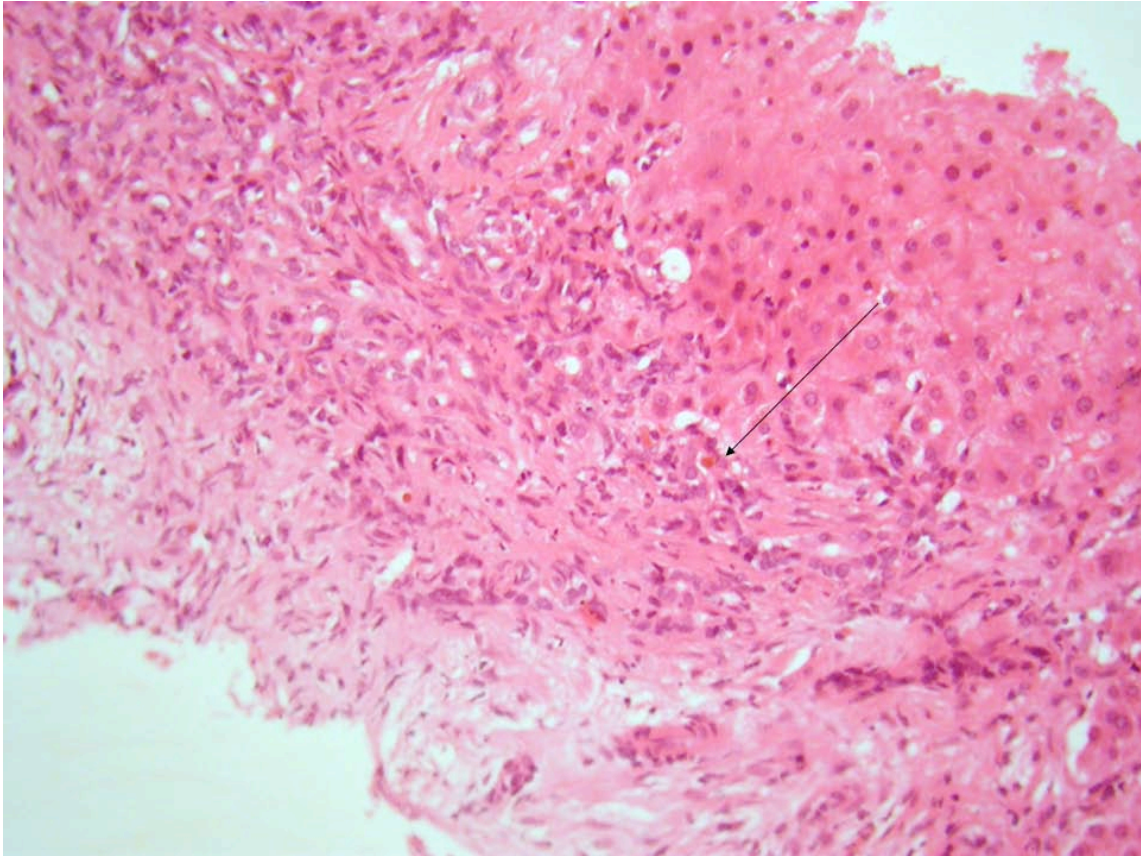


FIGURE 4.1 Patient 10 liver biopsy H&E immunohistochemistry, original magnification x200. Liver biopsy from patient 10 showing ductular transformation at the margin of an expanded portal tract. Some ductules contained bile plugs (arrow). Note that the pattern of biliary fibrosis; it does not resemble a ductal plate malformation.

Ten of the 355 patients were verified as having developed renal cysts either by abdominal ultrasound scan (nine of the children) or abdominal CT (one child) (Fig. 4.2). All ten patients had the perinatal (non-syndromic) form of BA. There was no reported family history of liver or renal disease and no children developed hepatic cysts. Nine of the ten children have undergone liver transplantation.

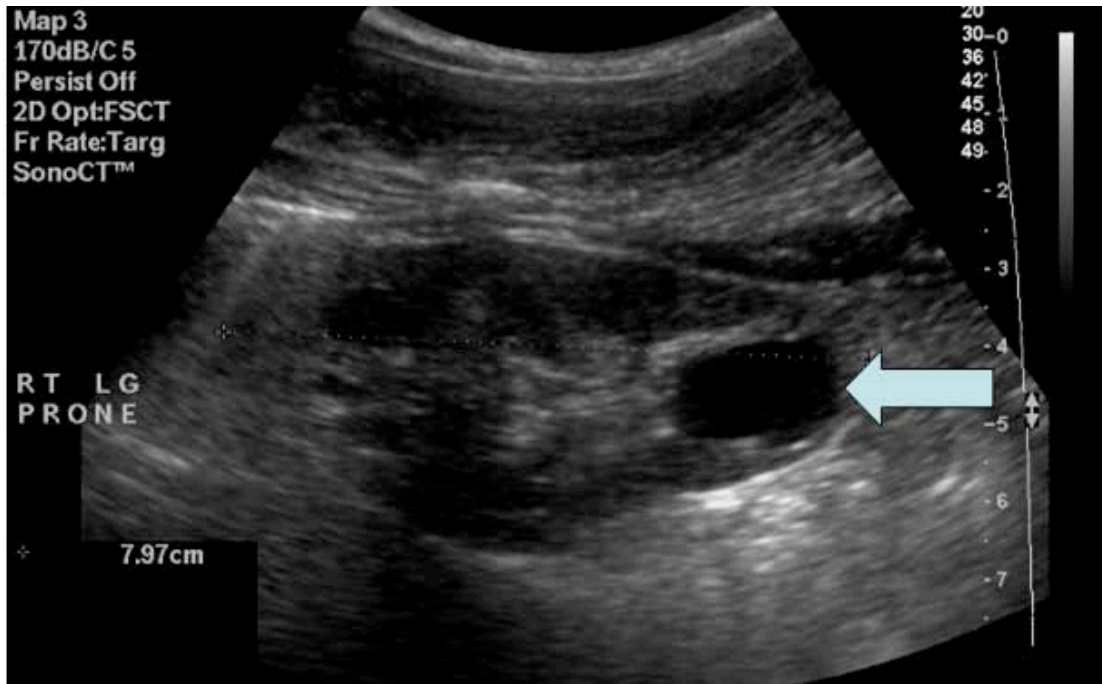
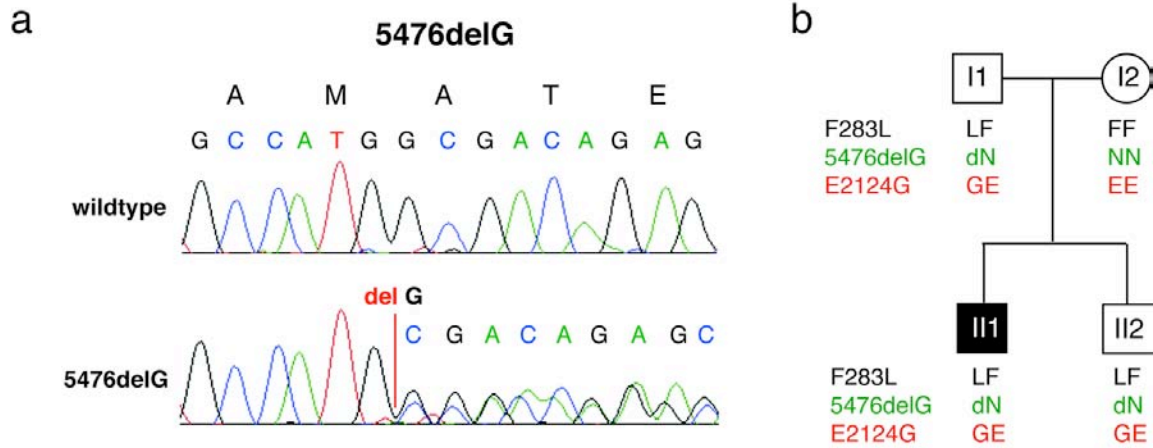


FIGURE 4.2 Renal cyst ultrasound. This renal ultrasound scan demonstrates a large cyst in the upper pole of the right kidney in child 10 (Arrow indicates cyst).

Patient 1 has had long-term success from the Kasai HPE and has not required a liver transplant, and has not yet developed renal dysfunction, and patient 7 developed renal cysts prior to transplantation. (Table 3.1). The median age at detection of renal cysts was 9.5 years (range 0.25 to 14 years). The natural history of the cysts was variable, ranging from a single cyst, which did not change with time, to a rapid increase in size and number of cysts (Table 3.1). Nine of the ten children had received a liver transplant at a median age of 0.83 years (range 0.66 to 5 years).

PKHD1 was analysed by DHPLC in genomic DNA from six children with BA and renal cysts. A further three cases (2, 7, and 8) along with further analysis of patient 10, were analysed by direct sequencing of *PKHD1*. Patient 10 was found to be a compound heterozygote with a frameshifting change in exon 34, c.5476delG (A1826fsX147) (Fig. 4.3). This frameshift results in an early termination product 147 amino acids after the occurrence of the deletion, in exon 37. The frameshift in exon 34 is not conserved in mouse, rat or chicken (Fig. 4.3c). The site of the premature stop in exon 37 is conserved in the mouse, rat, and chicken orthologues of *Pkhd1* (Fig. 4.3c).



C

Exon 34 cDNA sequence: Ch6: 51,882,208 - 51,882,427 (220bp)

5701 TGTGAGGCTGCCAGACACACCTATGTGCAGTGTGATTTGACAGTTGCCATGCGACAGAG
5425 TGTGAGGCTGCCAGACACACCTATGTGCAGTGTGATTTGACAGTTGCCATGCGACAGAG
1809 -C--E--A--A--R--H--T--Y--V--Q--C--D--L--T--V--A--M--A--T--E-

Alanine not conserved in mouse, rat, or chicken

gi 126157466 ref NP_694819.2 mouse	AEDSCKVRSSTYLRCDLTVSMGTERLPGSWPYVYLCESSLCLFEPDHW	1850
gi 109485870 ref XP_236979.4 rat	AEDSCGVSRTYLCQDLTVSVGMERLPGSWPYVYLCESSQGLFVPDHO	1437
gi 126131102 ref NP_619639.3 human	EEDSCEAARHTYVQCCLTVSMATEQLLESWPYLYICESSQCLFVDPHWA	1854
gi 118089204 ref XP_420050.2 chicken	SSANQEDRSTIIECDVQVAVVGSYRQRGPRSYLYLVCGESQAQQQGGDTG	1764

Exon 37 cDNA sequence: Ch6: 51,798,908 - 51,799,120 (213bp)

6181 AAAGGGGGCAAGCTGATTTTCATGGCCCCAGGACCCATCGAGCTCAGGGCACACGCCATC
5905 AAAGGGGGCAAGCTGATTTTCATGGCCCCAGGACCCATCGAGCTCAGGGCACACGCCATC
1969 -K--G--G--K--L--I--F--M--A--P--G--P--I--E--L--R--A--H--A--I--

Conserved in mouse, rat, and chicken

gi 126157466 ref NP_694819.2 mouse	LLDANTSFLNSLHIKGGKIFMDPGPIELRAHSILITDGGELHIGSEKP	2000
gi 109485870 ref XP_236979.4 rat	LLDANTSLLNSLHIKGGKIFMEPGPIDLRAHSILITDGGELHIGSEDKP	1585
gi 126131102 ref NP_619639.3 human	LLDTNTSILNLLHIKGGKIFMAPGPIELRAHAILVSDGGELRIGSEDKP	2004
gi 118089204 ref XP_420050.2 chicken	LLGAATAALHLLHLRGGKIFTPGGPVELHAHYILISDGGELRVGSSEAR	1911

FIGURE 4.3 Mutational analysis of *PKHD1*. (a) Direct sequencing of the *PKHD1* gene in patient 10 and normal control shows the deletion c.5476delG that results in a frameshift in exon 34. (b) Segregation analysis shows co-segregation of the deletion and the two missense changes E2124G and F283L in the father (I1), the affected child (II1) and the unaffected sibling (II2). (c) cDNA and protein sequences of *PKHD1* at the site the frameshift deletion in exon 34, and the resulting premature stop codon in exon 37. The deletion at exon 34 shifts the entire coding sequence by one base changing the following 147 amino acids downstream, finally resulting in the STOP codon TGA at exon 37, which sits within a region conserved in the mouse, rat, and chicken orthologues of *Pkhd1*. This is highlighted in the sequence alignment of the three species with the human *PKHD1* sequence.

In addition, two novel non-synonymous missense changes were detected F283L (847 T→C) and E2124G (6371 A→G). F283L (phenylalanine to leucine) is a conservative change, from one hydrophobic amino acid to another, at a site conserved in the mouse, rat, and chicken orthologs (Fig. 4.4a). E2124G (glutamic acid to glycine) is a non-conservative change, from a negatively charged amino acid to a small neutral, non-polar amino acid, but at a poorly conserved site (Fig. 4.4b). Extended analysis of patient 10's family, who are phenotypically normal (including normal ultrasound scan imaging of the kidneys), revealed a sibling and the father to have the deletion mutation and both missense changes. This indicates that the missense changes are unlikely to be pathogenic (Fig. 4.3b), making the deletion the only change likely to be pathogenic. No other likely pathogenic changes to *PKHD1* were found in any of the other cases, or controls.



FIGURE 4.4 Mutational analysis of *PKHD1*. Direct sequencing of the *PKHD1* gene in patient 10 and normal control shows the missense mutations in exons 12 and 39. (A) The mutation in exon 12 results in a conservative change at a site conserved in the mouse, rat, and chicken orthologues of *Pkhd1*. (B) The mutation in exon 39 results in a non-conservative change at a site conserved only in the murine ortholog of *Pkhd1*.

4.4 CONCLUSIONS

The observation of renal cysts in paediatric liver disease is an established clinical association. However, in this project the aim was to determine if this association is greater in patients with BA than other liver diseases, which would suggest that BA is associated with renal cyst development.

Of 659 children who received a liver transplant at BCHLU, 206 were transplanted for BA; further to this the BCHLU identified the development of renal cysts in 10 of 355 (2.8%) patients with BA. Nine of the 206 (4%) patients with BA who were transplanted had renal cysts as compared with cyst identification in 9 of 463 (2%) children with other forms of liver disease. However, the observed differences are not significant, and give no indication of an increased association of renal cysts with BA relative to other paediatric liver diseases.

The identification of a compound heterozygote BA patient with renal cysts does not support a role for *PKHD1* in the pathogenesis of BA alone. This is further supported by the fact these changes were also carried by other family members.

In light of the findings, it was decided to suspend mutational screening of *PKHD1* in a larger more stratified cohort of BA patients until a second, more convincing mutation was identified in BA patients with associated renal cysts. Unfortunately this could not be achieved before the completion of this project. Thus from these particular findings it can be concluded that

PKHD1 does not appear to contribute to the pathogenesis of BA, or the occurrence of renal cysts in BA.

The apparent lack of an increased association of renal cysts and BA does not however mean that there is no association between hepatic disorders and renal cystic disease caused by mutations in *PKHD1*. Thus the main aim of this work moved away from investigating the pathogenetic role of *PKHD1* in BA specifically, becoming a study of the phenotypic variability of *PKHD1* associated disease in human liver disorders and animal models of ARPKD.

4.5 DISCUSSION

Simple renal cysts in childhood are a rare finding, occurring in 0.1% of children [Mir et al., 1983]. Renal cyst formation may be secondary to renal dysplasia as an isolated developmental abnormality or they may be a clinical feature of a syndrome. Renal cysts may also be acquired and develop in long term renal dialysis patients [Thomsen et al., 1997]. The development of renal cysts is also a common feature of ciliopathies. This was taken into careful consideration during this study and renal function was calculated for all patients in the cohort using the Schwartz formula ($\text{height (cm)} \times 40 / \text{creatinine } (\mu\text{mol/l})$) as an approximation for glomerular filtration rate (GFR) with a normal calculated GFR being greater than $60\text{ml/minute}/1.73\text{cm}^2$ [Hogg et al., 2003]. No patient within the cohort studies displayed renal dysfunction prior to liver transplantation (Table 3.1). Thus, the presence of cysts suggests an underlying pathological process.

Interestingly, Calvo-Garcia [Calvo-Garcia et al., 2008] compared cyst association between BA and other paediatric liver diseases in a cohort of post-transplanted patients. They also found there was no increased association of renal cysts in cases of BA when compared to other paediatric liver diseases. None of their cohort developed renal cysts prior to transplantation, and the development of cysts was attributed to renal dysfunction due to the transplant process, in particular the use of calcineurin inhibitors (CNI). In the cohort of patients with BA and renal cysts included within the current study, renal dysfunction was identified in five children post-transplantation, while renal function improved significantly upon discontinuation of CNI in four (Table 3.1). The onset of renal dysfunction was not found to correlate with the identification of renal cysts, indeed in several patients the number and size of cysts increased despite an improvement in renal function subsequent to discontinuing CNIs. This suggests that in cases such as these the development and progression of renal cysts can be independent to renal dysfunction and CNIs. Two individuals from the cohort developed renal cysts following HPE and prior to liver transplantation, providing reasonable doubt of whether the transplantation process is the sole cause of cyst formation in these cases. The findings of this investigation suggests renal cyst formation in paediatric liver disease can be independent of the transplant process or renal function, and therefore cannot be the sole aetiology for the development of renal cysts in such cases. The development of cysts prior to transplantation, and the association of renal cysts in BA does indicate that they may have formed as part of the primary aetiology.

However, it is the very nature of these cysts that argues against an association with *PKHD1* mutations. Phenotypically the renal cysts of ARPKD patients are small, and great in number,

resulting in bilateral sponge-like enlarged echogenic kidneys. In contrast, the renal cysts observed in this cohort were isolated single cysts in the majority of cases (Table 3.1). Only patient 10 presented with renal cystic disease that resembled typical ARPKD [Menezes and Onuchic, 2006; Rossetti et al., 2003; Ward et al., 2002]. However, the slight difference between the renal cystic phenotype observed in this cohort, and that typically in patients with ARPKD cannot lead to a complete dismissal of this observation as chance. A retrospective review of cases of ARPKD and CHF patients at the Mayo clinic by Adeva *et al* [2006] concluded that although ARPKD typically presents with greatly enlarged echogenic kidneys, mutations in *PKHD1* can result in CHF with minimal kidney involvement [Adeva et al., 2006], including cases with only 1 or 2 isolated renal cysts. Whilst previous studies have identified the existence of genotype/phenotype correlations in ARPKD [Bergmann et al., 2005a; Bergmann et al., 2003; Furu et al., 2003; Rossetti et al., 2003], patients with two truncating mutations typically have a severe renal presentation that results in neonatal death. Patients with at least one mutation typically have a milder renal presentation, suggesting that some missense changes may be hypomorphic alleles [Furu et al., 2003; Rossetti et al., 2003].

In this series, sequencing the *PKHD1* gene revealed three novel changes in a single family. The affected child, and both the unaffected father and brother carried the same alleles at the three sites. These changes were not found in the control samples, which included both normal and diagnosed ARPKD patients. Thus, no population frequency data for these changes is available. Given a carrier frequency of approximately 1:70 for disease causing *PKHD1* mutations in non-isolated populations, and the vast number of private alleles, the prevalence of any individual mutation would be expected to be low in the normal population

[Bergmann et al., 2004; Zerres et al., 1998a; Zerres et al., 1998b]. However, the small number of cases in this study renders these findings meaningless. Making it unclear at this stage whether mutations in *PKHD1* are associated with the BA with renal cysts phenotype, thus no clear conclusion could be drawn.

What is clear however is that the variability of the disease presentation and course of ARPKD and BA most likely reflects the importance of susceptibility and modifier genes in such diseases as well as environmental influences, making this a complex case to solve.

CHAPTER 5 INCREASED ACETYLATION OF α -TUBULIN AND DECREASED EXPRESSION OF FIBROCYSTIN ARE SENSITIVE MARKERS OF CELLULAR DAMAGE AND ACTIVATION IN INFLAMMATORY LIVER DISEASE

5.1 INTRODUCTION

Preliminary immunohistochemical studies, using a mouse monoclonal antibody specific for the intracellular domain of the wildtype fibrocystin protein [Ward et al., 2003], showed that in liver tissue from end-stage BA patients, bile ducts were consistently negative. The very nature of the pathology of BA may cause an alteration in cell function and protein expression over time as the disease progresses. Thus the absence of fibrocystin staining in end-stage diseased liver does not indicate if expression is lacking at the initiation of the disease, diminishes as a result of the disease process, or was never expressed in these tissues to begin with. This is something that must be clarified not only in BA, but other human liver diseases, in order to determine the role of fibrocystin in the pathogenesis of BA.

Alpha-tubulin is a constitutively expressed component of MTs, the basal body, and the axoneme of primary cilia. Formation of these ordered structures requires MT stability, a feature that has also been correlated with acetylation [LeDizet and Piperno, 1986]. Hyperacetylation of α -tubulin in the hepatocytes of ethanol-fed rats was found to result in impaired tubulin polymerisation, and possible altered MT integrity and dynamics [Kannarket et al., 2006]. Because MTs are central to many cellular processes including mitosis, vesicular transport, organelle placement and transport, and primary ciliary formation, it is proposed

that altered microtubular dynamics could have far reaching effects on numerous cellular functions.

5.2 AIMS

- Determine if altered expression of fibrocystin and/or acetylated α -tubulin are specific or non-specific markers of biliary damage in human liver disease, using a cohort of adult patient samples, and paediatric BA patient samples.
- Determine if the primary cilia of biliary epithelial cells from a cohort of liver disease patients have structural defects.

5.3 RESULTS

5.3.1 Evaluation of fibrocystin immunostaining achieved with different fixatives on frozen tissue

Comparison of antigen preservation for immunohistochemical detectability between a panel of cross-linking and coagulant fixatives on frozen tissue sections indicated that detection of the antigen, depended very much upon the prior treatment of the tissue (Fig. 5.2). There was no obvious difference in the level of staining achieved with each of the different fixatives, except with acetone used alone. No staining above that of non-specific background was observed for methanol, methanol:acetone, ethanol, or formalin, when compared to the negative control (Figs. 5.1a and 5.2). A slightly elevated level of background staining was observed in paraformaldehyde fixed tissue, but no specific staining of the biliary epithelium

could be detected (Fig. 5.2). In contrast, samples fixed in acetone displayed high levels of positive staining, both within the bile ducts, as expected, but also within the sinusoids (Fig. 5.3). These results were consistent for both antibodies (clones 11 and 19) at all dilutions tested (all dilutions not shown). The absence of any specific fibrocystin staining with any of the fixatives used meant evaluation had to move to FFPE tissue.

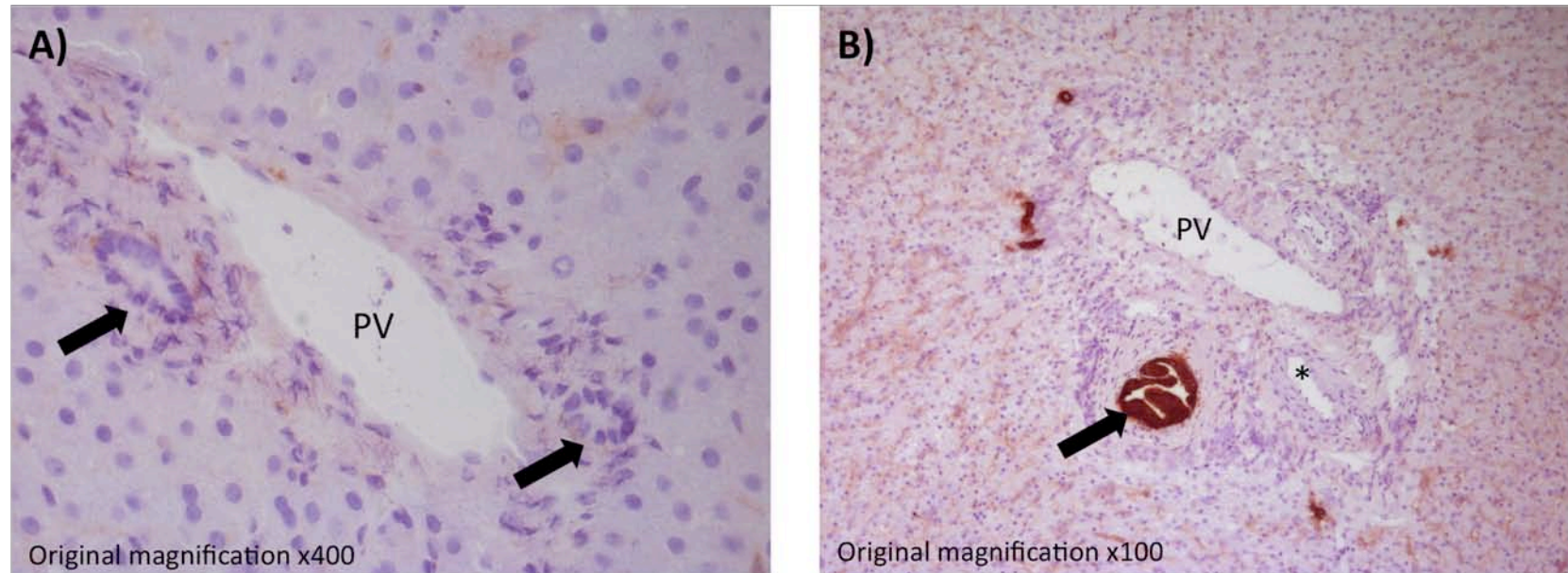


FIGURE 5.1 Sections of snap frozen normal human liver tissue stained using DAB immunohistochemistry. This method results in a brown reaction product exclusively where the target antibody is bound. (A) Negative control, no primary antibody. Block arrows indicate negative bile ducts within portal tract. (B) Positive control, human epithelial antigen 125 (HEA125), also known as epithelial cell adhesion molecule (EpCAM). Block arrow indicates positive bile duct located within a portal tract. * Indicates hepatic artery branch. PV = portal vein.

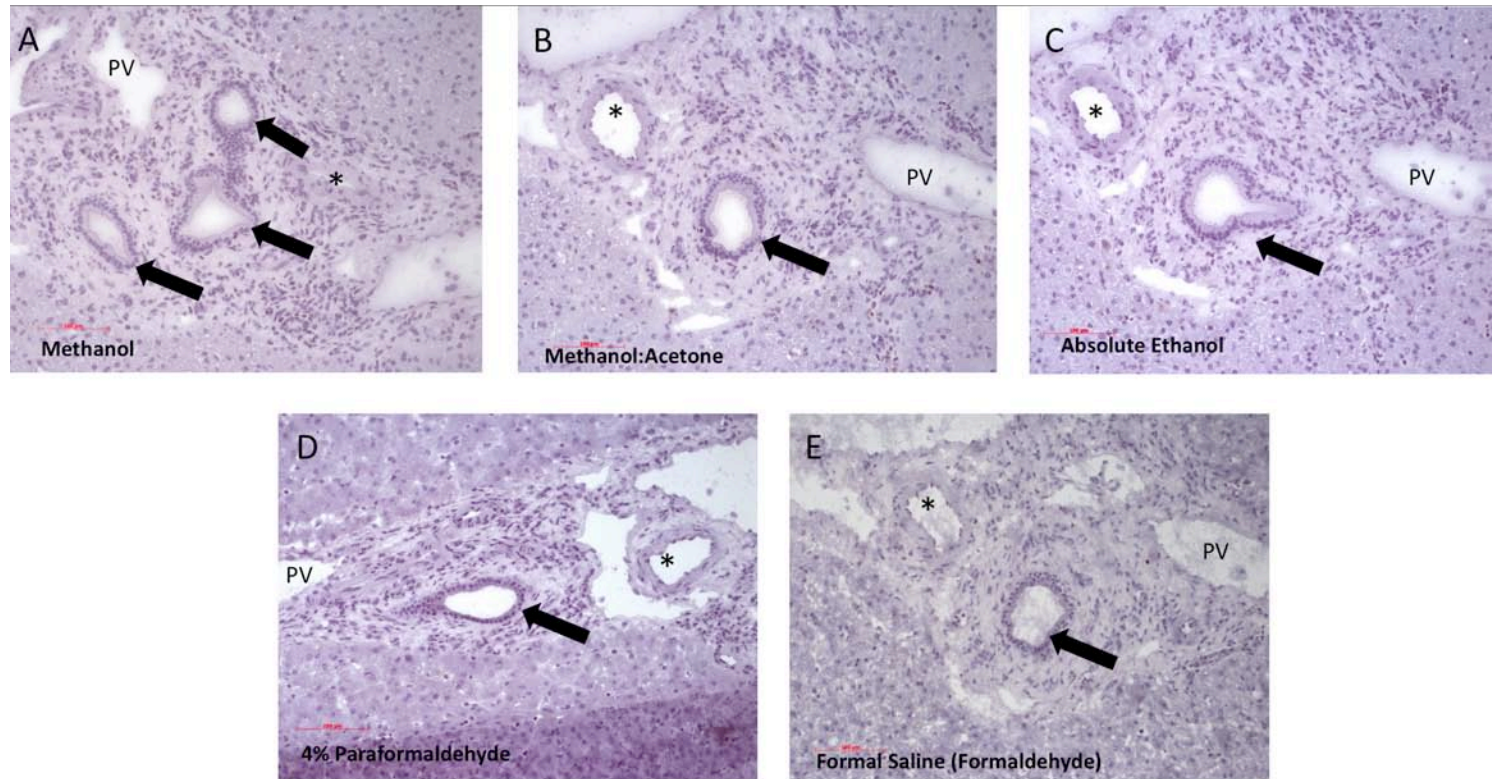


FIGURE 5.2 Immunohistochemical fixative panel performed on sections of snap frozen normal human liver tissue. Frozen tissue sections were stained for fibrocystin using DAB. This method results in a brown reaction product exclusively where fibrocystin is expressed. Each panel clearly shows at least one bile duct located within a portal tract (block arrows). In none of the sections can positive staining be seen. Note the absence of any non-specific staining within any of the tissue, indicating the staining to be highly specific. (A) Methanol fixed, (B) Methanol: Acetone (1:1) fixed, (C) Absolute ethanol fixed, (D) 4% w/v paraformaldehyde fixed, (E) formaldehyde fixed. Original magnification: x200. Scale bar = 100 μ m. PV = portal vein. * = Hepatic artery branch.

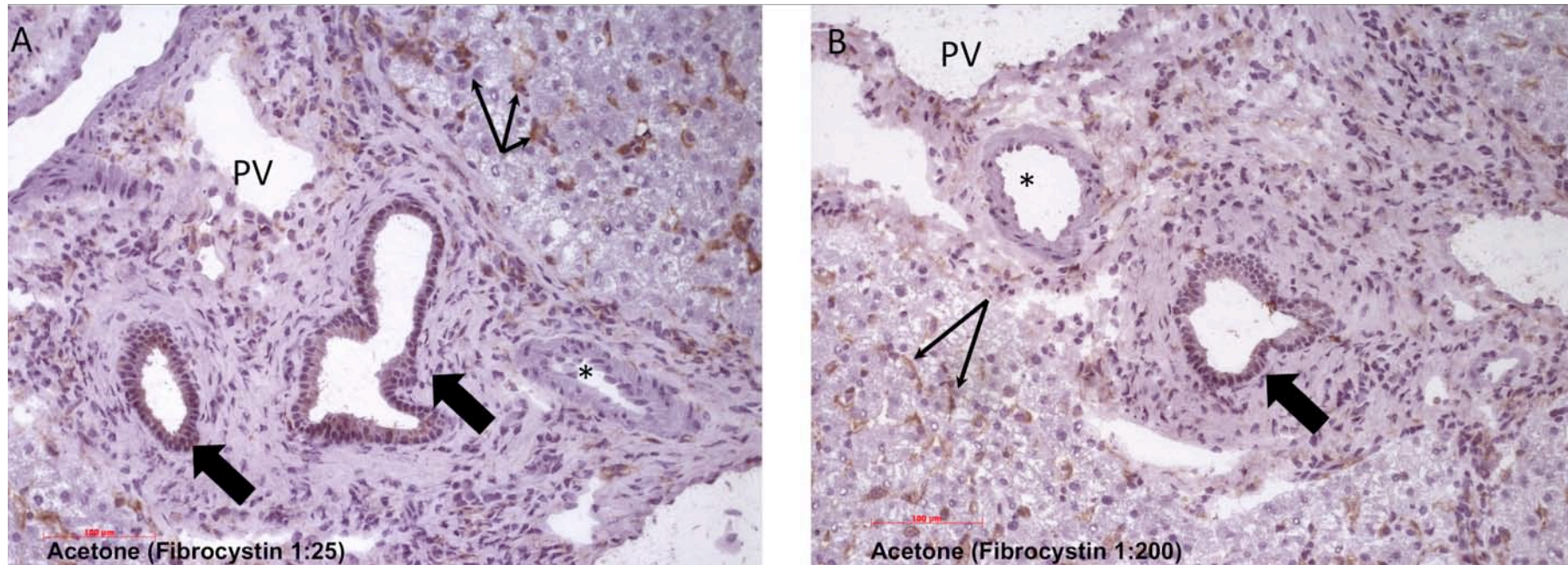


FIGURE 5.3 Acetone fixed sections of snap frozen normal human liver tissue. Frozen tissue sections were stained for fibrocystin using DAB immunohistochemistry. This method results in a brown reaction product exclusively where fibrocystin is expressed. Each panel clearly shows at least one bile duct located within a portal tract. The sections show bile ducts stain positively for fibrocystin (block arrows). Line arrows indicate the location of background sinusoidal staining. (A) Fibrocystin dilution 1:25. (B) Fibrocystin dilution 1:200. Original magnification: x200. Scale bar = 100 μ m. PV = portal vein. * = hepatic artery branch.

5.3.2 Optimisation of monoclonal antibodies for immunohistochemical study

In order to perform a full immunohistochemical screen of fibrocystin and acetylated α -tubulin expression in the cohort of liver diseases, the appropriate final working dilutions of the antibodies to be used had to be determined. Not only this, but the most appropriate of five fibrocystin clones available had to be determined. A serial titration was carried out for each antibody on normal liver for fibrocystin, and normal liver and liver from a PBC patient for acetylated α -tubulin.

The results of the titrations indicated that the optimum working dilution for the acetylated α -tubulin antibody (6-11B-1) on FFPE was 1:200, for the specific detection within biliary epithelia with minimum background (Fig. 5.4). At higher concentrations, the level of background became unacceptable, making it difficult to determine a true positive result (Fig. 5.4).

ANTIBODY DILUTION

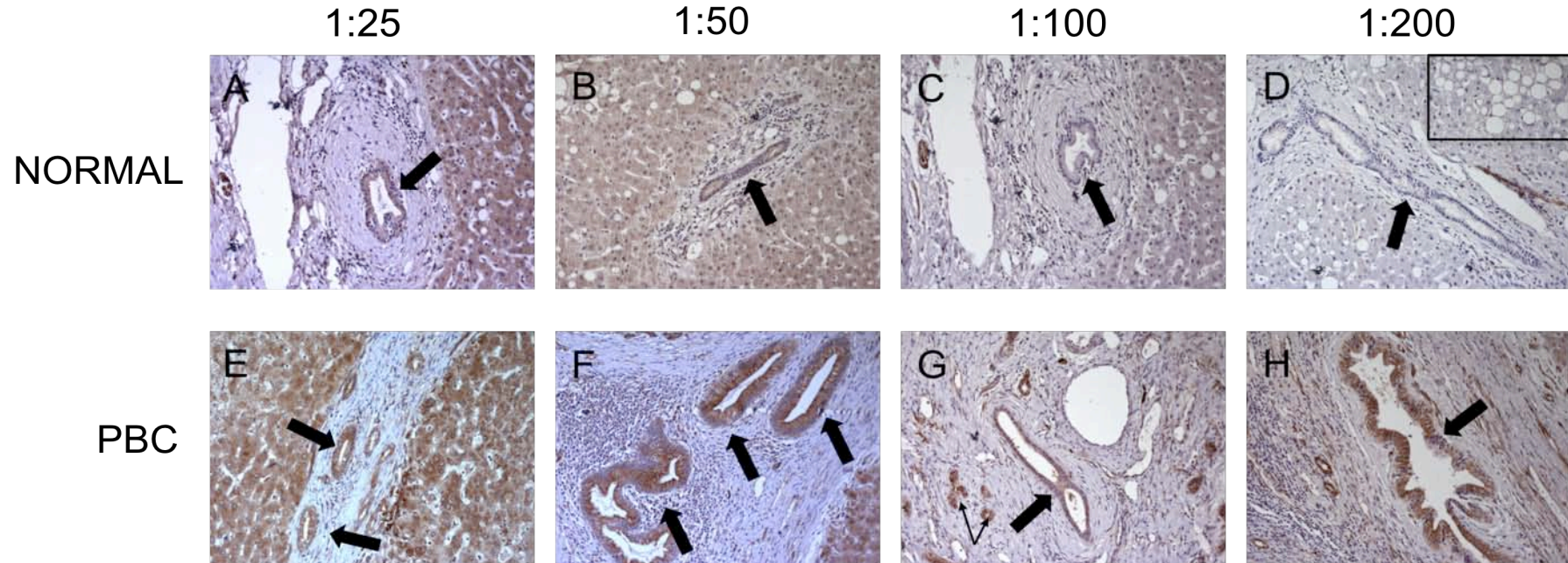


FIGURE 5.4 Acetylated α -tubulin antibody titrations on sections of formalin-fixed paraffin embedded human liver stained using DAB immunohistochemistry. The anti-acetylated α -tubulin antibody (6-11B-1) was serially titrated to determine the dilution at which optimal specific staining would be achieved, with minimal non-specific staining. Positive bile ducts are stained brown where acetylated α -tubulin can be detected (block arrows). Both normal and PBC tissue was used, as the levels of expression in either states was not known. While staining was strongest in tissue taken from PBC liver, the dilution at which the antibody performed best for both tissue types was determined to be 1:200 (D and H). In both types of tissue high levels of background was evident at lower dilutions (A-C, and E-G). Note the evidence of bile ductular proliferation in panel G (line arrows). Evidence of steatosis in the normal liver sections is highlighted by the rectangle in the top right corner of panel D. Original magnifications: panels A, C-H: x200; panel B: x100.

Immunostaining with the five fibrocystin antibodies directed against various epitopes within the protein structure was assessed by a pathologist (GMR) using three points of reference; non-specific background, kupffer cell, and BEC staining (Table 5.1). Specific staining was classed as maximal signal within bile ducts with minimal detectable in other structures. All five clones exhibited high levels of non-specific staining at very high concentrations (Figs. 5.5 a-e). Clone 14 failed to detect fibrocystin within biliary epithelia at all, while clone 19 was only able to detect fibrocystin within bile ducts at very high concentrations (Fig. 5.5 c and e). Both clone 11 and 18 were able to detect fibrocystin within biliary epithelia at a number of dilutions (Figs. 5.5 b and d), however the level of non-specific staining was unacceptable, as it would increase the probability of declaring a false positive when assessing specific staining. Finally, clone 5a proved optimal, detecting fibrocystin within bile ducts at a range of concentrations with very little non-specific staining (Fig. 5.5a). Thus the optimal working dilution for clone 5a, and that used in the full study was 1:100.

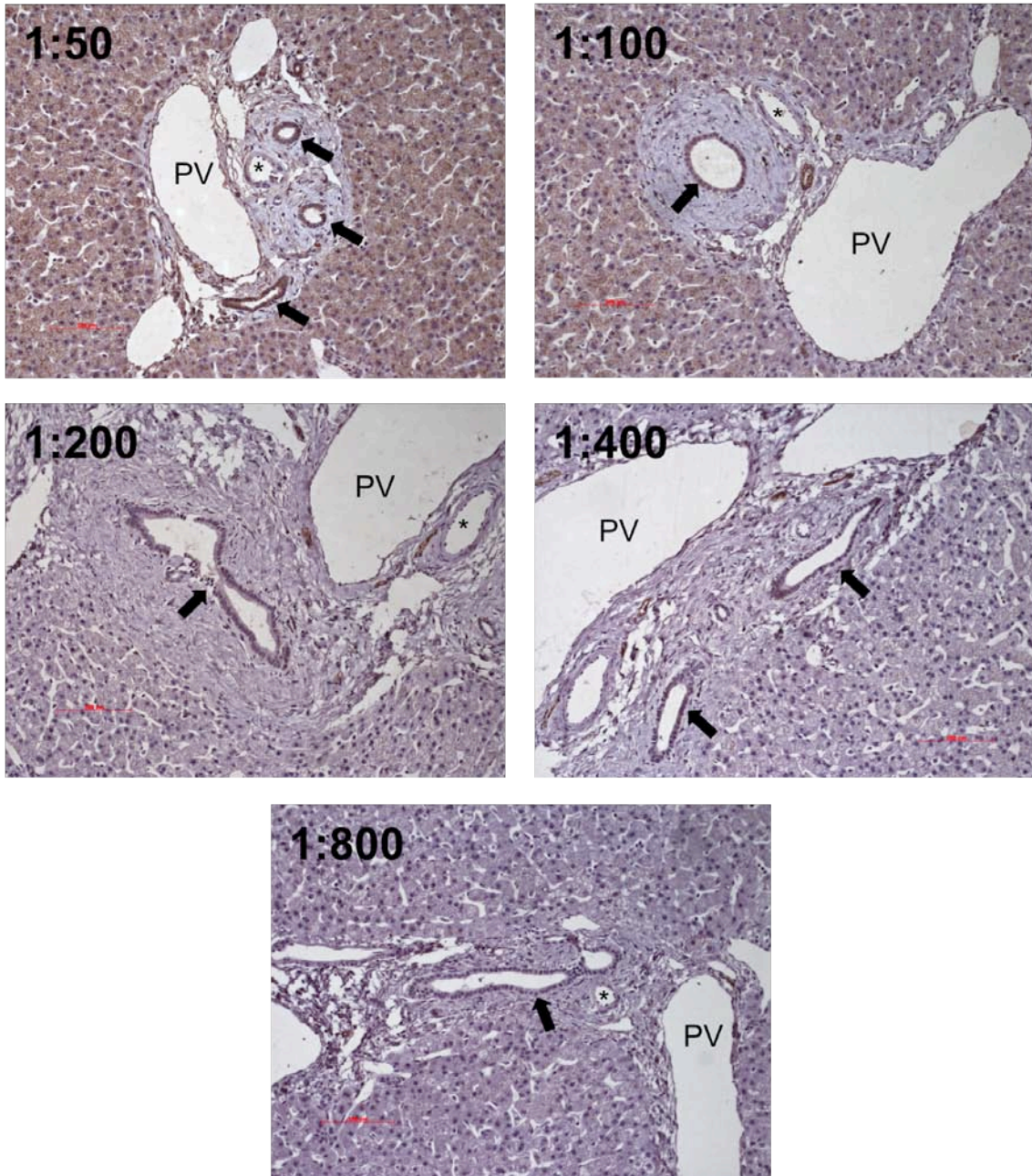


FIGURE 5.5a Fibrocystin antibody (clone 5a) titration on sections of formalin-fixed paraffin embedded human liver tissue stained using DAB immunohistochemistry. Anti-fibrocystin monoclonal antibody clone 5a was serially diluted, and tested on normal human liver tissue to determine the optimal dilution that would produce maximal specific staining of the biliary epithelium with minimal non-specific staining. A brown stain is evident in bile ducts positive for fibrocystin (block arrows). Optimal staining was achieved at a dilution of 1:100 (See table 5.1). PV = portal vein; * = hepatic artery branch; scale bar = 100 μ m. Original magnification: x200.

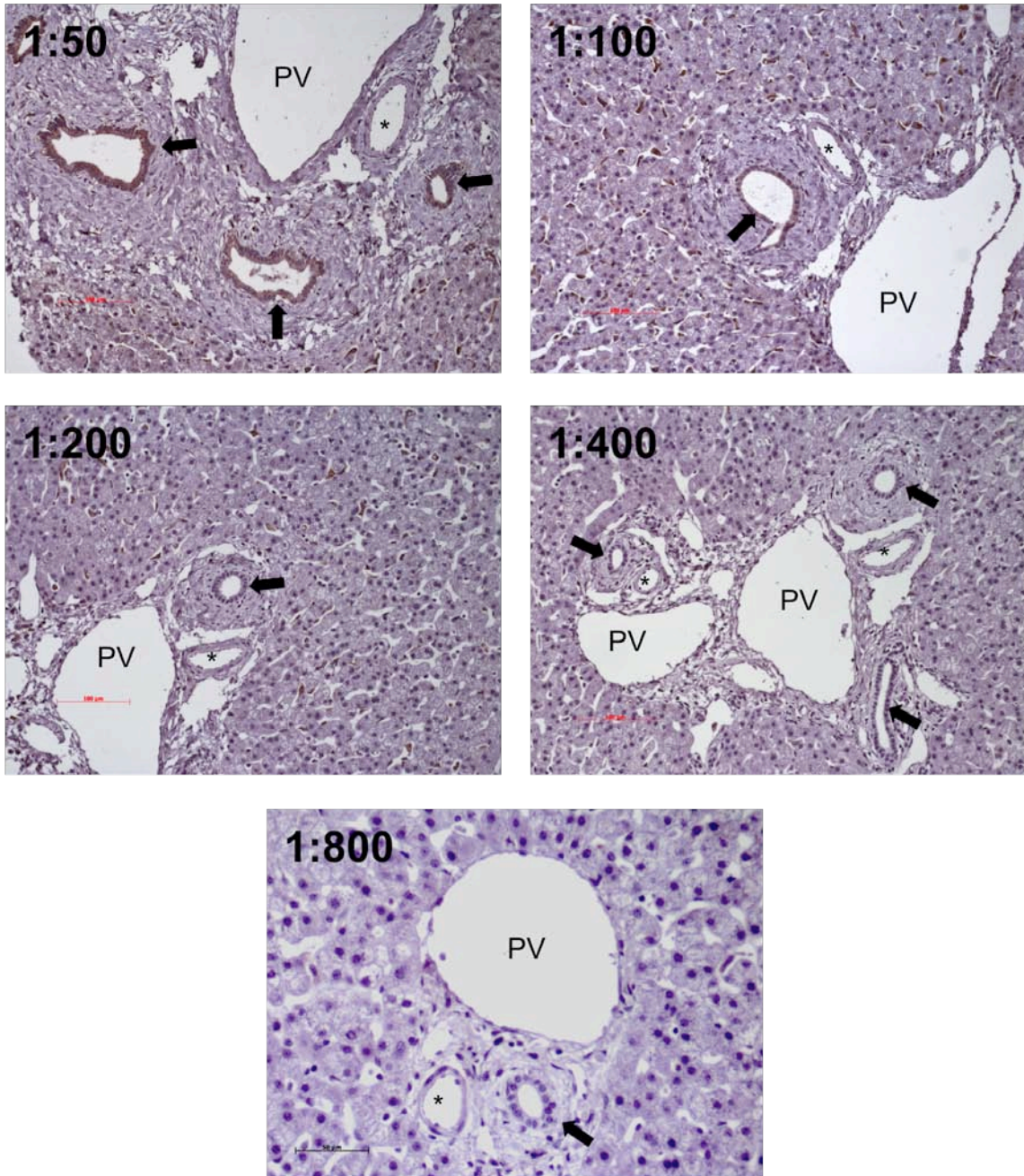


FIGURE 5.5b Fibrocystin antibody (clone 11) titration on sections of formalin-fixed paraffin embedded human liver tissue stained using DAB immunohistochemistry. Anti-fibrocystin monoclonal antibody clone 11 was serially diluted, and tested on normal human liver tissue to determine the optimal dilution that would produce maximal specific staining of the biliary epithelium with minimal non-specific staining. A brown stain is evident in bile ducts positive for fibrocystin (block arrows). Optimal staining was not achieved at any dilution for this clone (See table 5.1). PV = portal vein; * = hepatic artery branch. Original magnification of 1:50, 1:100, 1:200, and 1:400: x200; Scale bar = 100 μ m. Original magnification for 1:800: x400; Scale bar = 50 μ m.

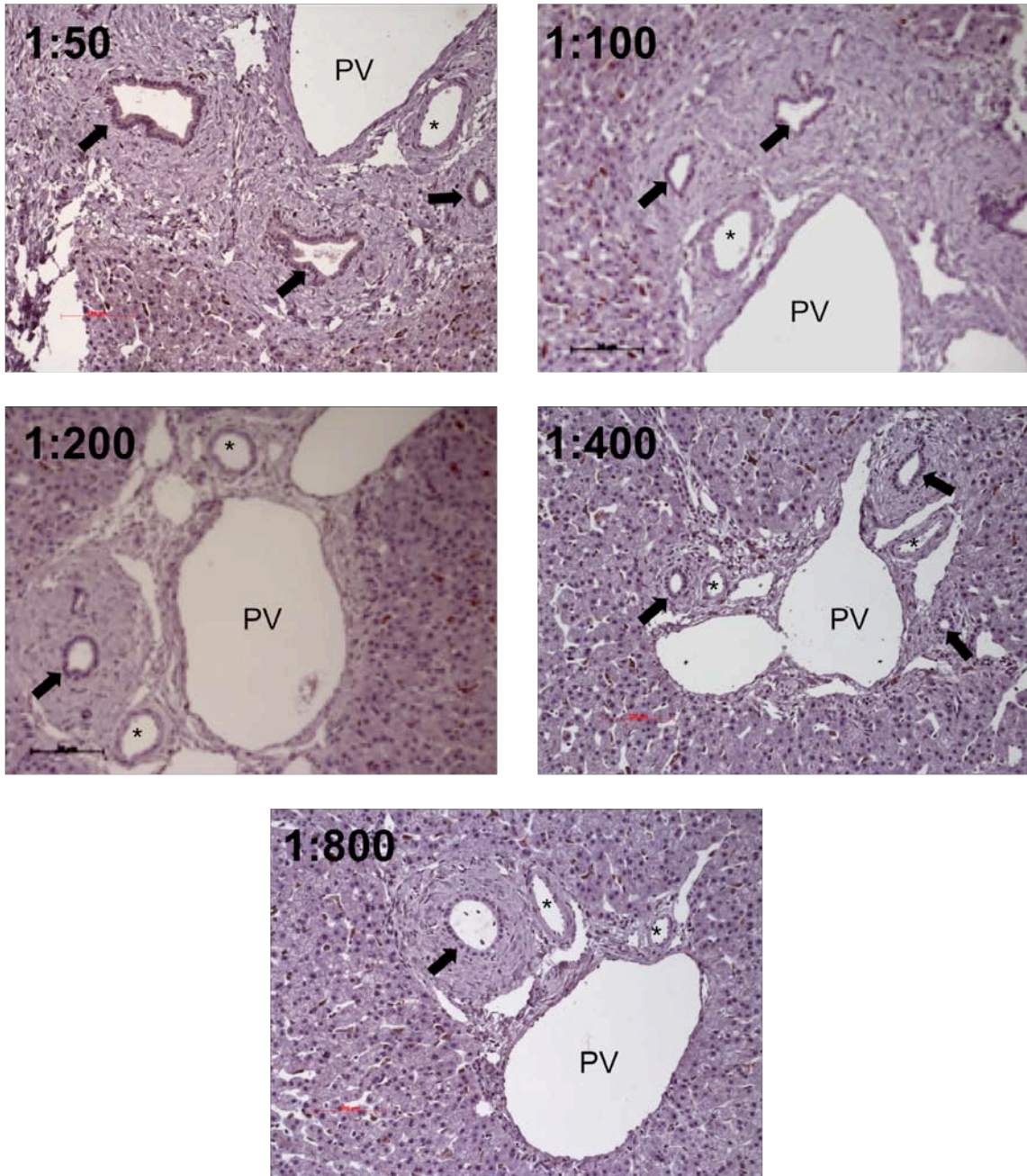


FIGURE 5.5c Fibrocystin antibody (clone 14) titration on sections of formalin-fixed paraffin embedded human liver tissue stained using DAB immunohistochemistry. Anti-fibrocystin monoclonal antibody clone 14 was serially diluted, and tested on normal human liver tissue to determine the optimal dilution that would produce maximal specific staining of the biliary epithelium with minimal non-specific staining. A brown stain is evident in bile ducts positive for fibrocystin (block arrows). Optimal staining was not achieved at any dilution for this clone (See table 5.1). PV = portal vein; * = hepatic artery branch. Scale bar = 100 μ m. Original magnification x200.

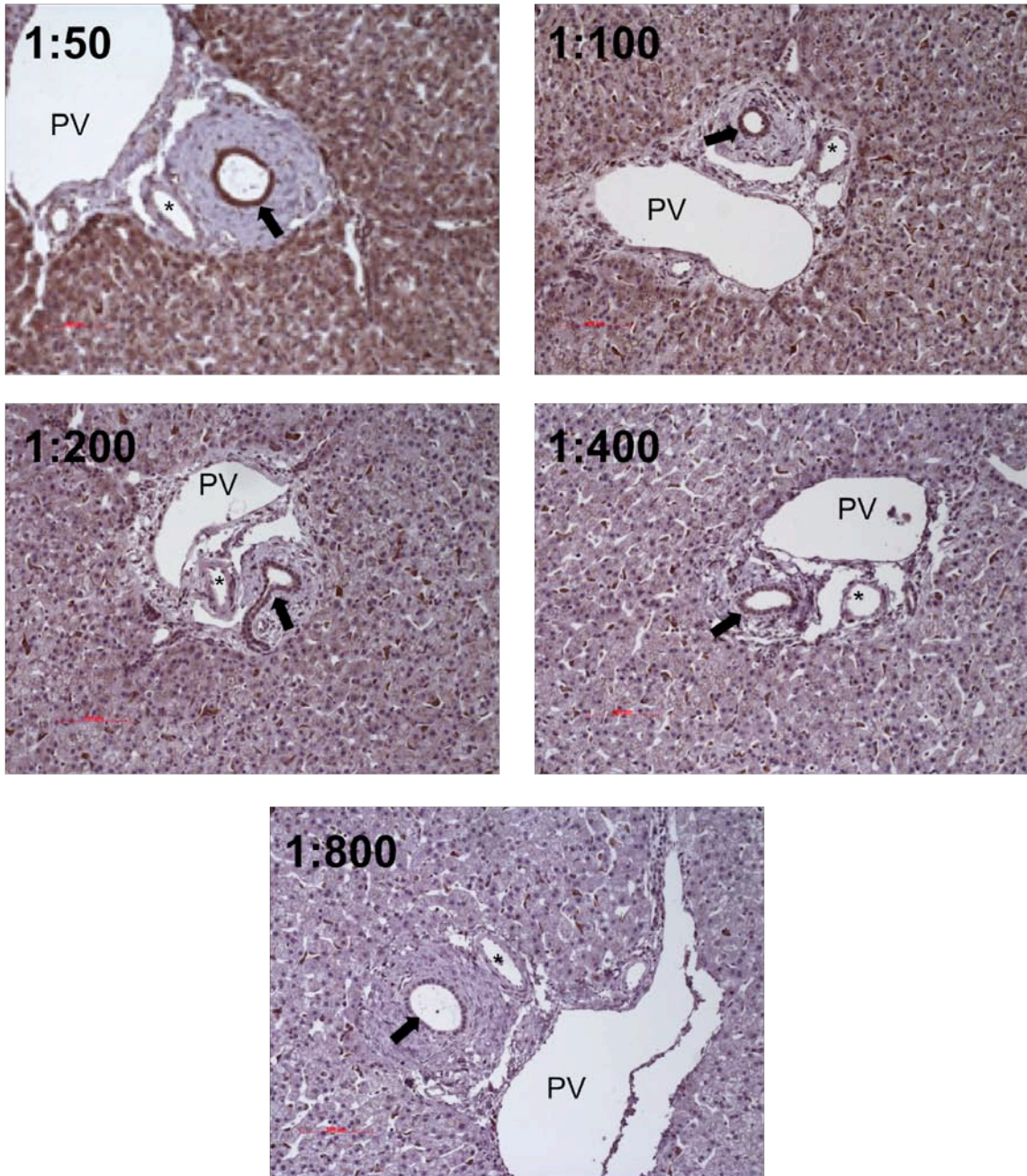


FIGURE 5.5d Fibrocystin antibody (clone 18) titration on sections of formalin-fixed paraffin embedded human liver tissue stained using DAB immunohistochemistry. Anti-fibrocystin monoclonal antibody clone 18 was serially diluted, and tested on normal human liver tissue to determine the optimal dilution that would produce maximal specific staining of the biliary epithelium with minimal non-specific staining. A brown stain is evident in bile ducts positive for fibrocystin (block arrows). Optimal staining was not achieved at any dilution for this clone (See table 5.1). PV = portal vein; * = hepatic artery branch. Scale bar = 100 μ m. Original magnification x200.

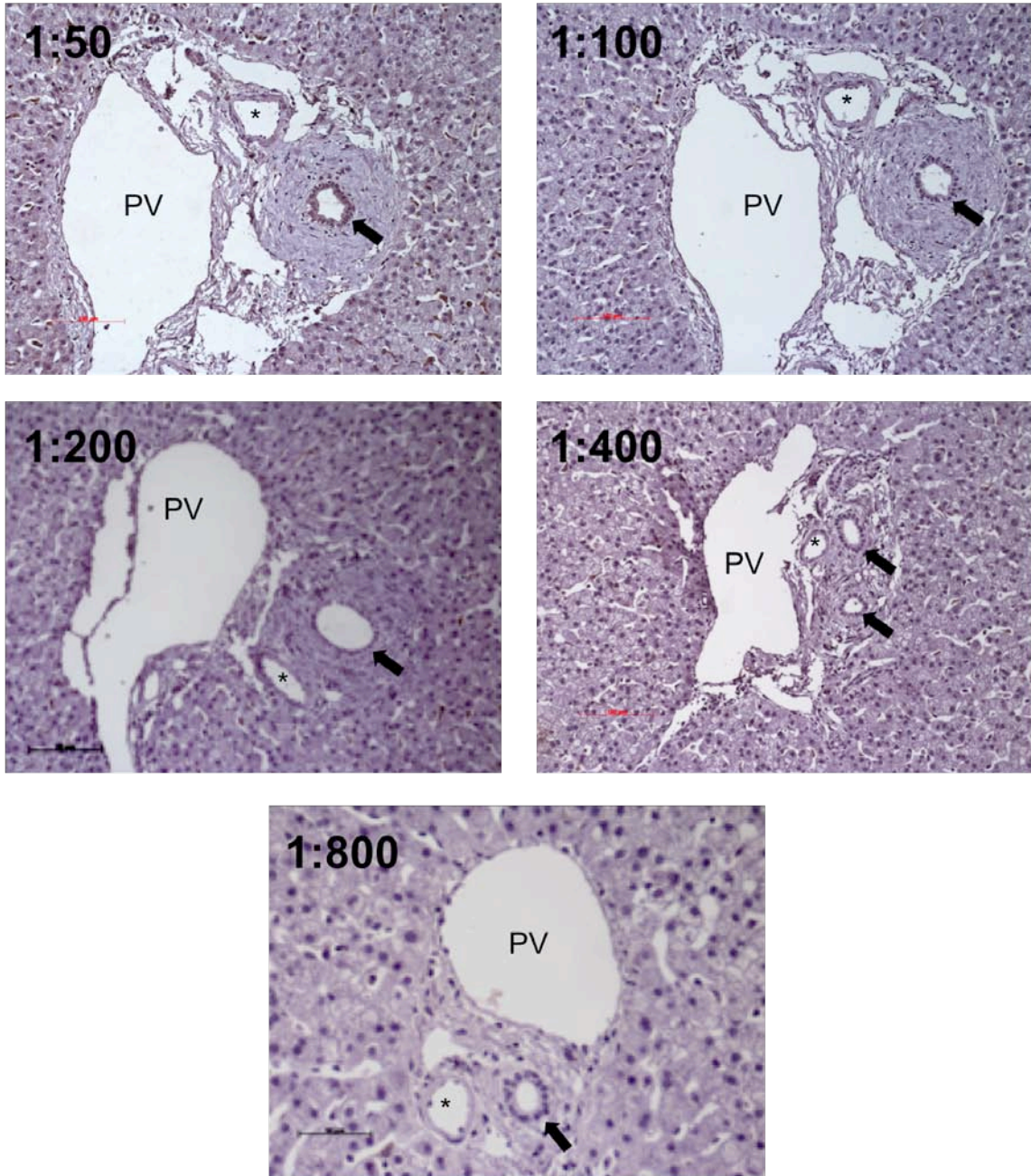


FIGURE 5.5e Fibrocystin antibody (clone 19) titration on sections of formalin-fixed paraffin embedded human liver tissue stained using DAB immunohistochemistry. Anti-fibrocystin monoclonal antibody clone 19 was serially diluted, and tested on normal human liver to determine the optimal dilution that would produce maximal specific staining of the biliary epithelium with minimal non-specific staining. A brown stain is evident in bile ducts positive for fibrocystin (block arrows). Optimal staining was not achieved at any dilution for this clone (See table 5.1). PV = portal vein; * = hepatic artery branch. Original magnification of 1:50, 1:100, 1:200, and 1:400: x200; Scale bar = 100 μ m. Original magnification at 1:800: x400; Scale bar = 50 μ m.

TABLE 5.1 Fibrocystin antibody titration on FFPE human liver tissue sections

Clone (epitope location) (Stock concentration)	Structure	Antibody Dilution				
		1:50	1:100	1:200	1:400	1:800
5a (C-terminal) (0.50 mg/ml)	BD	+++	++	+	-	-
	KC	-	-	-	-	-
	b/g	+	-	-	-	-
11 (N-terminal) (0.30 mg/ml)	BD	++	+	-	-	-
	KC	+++	++	+	-	-
	b/g	-	-	-	-	-
14 (N-terminal) (0.57 mg/ml)	BD	-	-	-	-	-
	KC	+++	+++	+++	++	+
	b/g	-	-	-	-	-
18 (N-terminal) (0.27 mg/ml)	BD	+++	+++	++	+	-
	KC	+++	+++	+++	++	++
	b/g	+++	++	+	-	-
19 (N-terminal) (0.59 mg/ml)	BD	+	-	-	-	-
	KC	++	+	+	-	-
	b/g	-	-	-	-	-

Key: -, no visible staining; +, faint staining on cells; ++, moderate staining on most cells; +++ intense staining on cells; BD, bile ducts; KC, kupffer cells; b/g, background (non-specific). Optimal staining was judged as the antibody giving maximal optimal signal, with minimal background, and nonspecific staining. This was obtained with clone 5a at a dilution of 1:100, as it provided strong specific staining, with no background or non-specific staining.

5.3.3 Increased levels of acetylated α -tubulin and decreased levels of fibrocystin expression are detected in a cohort of various adult liver diseases

Fibrocystin expression in BEC within tissue specimens taken from a variety of end-stage inflammatory and non-inflammatory liver diseases was variable within different structures for each disease type included (Table 5.4). Fibrocystin expression was also documented in nerve bundles, inflammatory cells, and portal vessels within tissue sections for most cases studied, but was not always evident in these structures (not shown). In normal tissue, bile ducts were consistently positive for fibrocystin, whereas staining was frequently low or absent in all end-stage liver disease tissue including end-stage BA (Figs. 5.6 and 5.7). Kasai wedge biopsies, taken at the time of HPE surgery during the earlier stages of BA, showed ductules strongly expressing fibrocystin (Fig. 5.7).

The count data analyses for the number of positive ducts per section, and per case are shown in table 5.3 and figures 5.8 and 5.9. Raw count data can be found in appendix 2, table 2.1. The overall intensity of staining for each disease group shows staining intensity was diminished overall in all end-stage tissue, if staining was at all present. For all end-stage diseases, the reduction in the number of positive cells relative to normal tissue is statistically significant, at $p < 0.05$ (Table 5.3).

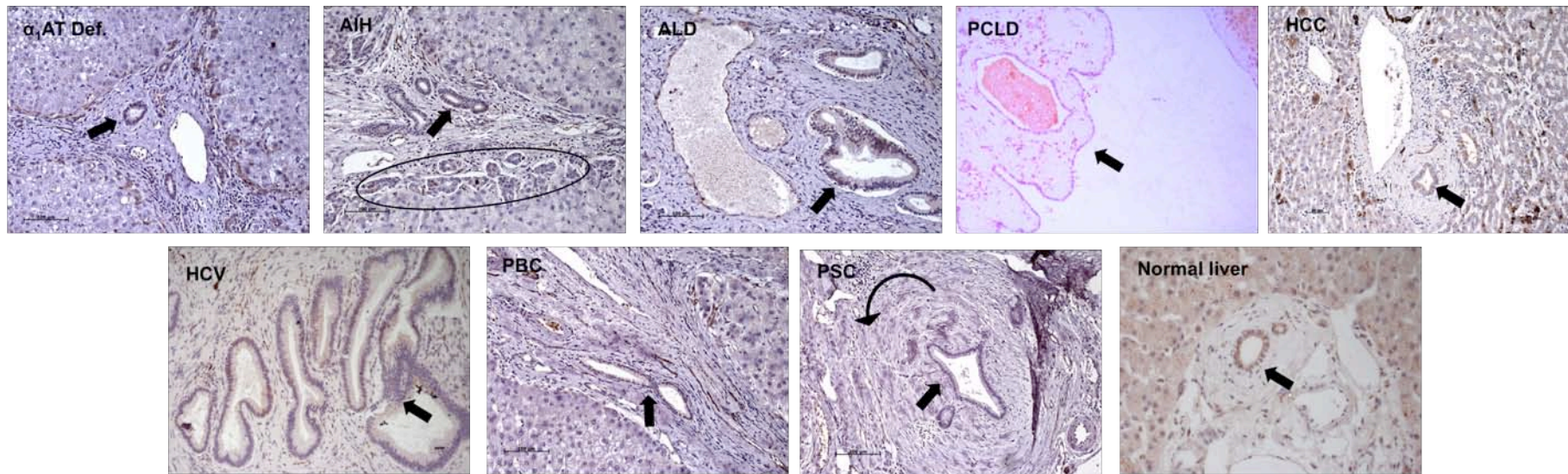


FIGURE 5.6 Fibrocystin expression on sections of formalin-fixed paraffin-embedded adult human end-stage liver disease tissue stained using DAB immunohistochemistry. This method results in a brown reaction product where fibrocystin is expressed. Expression of fibrocystin was frequently low or absent in bile ducts from all end stage liver disease tissue (block arrows). In contrast, most bile ducts in normal liver tissue were strongly positive (block arrow in bottom, right panel). Evidence of ductular proliferation is also evident in the section of AIH liver tissue (black oval). Note also the characteristic concentric oblitative fibrosis of PSC surrounding the bile duct (curved black arrow). α_1 AT Def. - α_1 -antitrypsin deficiency (n=5); AIH - autoimmune hepatitis (n=5); ALD - alcoholic liver disease (n=5); PCLD - polycystic liver disease (n=6); HCC - hepatocellular carcinoma (n=5); HCV - hepatitis C viral infection (n=5); PBC - primary biliary cirrhosis (n=5); PSC - primary sclerosing cholangitis (n=5). Original magnification of normal liver section: x400. Original magnification of all other sections: x200.

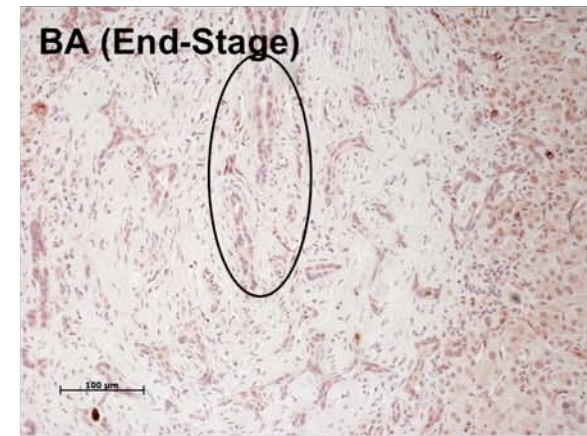
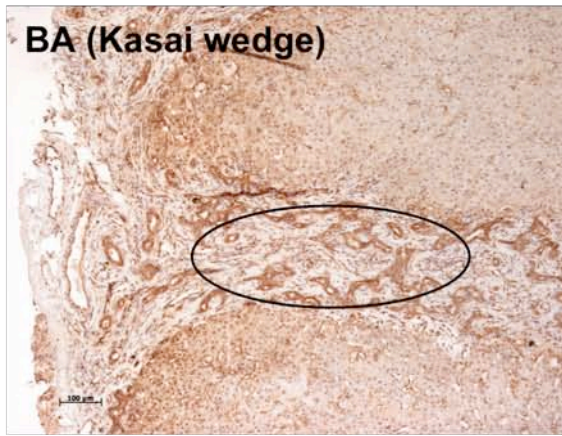
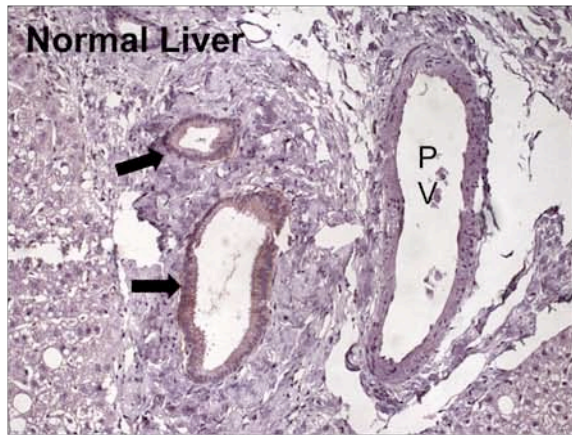


FIGURE 5.7 Fibrocystin expression on sections of formalin-fixed paraffin embedded human biliary atresia liver tissue. Sections were stained using DAB histochemistry, which produces a brown stain exclusively where fibrocystin is present. In normal tissue bile ducts were consistently positive for fibrocystin (block arrows). Kasai wedge biopsies taken at the time of hepatobiliary surgery during the earlier stages of biliary atresia show intense proliferation of biliary epithelial cells. Ductules retain positivity for fibrocystin in the early stages of biliary atresia (ductular structures within oval). Staining of fibrocystin in bile ducts and ductules in end-stage biliary atresia is absent (ductular structures within oval); indicating that expression of fibrocystin is eventually lost at the point of end stage disease. Normal Liver: original magnification x200. BA (Kasai wedge): original magnification x100, scale bar = 100µm. BA (end-stage): original magnification x200, scale bar = 100µm. PV – portal vein; BA – biliary atresia.

TABLE 5.2 Expression levels of fibrocystin in various structures within human liver tissue sections. Table shows qualitative representation of the overall staining intensity observed within all cases of the cohort. Staining was carried out on FFPE tissue sections using the anti-fibrocystin antibody 5a.

Specimen type	Ducts	Hepatocytes	Vessels	Infiltrate	Stroma	Other
NL (n=5)	++	-	-	-	-	Nerve bundles +++
PCLD (n=6)	+	-	-	-	-	Occasional cyst +
PBC (n=5)	+	-	-	-	-	Nerve bundles +++
PSC (n=5)	-	-	-	-	-	Nerve bundles +++
AIH (n=5)	+/-	-	-	-	-	Nerve bundles +++
ALD (n=5)	-	-	-	-	-	Nerve bundles +++
α_1 AT Def. (n=5)	-	-	-	-	-	
HCC (n=5)	+/-	-	-	+++	-	
HCV (n=5)	+/-	-	++	+	-	
BA (HPE) (n=5)	++	-	++	-	-	
BA (End-stage) (n=6)	-	-	+	-	-	

Key: -, no visible staining; +, faint staining on cells; ++, moderate staining on most cells; +++, intense staining on cells; NL, normal liver; PCLD, polycystic liver disease; PBC, primary biliary cirrhosis; PSC, primary sclerosing cholangitis; AIH, autoimmune hepatitis; ALD, alcoholic liver disease; α_1 AT Def, α_1 -antitrypsin deficiency; HCC, hepatocellular carcinoma; HCV, hepatitis C viral infection; BA, biliary atresia; HPE, hepatportoenterostomy.

TABLE 5.3 Fibrocystin immunohistochemical staining data analysis

Specimen type	Number of cases	Total positively staining bile ducts	Total % positive	Mean % positive	Standard deviation	Intensity	Cysts	P-value*
NL	5	144/204	71	67	24.496	++	N/A	-
PCLD	6	54/281	19	24	34.349	+	Occ. +	0.020
PBC	5	10/130	8	8	8.373	+	N/A	0.002
PSC	5	13/188	7	4.26	9.526	-	N/A	0.002
AIH	5	21/108	19	11	11.563	+/-	N/A	0.002
ALD	5	13/52	25	5	11.180	-	N/A	0.001
α_1 AT Def.	5	20/60	33	7	14.892	-	N/A	0.001
HCC	5	29/99	29	24	34.866	+/-	N/A	0.031
HCV	5	8/270	3	6	10.654	+/-	N/A	0.002
BA	11	0/418	0	0	0	-	N/A	0.002

Key: -, no visible staining; +, faint staining on cells; ++, moderate staining on most cells; +++, intense staining on cells; NL, normal liver; PCLD, polycystic liver disease; PBC, primary biliary cirrhosis; PSC, primary sclerosing cholangitis; AIH, autoimmune hepatitis; ALD, alcoholic liver disease; α_1 AT Def, α_1 -antitrypsin deficiency; HCC, hepatocellular carcinoma; HCV, hepatitis C viral infection; BA, biliary atresia; Occ., occasional. P-value relative to normal liver for a 1-tailed unpaired t-test with assumption of unequal variance, significance $p < 0.05$.

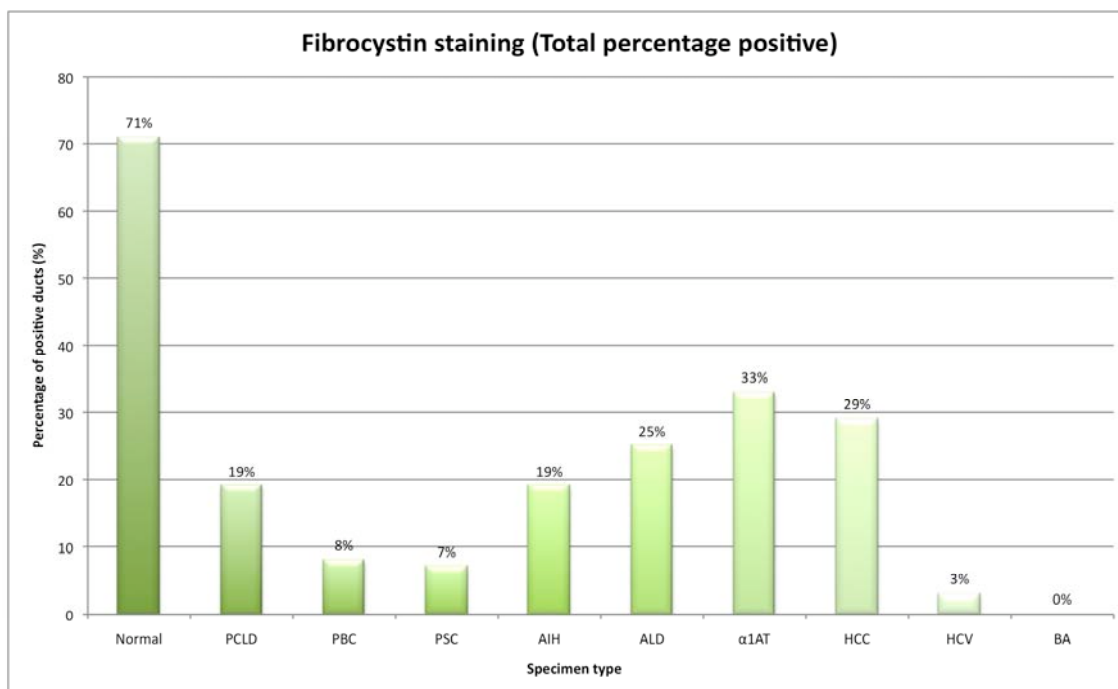


FIGURE 5.8 Fibrocystin cohort staining count data: total percentage of positive ducts. All visible bile ducts, and ductules on stained sections were counted, and analysed. The number of positively staining bile ducts, for each disease group, is expressed as a percentage of the total ducts counted, for that group. The total number of positive ducts, from normal liver is 71%. The percentage of positive ducts is significantly decreased in all end-stage liver diseases, when compared to levels of staining in normal tissue. PCLD, polycystic liver disease; PBC, primary biliary cirrhosis; PSC, primary sclerosing cholangitis; AIH, autoimmune hepatitis; ALD, alcoholic liver disease; α₁AT, α₁-antitrypsin deficiency; HCC, hepatocellular carcinoma; HCV, hepatitis C viral infection; BA, biliary atresia.

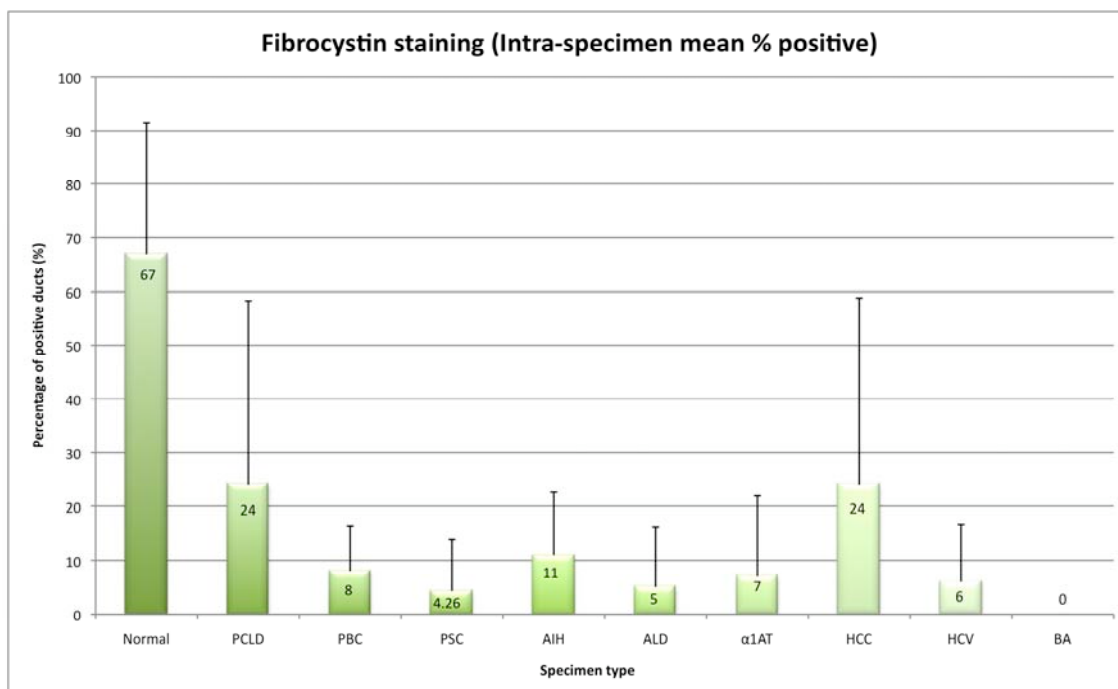


FIGURE 5.9 Fibrocystin cohort staining count data: intra-specimen mean percentage of positive ducts. Chart representing the mean percentage of bile ducts that stained positive for fibrocystin within each disease group. All visible bile ducts, and ductules on stained sections were counted, and analysed. The number of positively staining bile ducts, for each specimen, within each disease group, is expressed as a percentage of the total ducts counted. The mean number of positive ducts, from normal liver is 67%. On average, the mean percentage of positive bile ducts within each specimen of end-stage liver disease tissue is significantly lower, when compared to normal tissue. PCLD, polycystic liver disease; PBC, primary biliary cirrhosis; PSC, primary sclerosing cholangitis; AIH, autoimmune hepatitis; ALD, alcoholic liver disease; α₁AT, α₁-antitrypsin deficiency; HCC, hepatocellular carcinoma; HCV, hepatitis C viral infection; BA, biliary atresia. Error bars represent standard deviation for each disease.

Expression of acetylated α -tubulin by BEC within the tissue sections studied juxtaposes that of fibrocytin. Expression was consistently negative in normal liver. However, one out of the five normal specimens presented with mild/moderate steatosis and contained weakly positive bile ducts, hepatocytes, and stellate cells (not shown). All disease groups showed very strong acetylated α -tubulin staining of bile ducts, particularly in periseptal regions of ductular reactivity (Fig. 5.11). Periseptal/peripoportal hepatocytes and bile ducts were strongly positive in ALD, HCC, and HCV (not shown). Staining for acetylated α -tubulin in BA biopsies taken at Kasai HPE was identical to that seen in all end-stage livers (Fig. 5.12). Strong acetylated α -tubulin staining was present in both the early and late stages of BA in ductules and hepatocytes, consistent with the observations made in other cohorts of end-stage adult liver disease (Fig. 5.13).

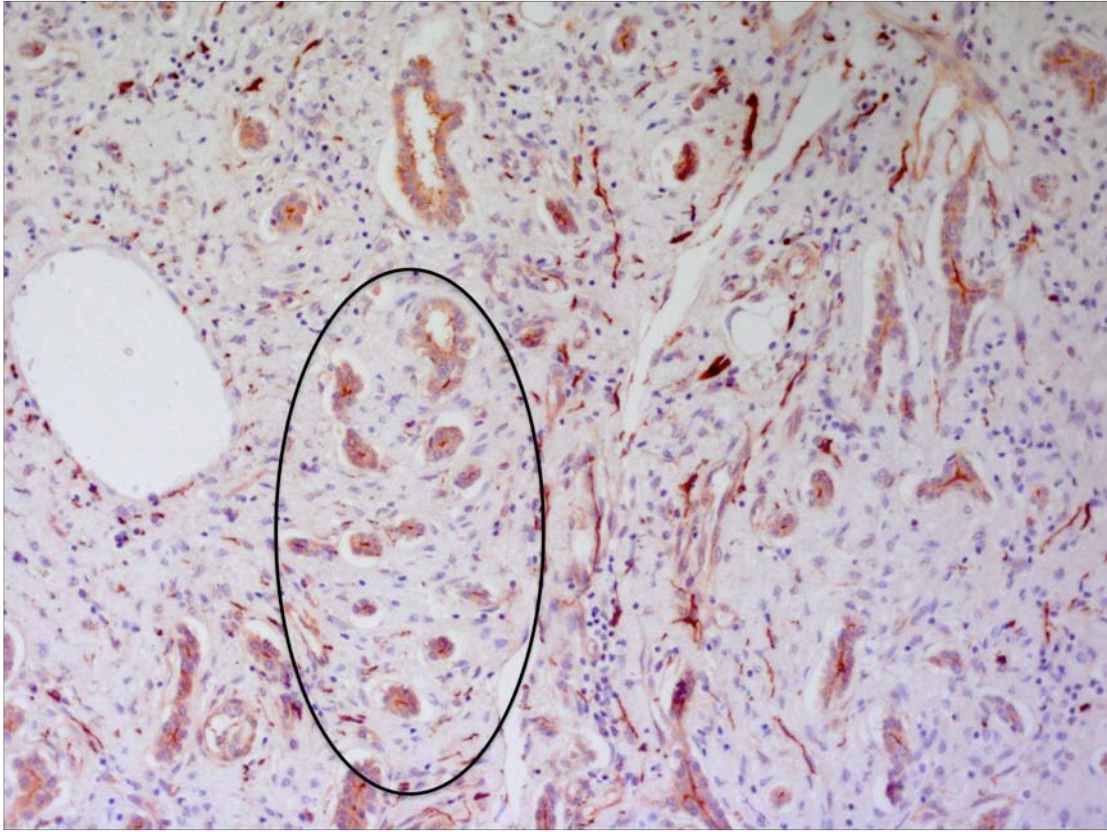


FIGURE 5.10 Section of end-stage autoimmune hepatitis human liver tissue displaying periseptal ductular reactivity. Formalin-fixed paraffin-embedded section stained with acetylated α -tubulin histochemistry. The stained section shows positively staining, periseptal ductular proliferation in response to inflammation and fibrosis (highlighted area). Original magnification: x200.

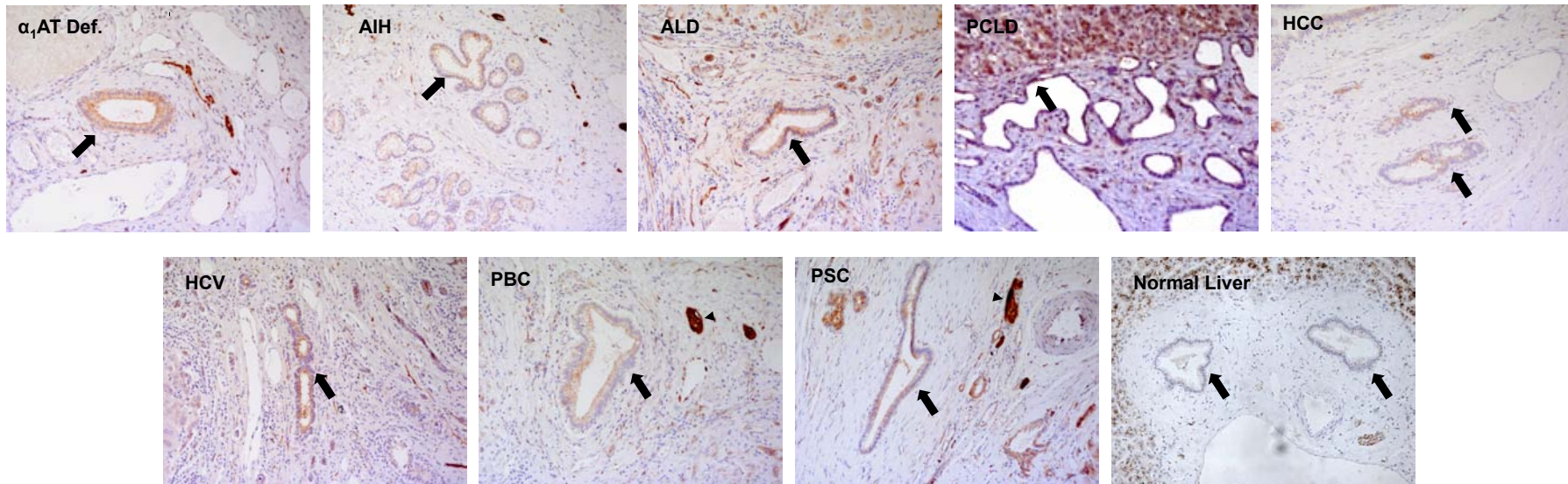


FIGURE 5.11 Acetylated α -tubulin expression on sections of formalin-fixed paraffin-embedded human end-stage liver disease tissue stained using DAB immunohistochemistry. This method results in a brown reaction product where acetylated α -tubulin is expressed. Expression of acetylated α -tubulin was completely absent from bile ducts in normal donor liver (bottom, far left panel, block arrows). In contrast, most disease groups showed strong positive staining in bile ducts and reactive ductules (block arrows). Strong expression of acetylated α -tubulin was seen in periseptal hepatocytes in HCV and ALD. Inflammatory cells were generally negative. Malignant cells of HCC were strongly positive whereas cystic epithelium in adult PCLD was generally negative (block arrow). Nerve bundles were also stained strongly for acetylated α -tubulin in several of the disease groups (line arrows). α_1 AT Def. - α_1 -antitrypsin deficiency; AIH - autoimmune hepatitis; ALD - alcoholic liver disease; PCLD - polycystic liver disease; HCC - hepatocellular carcinoma; HCV - hepatitis C viral infection; PBC - primary biliary cirrhosis; PSC - primary sclerosing cholangitis. Original magnification: x200.



FIGURE 5.12 Acetylated α -tubulin expression on sections of formalin-fixed paraffin-embedded human biliary atresia liver tissue. Sections were stained using DAB histochemistry, which produces a brown stain where acetylated α -tubulin is present. In normal tissue bile ducts were consistently negative for acetylated α -tubulin (far left panel, line arrows). Kasai wedge biopsies taken at the time of hepatobiliary surgery during the earlier stages of biliary atresia show intense proliferation of biliary epithelial cells. Strong acetylated α -tubulin staining was present in both the early (middle panel, oval), and late stages of biliary atresia (far right panel, oval), in ductules and hepatocytes, consistent with the observations made in other cohorts of end stage adult liver disease. BA – biliary atresia. Original magnification: Normal liver, and BA Kasai wedge, x200; BA end-stage x100.

TABLE 5.4 Expression levels of acetylated α -tubulin in a number of structures within human liver tissue sections. Table shows qualitative representation of the overall staining intensity observed within all cases of the cohort. Staining was carried out on FFPE tissue sections using the anti-acetylated α -tubulin antibody 6-11B-1.

Specimen type	Ducts	Hepatocytes	Vessels	Infiltrate	Stroma	Other
NL	-	-	-	-	-	
PCLD	++	-	-	-	-	Cysts +
PBC	++	-	-	-	-	
PSC	++	-	-	-	-	
AIH	++	+	-	-	-	
ALD	++	++	-	-	+	
α_1 AT def.	++	+	-	-	-	
HCC	++	+	-	-	-	Tumour cells+
HCV	++	+	-	-	-	
BA (HPE)	++	+/-	-	-	-	
BA (end-stage)	++	+	-	-	-	

Key: -, no visible staining; +, faint staining on cells; ++, moderate staining on most cells; +++ intense staining on cells; NL, normal liver; PCLD, polycystic liver disease; PBC, primary biliary cirrhosis; PSC, primary sclerosing cholangitis; AIH, autoimmune hepatitis; ALD, alcoholic liver disease; α_1 AT Def, α_1 -antitrypsin deficiency; HCC, hepatocellular carcinoma; HCV, hepatitis C viral infection; BA, biliary atresia.

To summarise, normal tissue bile ducts were consistently positive for fibrocystin, and negative for acetylated α -tubulin. In all end-stage liver disease tissue studied, bile ducts were consistently negative for fibrocystin, and positive for acetylated α -tubulin. Kasai wedge biopsies taken at the earlier stages of BA, showed that ductules retain positivity for fibrocystin, but that it is eventually lost at the point of end-stage disease, whilst retaining expression of acetylated α -tubulin.

5.3.4 Immunofluorescence analysis of primary ciliary expression in HEK293 cells: time-course evaluation

Cells were evaluated for the expression of primary cilia 1, 3, or 5 days post-confluency, by staining with the ciliary marker acetylated α -tubulin, and the ciliary protein fibrocystin as an additional confirmation. At none of the above time points were cilia uniformly expressed by

HEK293 cells under the culture conditions used. Ciliary like structures were however observed in isolated cells, see figure 5.13.

5.3.5 Immunofluorescence analysis of primary ciliary expression in primary BEC: substratum, ECM, and time-course evaluation

Primary BEC were evaluated for ciliary expression after culture on a variety of substrata coated with different matrix components, using the ciliary marker acetylated α -tubulin, and the ciliary protein fibrocystin as additional confirmation that the structure observed was a primary cilium. Cells did not always achieve 100% confluency on all the substrates investigated and so a time-course of 1, 3, or 5 days post-confluence could not always be strictly adhered to. Where cells did reach 100% confluency the time-course was followed. Cells that could not maintain 100% confluency due to cells washing off during feeding were examined the same number of days post-plating as cells that were able to maintain 100% confluency. Primary BEC, isolated from liver tissue taken from patients suffering end-stage liver disease where cholangiocyte damage is not the primary pathology e.g. Non-alcoholic steatohepatitis, did not uniformly express primary cilia under any of the culture conditions used. However, cilia were found on isolated cells under certain conditions. Where observed, both acetylated α -tubulin and fibrocystin co-localised to the structure, providing confirmatory evidence (Figure 5.14). In summary, none of the cell types used were able to uniformly express primary cilia under any of the conditions tested, and therefore were unsuitable for any further studies into ciliary expression, structure, or function *in vitro*. All results are also summarised in table 5.5.

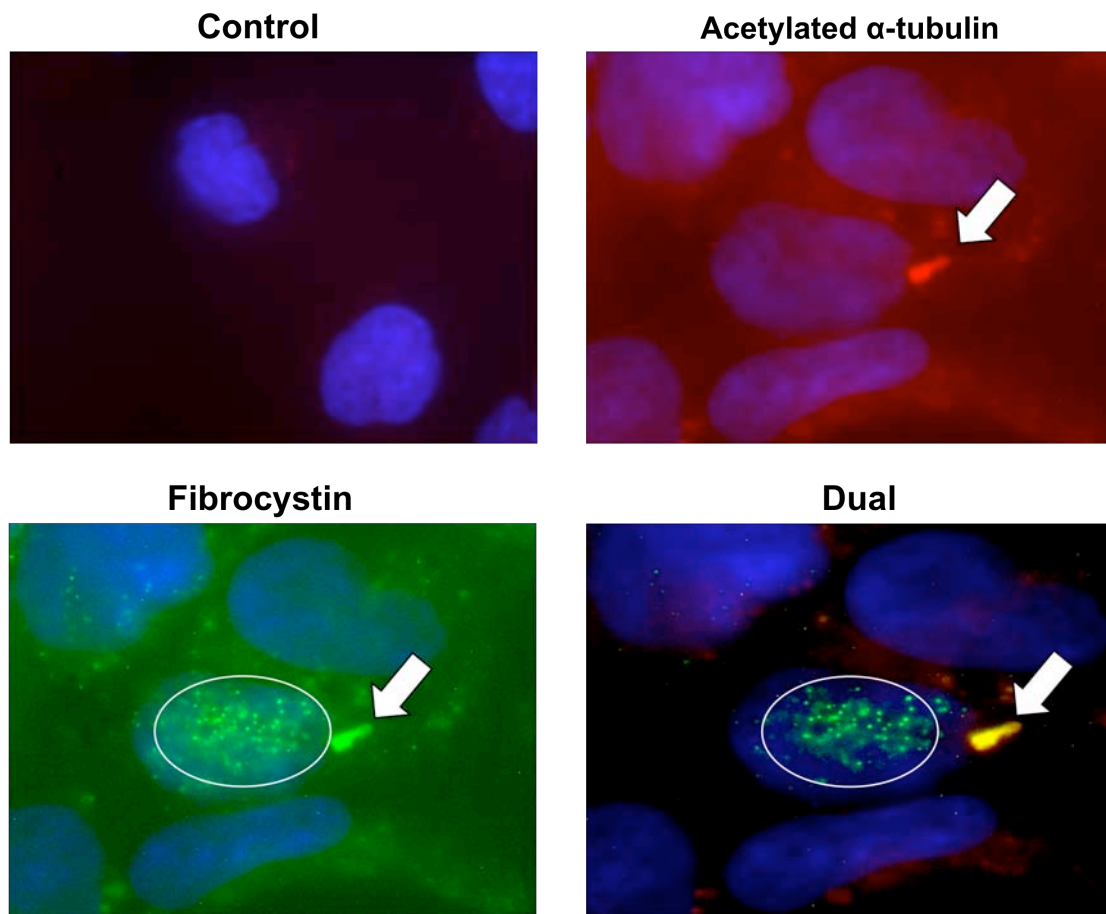


FIGURE 5.13 Representative images of a primary cilium observed on an isolated cell from 100% confluent HEK293 cells grown on gelatine coated glass coverslips. HEK293 cells in culture did not uniformly express primary cilia, but cilia were observed on isolated cells within monolayers. Top left panel shows control where the primary antibody has been excluded in order to determine the levels of nonspecific secondary staining. Levels of non-specific staining were extremely low and very acceptable. Top right panel shows only the TxRed channel representing acetylated α -tubulin staining. Acetylated α -tubulin is localised to what appears to be the axoneme of a primary cilium (block arrow). Bottom left panel shows only the FITC channel representing fibrocystin staining. Fibrocystin localises to the axoneme of the primary cilium, confirming the structure to be a primary cilium (block arrow). Fibrocystin also appears to be speckled throughout the cytoplasm, as observed by [Nagano et al., 2005] (white circle). Bottom right panel shows the TxRed and FITC channels merged confirming the colocalisation of acetylated α -tubulin and fibrocystin to the primary cilia of HEK293 cells when present. Key: Red, acetylated α -tubulin; Green, fibrocystin; Blue, DNA.

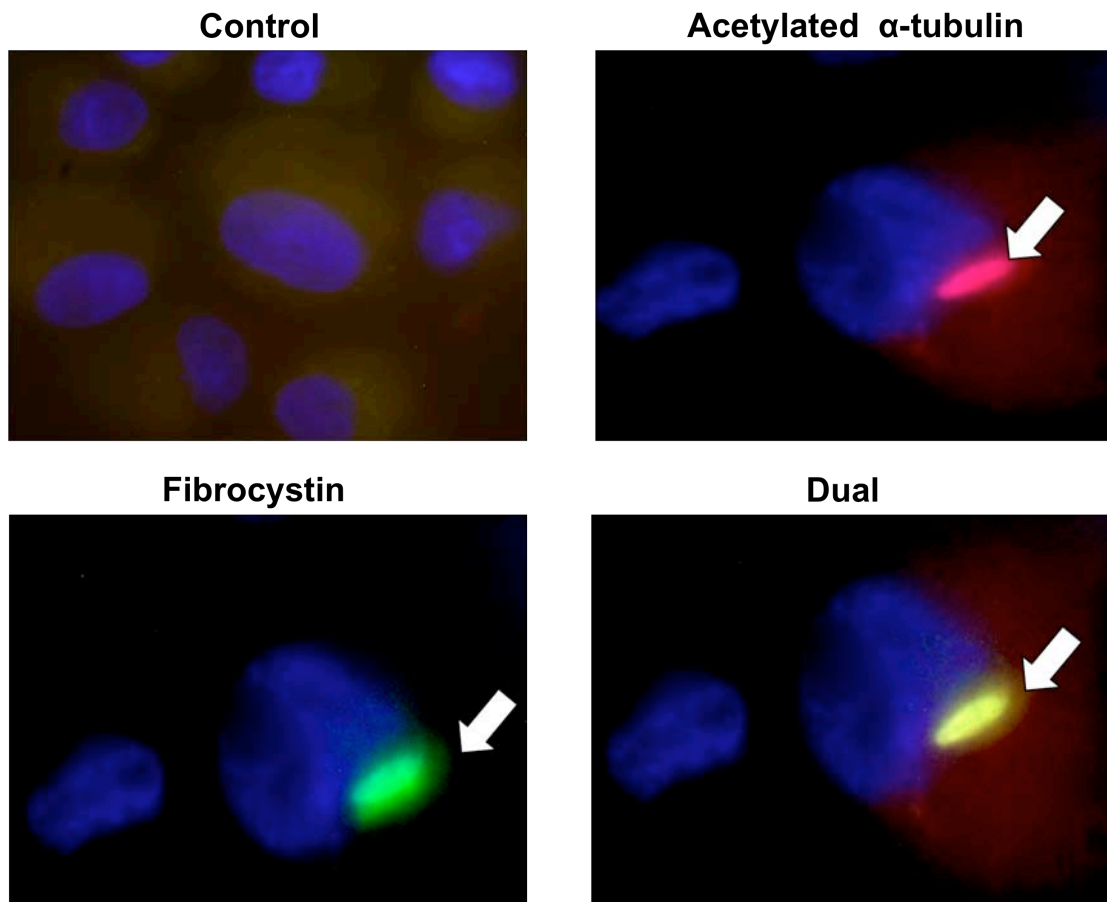


FIGURE 5.14 Representative images of a primary cilium observed on an isolated cell from sub-confluent BEC grown on gelatine coated glass coverslips. BEC in culture did not uniformly express primary cilia, but cilia were observed on isolated cells within monolayers. Top left panel shows control where the primary antibody has been excluded in order to determine the levels of non-specific secondary staining. Levels of non-specific staining were extremely low and acceptable. Top right panel shows only the TxRed channel representing acetylated α -tubulin staining. Acetylated α -tubulin is localised to what appears to be the axoneme of a primary cilium (block arrow). Bottom left panel shows only the FITC channel representing fibrocystin staining. Fibrocystin localises to the axoneme of the primary cilium, confirming the structure to be a primary cilium (block arrow). Bottom right panel shows the TxRed and FITC channels merged confirming the co-localisation of acetylated α -tubulin and fibrocystin to the primary cilia of BEC cells when expressed. Key: Red, acetylated α -tubulin; Green, fibrocystin; Blue, DNA.

TABLE 5.5 Summary of BEC substratum and ECM ciliary expression optimisations

MATRIX SUBSTRATE	Uncoated	Gelatine coated	Collagen coated	Poly-lysine coated
Permanox® chamber slides	Cells did not attached adequately to allow cells to grow to confluency. Transmission microscopy showed cellular morphology was also poor.			
Thermanox® coverslips	High levels of background autofluorescence in all channels from the coverslips prevented accurate assessment of ciliary expression. Transmission microscopy showed good epithelial morphology			
Glass coverslips	Cells grew well. No cilia observed.	Cells grew well. Cilia observed on isolated cells.	Cells grew well. No cilia observed.	Cells grew well. No cilia observed.
Acid-washed glass coverslips	Good cellular growth, but cells tended to wash away upon feeding.	Good cellular growth. No cilia observed.	Cells grew well. No cilia observed.	Good cellular growth. Primary cilia observed on isolated cells.

5.4 CONCLUSIONS

The main finding of this chapter is the novel observation that decreased expression of fibrocystin in biliary epithelium is associated with elevated levels of α -tubulin acetylation in both inflammatory and non-inflammatory adult end-stage liver diseases. This observation is also true in end-stage BA with and without cysts. In contrast, in the early stages of BA fibrocystin expression is still evident, despite elevated levels of α -tubulin acetylation. The consequences of this are not obvious, however, as they are not limited to one disease it does suggest that these events occur secondary to the primary disease process and are not causative. What can be concluded from this immunohistochemical work is that decreased expression of fibrocystin and increased α -tubulin acetylation in biliary epithelial cells could be a non-specific marker of an ongoing assault to the biliary tree in a multitude of hepatic disorders.

Secondary to the immunohistochemical characterisation of fibrocystin expression in patient samples, the next aim of this chapter was to examine the structure and/or function of BEC primary cilia *in vitro*. Unfortunately the failure of the cells used to produce uniform ciliary expression meant this section of the project completely failed to meet the aims set-out.

The findings of the work carried out to try to obtain uniform ciliary expression in the human embryonic kidney epithelial cell line HEK293 were that, although HEK293 cells are capable of expressing primary cilia in culture, uniform expression cannot be obtained in 2-dimensional culture on an impermeable substratum. The findings for primary BEC is identical to that of HEK293 cells. As a result of this all aims based upon the visualisation and characterisation of primary cilia on cells *in vitro* were abandoned, however they will be discussed later.

5.5 DISCUSSION

The absence of fibrocystin staining in the liver sections from children with biliary atresia and renal cyst may be due to lack of expression by *PKHD1* due to a molecular defect within the gene. This would support the overall project hypothesis of abnormal ciliary development in the aetiology of BA. Alternatively, as the observation was also made in liver sections from a mixed cohort of adult end-stage liver diseases, the absence of fibrocystin may be related to loss of expression secondary to advanced biliary disease, and could be a non-specific marker of liver damage, along with elevated levels of α -tubulin acetylation. If this is indeed the case, this raises the following questions; what causes this change in fibrocystin expression and α -tubulin

acetylation, and what are the resultant effects? At this point the answers to these questions can only be speculated upon.

In terms of fibrocystin expression, the reasons for a decrease in expression are difficult to speculate as the basic function of this protein is yet to be fully understood. However, with the knowledge that mutations in the gene encoding fibrocystin, *PKHD1*, are responsible for ARPKD, clues as to its function are beginning to be elucidated. ARPKD is characterised by the cystic dilatation of the PTs of the kidneys, and bile ducts with CHF. Characterisation of cystic BEC by multiple groups has determined that fibrocystin is absent from the primary cilia of these cells, which in some cases also display an abnormal axonemal architecture [Haycraft et al., 2001; T. V. Masyuk et al., 2003; Pazour et al., 2000]. Upon further characterisation of the cystic epithelia it was discovered that the epithelial cells surrounding the cysts are usually less well differentiated [Lin and Satlin, 2004], suggesting fibrocystin expression is tied into the differentiation state of tubular epithelia. Although it does not appear that tubular epithelia differentiation is dependent upon fibrocystin expression, when it is lost, cells either fail to become fully differentiated, or become dedifferentiated. Despite the fact that not all of the diseases included in the present cohort display a cystic phenotype, the loss of fibrocystin expression could indeed indicate that an altered cellular state occurs as a result of bile ductal damage. Abnormalities in cell polarity have also been described in ARPKD [Calvet, 1994; J. J. Grantham, 1993; 2001; Murcia et al., 1999; P. D. Wilson, 1997]. Thus, the primary cilium is also thought to contribute to the maintenance of cellular polarity within tubular structures and that loss of this organelle can result in/contribute to loss of PCP. Again, although only one of the diseases included in the cohort displays cysts as a main phenotypic characteristic,

loss of BEC polarity is reported in HCV infection [Delladetsima et al., 1996; Goldin et al., 1996; Mihm et al., 1997], PBC [Nakanuma et al., 2001], and AIH [Zen et al., 2005]. Therefore the loss/decrease of fibrocystin expression may also correlate with a loss of epithelia polarity as a result of ductular damage. Unfortunately, the clear visualisation of primary cilia and/or centrosomes in tissue is very difficult due to the many layers of cells present, thus it was not possible to determine if the BECs which lacked fibrocystin staining had altered polarity.

Upon initiation of this project it was not predicted that levels of α -tubulin acetylation would correlate with ductular damage. Immunohistochemical staining for acetylated α -tubulin was included because it was a known marker of primary cilia, and because hyperacetylation of α -tubulin had been associated with hepatocyte damage in ethanol-fed rats. Speculation as to why the acetylation of α -tubulin increases during ductular damage is perhaps a little less extraneous than for the observed decrease in fibrocystin. For instance, protein acetylation is thought to regulate a diverse set of functions [Kouzarides, 2000]. Interestingly, several environmental stresses; ageing, diet, and disease all affect the regulation of the protein acetylation status in cells [Chang and Min, 2002; Deckert and Struhl, 2001; Timmermann et al., 2001]. Recent studies indicate that histone/protein acetylation also regulates the extent of inflammatory responses [Blanchard et al., 2002; Ito et al., 2002; Rahman, 2002]. For example, in allergic diseases such as asthma, enhanced histone acetylation is associated with inflammation, and reduced acetylation with decreased inflammation [Bhavsar et al., 2008]. The relevance of this to α -tubulin acetylation, is that a number of the histone deacetylases (HDACs) and histone acetylases (HATs), are also able to acetylate a variety of non-histone proteins, including α -tubulin [Polevoda and Sherman, 2002]. Therefore, the increase in α -

tubulin acetylation observed in this study could simply be a reflection of an inflammatory response. Or in the case of those disorders not characterised by overt inflammation, the acetylation could reflect an ongoing cellular response to epithelial damage. Interestingly, such functions have also been implicated in cellular polarity [Boyault et al., 2007].

Acetylation of α -tubulin at lysine 40 is an established marker of MT stability [Piperno et al., 1987]. Thus, the amount of acetylated α -tubulin is thought to be proportional to the stability of the MTs. However, it has been reported by several groups that although MT stability is correlated with α -tubulin acetylation, stabilisation is not promoted by α -tubulin acetylation [Palazzo et al., 2003]. In fact, it has recently been shown that increased α -tubulin acetylation does not increase levels of stable MTs; rather MTs must be stabilised by other mechanisms (such as capping [Infante et al., 2000; Piperno et al., 1987]), and then these stable MTs accumulate acetylated α -tubulin [Palazzo et al., 2003]. This is consistent with results showing that tubulin acetylation has no effect on *in vitro* MT assembly [Maruta et al., 1986] and that acetylated tubulin is only detectable in long-lived stable MTs *in vivo* [Webster and Borisy, 1989]. This is further supported by the finding that tubacin, an inhibitor of α -tubulin deacetylation in mammalian cells, causes an increase in α -tubulin acetylation without directly stabilising MTs [Haggarty et al., 2003]. It is also hypothesised that because α -tubulin acetylation alone does not appear to drastically change MT stability, it may instead affect the activity of MT associated proteins (MAPs) or MT motors [Palazzo et al., 2003], enabling the binding of specific MAPs to MTs within specialised domains [Maruta et al., 1986; Mizuno and Singer, 1994].

While it could be argued, that the increased levels of α -tubulin acetylation goes against the proliferative response to ductular damage observed in some of the diseases studied. There are studies that suggest α -tubulin acetylation per se does not play an essential role in some of the functions of MTs such as mitosis in the cell cycle [Gaertig et al., 1995]. Indeed, acetylated α -tubulin is present within the mitotic spindle of several cell types [Piperno et al., 1987]. It is clear however, that the exact functions of α -tubulin acetylation are still to be fully understood. What is clear from this study and many others is that alterations in basal levels of MT acetylation are an indication of an altered cell state.

In summary, the immunohistochemical study of fibrocystin expression in samples of patient tissue has revealed the novel observation that decreased expression of fibrocystin and increased α -tubulin acetylation are non-specific markers of biliary damage in adult end-stage liver disease, and end-stage BA. It also reveals that the observed changes in protein expression are a secondary consequence of the primary disease process rather than a causative event. The study has also shown that α -tubulin acetylation is markedly increased in most common inflammatory liver diseases, highlighting a state of increased cellular activation during the inflammatory process. Thus, on the basis of these findings, it can be concluded that acetylation of α -tubulin is a highly sensitive marker of cellular activation in most common inflammatory liver diseases and the absence of fibrocystin staining reflects ongoing damage to the intrahepatic biliary tree, rather than a phenomenon specific to ciliopathies.

The *in vitro* cell culture work carried out in this chapter, although incomplete, highlights the many requirements that must be met to form a solid foundation to support the aims of any research project that relies upon such a technique. To recapitulate, these include, but are not limited to, identifying a cell line that is suitable to the needs of the investigation, and optimising the isolation and growth conditions of the chosen cells. All of the above factors should have been considered and set-in place before a full study of primary cilia in the chosen cells began. The inability to optimise the most basic complementary techniques required to support this section of the study resulted in the deferral of this part of the project.

The selection of a ciliated human epithelial cell line for the optimisation was challenging. The obvious choice for a project studying bile duct damage would be a BEC line. Unfortunately, the human cholangiocyte cell lines have lost a number of the specialised characteristics of BEC, and none are reported to be ciliated in the literature. The human cell line HEK293 was selected as a candidate, as a tubular epithelial cell. However, many cell lines derived from cells that were originally ciliated *in vivo* do not assemble cilia in culture [Pazour and Witman, 2003], HEK293 cells are no exception to this. HEK293 cells were selected to be studied before the realisation they were entirely unsuitable. HEK293 cells do not fully polarise in culture, explaining the lack of primary ciliary expression [M-Z Zhang et al., 2004b]. Many of the non-human ciliated cell lines are fully polarised in culture, enabling them to produce primary cilia. As the work in this project demonstrates, HEK293 cells may be capable of primary cilia expression in culture under the right conditions. Culture techniques such as collagen-gels and semi-permeable culture inserts, which promote polarisation of the cells, may therefore induce a more uniform expression of primary cilia. Another method that could have

been used to induce ciliary expression in this study is serum starvation, a technique used to induce ciliary expression in cells grown *in vitro*. It is thought this method “aligns” cells for particular properties, such as ciliary expression, a property influenced by the cell-cycle [Cooper and Gonzalez-Hernandez, 2009; Pan and Snell, 2007]. Additionally, a study to identify or generate an alternative human ciliated cholangiocyte cell line would be advantageous to the continuation of this project.

The relevance of primary cultures of isolated BEC for the functional study of fibrocystin in relation to BA is obvious. However, the availability of viable human liver tissue is a limiting factor when conducting an investigation that is dependent upon such a scarce resource. A further limitation is the need to consider the disease affecting the tissue. As this project required viable BEC, diseases characterised by severe cholangiopathy may not produce viable cells, further narrowing the selection of tissue available for the study.

Primary cultures of isolated BEC are also temperamental, with high levels of inter- and intra-sample variability in viability, and yield. Thus, to establish a model system of uniform ciliary expression in primary BEC is challenging. The measures used to develop a system in this project focused around maintaining ease of manipulation, analysis, and image capture. However, it is clear from this work that a culture system more akin to the *in vivo* environment of these cells utilising three-dimensional culture systems such as collagen-gels or semi-permeable cell culture inserts, might have proven more successful. Such systems would however introduce further complications in terms of ease of manipulation, and subsequent

analyses. Although less complex alternative options were available for consideration, again the very nature of primary BEC in culture needed to be carefully considered. Whilst serum starvation has been shown to induce ciliary expression in a number of cell lines [Pan and Snell, 2007], the effect of serum starvation on such a temperamental cell type could be catastrophic. Alternative methods considered also included the culture of the primary isolated BEC in a flow chamber. The constant flow of media over the apical surface of the cells may aid polarisation, inducing ciliary expression. Again, such a system would also introduce complications in terms of subsequent manipulation and image capture, although this could be overcome.

In summary, the main initial project aims that relied upon the establishment of an *in vitro* ciliated cell population could not be met, resulting in a change of focus which led to the novel observation of fibrocystin and α -tubulin acetylation as markers of non-specific BEC damage.

CHAPTER 6 KNOCKDOWN OF *PKHD1* DOES NOT INCREASE OESTROGEN DRIVEN CENTROSOMAL AMPLIFICATION IN PRIMARY MURINE PROXIMAL TUBULE EPITHELIAL CELLS

6.1 INTRODUCTION

Knockdown of *Pkhd1* in the *Del2* mouse model results in what appears to be a gender specific renal cystic disease, with a 'star-burst' ciliary phenotype in the cystic renal epithelia of both sexes. The cause of the gender difference is speculated to be due to differences in the expression of androgenic hormones in the two sexes. The reported association of oestrogen with increased levels of cystic disease in ADPKD prompted the hypothesis that the observed difference of renal cystic phenotype in this mouse model is possibly due to the actions of oestrogen in the proximal tubular epithelium, resulting in centrosomal amplification and 'star-burst' cilia, leading to accelerated cystogenesis. This theory was further supported by studies that shed light on the mechanism of centrosomal amplification, by which, oestrogen may drive an abnormal proliferative response in epithelial tissues that may result not only in cysts alone, but may be characteristic of any tissue displaying abnormal proliferative behaviour, such as tumours or the reactive cholangiocytes observed in a number of cholestatic liver diseases, such as BA.

The observation of significant centrosomal amplification in the epithelia lining cysts in the *Pkd1* knockout, and *PKDI* transgenic mouse models, as well as human ADPKD patients provided evidence that centrosomal amplification does indeed play a role in cystic development. Furthermore, these observations indicate that cystoproteins may also play a role

in centrosomal amplification. Taken together, this evidence forms the basis of the following hypothesis:

Knockdown of fibrocystin results in centrosomal amplification, resulting in cystic disease of the renal tubules and bile ducts. The mitogenic effects of oestrogen on receptive tissues, and implication in centrosomal amplification means it may act in synergy to promote a more severe cystic phenotype.

6.2 AIMS

In order to investigate this hypothesis, the following aims were set out:

- Investigate if *Pkhd1* knockdown and/or oestrogen drives centrosomal amplification in primary murine PTCs.
- Determine the age at which the proximal tubules begin to dilate in *Del2* mice.
- Determine the age at which 'star-burst' cilia and centrosomal amplification first appear in the proximal tubules of both male and female *Del2* mice.
- Determine if centrosomal amplification precedes cystogenesis or occurs as a result of cystogenesis when fibrocystin is knocked down.

These aims were set out in order to determine if the lack of fibrocystin expression in the presence of oestrogen act in synergy to further boost centrosomal amplification in proximal tubular epithelial cells, possibly accounting for the gender specific renal cystic phenotype observed in the *Del2* mice. Providing further insight into the functional roles of fibrocystin in tubular epithelium.

6.3 RESULTS AND ANALYSIS

6.3.1 Treatment of primary murine proximal tubular epithelial cells *in vitro* drives centrosomal overduplication

In order to determine if exposing primary PTCs to E2 in culture resulted in an increase in centrosomal overduplication, statistical analysis of the mean percentages of cells displaying more than 2 centrosomes from control samples was compared to samples treated with E2. This analysis was performed for age-matched animals, one, three, six, and nine months, in order to examine if there is a gender dependent difference in the observed level of centrosomal amplification. Comparison of wt male versus wt female, and *Del2* male versus *Del2* female was also carried out to determine if a gender dependent effect was more evident in wt or *Del2* mice.

A total of 52 mice were used in this study, 26 wt and 26 *Del2* animals, with an average cell count of ≥ 100 cells counted for each animal and all treatments, detailed in appendix 3. The number of cells displaying centrosomal overduplication (>2 centrosomes) is expressed as a percentage of the total number of cells counted.

6.3.1.1 One-month-old wt animals

Counts of at least 100 cells were performed at all four treatments of β -estradiol: 0pg/ml, 25pg/ml, 75pg/ml, and 500pg/ml. For one-month-old wt animals counts were collected from 4 male and 4 female mice. For wt male mice the mean number of cells displaying centrosomal overduplication does not show a linear increase with increasing levels of E2 (Fig. 6.1). In comparison, levels of centrosomal overduplication in proximal tubular epithelial cells derived from one-month-old wt females exhibit a clear linear increase with increasing levels of E2 (Fig. 6.1). For males, when the mean number of cells displaying centrosomal overduplication at 25pg/ml, 75pg/ml, and 500pg/ml E2 are compared with the control sample, there is a significant increase in the number of cells displaying centrosomal amplification at all three treatment levels, relative to the control (Table 6.1). In comparison, when the mean number of treated cells displaying centrosomal amplification from female mice are compared to the control cells (0pg/ml), a significant increase in the number of cells with centrosomal overduplication is evident at only high physiological and excess levels of E2 (75pg/ml, and 500pg/ml E2 respectively), table 6.2.

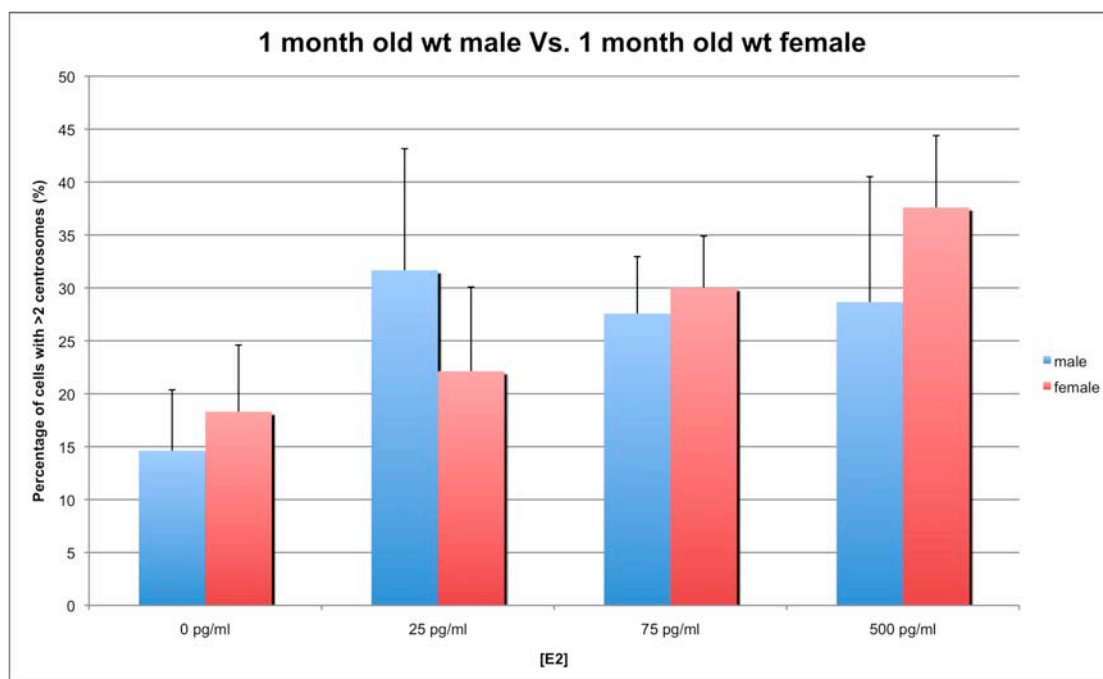


FIGURE 6.1 One-month-old wt: Mean percentage of primary proximal tubular cells displaying centrosomal overduplication. Cells isolated from female mice (red bars) show a positive correlation with levels of abnormal cells (>2 centrosome) increasing with increasing levels of E2. In contrast, those cells isolated from male mice (blue bars) show an ‘all-or-nothing’ type increase in abnormal cells when treated with E2, with no gradual increase with higher levels of E2. The increase in the levels of abnormal cells upon addition of E2 relative to the control sample are statistically significant at all levels of E2 for male mice (Table 6.1). For cells isolated from female animals the observed increase only becomes significant compared to the control at 75pg/ml and 500pg/ml E2 (Table 6.2).

TABLE 6.1 Cell count data analysis for one-month-old wt males

Sample: E2 (pg/ml)	Mean % of cells with >2 centrosomes	Standard deviation	p-value*
0	15	5.749	
25	32	11.488	0.026
75	28	5.382	0.008
500	29	11.847	0.047

*p-values relative to control (0pg/ml). t-test: 1-sided, unequal variance assumed, p<0.05 significance.

TABLE 6.2 Cell count data analysis for one-month-old wt females

Sample: E2 (pg/ml)	Mean % of cells with >2 centrosomes	Standard deviation	p-value*
0	18	6.295	
25	22	7.956	0.241
75	30	4.884	0.014
500	38	6.800	0.003

*p-values relative to control (0pg/ml). t-test: 1-sided, unequal variance assumed, p<0.05 significance.

Comparison of the level of centrosomal amplification at matched levels of E2 treatment for male and female mice showed that there is no significant difference between the levels of centrosomal overduplication observed in primary proximal tubular epithelial cells isolated from males and females (Table 6.3), further illustrated in Appendix 3, Fig. 3.1.

TABLE 6.3 Cell count data analysis for one-month-old wt males Vs. females

Sample: E2 (pg/ml)	Mean % of cells with >2 centrosomes (male)	Mean % of cells with >2 centrosomes (female)	p- value*
0	15	18	0.210
25	32	22	0.113
75	28	30	0.263
500	29	38	0.125
*t-test: mean of male Vs. female. t-test: 1-sided, unequal variance assumed, p<0.05 significance.			

6.3.1.2 One-month-old *Del2* animals

100 or more cells were counted at all four levels of β -estradiol treatment for one-month-old *Del2* male mice (n of 3). Those cells with more than 2 centrosomes were expressed as a percentage of total cells counted. The mean number of cells displaying centrosomal amplification did not show a linear increase in abnormal cells with increasing levels of E2 (Fig. 6.2). When the mean percentage of abnormal cells at 25pg/ml, 75pg/ml, and 500pg/ml E2 were compared to the mean percentage of abnormal cells in the control sample (0pg/ml E2), cells treated with 75pg/ml, and 500pg/ml E2 had a significantly higher percentage of abnormal cells (Table 6.4).

Similar counts for cells isolated from four one-month-old female *Del2* mice revealed a linear increase in the mean number of abnormal cells with increasing levels of E2 (Fig 6.2). When the mean percentage of abnormal cells in the control sample (0pg/ml E2) was compared with the mean percentage of abnormal cells in treated samples, samples treated with 75pg/ml and 500pg/ml E2 displayed a significantly higher mean percentage of abnormal cells (Table 6.5).

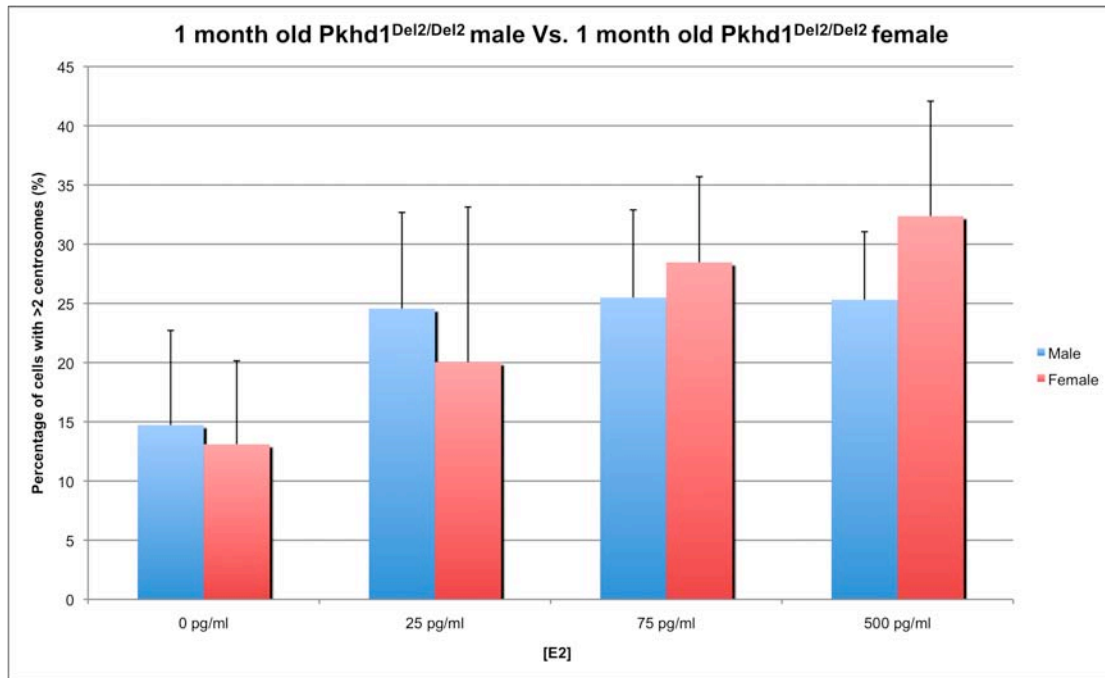


FIGURE 6.2 One-month-old *Del2*: Mean percentage of primary proximal tubular cells displaying centrosomal overduplication. Cells isolated from female mice (red bars) display a linear increase in the number of abnormal cells (>2 centrosomes) in correlation with increasing levels of E2. In contrast, those cells isolated from male mice (blue bars) show a maximal response upon administration of E2 at all levels. The increase in the levels of abnormal cells upon addition of E2 relative to the control samples are statistically significant at 75pg/ml, ad 500pg/ml E2 for male and female mice (Table 6.4 and 6.5).

TABLE 6.4 Cell count data analysis for one-month-old *Del2* males

Sample: E2 (pg/ml)	Mean % of cells with >2 centrosomes	Standard deviation	p-value*
0	14.7	7.986	
25	25.6	8.121	0.068
75	25.3	7.398	0.048
500	25.3	5.752	0.040

*p-values relative to control (0pg/ml). t-test: 1-sided, unequal variance assumed, p<0.05 significance.

TABLE 6.5 Cell count data analysis for one-month-old *Del2* females

Sample: E2 (pg/ml)	Mean % of cells with >2 centrosomes	Standard deviation	p-value*
0	13	7.054	
25	20	13.095	0.199
75	28	7.233	0.011
500	33	9.703	0.010

*p-values relative to control (0pg/ml). t-test: 1-sided, unequal variance assumed, p<0.05 significance.

Comparison of the level of centrosomal amplification at matched levels of E2 treatment for one-month-old *Del2* male and female mice showed that there is no significant difference between the levels of centrosomal overduplication observed in primary proximal tubular epithelial cells isolated from males and females (Table 6.6), further illustrated in Appendix 3 Fig. 3.2.

TABLE 6.6 Cell count data analysis for one-month-old *Del2* males Vs. females

Sample: E2 (pg/ml)	Mean % cells with >2 centrosomes (male)	Mean % cells with >2 centrosomes (female)	p-value*
0	14.7	13	0.385
25	25.6	20	0.291
75	25.5	28	0.294
500	25.3	33	0.133
*t-test: mean of male Vs. female. t-test: 1-sided, unequal variance assumed, p<0.05 significance.			

6.3.1.3 Three-month-old wt animals

Counts of 100 or more cells were performed at all four levels of β -estradiol treatment: 0pg/ml, 25pg/ml, 75pg/ml, and 500pg/ml. For three-month-old wt animals counts were collected from 3 male and 3 female mice, the mean percentage of abnormal cells was used for the following analysis. Levels of centrosomal overduplication in primary PTCs from wt male and female animals show an almost linear increase with increasing levels of E2 (Fig. 6.3). For both sexes the number of cells displaying centrosomal amplification when compared to the control show a significant increase at high physiological and excess to physiological levels of E2, 75pg/ml and 500pg/ml, respectively (Tables 6.7 and 6.8).

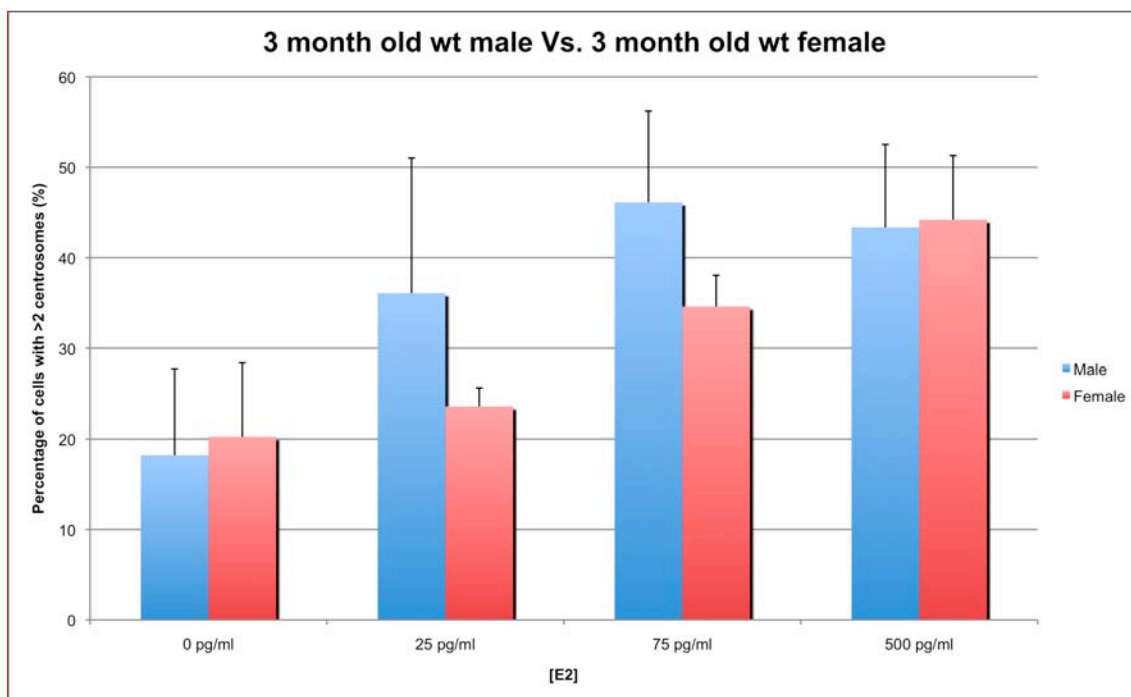


FIGURE 6.3 Three-month-old wt: Mean percentage of primary proximal tubular cells displaying centrosomal overduplication. Cells isolated from female mice (red bars) show a linear increase in the number of abnormal cells (those expressing >2 centrosomes) with respect to increasing levels of E2. Whilst cells isolated from male mice (blue bars) show an initial linear increase in the mean number of abnormal cells, a maximal level appears to be reached at 75pg/ml E2. The increase in the levels of abnormal cells upon addition of E2 relative to the control sample are statistically significant at 75pg/ml and 500pg/ml E2 for both male and female mice (Tables 6.7 and 6.8).

TABLE 6.7 Cell count data analysis for three-month-old wt males

Sample: E2 (pg/ml)	Mean % of cells with >2 centrosomes	Standard deviation	p-value*
0	18.2	9.543	
25	36.1	14.938	0.084
75	46.1	5.823	0.013
500	43.3	5.296	0.015

*p-values relative to control (0pg/ml). t-test: 1-sided, unequal variance assumed, p<0.05 significance.

TABLE 6.8 Cell count data analysis for three-month-old wt females

Sample: E2 (pg/ml)	Mean % of cells with >2 centrosomes	Standard deviation	p-value*
0	20.2	8.133	
25	23.6	2.043	0.276
75	34.6	3.444	0.038
500	44.2	7.092	0.010

*p-values relative to control (0pg/ml). t-test: 1-sided, unequal variance assumed, p<0.05 significance.

Comparison of the level of centrosomal amplification at matched levels of E2 treatment for male and female mice showed that there is no significant difference between the levels of centrosomal overduplication observed in primary proximal tubular epithelial cells isolated from males and females (Table 6.9), further illustrated in Appendix 3 Fig. 3.3.

TABLE 6.9 Cell count data analysis for three-month-old wt males Vs. females

Sample: E2 (pg/ml)	Mean % cells with >2 centrosomes (male)	Mean % cells >2 centrosomes (female)	p- value*
0	18.2	20.2	0.397
25	36.1	23.6	0.142
75	46.1	34.6	0.089
500	43.3	44.2	0.453
*t-test: mean of male Vs. female. t-test: 1-sided, unequal variance assumed, p<0.05 significance.			

6.3.1.4 Three-month-old *Del2* animals

Counts of 100 or more cells were performed at all four levels of E2 treatment: 0pg/ml, 25pg/ml, 75pg/ml, and 500pg/ml. For three-month-old *Del2* animals counts were collected for 3 male and 3 female mice, and the mean percentage of abnormal cells used for the following analysis. The mean percentage of cells displaying an abnormal centrosomal complement from male mice does not display a linear increase at higher doses of E2. Reaching an almost maximal response at 25pg/ml E2, comparable to low physiological levels, increasing very little at 75pg/ml E2 (Fig.6.4). When compared to levels of abnormal cells from the control sample (0pg/ml E2) the mean percentage of abnormal cells treated with 25pg/ml, and 500pg/ml E2 are significantly higher (Table 6.10). This is the same for proximal tubular epithelial cells isolated from three-month-old *Del2* female mice (Fig 6.4, Table 6.11).

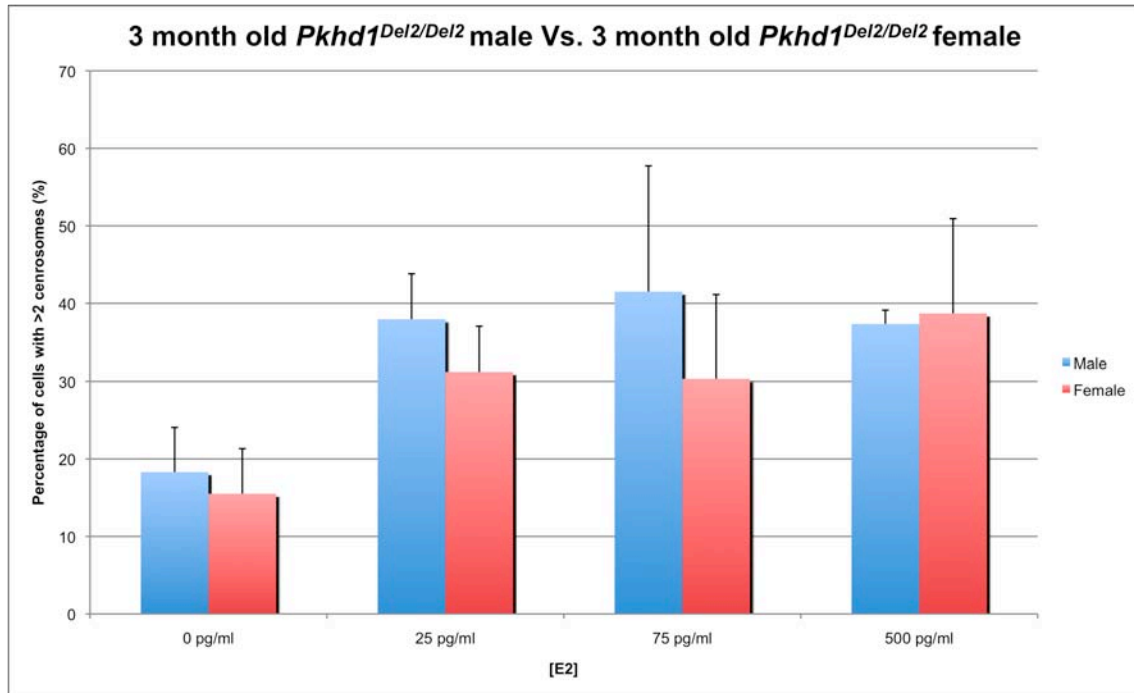


FIGURE 6.4 Three-month-old *Del2*: Mean percentage of primary proximal tubular cells displaying centrosomal overduplication. Cells isolated from female mice (red bars) and male mice (blue bars) both show a maximal response to treatment with E2 at low physiological levels (25pg/ml E2), with little increase with increasing levels of E2. The increase in the levels of abnormal cells upon addition of E2 relative to the control sample are statistically significant at 25pg/ml and 500pg/ml E2 for both male and female mice.

TABLE 6.10 Cell count data analysis for three-month-old *Del2* males

Sample: E2 (pg/ml)	Mean % of cells with >2 centrosomes	Standard deviation	p-value*
0	18.3	5.755	
25	37.9	5.858	0.007
75	41.5	16.232	0.060
500	37.3	1.778	0.010

*p-values relative to control (0pg/ml). t-test: 1-sided, unequal variance assumed, p<0.05 significance.

TABLE 6.11 Cell count data analysis for three-month-old *Del2* females

Sample: E2 (pg/ml)	Mean % of cells with >2 centrosomes	Standard deviation	p-value*
0	15.5	5.818	
25	31.2	5.824	0.015
75	30.3	10.795	0.063
500	38.7	12.225	0.031

*p-values relative to control (0pg/ml). t-test: 1-sided, unequal variance assumed, p<0.05 significance.

Comparison of the levels of centrosomal amplification at matched levels of E2 treatment for male and female mice showed that there is no significant difference in the level of centrosomal overduplication observed in primary proximal tubular epithelial cells between the two genders *in vitro* (Table 6.12), further illustrated in Appendix 3, Fig. 3.4.

TABLE 6.12 Cell count data analysis for three-month-old *Del2* males Vs. females

Sample: E2 (pg/ml)	Mean % cells >2 centrosomes (male)	Mean % cells >2 centrosomes (female)	p- value*
0	18.3	15.5	0.293
25	37.9	31.2	0.115
75	41.5	30.3	0.193
500	37.3	38.7	0.433

*t-test: mean of male Vs. female. t-test: 1-sided, unequal variance assumed, p<0.05 significance.

6.3.1.5 Six-month-old wt animals

100 plus cells were counted at all four levels of β -estradiol treatment (0pg/ml, 25pg/ml, 75pg/ml, and 500pg/ml E2) for six-month-old wt mice. Counts were collected, and the mean percentage of abnormal cells from total cells calculated and analysed, with an n of 3 for male and female mice. The mean percentage of cells displaying centrosomal overduplication from male wt animals shows no significant increase with increasing levels of E2 treatment (Fig. 6.5). Basal levels of centrosomal amplification are high in the control sample, with a mean of 30% abnormal cells (n of 3) (Fig. 6.5). In contrast, identical counts and analysis for female wt mice show a positive linear correlation with increasing E2 levels (Fig. 6.5). On comparison of the mean number of abnormal cells between control and treated samples for male animals, there is no significant difference between the treatments (Table 6.13). When the same comparison is made for the female data, the level of centrosomal overduplication at only 500pg/ml E2 (excessive to physiological) is significantly higher compared to the control (0pg/ml) (Table 6.14).

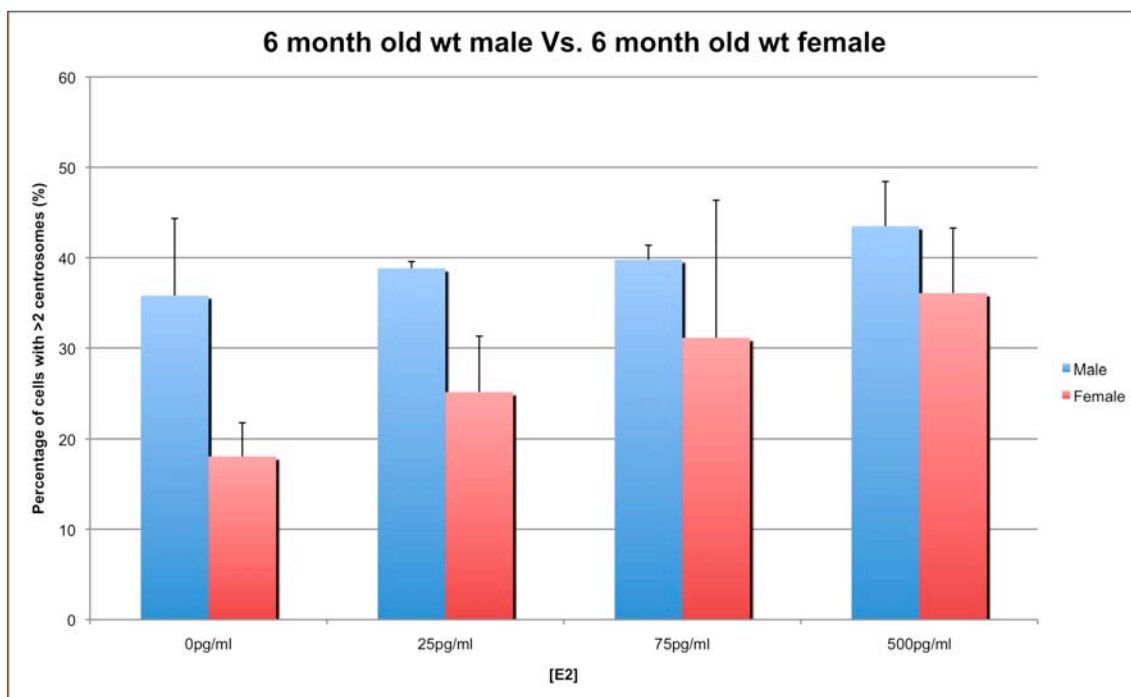


FIGURE 6.5 Six-month-old wt: Mean percentage of primary proximal tubular cells displaying centrosomal overduplication. Cells isolated from female mice (red bars), and male mice (blue bars) both show a linear increase in the number of abnormal cells with respect to increasing levels of E2, albeit more pronounced in the female samples). The increase in the levels of abnormal cells upon addition of E2 relative to the control sample is only statistically significant at 500pg/ml E2 for cells isolated from female mice.

TABLE 6.13 Cell count data analysis for six-month-old wt males

Sample: E2 (pg/ml)	Mean % of cells with >2 centrosomes	Standard deviation	p-value*
0	35.8	8.539	
25	38.8	0.742	0.301
75	39.8	1.599	0.523
500	43.5	4.932	0.132

*p-values relative to control (0pg/ml). t-test: 1-sided, unequal variance assumed, p<0.05 significance.

TABLE 6.14 Cell count data analysis for six-month-old wt females

Sample: E2 (pg/ml)	Mean % of cells with >2 centrosomes	Standard deviation	p-value*
0	18.1	3.729	
25	25.2	6.121	0.088
75	31.1	15.224	0.136
500	36.1	7.213	0.016

*p-values relative to control (0pg/ml). t-test: 1-sided, unequal variance assumed, p<0.05 significance.

In order to determine if there is a gender difference in the level of centrosomal amplification upon administration of E2, comparison of the mean percentage of abnormal cells at matched levels of E2 treatment for males versus females was carried out. When comparing the mean percentage of abnormal cells between male and female samples, levels of abnormal cells were significantly higher in cells derived from male mice than female mice at 0pg/ml E2 (control), and 25pg/ml E2 (low physiological) (Table 6.15), further illustrated in Appendix 3, Fig. 3.5.

TABLE 6.15 Cell count data analysis for six-month-old wt males Vs. females

Sample: E2 (pg/ml)	Mean % cells >2 centrosomes (male)	Mean % cells >2 centrosomes (female)	p-value*
0	35.8	18.1	0.026
25	38.8	25.2	0.030
75	39.8	31.1	0.215
500	43.5	36.1	0.112

*t-test: mean of male Vs. female. t-test: 1-sided, unequal variance assumed, p<0.05 significance.

6.3.1.6 Six-month-old Del2 animals

Counts of 100 or more cells were performed at all four levels of E2 treatment: 0pg/ml, 25pg/ml, 75pg/ml, and 500pg/ml. For six-month-old *Del2* animals, counts were collected for 3 male and 3 female mice, and the mean percentage of abnormal cells used for the following analysis. Analysis of the mean percentage of cells displaying an abnormal centrosomal complement from male and female mice reveals a linear increase that correlates positively with E2 dose (Fig. 6.6). Comparison of the mean percentage of abnormal cells between control and treated samples taken from male mice shows there is a significantly higher level of abnormal cells in treated samples at all doses, table 6.16. When the same analysis is performed for female samples there is also a statistically significant increase in the number of abnormal cells in treated samples compared to the control (Table 6.17).

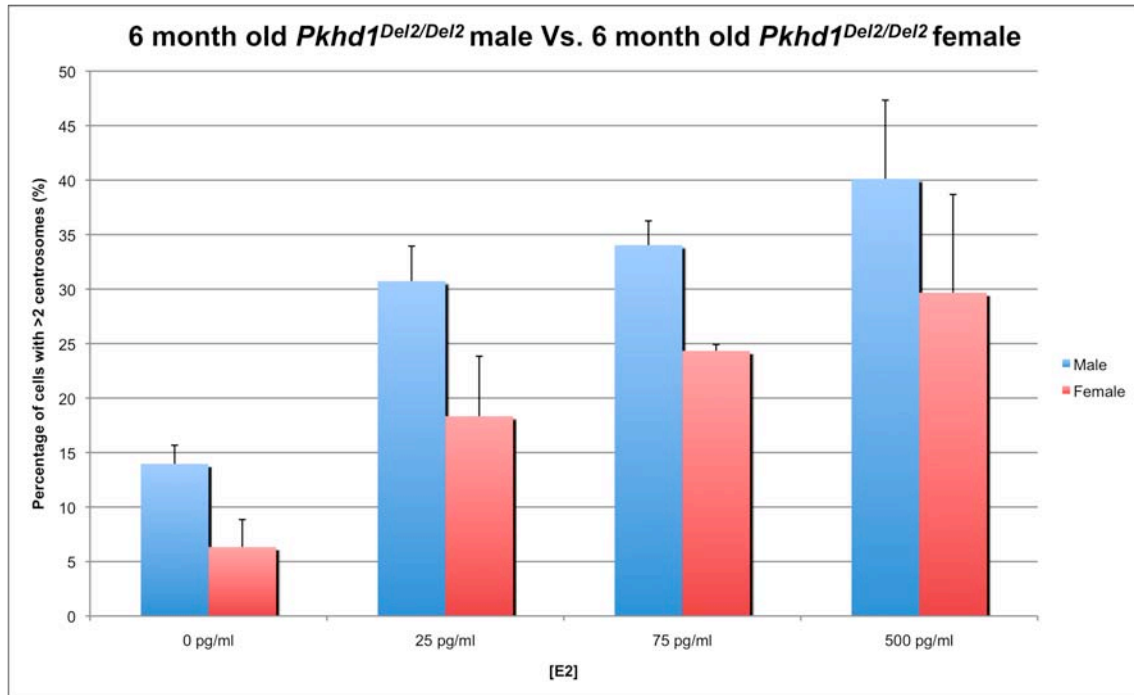


FIGURE 6.6 Six-month-old *Del2*: Mean percentage of primary proximal tubular cells displaying centrosomal overduplication. Cells isolated from female mice (red bars) and male mice (blue bars) both show a linear increase in the number of abnormal cells (those expressing >2 centrosomes) with respect to increasing levels of E2. The increase in the levels of abnormal cells upon addition of E2 relative to the control sample are statistically significant at all levels of E2 for cells isolated from both male and female mice (Table 6.16 and 6.17).

TABLE 6.16 Cell count data analysis for six-month-old *Del2* males

Sample: E2 (pg/ml)	Mean % of cells with >2 centrosomes	Standard deviation	p-value*
0	14.0	1.706	
25	30.7	3.211	0.002
75	34.0	2.224	0.0002
500	40.1	7.217	0.010

*p-values relative to control (0pg/ml). t-test: 1-sided, unequal variance assumed, p<0.05 significance.

TABLE 6.17 Cell count data analysis for six-month-old *Del2* females

Sample: E2 (pg/ml)	Mean % of cells with >2 centrosomes	Standard deviation	p-value*
0	6.3	2.517	
25	18.3	5.508	0.023
75	24.3	0.577	0.002
500	29.7	9.018	0.019

*p-values relative to control (0pg/ml). t-test: 1-sided, unequal variance assumed, p<0.05 significance.

Upon further analysis, comparison of centrosomal amplification between the genders at matched levels of β -estradiol treatment (0pg/ml, 25pg/ml, 75pg/ml, and 500pg/ml) reveals that levels of centrosomal amplification are significantly higher in cells derived from male animals at 0pg/ml E2, 25pg/ml E2, and 75pg/ml E2. Although this difference is not statistically significant at 500pg/ml E2 it is still evident (Table 6.18), further illustrated in Appendix3, Fig. 3.6.

TABLE 6.18 Cell count data analysis for six-month-old *Del2* males Vs. females

Sample: E2 (pg/ml)	Mean % cells >2 centrosomes (male)	Mean % cells >2 centrosomes (female)	p- value*
0	14.0	6.3	0.008
25	30.7	18.3	0.020
75	34.0	24.3	0.006
500	40.1	29.7	0.098

*t-test: mean of male Vs. female. t-test: 1-sided, unequal variance assumed, $p < 0.05$ significance.

6.3.1.7 Nine-month-old wt animals

Counts of at least 100 cells were performed at all four doses of β -estradiol: 0pg/ml, 25pg/ml, 75pg/ml, and 500pg/ml. For nine-month-old wt animals counts were collected for 3 male and 3 female mice. For both the male and female samples the mean percentage of abnormal cells revealed no real trend with increasing levels of E2 treatment (Fig. 6.7). Levels of centrosomal amplification were consistently high across all experimental conditions. Comparison of the mean percentage of abnormal cells between treated and control samples reveals that for cells derived from male mice there is only a significant increase in the level of abnormal cells at 500pg/ml E2 (Table 6.19). Similar analysis for cells derived from female mice reveals there is no significant difference in the level of centrosomal amplification between treated and control cells (Table 6.20).

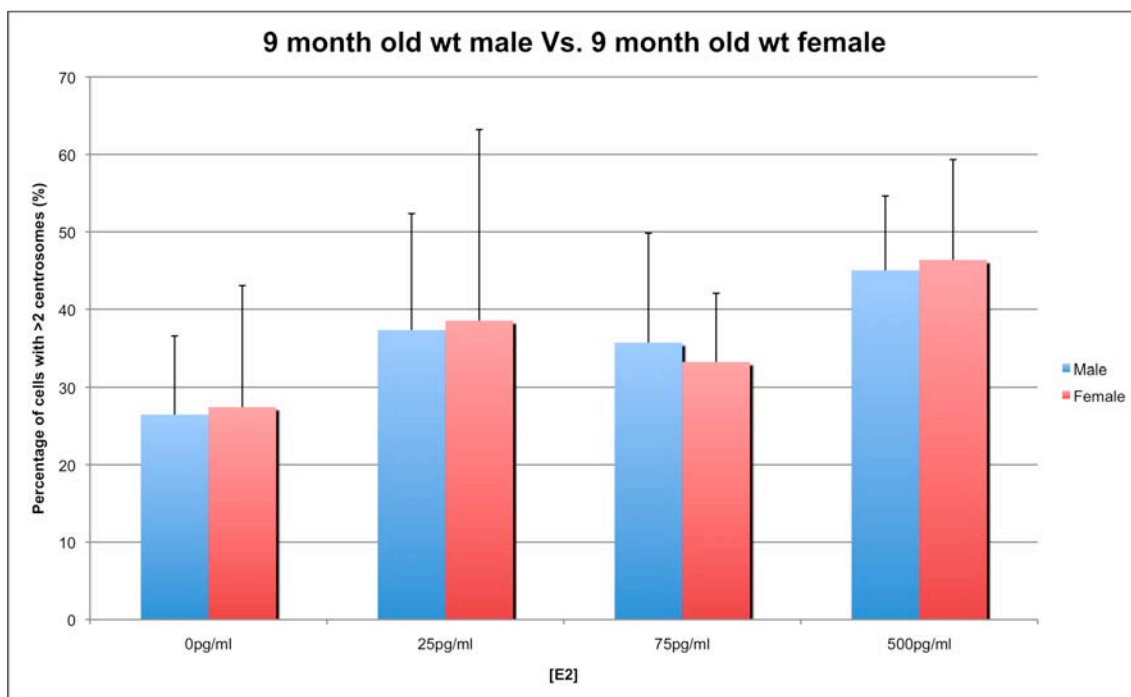


FIGURE 6.7 Nine-month-old wt: Mean percentage of primary proximal tubular cells displaying centrosomal overduplication. Cells isolated from female mice (red bars) and male mice (blue bars) both show no particular pattern in the number of increasing abnormal cells (those expressing >2 centrosomes) with increasing levels of E2. The increase in the levels of abnormal cells upon addition of E2 relative to the control sample are statistically significant only at 500pg/ml E2 for cells isolated from male mice.

TABLE 6.19 Cell count data analysis for nine-month-old wt males

Sample: E2 (pg/ml)	Mean % of cells with >2 centrosomes	Standard deviation	p-value*
0	26.5	10.079	
25	37.3	15.035	0.183
75	35.7	14.145	0.208
500	45.0	9.612	0.041

*p-values relative to control (0pg/ml). t-test: 1-sided, unequal variance assumed, p<0.05 significance.

TABLE 6.20 Cell count data analysis for nine-month-old wt females

Sample: E2 (pg/ml)	Mean % of cells with >2 centrosomes	Standard deviation	p-value*
0	27.4	15.618	
25	38.5	24.679	0.276
75	33.2	8.878	0.308
500	46.4	12.963	0.092

*p-values relative to control (0pg/ml). t-test: 1-sided, unequal variance assumed, p<0.05 significance.

Further analysis, comparing the mean percentage of abnormal cells at matched levels of E2 for male versus female samples revealed there is no significant difference between samples derived from the difference genders (Table 6.21), further illustrated in Appendix 3, Fig. 3.7.

TABLE 6.21 Cell count data analysis for nine-month-old wt males Vs. females

Sample: E2 (pg/ml)	Mean % cells >2 centrosomes (male)	Mean % cells >2 centrosomes (female)	p- value*
0	26.5	27.4	0.467
25	37.3	38.5	0.473
75	35.7	33.2	0.405
500	45.0	46.4	0.447
*t-test: mean of male Vs. female. t-test: 1-sided, unequal variance assumed, p<0.05 significance.			

6.3.1.8 Nine-month-old Del2 animals

Counts of at least 100 cells were performed at all four doses of β -estradiol: 0pg/ml, 25pg/ml, 75pg/ml, and 500pg/ml. For nine-month-old *Del2* animals, counts were collected from 3 male, and 3 female mice. The mean percentage of abnormal cells was consistently high in all doses of E2 for both male and female samples (Fig. 6.8). Statistical comparison of the mean number of abnormal cells in control and treated cells isolated from male animals revealed there was no significant difference in the level of centrosomal amplification (Table 6.22). The same analysis performed for female samples revealed that at 75pg/ml and 500pg/ml E2 treated cells had significantly higher levels of centrosomal overduplication when compared to the control (Table 6.23).

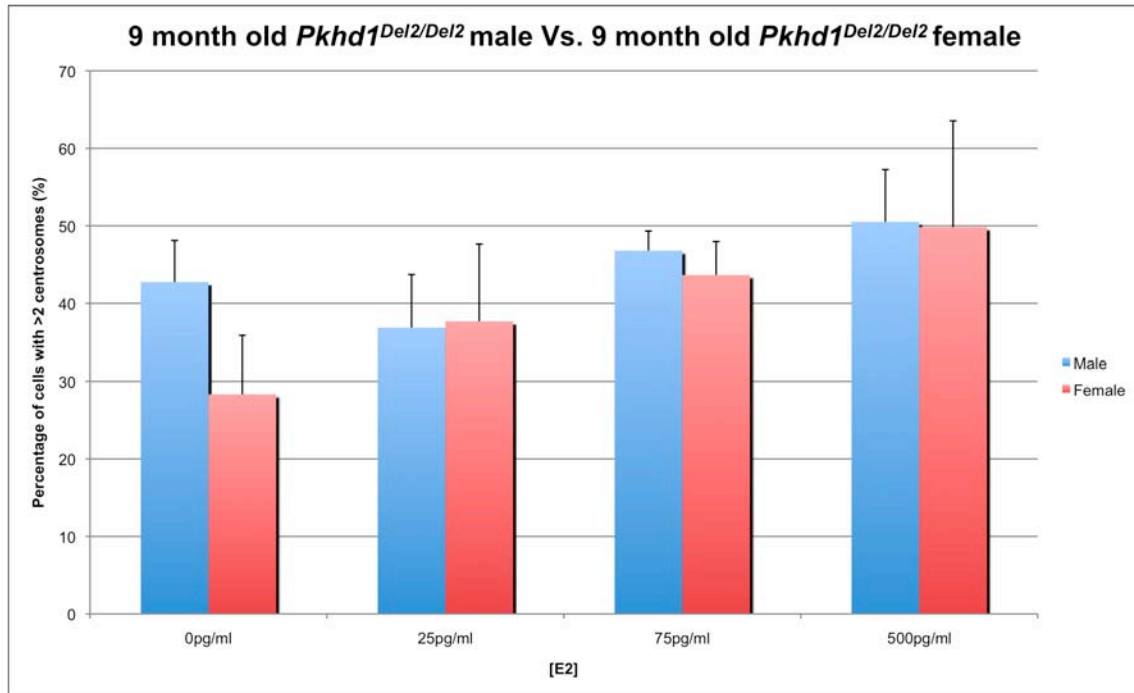


FIGURE 6.8 Nine-month-old *Del2*: Mean percentage of primary proximal tubular cells displaying centrosomal overduplication. Cells isolated from female mice (red bars) show a subtle linear increase in the number of abnormal cells (those expressing >2 centrosomes) with respect to increasing levels of E2. In contrast, those cells isolated from male mice (blue bars) show no real pattern of increasing levels of abnormal cells upon administration of E2. The increase in the level of abnormal cells upon addition of E2 relative to the control sample are statistically significant at 75pg/ml and 500pg/ml E2 for only female primary proximal tubular epithelial cells.

TABLE 6.22 Cell count data analysis for nine-month-old *Del2* males

Sample: E2 (pg/ml)	Mean % of cells with >2 centrosomes	Standard deviation	p-value*
0	42.7	5.367	
25	36.9	6.860	0.155
75	46.8	2.533	0.163
500	50.5	6.753	0.099

*p-values relative to control (0pg/ml). t-test: 1-sided, unequal variance assumed, p<0.05 significance.

TABLE 6.23 Cell count data analysis for nine-month-old *Del2* females

Sample: E2 (pg/ml)	Mean % of cells with >2 centrosomes	Standard deviation	p-value*
0	28.3	7.546	
25	37.7	9.970	0.135
75	43.6	4.320	0.026
500	49.8	13.722	0.047

*p-values relative to control (0pg/ml). t-test: 1-sided, unequal variance assumed, p<0.05 significance.

Comparison of the level of centrosomal amplification at matched levels of E2 treatment for male and female mice showed that in the control samples cells derived from male mice had significantly higher levels of abnormal cells (>2 centrosome). However, there is no difference between male and female samples treated with E2 (Table 6.24), further illustrated by Appendix 3, Fig. 3.8.

TABLE 6.24 Cell count data analysis for nine-month-old *Del2* males Vs. females

Sample: E2 (pg/ml)	Mean % cells >2 centrosomes (male)	Mean % cells >2 centrosomes (female)	p- value*
0	42.7	28.3	0.030
25	36.9	37.7	0.457
75	46.8	43.6	0.175
500	50.5	49.8	0.472
*t-test: mean of male Vs. female. t-test: 1-sided, unequal variance assumed, p<0.05 significance.			

6.3.1.9 *Primary murine proximal tubular epithelial cells display abnormal cellular morphology upon treatment with 17 β -estradiol in vitro*

The severity of centrosomal amplification, and the associated morphological implications were not formally documented or measured in this study. Cellular morphology was generally assessed by immunofluorescent immunohistochemistry in order to further understand the possible mechanism by which E2 may drive abnormal epithelial proliferation. An overall assessment of nuclear morphology, centrosome number per cell, and cilia expression was carried out whilst cell counts were performed.

Proximal tubular epithelial cells isolated from wt and *Del2* animals showed little evidence of centrosomal amplification in control samples. Where centrosomal overduplication was evident the number of centrosomes present rarely exceeded more than four per cell. An associated increase in the number of primary cilia expressed was also evident in control samples, rarely exceeding more than 2 primary cilia per cell. Nuclear morphology, a good representation of any significant chromosomal instability present, was also rarely abnormal in control samples from both wt and *Del2* animals (Fig. 6.9 and 6.10).

Severity of centrosomal overduplication, and the associated anomalies of primary cilia expression and abnormal nuclear morphology increased in correlation with increasing levels of E2 treatment. This occurred in cells isolated from both wt and *Del2* animals (Fig. 6.9 and 6.10).

Overall, the severity of centrosomal overduplication observed was greater in cells isolated from *Del2* mice, when compared to wt samples at matched levels of E2 treatment, including control samples (Fig. 6.9 and 6.10). Cells in which multiple centrosomes were present in large numbers (>5 centrosomes per cell) generally displayed an abnormal nuclear morphology, with multiple nuclei, or small micronuclear fragments. Such cells were observed in PTC samples derived from wt and *Del2* animals at all levels of E2 treatment. However, the degree of nuclear dysmorphia observed increased in severity with increasing levels of E2 treatment (Fig. 6.9 and 6.10). The degree of nuclear dysmorphia also appeared to be more severe in cells isolated from *Del2* mice when compared to cells isolated from wt mice matched for age, and E2 treatment (Fig.6.9 and 6.10).

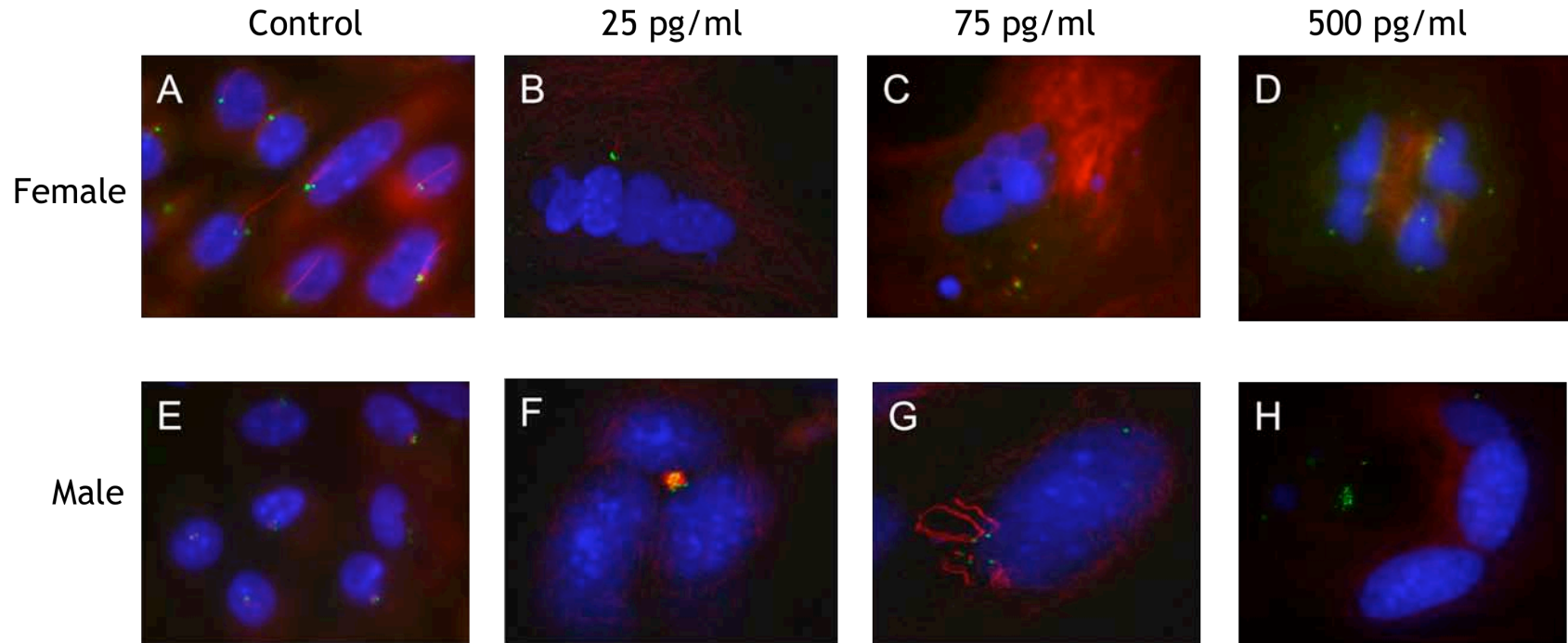


FIGURE 6.9 Immunofluorescence staining of 17 β -estradiol treated primary proximal tubular epithelial cells isolated from wildtype mice. Images show increasing complexity of centrosomal amplification and consequent ciliary and nuclear abnormalities in correlation with increasing levels of E2. Cells treated with E2 in which multiple centrosomes are present also express multiple primary cilia, much like the starburst phenotype seen in the cystic epithelium of *Del2* animals (G). Control samples (A, and E), for both female and male animals respectively, show a number of cells with the expected complement of centrosomes (≤ 2 centrosomes per cell), with a single primary cilium. Upon treatment with E2, cells begin to display a number of abnormal characteristics, including: abnormal numbers of centrosomes (>2 per cell), evident in panels B-D, and F-H, representing cells treated with E2. Multiple primary cilia are evident in panel G, with a single PTC from a male animal treated with 75pg/ml E2. Dysmorphic nuclei, an increase in the number of nuclei proper, and micronuclei, all of which are especially evident in panel B, with a single large dysmorphic PTC from a female animals treated with 25pg/ml E2. This cell (B), displays 4 large nuclei with at least 3 micronuclei, with a cluster of centrosomes and associated multiple primary cilia lying above the nuclei. The presence of multiple centrosomes also results in abnormal mitoses, where the nuclear material is pulled in multiple directions, as opposed to two well-defined poles. This is evident in panel D, a single PTC from a female animal treated with 500pg/ml E2, 8 centrosomes can be visualised clearly, the nuclear material is being pulled to four separate poles. Key: Red, acetylated α -tubulin; Green, γ -tubulin; Blue, DAPI stained DNA.

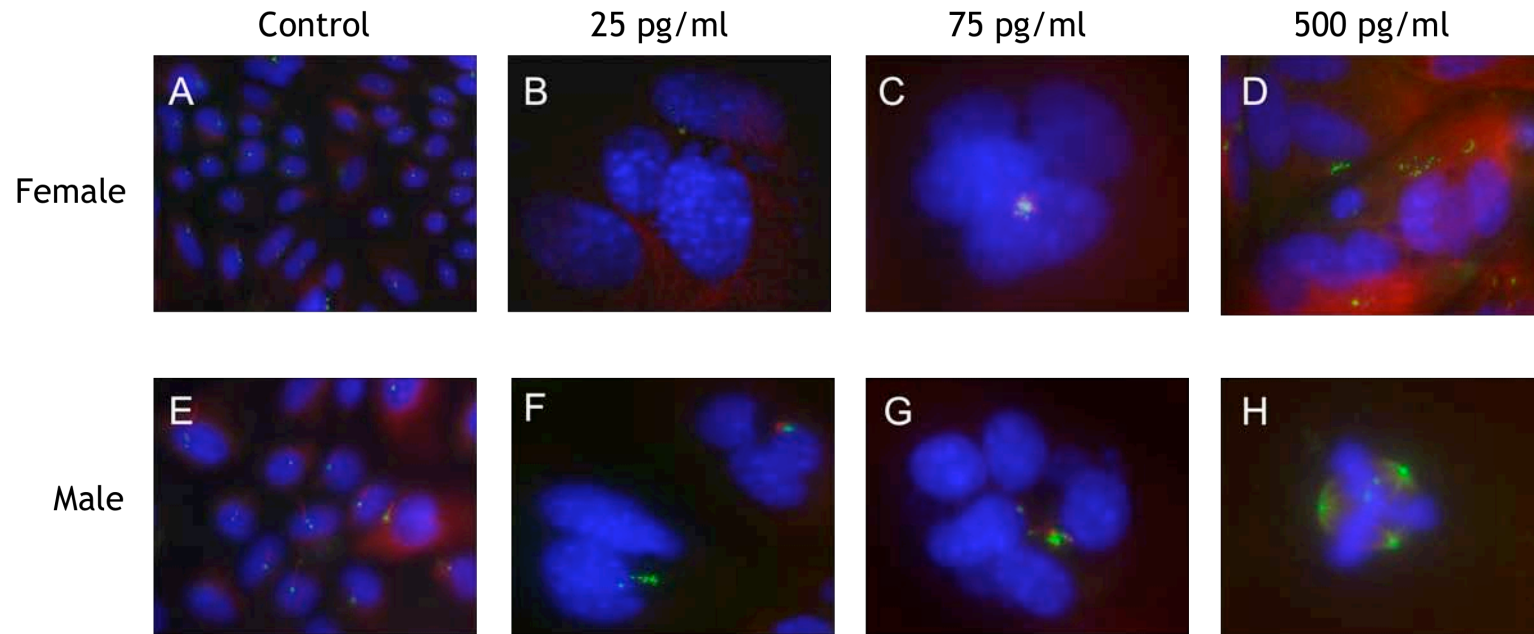


FIGURE 6.10 Immunofluorescence staining of 17 β -estradiol treated primary proximal tubular epithelial cells isolated from *Del2* mice. Images illustrating the increasing complexity of the centrosomal anomalies, and consequent ciliary and nuclear abnormalities, present in primary PTCs when cultured with increasing levels of E2 *in vitro*. Cells in which multiple centrosomes are present also express multiple cilia, much like the star-burst phenotype seen in the cystic epithelium of *Del2* animals. Often these primary cilia are seen as a nest of acetylated α -tubulin positive structures surrounding a cluster of centrosomes panels C and G. Control samples for both female, and male animals (A and E, respectively), show a number of cells with the expected complement of centrosomes (≤ 2 centrosomes per cell), with a single primary cilium, and a small fraction of the cells displaying between 3 and 4 centrosomes with 2 primary cilia. Upon treatment with 17 β -estradiol, cells begin to display a number of abnormal characteristics, including; abnormal numbers of centrosomes (>2 centrosome per cell), evident in panels B-D and F-H. Multiple primary cilia, evident in panel G, with a single PTC from a male animal treated with 75pg/ml E2. Dymorphic nuclei, an increase in the number of nuclei proper, and micronuclei, all of which are especially evident in panel B, with a single large dymorphic PTC from a female animal treated with 25pg/ml E2. This cell (B) displays 4 large nuclei with at least 8 micronuclei, with a cluster of centrosomes and associated primary cilia lying above the nuclei. The presence of multiple centrosomes also results in abnormal mitoses, where the nuclear material is pulled in multiple directions, as opposed to two well-defined poles. This is evident in panel H, a single PTC from a male mouse treated with 500pg/ml E2, at least 3 centrosomes can be visualised clearly, with the nuclear material being pulled to 3 separate poles. Key: Red, acetylated α -tubulin; Green, γ -tubulin; Blue, DAPI stained DNA.

6.3.2 Susceptibility of primary murine proximal tubular epithelial cells to E2 driven centrosomal overduplication is age dependent

To determine if age alone is a significant factor in susceptibility to centrosomal overduplication in primary proximal tubular epithelial cells, the mean percentage of cells displaying an abnormal complement of centrosomes from one-month-old wt and *Del2* mice were compared with cells isolated from older wt and *Del2* animals, respectively. This was done to examine the effect of age alone on centrosomal amplification by matching all other variables. Comparing young and old wt animals excludes any effect of fibrocystin knockdown on centrosomal overduplication. But comparing young and old *Del2* animals this allows comparison of cells derived from proximal tubules that are only just beginning to dilate with those that are fully cystic.

6.3.2.1 *Three-month-old wt animals*

Comparison of the mean percentage of abnormal cells observed in PTCs derived from wt male and wt female animals at the ages of one month (n of 4 for both males and females), and three months (n of 3 for both males and females), reveals levels of abnormal cells are consistently higher in samples derived from three-month-old wt animals (Fig. 6.11). Statistically, this observation is only significant for cells isolated from male mice, treated with 75pg/ml E2 (Table 6.25). In all other samples this general increase is not significantly different (Table 6.25 and 6.26).

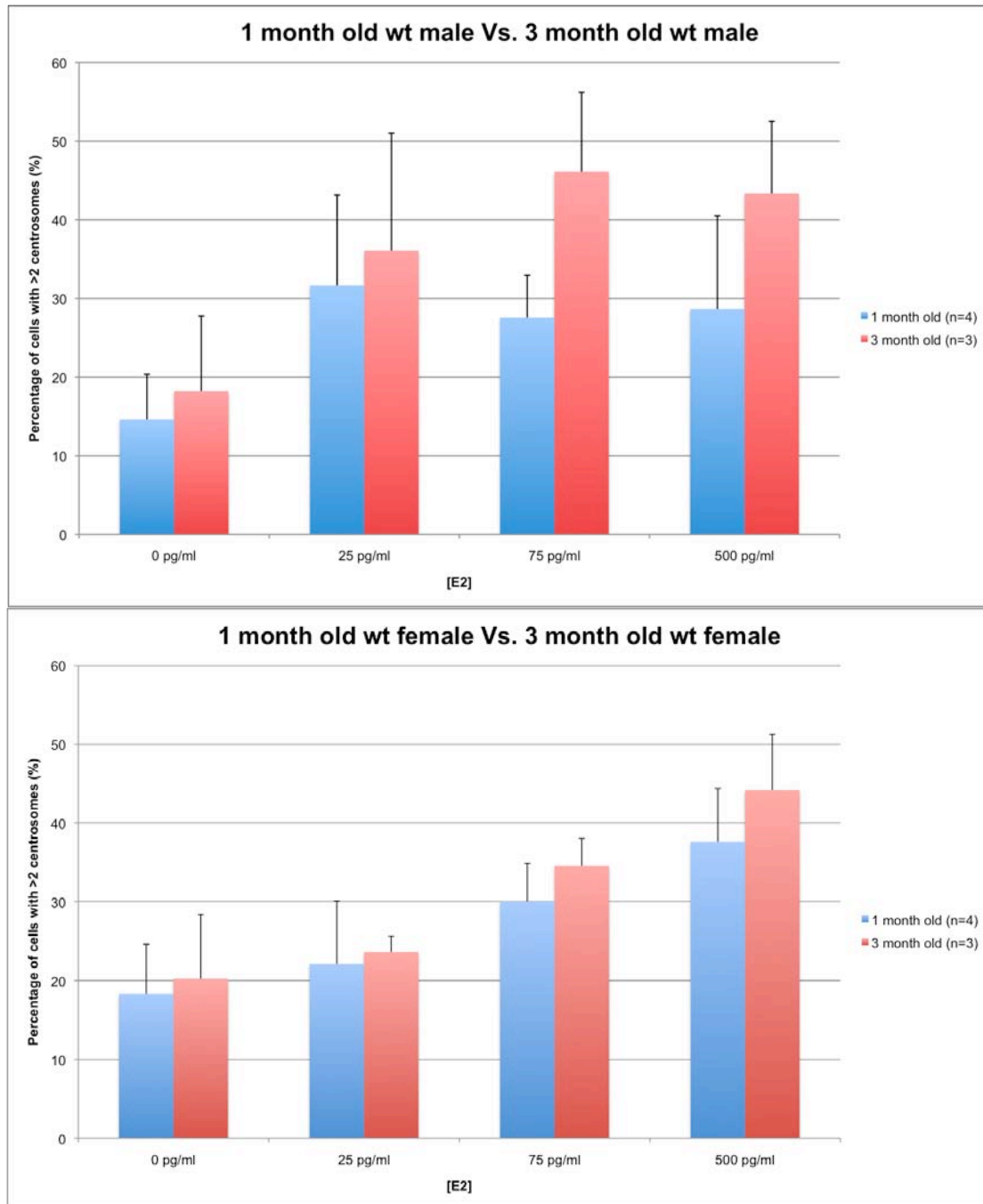


FIGURE 6.11 One-month-old Vs three-month-old wt: comparison of centrosomal amplification in 17 β -estradiol treated primary proximal tubular epithelial cells. The number of cells displaying centrosomal overduplication, represented as the mean percentage of cells with more than 2 centrosomes, from one-month-old (blue bars), and three-month-old (red bars) mice were compared to determine if levels were significantly higher in cells isolated from older animals. Levels were found to be consistently higher in both male (upper chart), and female (lower chart) three-month-old animals.

TABLE 6.25 Cell count data analysis for one-month-old versus three-month-old wt males

Sample: E2 (pg/ml)	Mean % of cells with >2 centrosomes (one month)	Mean % of cells with >2 centrosomes (three months)	p-value *
0	15	18.2	0.300
25	32	36.1	0.347
75	28	46.1	0.033
500	29	43.3	0.062
*p-value calculated from 1-sided t-test with unequal variance assumed, p<0.05 significance			

TABLE 6.26 Cell count data analysis for one-month-old versus three-month-old wt females

Sample: E2 (pg/ml)	Mean % of cells with >2 centrosomes (one month)	Mean % of cells with >2 centrosomes (three months)	p-value *
0	18	20.2	0.374
25	22	23.6	0.372
75	30	34.6	0.103
500	38	44.2	0.139
*p-value calculated from 1-sided t-test with unequal variance assumed, p<0.05 significance			

6.3.2.2 Three-month-old *Del2* animals

Comparison of the mean percentage of abnormal cells observed in PTCs derived from *Del2* male, and *Del2* female animals at the ages of one month (n of 4 for both males and females), and three months (n of 3 for both males and females) reveals the number of cells displaying centrosomal overduplication to be higher in samples derived from three-month-old mice (Fig. 6.12). Statistically this increase is only significant in PTCs derived from male *Del2* mice treated with 25pg/ml E2 (comparable to low physiological levels), and 500pg/ml E2 (levels excess to physiological) (Tables 6.27 and 6.28).

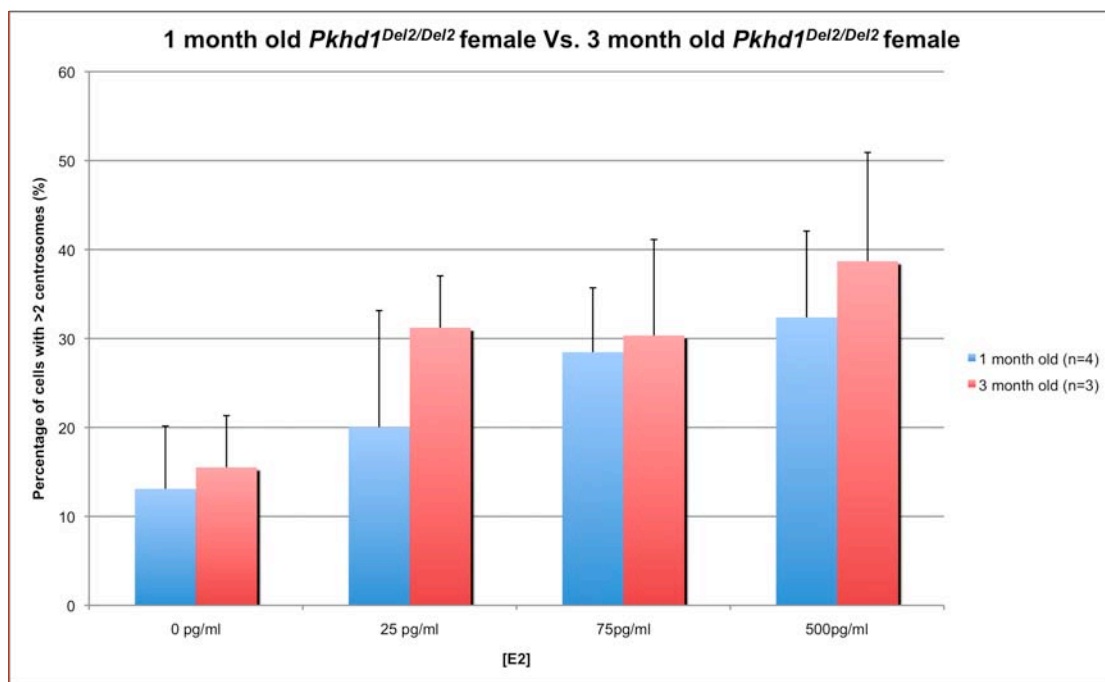
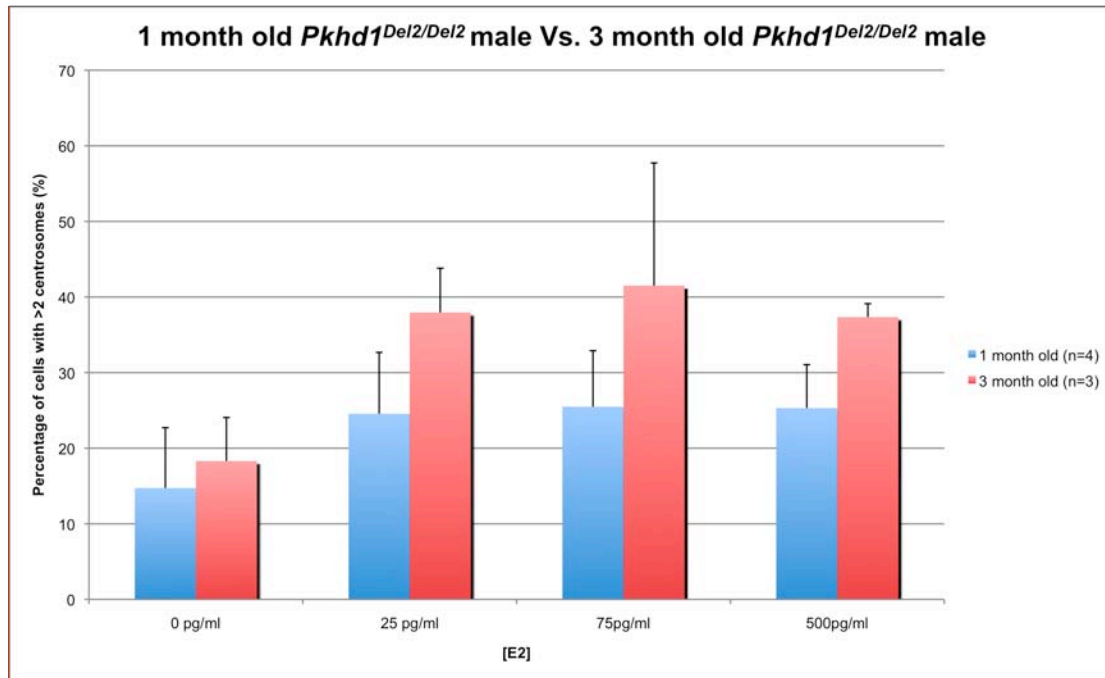


FIGURE 6.12 One-month-old Vs three-month-old *Del2*: comparison of centrosomal amplification in 17 β -estradiol treated primary proximal tubular epithelial cells. The number of cells displaying centrosomal overduplication, represented as the mean percentage of cells with more than 2 centrosomes, from one-month-old (blue bars), and three-month-old (red bars) mice were compared to determine if levels were significantly higher in cells isolated from older animals. Levels were found to be consistently higher in both male (upper chart), and female (lower chart) three-month-old animals.

TABLE 6.27 Cell count data analysis for one-month-old versus three-month-old *Del2* males

Sample: E2 (pg/ml)	Mean % of cells with >2 centrosomes (one month)	Mean % of cells with >2 centrosomes (three months)	p-value *
0	14.7	18.3	0.261
25	25.6	37.9	0.026
75	25.5	41.5	0.111
500	25.3	37.3	0.010
*p-value calculated from 1-sided t-test with unequal variance assumed, p<0.05 significance			

TABLE 6.28 Cell count data analysis for one-month-old versus three-month-old *Del2* females

Sample: E2 (pg/ml)	Mean % of cells with >2 centrosomes (one month)	Mean % of cells with >2 centrosomes (three months)	p-value *
0	13	15.5	0.321
25	20	31.2	0.099
75	28	30.3	0.405
500	33	38.7	0.252
*p-value calculated from 1-sided t-test with unequal variance assumed, p<0.05 significance			

6.3.2.3 Six-month-old wt animals

Comparing the mean number of cells displaying centrosomal amplification between one-month-old (n of 4 for both males and females), and six-month-old (n of 3 for both males and females) wt animals reveals, samples isolated from the older animals generally display higher numbers of abnormal cells (Fig. 6.13). Statistically, there is very little difference between the levels of abnormal cells in samples derived from female mice (Table 6.30). In contrast cells derived from six-month-old male mice show a significant increase in the number of cells displaying centrosomal amplification when compared to cells isolated from one-month-old males (Table 6.29).

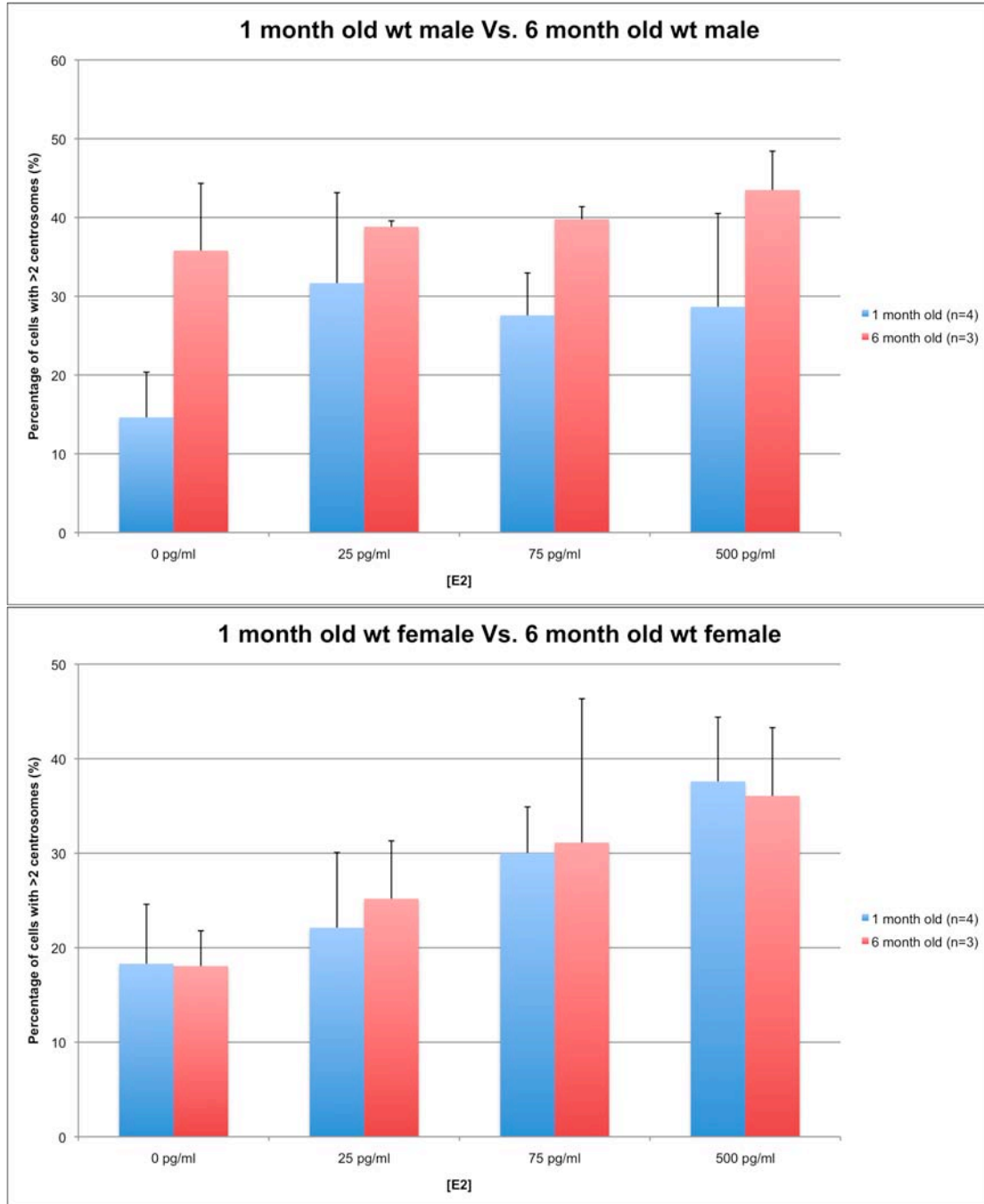


FIGURE 6.13 One-month-old Vs six-month-old wt: comparison of centrosomal amplification in 17 β -estradiol treated primary proximal tubular epithelial cells. The number of cells displaying centrosomal overduplication, represented as the mean percentage of cells with more than 2 centrosomes, from one-month-old (blue bars), and six-month-old (red bars) mice were compared to determine if levels were significantly higher in cells isolated from older animals. Levels were found to be consistently higher in samples isolated from six-month-old male mice (upper chart). In contrast, levels were variable in cells isolated from female mice.

TABLE 6.29 Cell count data analysis for one-month-old versus six-month-old wt males

Sample: E2 (pg/ml)	Mean % of cells with >2 centrosomes (one month)	Mean % of cells with >2 centrosomes (three months)	p-value *
0	15	35.8	0.048
25	32	38.8	0.151
75	28	39.8	0.008
500	29	43.5	0.042
*p-value calculated from 1-sided t-test with unequal variance assumed, p<0.05 significance			

TABLE 6.30 Cell count data analysis for one-month-old versus six-month-old wt females

Sample: E2 (pg/ml)	Mean % of cells with >2 centrosomes (one month)	Mean % of cells with >2 centrosomes (three months)	p-value *
0	18	18.1	0.476
25	22	25.2	0.295
75	30	31.1	0.457
500	38	36.1	0.395
*p-value calculated from 1-sided t-test with unequal variance assumed, p<0.05 significance			

6.3.2.4 Six-month-old *Del2* animals

Comparing the mean number of cells displaying centrosomal amplification between one-month-old (n of 4 for both males and females), and six-month-old (n of 3 for both males and females) *Del2* animals reveals, samples isolated from six-month-old male animals generally display higher levels of centrosomal overduplication when treated with E2 (Fig. 6.14). However, only at 500pg/ml E2 does this become statistically significant (Table 6.31). With the mean percentage of cells displaying centrosomal overduplication in one-month-old and six-month-old male control samples being relatively equal (Fig. 6.31). In contrast, cells isolated from female mice display higher levels of centrosomal amplification in cells isolated from one-month-old animals at all levels of E2 treatment (Fig.6.14). None of which is statistically significant (Table 6.32).

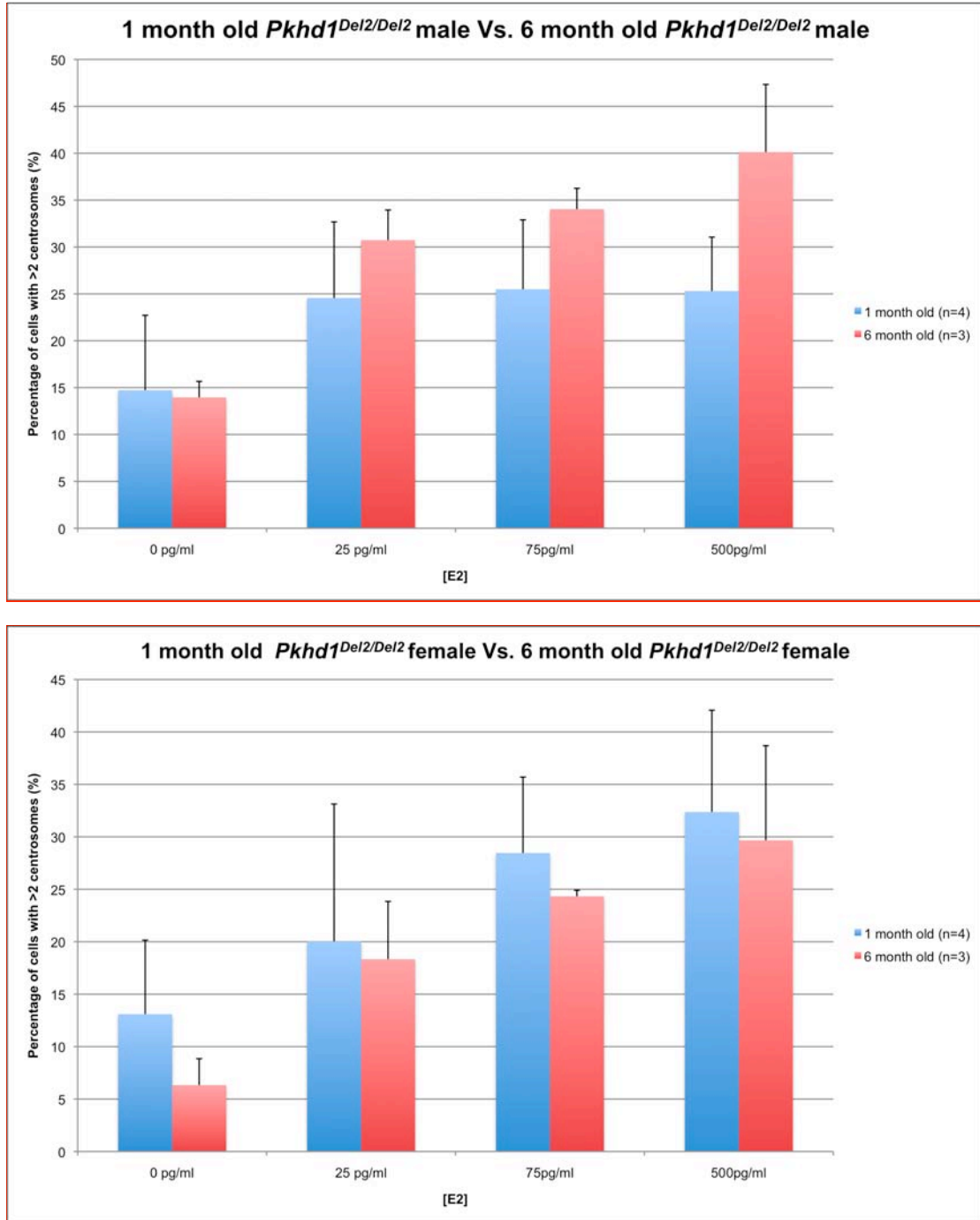


FIGURE 6.14 One-month-old Vs six-month-old *Del2*: comparison of centrosomal amplification in 17 β -estradiol treated primary proximal tubular epithelial cells. The number of cells displaying centrosomal overduplication, represented as the mean percentage of cells with more than 2 centrosomes, from one-month-old (blue bars), and six-month-old (red bars) mice were compared to determine if levels were significantly higher in cells isolated from older animals. Levels were found to be consistently higher in E2 treated samples isolated from six-month-old male mice (upper chart). In contrast, levels were found to be consistently higher in cells isolated from one-month-old female mice.

TABLE 6.31 Cell count data analysis for one-month-old versus six-month-old *Del2* males

Sample: E2 (pg/ml)	Mean % of cells with >2 centrosomes (one month)	Mean % of cells with >2 centrosomes (three months)	p-value *
0	14.7	14.0	0.432
25	25.6	30.7	0.118
75	25.5	34.0	0.05
500	25.3	40.1	0.023
*p-value calculated from 1-sided t-test with unequal variance assumed, p<0.05 significance			

TABLE 6.32 Cell count data analysis for one-month-old versus six-month-old *Del2* females

Sample: E2 (pg/ml)	Mean % of cells with >2 centrosomes (one month)	Mean % of cells with >2 centrosomes (three months)	p-value *
0	13	6.3	0.076
25	20	18.3	0.413
75	28	24.3	0.168
500	33	29.7	0.360
*p-value calculated from 1-sided t-test with unequal variance assumed, p<0.05 significance			

6.3.2.5 Nine-month-old wt animals

Analysis of the mean percentage of cells displaying centrosomal overduplication from nine-month-old (n of 3) and one-month-old (n of 4) wt male and female mice shows that overall, levels are consistently higher in cells derived from nine-month-old animals (Fig. 6.15). However, this observation is not significant at any level of E2 treatment for either gender (Tables 6.33 and 6.34).

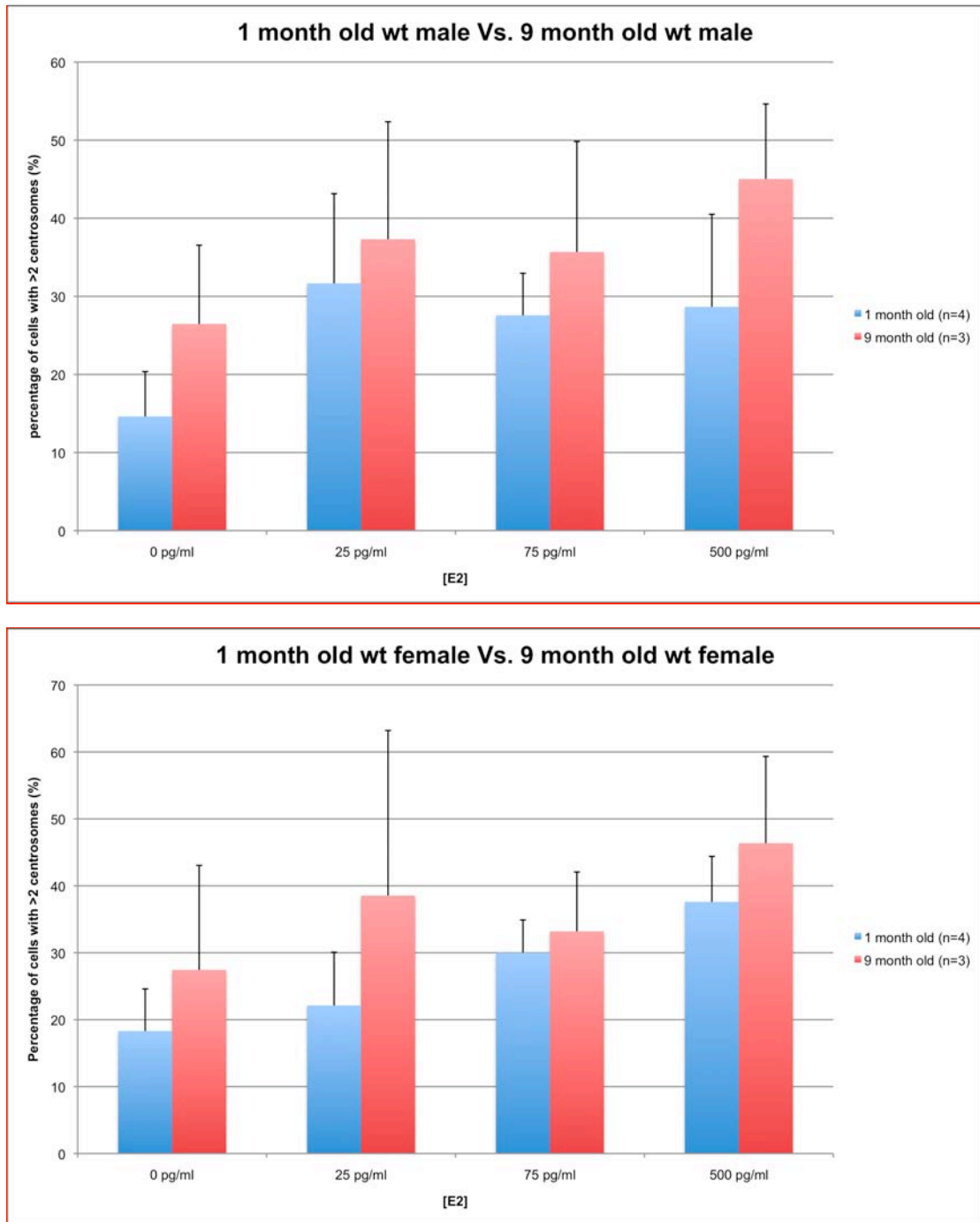


FIGURE 6.15 One-month-old Vs nine-month-old wt: comparison of centrosomal amplification in 17 β -estradiol treated primary proximal tubular epithelial cells. The number of cells displaying centrosomal overduplication, represented as the mean percentage of cells with more than 2 centrosomes, from one-month-old (blue bars), and nine-month-old (red bars) mice were compared to determine if levels were significantly higher in cells isolated from older animals. Levels were found to be consistently higher in E2 treated samples isolated from nine-month-old male mice (upper chart), and female mice (lower chart).

TABLE 6.33 Cell count data analysis for one-month-old versus nine-month-old wt males

Sample: E2 (pg/ml)	Mean % of cells with >2 centrosomes (one month)	Mean % of cells with >2 centrosomes (three months)	p-value *
0	15	26.5	0.083
25	32	37.3	0.309
75	28	35.7	0.215
500	29	45.0	0.050
*p-value calculated from 1-sided t-test with unequal variance assumed, p<0.05 significance			

TABLE 6.34 Cell count data analysis for one-month-old versus nine-month-old wt females

Sample: E2 (pg/ml)	Mean % of cells with >2 centrosomes (one month)	Mean % of cells with >2 centrosomes (three months)	p-value *
0	18	27.4	0.211
25	22	38.5	0.185
75	30	33.2	0.308
500	38	46.4	0.184
*p-value calculated from 1-sided t-test with unequal variance assumed, p<0.05 significance			

6.3.2.6 Nine-month-old *Del2* animals

Analysis of the mean percentage of cells displaying centrosomal amplification from one-month-old (n of 4), and nine-month-old (n of 3) *Del2* male and female mice show that the number of abnormal cells is consistently higher in cells derived from nine-month-old animals (Fig. 6.16). In samples isolated from male mice the observed increase is statistically significant at all levels of E2 treatment, also true for the control (Table 6.35). For female mice, the increase in levels of centrosome overduplication was significant at 0pg/ml, 25pg/ml, and 75pg/ml E2 (Table 6.36).

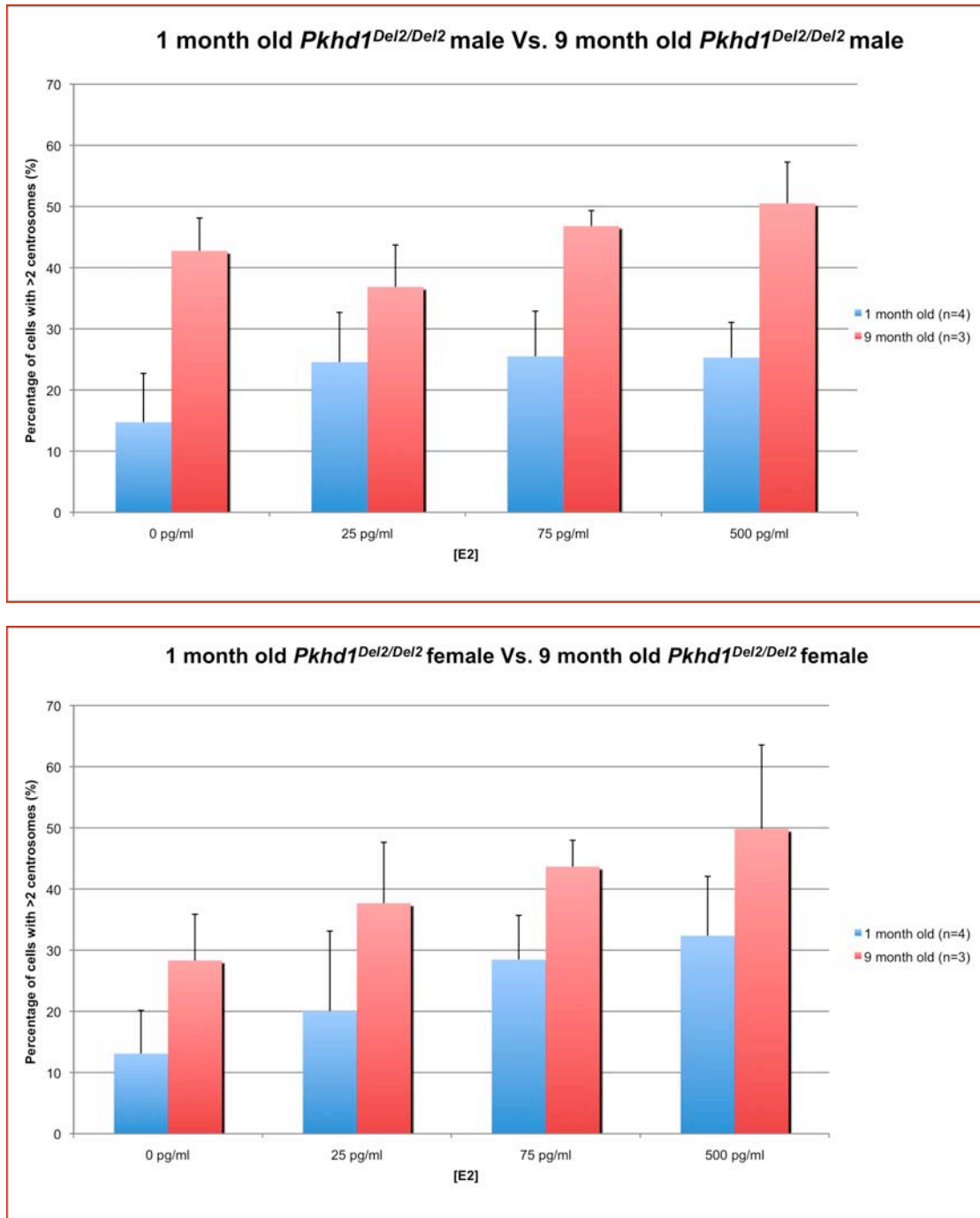


FIGURE 6.16 One-month-old Vs nine-month-old *Del2*: comparison of centrosomal amplification in 17 β -estradiol treated primary proximal tubular epithelial cells. The number of cells displaying centrosomal overduplication, represented as the mean percentage of cells with more than 2 centrosomes, from one-month-old (blue bars), and nine-month-old (red bars) mice were compared to determine if levels were significantly higher in cells isolated from older animals. Levels were found to be consistently higher in all samples isolated from nine-month-old male mice (upper chart), and female mice (lower chart).

TABLE 6.35 Cell count data analysis for one-month-old versus nine-month-old *Del2* males

Sample: E2 (pg/ml)	Mean % of cells with >2 centrosomes (one month)	Mean % of cells with >2 centrosomes (three months)	p-value *
0	14.7	42.7	0.001
25	25.6	36.9	0.041
75	25.5	46.8	0.003
500	25.3	50.5	0.003
*p-value calculated from 1-sided t-test with unequal variance assumed, p<0.05 significance			

TABLE 6.36 Cell count data analysis for one-month-old versus nine-month-old *Del2* females

Sample: E2 (pg/ml)	Mean % of cells with >2 centrosomes (one month)	Mean % of cells with >2 centrosomes (three months)	p-value *
0	13	28.3	0.025
25	20	37.7	0.050
75	28	43.6	0.009
500	33	49.8	0.072
*p-value calculated from 1-sided t-test with unequal variance assumed, p<0.05 significance			

6.3.3 Knockdown of fibrocystin in primary proximal tubular epithelial cells has no effect on 17 β -estradiol driven centrosomal overduplication

Statistical analysis to compare the mean number of cells displaying centrosomal overduplication in age-matched wt and *Del2* animals was carried out to determine if knockdown of fibrocystin resulted in a significant increase in the incidence of centrosomal amplification in primary PTCs. Age-matched analysis for the four age-points was performed to examine whether levels in cells derived from cystic versus non-cystic tubules would differ.

6.3.3.1 One month old animals

Comparing the mean percentage of abnormal proximal tubular epithelial cells derived from counts of 100 or more cell for one-month-old wt (n of 4) and one-month-old *Del2* (n of 4) male and female mice revealed, the number of abnormal cells is higher in samples isolated from wt mice (Fig. 6.17). The difference in the levels of centrosomal overduplication between wt and *Del2* mice when compared is not statistically significant at any level of E2 treatment (Tables 6.37 and 6.38).

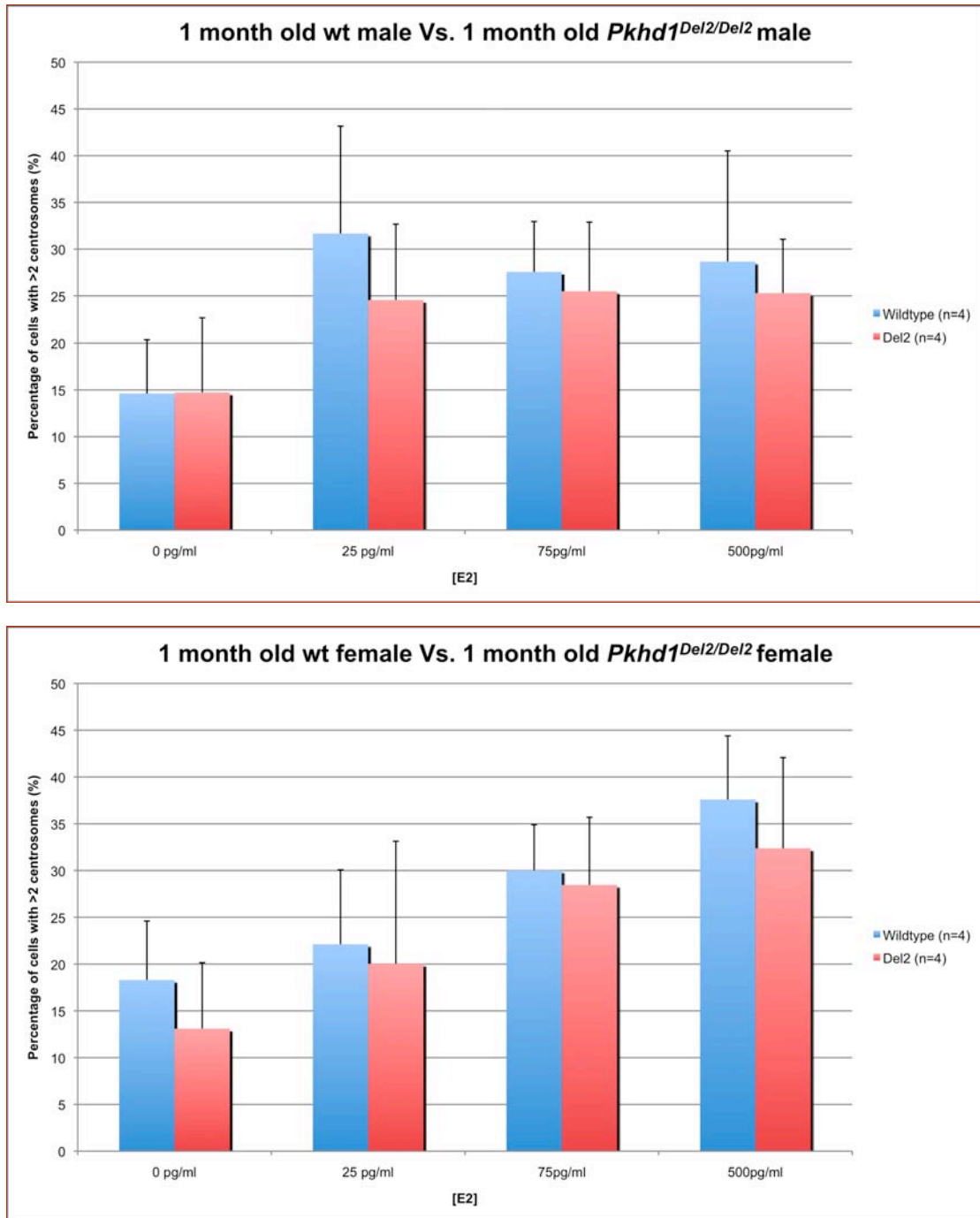


FIGURE 6.17 Age-matched comparison of the mean percentage of primary proximal tubular epithelial cells displaying centrosomal amplification from one-month-old wt and *Del2* animals. Levels of centrosomal amplification, represented as the mean number of cells with more than two centrosomes per sample, from wt (blue bars) and *Del2* (red bars) mice were compared to determine if levels were significantly higher in cells isolated from *Del2* animals. Levels were found to be consistently higher in both male (top chart) and female (lower chart) wt animals.

TABLE 6.37 Cell count data analysis for one-month-old wt versus one-month-old *Del2* males

Sample: E2 (pg/ml)	Mean % of cells with >2 centrosomes (wt)	Mean percentage of cells with >2 centrosomes (<i>Del2</i>)	p-value*
0	15	14.7	0.491
25	32	25.6	0.177
75	28	25.5	0.334
500	29	25.3	0.317
*p-values calculated from 1-sided t-test with unequal variance assumed, p<0.05 significance			

TABLE 6.38 Cell count data analysis for one-month-old wt versus one-month-old *Del2* females

Sample: E2 (pg/ml)	Mean % of cells with >2 centrosomes (wt)	Mean percentage of cells with >2 centrosomes (<i>Del2</i>)	p-value*
0	18	13	0.157
25	22	20	0.398
75	30	28	0.368
500	38	33	0.208
*p-values calculated from 1-sided t-test with unequal variance assumed, p<0.05 significance			

6.3.3.2 Three-month-old animals

Analysis comparing the mean percentage of abnormal proximal tubular epithelial cells isolated from three-month-old wt (n of 3), and three-month-old *Del2* (n of 3) male and female mice revealed, differences between wt and *Del2* samples to be inconsistent (Fig. 6.18). Although cells from both wt and *Del2* animals show a similar response to increasing levels of E2, cells isolated from neither genotype show a consistently higher level of centrosomal amplification compared to the other (Fig. 6.18).

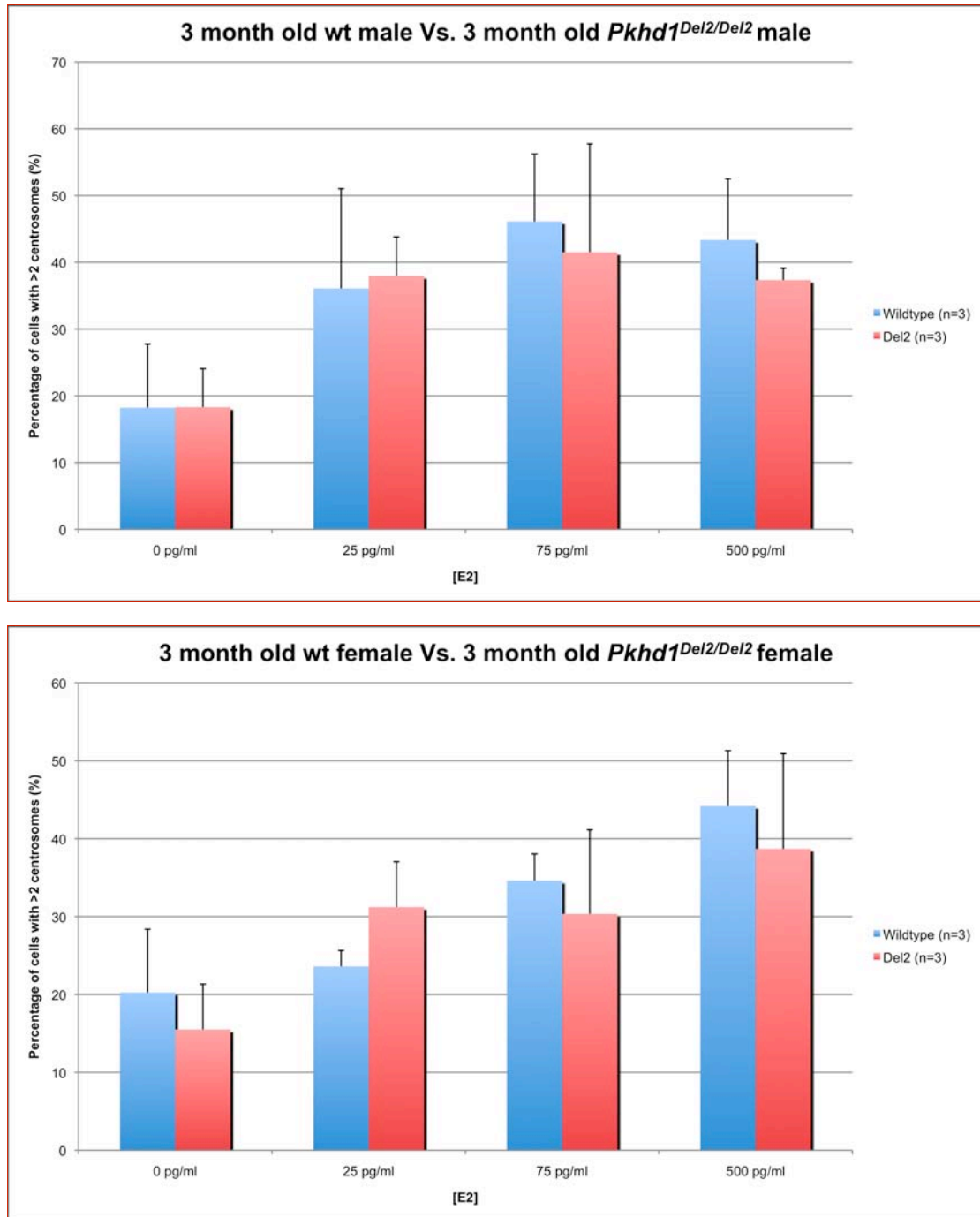


FIGURE 6.18 Age-matched comparison of the mean percentage of primary proximal tubular epithelial cells displaying centrosomal amplification from three-month-old wt and *Del2* animals. Levels of centrosomal amplification, represented as the mean number of cells with more than two centrosomes per sample, from wt (blue bars) and *Del2* (red bars) mice were compared to determine if levels were significantly higher in cells isolated from *Del2* animals. Levels were not found to be consistently higher in either wt or *Del2* animals.

TABLE 6.39 Cell count data analysis for three-month-old wt versus three-month-old *Del2* males

Sample: E2 (pg/ml)	Mean % of cells with >2 centrosomes (wt)	Mean percentage of cells with >2 centrosomes (<i>Del2</i>)	p-value*
0	18.2	18.3	0.495
25	36.1	37.9	0.427
75	46.1	41.5	0.350
500	43.3	37.3	0.187
*p-values calculated from 1-sided t-test with unequal variance assumed, p<0.05 significance			

TABLE 6.40 Cell count data analysis for three-month-old wt versus three-month-old *Del2* females

Sample: E2 (pg/ml)	Mean % of cells with >2 centrosomes (wt)	Mean percentage of cells with >2 centrosomes (<i>Del2</i>)	p-value*
0	20.2	15.5	0.231
25	23.6	31.2	0.070
75	34.6	30.3	0.286
500	44.2	38.7	0.273
*p-values calculated from 1-sided t-test with unequal variance assumed, p<0.05 significance			

6.3.3.3 Six-month-old animals

Analysis of the mean percentage of cells displaying centrosomal overduplication from six-month-old wt (n of 3), and six-month-old *Del2* (n of 3) male and female mice reveals that upon comparison, levels of abnormal cells are consistently higher in samples isolated from wt animals (Fig. 6.19). This difference is statistically significant at 25pg/ml and 75pg/ml E2 in male samples (Table 6.41), and notably in control samples for both male and female isolates (Table 6.41 and 6.42).

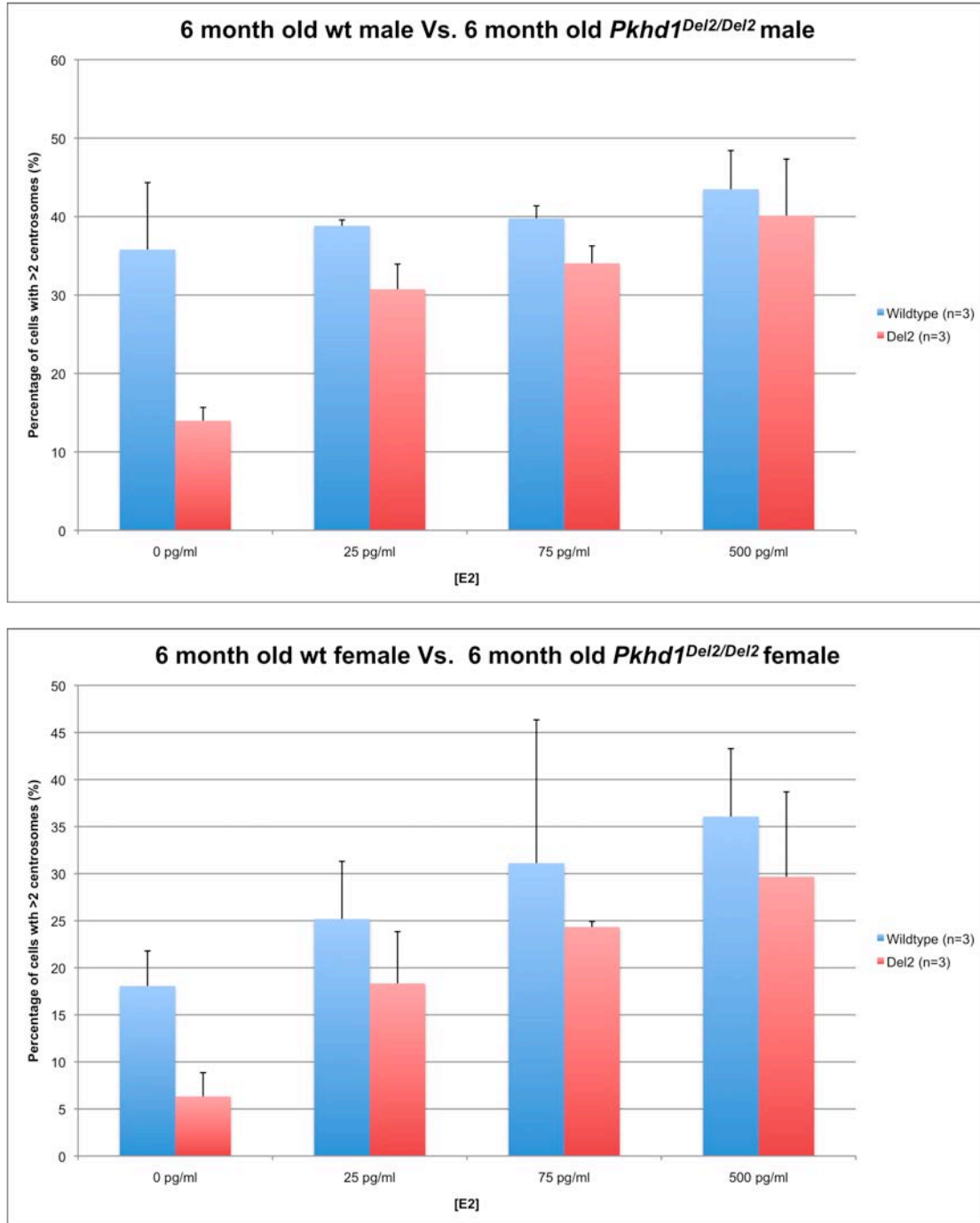


FIGURE 6.19 Age-matched comparison of the mean percentage of primary proximal tubular epithelial cells displaying centrosomal amplification from six-month-old wt and *Del2* animals. Levels of centrosomal amplification, represented as the mean number of cells with more than two centrosomes per sample, from wt (blue bars) and *Del2* (red bars) mice were compared to determine if levels were significantly higher in cells isolated from *Del2* animals. Levels were found to be consistently higher in both male (top chart) and female (lower chart) wt animals.

TABLE 6.41 Cell count data analysis for six-month-old wt versus six-month-old *Del2* males

Sample: E2 (pg/ml)	Mean % of cells with >2 centrosomes (wt)	Mean percentage of cells with >2 centrosomes (<i>Del2</i>)	p-value*
0	35.8	14.0	0.050
25	38.8	30.7	0.021
75	39.8	34.0	0.013
500	43.5	40.1	0.273
*p-values calculated from 1-sided t-test with unequal variance assumed, p<0.05 significance			

TABLE 6.42 Cell count data analysis for six-month-old wt versus six-month-old *Del2* females

Sample: E2 (pg/ml)	Mean % of cells with >2 centrosomes (wt)	Mean percentage of cells with >2 centrosomes (<i>Del2</i>)	p-value*
0	18.8	6.3	0.007
25	25.2	18.3	0.112
75	31.1	24.3	0.260
500	36.1	29.7	0.197
*p-values calculated from 1-sided t-test with unequal variance assumed, p<0.05 significance			

6.3.3.4 Nine-month-old animals

Age-matched comparison of the mean percentage of proximal tubular cells displaying an abnormal centrosomal complement between wt and *Del2* mice reveals that, although levels of abnormal cells increase with higher doses of 17 β -estradiol, the incidence of centrosomal overduplication is higher in samples derived from *Del2* animals (Fig. 6.20). However, statistical analysis shows that the higher incidence of centrosomal overduplication in *Del2* samples is not statistically significant (Table 6.43 and 6.44).

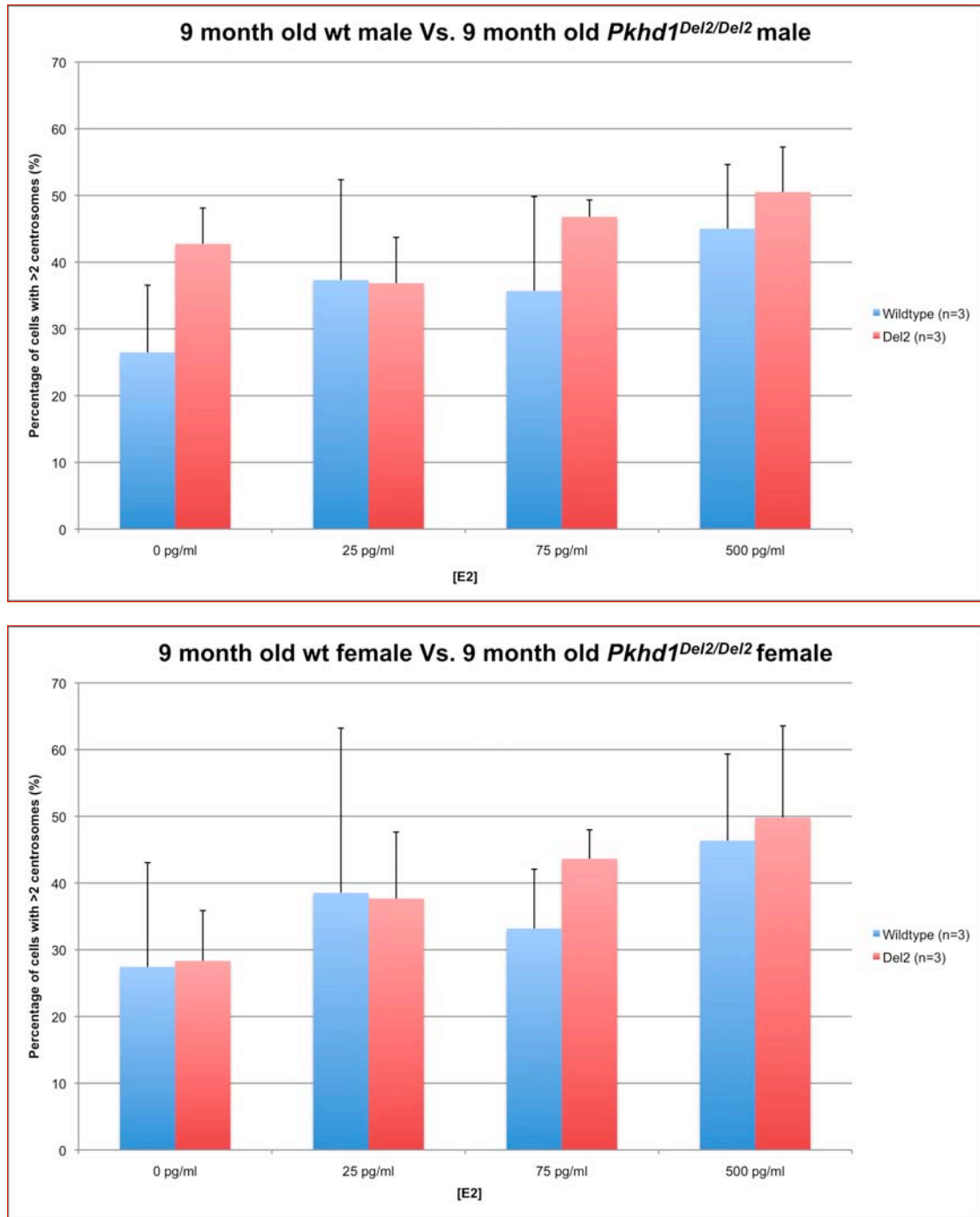


FIGURE 6.20 Age-matched comparison of the mean percentage of primary proximal tubular epithelial cells displaying centrosomal amplification from nine-month-old wt and *Del2* animals. Levels of centrosomal amplification, represented as the mean number of cells with more than two centrosomes per sample, from wt (blue bars) and *Del2* (red bars) mice were compared to determine if levels were significantly higher in cells isolated from *Del2* animals. Levels varied between wt and *Del2* PTCs, but were found to be generally higher in *Del2* samples.

TABLE 6.43 Cell count data analysis for nine-month-old wt versus nine-month-old *Del2* males

Sample: E2 (pg/ml)	Mean % of cells with >2 centrosomes (wt)	Mean percentage of cells with >2 centrosomes (<i>Del2</i>)	p-value*
0	26.5	42.7	0.044
25	37.3	36.9	0.482
75	35.7	46.8	0.153
500	45.0	50.5	0.235
*p-values calculated from 1-sided t-test with unequal variance assumed, p<0.05 significance			

TABLE 6.44 Cell count data analysis for nine-month-old wt versus nine-month-old *Del2* females

Sample: E2 (pg/ml)	Mean % of cells with >2 centrosomes (wt)	Mean percentage of cells with >2 centrosomes (<i>Del2</i>)	p-value*
0	27.4	28.3	0.468
25	38.5	37.7	0.480
75	33.2	43.6	0.084
500	46.4	49.8	0.383
*p-values calculated from 1-sided t-test with unequal variance assumed, p<0.05 significance			

6.3.4 At what age do ‘star-burst’ primary cilia occur in *Pkhd2*^{*Del2/Del2*} animals?

Fluorescent immunohistochemical staining of kidney and liver tissue from a number of one and four-month-old *Del2* animals was carried out in order to determine the approximate age at which ‘star-burst’ cilia and associated centrosomal overduplication may begin to occur. In order to confirm that the tubular segments under observation were indeed the proximal tubules or bile ducts, kidneys were stained with the proximal tubule specific marker, LTA, and liver with the bile duct specific marker, DBA.

In one-month-old fully inbred (past 10th generation inbred) male *Del2* mice, no evidence of dilation of the proximal tubules was found (Fig. 6.21b). At four months, tubules appeared slightly dilated (Fig. 6.21c). Primary cilia were visible within the tubule lumen of proximal

tubules in sections taken from male *Del2* mice (Fig. 6.21). In contrast, proximal tubules examined from one-month-old inbred *Del2* female mice displayed evidence of dilation, especially when compared to tubules within wt kidneys (Fig. 6.21e). By four-months of age the proximal tubules of female *Del2* mice were significantly dilated (Fig. 6.21e), with sparse stunted primary cilia visible (not shown).

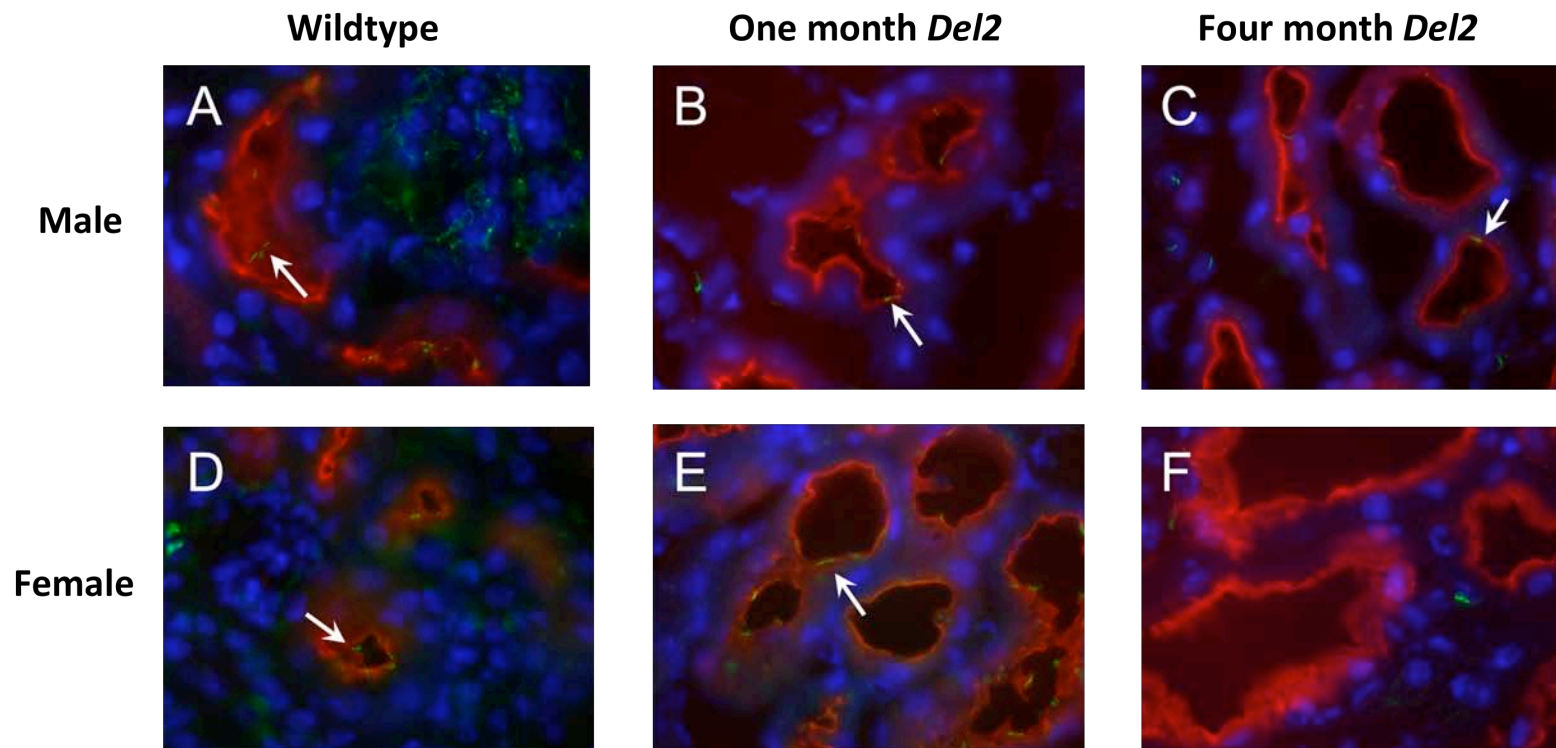


FIGURE 6.21 Fluorescent immunohistochemistry of wt and *Pkhd1*^{Del2/Del2} kidney tissue sections. These representative images show the general morphology of the proximal tubules in wt and *Del2* mice. The proximal tubule specific marker lotus tetragonolobus agglutinin (LTA) can be seen in red, highlighting the luminal surface of the epithelial cells lining the tubules. Nuclei of cells are stained blue with DAPI. Primary cilia stained with the marker acetylated α -tubulin, if present, are seen in green. In wild type kidney (Panels A and D) normal proximal tubular morphology of a small continuously labelled lumen is shown, with patent primary cilia. At one month of age proximal tubules of male *Del2* animals (Panel B) are undilated, with a few primary cilia visible. In contrast, proximal tubules from one-month-old female *Del2* mice (Panel E) have begun to dilate, however primary cilia remain present. At four month of age the proximal tubules of male *Del2* mice have begun to dilate slightly with fewer primary cilia present in the tubule lumen (Panel C). In contrast, the proximal tubules of female *Del2* animals at four month of age (Panel F) are highly dilated with no primary cilia visible.

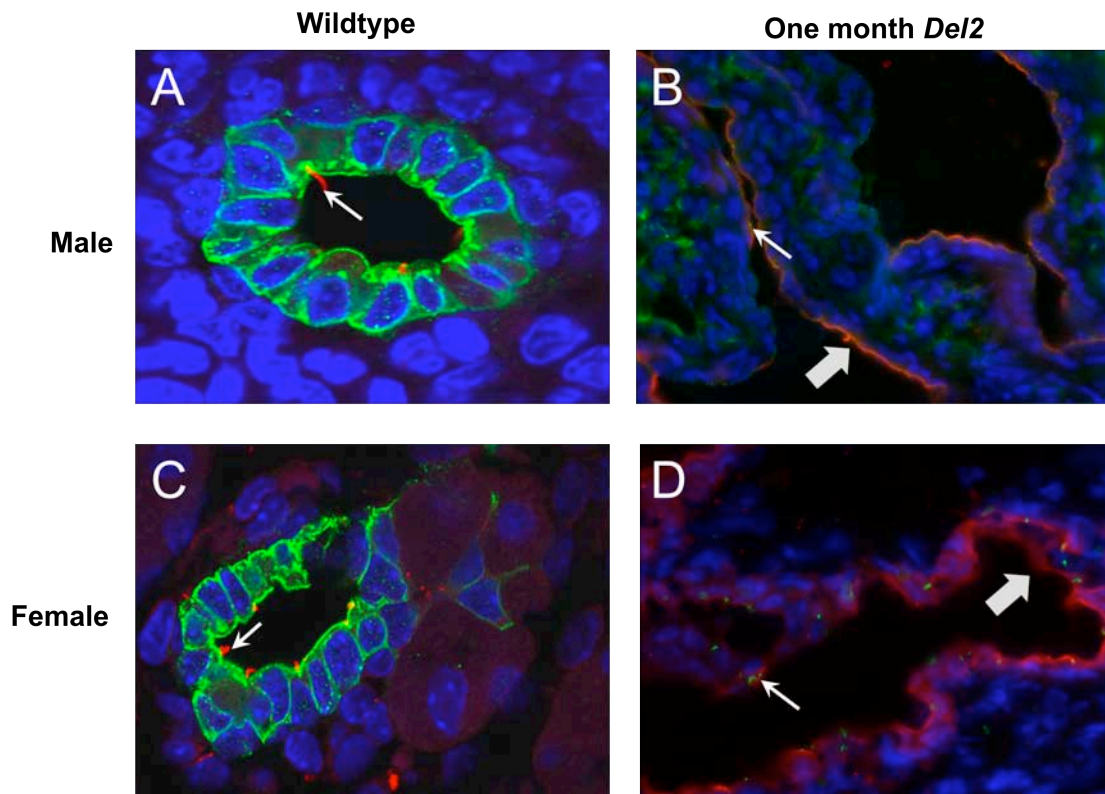


FIGURE 6.22 Fluorescent immunohistochemistry of wt and *Pkhd1*^{*Del2/Del2*} liver tissue sections. These representative images show the general morphology of the bile ducts in wt and *Del2* mice. The bile duct specific marker Dolichus biflorus agglutinin (DBA) can be seen in green in the sections taken from wt animals (Panels A and C), and in red in the sections taken from *Del2* mice (Panels B and D), highlighting the surface of the biliary epithelial cells lining the tubules (block arrows). Nuclei of cells are stained blue with DAPI. Primary cilia, stained with the marker acetylated α -tubulin, if present are seen in red in wt sections (Panels A and C), and green in *Del2* sections (Panels B and D). In wild-type liver, panels A and C, normal bile duct morphology of a small continuously labelled lumen is evident, with patent primary cilia. At one-month of age, bile ducts from both male and female *Del2* animals are cystic. Very few stunted primary cilia visible in *Del2* sections, (Panels B and D).

6.4 CONCLUSIONS AND DISCUSSION

6.4.1 Centrosomal amplification in primary murine proximal tubule epithelial cells shows positive correlation to increasing levels of 17 β -estradiol *in vitro*

The study has shown that the culture of primary murine proximal tubular epithelial cells with increasing levels of 17 β -estradiol drives a mitogenic response that results in the overduplication of centrosomes. In summary the main findings of this chapter are that primary proximal tubular epithelial cells derived from younger (one and three month old) male and female, wt and *Del2* mice display a significant susceptibility to E2 induced centrosomal overduplication *in vitro*. This is evident by the significant increase in the number of abnormal cells in samples cultured with E2 when compared to levels displayed in control samples. PTCs from older animals (six and nine months) also display an increased level of centrosomal amplification with increasing doses of E2 *in vitro*, however the increase in the number of abnormal cells in treated samples compared to control samples is less significant than in cells isolated from younger animals. The resulting increase in the number of centrosomes per cell is also associated with multiple primary cilia, and nuclear dysmorphia. So, although these findings are of little relevance to biliary atresia, or the functional study of fibrocystin, it does provide insight into the mechanism driving cystic development in tubular structures.

Analysis of the levels of centrosomal amplification induced in primary murine PTCs, when cultured with increasing doses in E2 shows there is a general positive correlation in cells derived from both wt and *Del2* animals. Although the trend was not always linear, there was a

definite overall increase in the incidence and severity of centrosomal amplification as levels of E2 increased. Comparison of the mean percentage of cells displaying centrosomal amplification in untreated control and treated samples were on the whole significantly different, with those wells treated with E2 displaying a higher incidence of abnormal cells. Abnormal cells being those with more than two centrosomes. Levels of abnormal PTCs derived from female animals did display a linear increase in the mean number of cell displaying more than two centrosomes in correlation with E2 doses. In contrast male cells displayed a more random response, despite the increasing levels of E2 used in culture. Once there was an initial increase in the level of abnormal cells upon introduction of the lowest dose of E2, levels remained relatively steady with little increase in the number of abnormal cells, despite increasing levels of E2. This could be due to difference in the *in vitro* environment from which these cells originated, as levels of circulating hormone such as E2 are innately different in male and female animals.

The expression profiles of the oestrogen receptor isoforms may also be responsible for the observed gender difference, if they do vary between male and female mice. Or it may be possible that differential expression of oestrogen receptor modulators may also contribute to this effect. Unfortunately, oestrogen receptor expression was not included in this study, and thus the above is only speculative.

In order to examine if there was a significant difference in the incidence of centrosomal amplification in primary PTCs, from male and female animals, age-matched comparison of

the mean number of abnormal cells observed was carried out. In order to determine if there was a significant difference in E2 responsiveness in primary PTCs isolated from male and female animals, E2 dose-matched comparison of the mean number of abnormal cells observed was also carried out. This analysis revealed there is very little difference in the severity of centrosomal amplification at matched levels of E2 treatment. Levels from neither sex were consistency greater than the other.

As primary PTCs isolated from both male and female mice displayed similar levels of centrosomal overduplication, these results provide no further clue towards the increased severity of cystic disease in female mice. However, what it does provide is evidence supporting a stimulatory role for E2 in the progression of renal cystic disease. This evidence also suggests it is the stimulatory effect of E2 in female *Del2* mice as opposed to a protective role of testosterone in male *Del2* animals that results in the more severe cystic phenotype in female mice. Similar to the cystogenic stimulatory effect of E2, that is also seen in polycystic liver disease in females receiving oestrogen therapy, or in those who are pregnant [Sherstha et al., 1997].

6.4.2 Severity of centrosomal amplification and the associated nuclear dysmorphia increases with increasing levels of 17 β -estradiol

The positive correlation between the number of abnormal cells, and E2 levels, is also associated with increasing severity of the type of centrosomal abnormalities observed. However, as this was not formally measured, its effects can only be speculated upon. It remains unclear how this would result in a more severe cystic phenotype in female *Del2* mice,

or how it could relate to an abnormal proliferative response, such as ductal proliferation in diseases such as BA, without leading to cancer, or cellular crisis. In order to better understand the functional relevance of centrosomal aberrations, and hence their biological significance, it is critical to consider the cellular context in which they occur [Duensing and Munger, 2002a; b; Nigg, 2002]. Centrosome anomalies are an astonishingly frequent finding in malignant tumours [Salisbury et al., 1999], with the degree of centrosomal aberrations often correlating with malignant progression [D'Assoro et al., 2002]. The frequent coincidence of centrosome aberrations, and cytogenetic changes, in primary tumours and tumour cell lines, has led to the conclusion that centrosomal abnormalities are a universal cause of genomic instability [Ghadimi et al., 2000; Pihan et al., 1998]. Despite the correlations between centrosome aberrations and clinical disease, a cause and effect relationship between centrosome aberrations, and tumour aggression has yet to be clearly proven. Indeed, centrosome aberrations have been detected in non-cancerous, inflammatory tissue [Battini et al., 2008; Lothschütz et al., 2002]. Malignant tumours have been observed to display centrosome anomalies in the presence of a diploid genome or a limited set of genetic alterations [Duensing and Munger, 2003]. Furthermore, genomically unstable neoplasms can possess a normal set of centrosomes [Martin-Subero et al., 2003], indicating that centrosome abnormalities may neither be sufficient nor necessary in cancer development. It is also acknowledged, that additional centrosomal changes are frequently detected in cancerous cells including; excess pericentriolar material, defects of centrosome maturation and microtubule-nucleating capacity, or misorientation of centrosomes within cells [Salisbury et al., 1999]. These findings not only question the significance of centrosome aberrations in chromosomal instability, they also underscore that centrosome anomalies are likely to represent a uniform cellular response




to a variety of cellular insults that do not necessarily result in cancer, but other proliferative disorders [Duensing, 2005].

Centrosome aberrations can be classified into subgroups, with presumably distinct biological impact [Duensing, 2005]. While strict categorisation of the centrosomal and genomic anomalies observed in these PTC studies was not implemented at the time cells were being counted, overall observations did detect noticeable differences in the kind of anomalies present. A tentative classification of the types of centrosomal abnormalities, observed in cancer cells by Duensing [2005], places centrosome overduplication into three basic categories: primary centrosome overduplication, transient accumulation, and permanent centrosome accumulation (Table 6.45). Whereas the first two categories of centrosome anomalies may lead to chromosomal instability if counter-regulatory cellular mechanisms fail, the latter category is unlikely to cause genomic instability. The first two categories are also able to generate multipolar anaphases that result in competent daughter cells, which also possess an abnormal centrosomal, and chromosomal complement. In this study, all three categories of centrosomal abnormalities were observed in PTCs from wt and *Del2* animals (Figs. 6.9 and 6.10). The predicted ability of those with primary centrosome overduplication and transient centrosome accumulation to produce viable daughter cells would explain how cells with an abnormal centrosome and chromosome complement are able to grow in culture. This ability may also result in abnormal proliferative behaviour in tubular epithelial cells, causing the phenotypes observed in PKD and hepatobiliary diseases such as BA. The difference between cystic ductular, and proliferative ductular responses, may be due to differences in the ratio of cells displaying permanent centrosomal accumulation, that are

unable to produce viable daughter cells, and cells that are able to produce viable daughter cells. It is possible that the lack of the additional centrosomal changes frequently detected in cancerous cells may provide the balance between the proliferative nature of ductular proliferation, cyst growth, and cancer.

TABLE 6.45 Proposed classification of centrosome abnormalities in tumour cells.

Taken from [Duensing, 2005]

Type of centrosome aberration	Primary centrosome overduplication	Transient centrosome accumulation	Permanent centrosome accumulation
Definition	Abnormal numbers of centrosomes in cells competent to generate daughter cells	Abnormal numbers of centrosomes together with altered ploidy in cells competent to generate daughter cells	Abnormal number of centrosomes in cells that are unable to generate viable daughter cells
Nuclear morphology	Normal	Enlarged, binucleated	Frequently multinucleated, micronuclei, nuclear enlargement
Chromosomal content	Normal	Tetraploid/polyploid	Polyploid/aneuploid \pm structural chromosomal aberrations
Persistent cell division defect	No	No	Frequent
Multipolar anaphases	Possible	Possible	Unlikely
Centrosome-mediated chromosomal instability	Possible	Possible	Unlikely
Examples of oncogenic mechanisms	HPV-16 E7	Aurora-A, Plk1 \pm p53 deficiency	HPV-16 E6; p21 ^{Cip1} or p53 deficiency after DNA damage
Cell morphology (gray, nuclei; black dots, centrosomes)			
	Normal nuclear morphology, diploid DNA content, multiple centrosomes	Binucleation and/or nuclear enlargement, tetra-/polyploidy, multiple centrosomes	Nuclear atypia, multinucleation, micronuclei, nuclear enlargement, poly-/aneuploidy, multiple centrosomes

6.4.3 PTC from older mice display increased susceptibility to E2 induced centrosomal overduplication

Analysis of the mean percentages of cells with centrosomal overduplication, from both male and female mice, at the ages of one, three, six, and nine months, shows that there is an almost consistent rise in the number of abnormal cells derived from older animals. This observation also holds true whether cells were isolated from wt or *Del2* animals. Overall, many differences observed were not statistically significant, making these observations meaningless.

Although not always statistically significant, the overall increase in the number of abnormal cells in samples isolated from older *Del2* animals correlates with the increasing severity of cytogenesis in *Del2* animals as they age. This observation could be attributed to the natural progression of the disease. It is reasonable to speculate, that cells isolated from tubules that have either begun to dilate, or are already very dilated/cystic may have already reached a steady state of centrosomal accumulation, whilst maintaining the ability to produce viable daughter cells. This may result in a higher proportion of those cells that are isolated possessing an abnormal centrosomal complement, whilst maintaining the ability to be cultured *in vitro*. However, this hypothesis cannot be applied to the increase seen in cells isolated from older wt animals. Woollard et al [2007] reported a significant increase in the PT diameter of female wt mice, this provides evidence that the age-related increase in tubule diameter is a physiological phenomenon. This suggests that as the animals age, tubular epithelial cells either lose their ability to maintain the optimal tubule diameter or a physiologically relevant mechanism results in this widening. Either way, it is not known whether the widening of the PT in wt mice is the result of abnormal cellular activity in response to the aging process, or an

important process related to homeostasis. Irrespective of this, it appears that whatever mechanism is driving this dilatation; it results in an increase in the number of cells with centrosomal overduplication, resulting in a higher proportion of isolated cells that possess an abnormal centrosomal complement.

6.4.4 Fibrocystin knockdown does not result in increased frequency or severity of centrosomal amplification in primary murine PTCs

Statistical comparisons of the mean number of PTCs displaying centrosomal overduplication, in cells derived from age-matched wt and *Del2* animals, shows knockdown of fibrocystin has no significant effect on the incidence of centrosomal amplification in primary PTCs. Indeed, in younger animals (one to six months), cells derived from wt animals displayed higher levels of centrosomal amplification at all levels of E2 treatment, when compared to levels observed in *Del2* samples. In contrast, cells derived from older *Del2* animals (9 months), displayed higher levels of centrosomal amplification when compared to cells derived from wt animals. Despite very few of these observations being statistically significant, these results can be interpreted in a number of ways. Firstly, it could simply be interpreted that the knockdown of fibrocystin simply has no effect on centrosomal amplification. However, although the exact functions of fibrocystin are not known, the chances of this are unlikely. Fibrocystin is a ciliary protein, shown in many studies to localise to the centrosome derived ciliary axoneme. Therefore, the likelihood of it having absolutely nothing to do with the structure, or function of the centrosome is improbable. Furthermore, the ciliary proteins PC-1 and PC-2, have both been found to play a role in centrosomal duplication despite not having any obvious direct link to centrosome structure, or function [Burtey et al., 2008; Fukasawa, 2005].

It is unknown whether a small functional fragment of the *Pkhd1* gene is still transcribed, and translated, in *Del2* animals. Targeted removal of exon 2, the first coding exon of the *Pkhd1* gene, removes the start codon, and the signal peptide from the ORF of the cDNA [Woollard et al., 2007]. Rapid amplification of 5' complementary DNA ends (5' RACE), and directed PCR analysis, confirms skipping of exon 2, and no possible alternative start site, indicate that *Del2* animals cannot make full-length fibrocystin. Western analysis with both rabbit anti-mouse fibrocystin and chicken anti-mouse fibrocystin, affinity purified antibodies, failed to detect fibrocystin in wt kidney membrane preparations, for reasons which remain unknown. Therefore, total loss of fibrocystin in *Del2* knockdown mice has yet to be verified [Woollard et al., 2007], but is being worked upon by the group who developed the *Del2* mouse (personal communication). If an alternative start codon is present within the ORF of the *Pkhd1* cDNA, an alternative smaller partially functional fragment may still be transcribed in *Del2* animals. Although this fragment may not be fully functional, it may still possess functions related to centrosome regulation.

Another explanation for the higher incidence of centrosomal amplification in wt cells, may be 'culture-shock.' Cells derived from a cystic environment, with accompanying fibrosis, inflammation, and the associated alterations in cytokine, and chemokine levels, would have altered expression of key homeostatic proteins enabling the cell to adapt to the changes within its immediate environment. However, this is entirely speculative.

6.4.5 The age at which ‘star-burst’ cilia and associated centrosomal amplification occurs in the PTs of *Del2* animals is not apparent upon examination of tissue from one and four month old animals

Although it is evident the PTs of female *Del2* mice begin to dilate from one month of age, there is no evidence of ‘star-burst’ cilia in the samples examined. By four months, the PTs of female *Del2* animals had very few stunted cilia, with most areas having no primary cilia. Expression of the PT marker, LTA, was also less defined, and appeared to be less restricted to the apical membrane, although this may be an artefact of staining. In contrast, male *Del2* kidney did not exhibit any tubular expansion at one month of age, although tubules did appear to have begun to dilate out by four months of age. Primary cilia were visible in PTs of male *Del2* animals, at one, and four months of age.

In comparison, the bile ducts of both male and female *Del2* animals were significantly dilated by one month of age, suggesting expansion is initiated very early in life. Expression of the bile duct marker DBA is discontinuous along the wall of the cysts, suggesting those cells lining the cyst have dedifferentiated. Primary cilia were sparse along the wall of the cyst, and where present were stunted in appearance, however no starburst cilia were observed.

The lack of evidence of ‘star-burst’ cilia in the PTs and bile ducts of one and four month old *Del2* animals resulted from, the timescale used in this study being inadequate to provide the resolution needed to accurately pinpoint the age at which ‘star-burst’ cilia may appear. The ages used did not cover an adequate age-range for the accurate determination of the age at which dilatation begins. The reasons for such an inadequate timescale, and age-range were

poor timing for the initiation of such a study, and the invaluable nature of the resource under investigation. The high cost and time-consuming nature of, aging-out animals, processing animals, and specimen preparation, all had to be taken into consideration. This meant, that in conjunction with the use of animals for the E2 primary culture studies, a limited supply of suitable archival tissue was available for this section of the study. However, despite these limitations this study highlights the pathogenetic role of *Pkhd1* knockdown in the liver. Providing more evidence supporting the importance of fibrocystin in hepatic tubulomorphogenesis. Although no definite evidence of *Pkhd1* knockdown driving centrosomal amplification was uncovered, this work has provided more data towards the investigation of the nature of tubular dilatation in *Del2* animals, and the levels of ciliary expression, an ongoing investigation by Dr C. Ward (Mayo Clinic, MN, USA).

In conclusion, the results obtained from this section of the current study indicate that, E2 drives centrosomal overduplication within murine primary proximal tubular cells in a dose dependent manner. As a consequence, nuclear dysmorphia and overexpression of primary cilia also display E2 sensitivity. These results also indicate that this response is age dependent. However, no evidence that this response is further promoted by knockdown of fibrocystin was obtained. Overall, the work contained within this chapter provides no direct answers to uncovering the aetiology of BA, or the function of fibrocystin. What it does provide is further insight into the process that drives fibrosis and cystogenesis in renal and hepatic tubules.

CHAPTER 7 DISCUSSION AND CONCLUSIONS

Overall, this project is a general investigation of *PKHD1* and fibrocystin in biliary duct injury, and the cellular phenotype of the *Pkhd1^{Del2/Del2}* mutant mouse. Although the main aims for this project initially set out to investigate a possible role of *PKHD1* sequence variants in cases of BA with renal cysts, inconclusive preliminary data meant the investigation had to broaden to include a wider range of diseases.

Despite the broadening of the investigation to encompass disorders not specifically related to BA, but becoming a more general study of fibrocystin and liver diseases this project did reveal a few interesting observations. These findings include the identification of three novel *PKHD1* sequence variants in a patient with BA and cysts. The identification of a non-specific marker of ongoing biliary duct damage in both cholangiopathic and non-cholangiopathic liver diseases. The functional investigation of the *Pkhd1* gene in the knockout mouse model, the *Del2* mouse revealed that although knockdown of *Pkhd1* does not result in any BA like hepatic morphological phenotype, the resulting altered epithelial cell behaviour and hepatic changes are shared by a number of cholangiopathies. Further investigation of the mechanisms related to altered epithelial behaviour uncovered cells that exhibit altered proliferative behaviour, common to a number of the cholangiopathies, including BA.

In conclusion, this thesis was unable to provide enough evidence to conclusively prove or disprove the hypotheses that “sequence variants and/or altered expression in the key gene

PKHD1 may be associated with cyst development and cellular damage in human liver disease.” The initial aim of this project was to investigate the phenotypic variability of *PKHD1* associated disease in human and animal models by meeting a number of key objectives that set out to fully characterise the role of fibrocystin *in vivo* and *in vitro*. The main finding of the investigations carried out to meet this aim is that altered expression of fibrocystin is a non-specific marker of biliary damage that is consequential of the disease process. An unexpected, and novel finding was that increased levels of α -tubulin acetylation is also another non-specific marker of biliary duct injury.

Investigations into the mechanism driving cystogenesis in the *Pkhd1*^{del2\del2} knockout mouse model were able to uncover that abnormalities in centrosomal duplication may play a role in abnormal tubulomorphogenesis, a feature common to all ciliopathies.

Questions that were not answered in this investigation include those that were reliant upon the establishment of a robust *in vitro* cell culture system. Thus, the structural and functional integrity of primary cilia in relation to BA, and *PKHD1* expression remains to be investigated. However, the main question this thesis was unable to answer was whether sequence variants of the gene *PKHD1* play a role in the acquired form of BA with or without renal cysts.

The main aim of the mutational screening was to determine if mutations in the *PKHD1* gene were associated with BA patients who displayed renal cysts, in order to establish a possible

genetic clue to the pathogenesis of this complex trait disorder particularly as most of these patients would not have lived long enough to develop cysts without transplantation. The reasoning behind this aim was that as the gene mutated in the nephropathy ARPKD, which presents with hepatic involvement in ~45% of cases, *PKHD1* is a candidate as a possible genetic link between non-syndromic and syndromic BA. Furthermore, the syndromic form of BA displays anomalies of situs determination, a feature common to the ciliopathies. Epithelial cells taken from the biliary tract of ARPKD patients lack fibrocystin staining, and primary cilia appear stunted. The identification of renal cysts in isolated BA led to the hypothesis that as a ciliary protein, fibrocystin and its encoding gene, *PKHD1*, are feasible candidates in the pathogenesis of BA.

As previously discussed, *PKHD1* is a large gene comprised of a minimum of 86 exons, with the longest open reading frame of fibrocystin containing a 67 exon transcript. It is mainly for this reason the mutational screening for this project was carried out by the Harris group. The primer design and optimisation necessary to screen a gene of this size is a considerable undertaking, and would be costly and time-consuming. Recruitment of a suitable pool of control samples would also have been extremely difficult to obtain.

Mutations in *PKHD1* associated with ARPKD have a carrier frequency of 1:70 [Bergmann et al., 2004; Zerres et al., 1998a; Zerres et al., 1998b], with ten case subjects in this project, a pool of at least 700 control samples would be needed in order to ensure any findings within a case sample was not coincidental. As project collaborators, the Harris group (Mayo Clinic, MN,

USA) have a long-standing *PKHD1* screening protocol in place with designed and optimised primers, access to a large pool of control DNA from both normal and ARPKD patients, and are collaborators in the Mutation Database Autosomal Recessive Polycystic Kidney Disease (<http://www.humgen.rwth-aachen.de/>). This allowed for quicker, and more accurate screening of the ten patients included in the initial screen, fully analysed data was received back from the Harris group for interpretation.

The identification of three sequence variants in patient 10 and two of their unaffected family members cannot be dismissed as purely coincidental, especially as none of these variants were found in any of the other controls. Furthermore, *PKHD1* displays complex patterns of splicing, which may contribute to the observed allelic heterogeneity observed in both animal models and patients with ARPKD. As described by Bergmann *et al* [2005b], who observed ARPKD patients with one or no detectable mutations in the longest ORF of *PKHD1*. In such cases mutations were found in alternatively spliced exons. Interestingly, the changes found in the alternatively spliced regions of the *PKHD1* gene are also observed in normal control samples [Bergmann *et al.*, 2005b]. Therefore, before the changes observed in patient 10 of this study can be classed as pathogenic mutations, or non-pathogenic polymorphisms, all 86 exons of the *PKHD1* gene would need to be screened to determine if any pathogenic mutations are present. Furthermore, the potential impact of these sequence variants would have to await the definition of transcripts containing alternative exons and their predicted reading frames.

As *PKHD1* is such a large gene the occurrence of pleiotropy is a possibility, such that mutations within different regions of the gene could result in similar or completely different phenotypic traits, a characteristic shared by a number of the genes involved in the ciliopathies [Hildebrandt and Zhou, 2007]. Features of BA such as hepatic cysts, fibrosis, ductular proliferation, and/or ductal plate malformation are all pleiotropic phenotypes common to the ciliopathies. Evidence of such a phenomenon in relation to *PKHD1* comes from the *ex40* mouse model [Moser et al., 2005], which expresses a modified *Pkhd1* transcript in which exon 40 is skipped. The *ex40* mouse develops severe malformations of the IHBDs, with progressive portal fibrosis and portal hypertension. However, in contrast to ARPKD patients, the *ex40* mouse develops morphologically and functionally normal kidneys [Moser et al., 2005]. The authors of this paper put this unexpected result down to a functionally divergent role for fibrocystin in the kidneys and liver, thus genetic pleiotropy could account for the observed phenotype. Therefore, such a phenomenon should also be considered for *PKHD1* in relation to BA.

Alternatively, the “second-hit” that may differentiate patient 10 from their unaffected family members may be located within another gene. While some diseases such as cystic fibrosis, α 1-antitrypsin deficiency, and phenylketonuria, are caused by mutations in a single gene loci inherited in a Mendelian fashion [Stickel and Osterreicher, 2006], a number of the ciliopathies and other liver diseases are polygenic, and could be classified as a “complex trait” [Beales, 2005; Czaja and Donaldson, 2000; Invernizzi and Mackay, 2008; Knisely, 2003; Zaghloul and Katsanis, 2009]. Indeed, studies suggest that ciliopathy associated genes have

the capacity to contribute pathogenic alleles to multiple ciliopathies [Zaghloul and Katsanis, 2009].

In genetics “complex traits” are defined as those where the mode of inheritance is unknown, that is: where a Mendelian autosomal dominant, autosomal recessive, or sex-linked pattern of inheritance attributable to a single gene locus does not apply [Donaldson, 2004]. Indeed, if “complex traits” were also defined as a disorder in which: “one or more genes acting alone or in concert increase or reduce the risk of that trait” [Haines and Pericak-Vance, 1998], such a definition would allow for all the possibilities (oligogenic, polygenic, and multifactorial) and covers two essential details. Firstly, genetic variation (mutations or polymorphisms) result in differences in the risk of disease, the mutations themselves do not confer disease. Secondly, the term ‘trait’ may refer to either the disease itself, a group of related diseases (syndrome), or to a particular clinical sub-group within a disease, such disease causing mutations may not only determine which diseases individuals develop, but also the clinical severity of the resulting disease [Donaldson, 2004].

As BA appears in several clinical forms, acquired, embryonic, and syndromic, this does suggest the disease is a common end-point to a number of primary diseases/disorders. If this is indeed the case, mutations in a number of genes that result in BA as a disease trait, or a BA type phenotype must be considered as candidates for mutational screening to identify genes that contribute to the phenotype. Considerable efforts would be required to determine the role of a single gene or group of genes, since their effect on disease manifestations are usually smaller

than crucial gene defects in monogenic disorders, but may also be masked/modified by other variants within the genome. In such cases, genetically modified animals are valuable tools in the analysis of disease-specific gene loci, by using knockout animal models, deficient for the gene of interest. In humans the detection of disease modulating genes is more difficult and challenging, as proven in this case. Currently, three different approaches can be applied to the identification of the genes responsible for 'complex trait' disorders: family-based linkage analysis, candidate gene association case-control studies, and genome-wide polymorphism studies. Family-based analysis, which requires large multiplex families, and genome-wide polymorphism studies are both time-consuming and expensive to undertake. In the absence of the appropriate families in which to use linkage-based approaches to study the genetic basis of complex disorders such as BA, the candidate gene approach is more commonly used. Therefore a multistage candidate gene association study was deemed more appropriate for this project as sample sizes were severely restricted, and it would uncover any possible associations between BA with cysts and *PKHD1* mutations relatively quickly [Hirschhorn and Daly, 2005]. Case-control association analysis has the advantage of taking into account sporadic (non-familial) cases and can provided the study groups are large enough, produce very powerful results. It is also a viable and informative option for the study of genes in diseases with a small heritable component. The major disadvantage of this approach compared with linkage analysis is that an association does not necessarily imply a primary relationship between the polymorphism and disease, but may be due to linkage disequilibrium between the polymorphism and disease causing mutation elsewhere in the same gene or a neighbouring gene [Donaldson, 2004]. In order to carry out a successful genetic case-control association study several important design points must be adhered to stringently, these are: careful

selection of the candidate gene, consideration of functional implications of genetic or splice variants, careful selection and stratification of cases and controls, and careful data analysis both before and after the study [Stickel and Osterreicher, 2006]. As the majority of these vital design points were not even considered during the design and application of this project, the reliability of the data produced by this study is non-existent. All that can be solidly concluded is that sequence variants were identified.

The selection of a candidate gene for an association study is usually based on biological plausibility, in that the gene chosen could play a putative role in the pathogenesis of the studied disease [Day, 2003]. The selection of a single candidate gene in terms of BA is challenging, especially when the possibility of the disorder being a ciliopathy is considered. The ciliopathies show a high degree of phenotypic pleiotropy, with many disorders sharing identical or similar phenotypes. In the case of BA with renal cysts, a number of disorders display significant hepatic involvement in association with renal cysts, however as previously explained the significant level of hepatic involvement in cases of the monogenic disease ARPKD made *PKHD1* an ideal first candidate for screening.

Another important task in genotype-phenotype association studies is the selection of appropriate cases and controls, another area where this project fails. A suitable recruitment strategy is required, and should control for potential confounders of an association such as age and gender. Specifically in the case of BA, an important confounder that had to be considered was if the patients selected had acquired, or syndromic BA. This approach is required to avoid

a confounding effect by population stratification due to a marked variation of the allele frequency of certain genes among subgroups with a different baseline risk for the disease [Cardon and Palmer, 2003]. Thus, both cases and controls need to be well characterised. In terms of the cases selected for the first stage of the mutational analysis of this project, the observation of renal cysts in patients with BA in a single transplantation centre could be argued to have been caused by selective bias. However, the observation of renal cysts in BA patients at independent centres suggests the association is feasible [Calvo-Garcia et al., 2008; Franchi-Abella et al., 2007]. The inclusion of a proportionate number of control subjects is equally important. This was not carefully factored into this study. Control subjects were not matched carefully for age or gender. Control subjects that were included in this study were from an extensive database maintained by the Harris group. Therefore the details of the control subjects were not made available. Control subjects did include normal individuals and ARPKD patients. Only data from the two unaffected family members of patient 10 was supplied. Upon finding the three changes in both family members, extension of the study was deemed inappropriate, as these results were not informative. Although none of the sequence variants detected were found in the control samples, with a carrier frequency of 1 in 70 [Bergmann et al., 2004; Zerres et al., 1998a; Zerres et al., 1998b], it is unlikely these findings are purely coincidental, nonetheless significantly more work would need to be done to prove this. However, limited subject samples also meant continuation of *PKHD1* mutational analysis had to be suspended.

Statistical issues have become increasingly complex in genetic studies, particularly statistical power. This is important as it reflects the probability that a statistically significant effect is

demonstrated when it really exists. In “under-powered” studies both a type I, or a type II error may occur. Type I errors refer to false-positive associations frequently seen in studies with low sample sizes, whereas type II errors represent false negative findings that may result from insufficient patient characterisation or population stratification [Stickel and Osterreicher, 2006]. Recently, a sample size of ≥ 150 has been defined as a critical threshold for the replication validity of genetic association studies [Ioannidis et al., 2001]. If taken into account, large numbers of carefully selected and stratified patients, and age and gender matched controls are necessary to give a study sufficient power to detect a significant effect [Cardon and Palmer, 2003]. Thus, the greatest shortcoming of this project was the woefully small sample size, an unavoidable hindrance of a retrospective study. Despite BA being the most common cause of hepatic transplantation in children, the disease is relatively rare within the general population [Chardot et al., 1999; Fischler et al., 2002; McKiernan et al., 2000; Yoon et al., 1997]. Therefore, when cases are stratified into groups of specific associated anomalies, numbers become even more restricted. Furthermore, when patient selection is limited to a single institution, restricted resources further compounded this problem. Consequently, a true association could have been missed due to insufficient sample size. The advantage of the multi-stage approach however, is that upon detection of an allelic variant associated with the phenotype of BA with renal cysts in the initial screen, an extended association study targeting the identified allelic variant would be cheaper and easier than complete resequencing of the entire *PKHD1* gene in all samples [Hirschhorn and Daly, 2005].

The immunohistochemical aspect of this project has demonstrated a statistically significant alteration in the expression levels of both acetylated α -tubulin and fibrocystin in bile ducts from a cohort of inflammatory and non-inflammatory liver diseases. Although most of the cases studied were those of adult end-stage liver diseases at the point of orthotopic transplantation, examination of biopsy specimens from early stage BA determined this alteration to be a consequence of disease progression rather than causative. This suggests that BA could not be caused by mutations in *PKHDI* alone. However, what must be considered is that it is difficult to draw any solid conclusion with the small number of Kasai biopsy samples examined. The reason for this is quite simply that such samples are very scarce, and therefore a limited resource. Human tissue is in general a precious resource, making it difficult to obtain a high number of cases, but when parameters such as early-stage BA Kasai biopsy samples with identifiable portal tracts are also applied, the supply becomes even more restricted. Often such biopsy samples are needle biopsies, or very small wedge biopsies taken for diagnostic purposes, therefore priority for use in studies such as this is not high. This being said, despite the small number of Kasai specimens examined it is clear that absence of fibrocystin in end-stage BA is due to a gradual loss of expression. The exact reason for this is not clear at this point, and can only be speculated upon. The most feasible explanation, which encompasses the decrease in fibrocystin in all end-stage diseases studied, is that stressed cells have an altered protein expression, with the levels of proteins that are not vital to cellular survival being reduced. Therefore, disease process that results in an altered cellular state appear to result in a loss of fibrocystin expression. Although the positive biliary epithelial cell marker, human epithelial antigen 125 (HEA125), was not used throughout the study,

inclusion of a more extensive panel of BEC markers, such as cytokeratin 19 (CK19) would have aided further identification of cells that had altered protein expression profiles.

Whilst using an expanded panel of BEC specific markers would have helped further characterise the exact state these cells were in, extensive study of BEC from the diseases in the cohort by the BCLR had revealed these cells do maintain their basic differentiated biliary epithelial cell phenotype (personal communication). Furthermore, work by the BCLR has also shown that BEC isolated from livers in this cohort of diseases are fully differentiated, displaying the BEC specific markers HEA125, CK18, and CK19, which allow for the immunological isolation and *in vitro* primary culture of these cells using the BEC specific marker HEA125. These HEA125 positive BEC have also been shown to only lose their specific epithelial cell markers after several passages *in vitro* (personal communication).

It is unfortunate that the resolution the tissue was examined at did not allow for the visualisation of primary cilia. The expression of primary cilia is indicative to the state a cell is in, if the cell expresses one under normal conditions, especially in regards to mitosis and polarity, and therefore would have provided yet another useful indicator of the state the cells that have lost fibrocystin expression are in. This would also help identify exactly where fibrocystin was being expressed in positive cells if not on the ciliary axoneme. Unfortunately, despite several attempts, the ability to clearly visualise primary cilia or centrosomes in tissue is extremely difficult within the 5µm tissue sections. Despite the use of confocal microscopy,

images were not clear enough to allow for cilia or centrosomes to be accurately characterised or counted.

The observed increase in α -tubulin acetylation in this project is also a significant observation. The exact cause of which can only be speculated upon at this point. All of the liver diseases included in the cohort display some degree of cholangiocyte activation, the exact nature of this cellular activation is not apparent when taking only the increased levels of α -tubulin acetylation into account. As with the observed decrease in fibrocystin, to uncover the mechanisms resulting in these alterations a more extensive panel of characterised markers would have been valuable. Markers such as proliferation cell nuclear antigen (PCNA), active caspase-3, and single-stranded DNA. Cholangiocytes may proliferate in response to liver injury [M. J. Phillips et al., 1989; Thung, 1990], however, such a response does not immediately correlate with increased levels of α -tubulin acetylation, which is thought to be a marker of stable MT populations. Thus, the inclusion of a marker that could identify cells that are actively proliferating, or undergoing apoptosis would help clarify exactly what state cells with increased levels of α -tubulin acetylation are in. This would help determine how cell state correlates to the changes in fibrocystin and acetylated α -tubulin expression.

As with all retrospective studies, there are limitations. As human tissue is a scarce resource, normal tissue especially, for each disease group included in the cohort there was no comparison with an age and gender matched group of normal samples, although the normal samples used did cover a range of ages. Another limitation is the samples of some diseases are

more abundant than others, due to incidence within the population. Thus, a set number of samples had to be decided upon for each disease group before commencement of the study that would ensure equal numbers of specimens to be examined for each disease group included. The difficulty in this was that in certain disorders or specimen types the number of identifiable portal tracts, ducts, and ductular structures varied widely. It is generally accepted that it is necessary to have an aggregate of twenty portal tracts to assess the number of bile ducts adequately in an individual patient [Ludwig et al., 1987]. Unfortunately, as some samples were needle biopsies, or displaying significant levels of ductopenia and portal fibrosis, not all specimens from individual patients had enough portal tracts to apply this criterion. In order to ensure a more uniform number of ducts had been counted for each disease group, the level of duct loss and the size of specimen should have been taken into account, allowing for a more uniform comparison between the groups. To overcome this, data was expressed and analysed as a percentage of the total number of ducts observed per disease group.

Another area the scarcity of human tissue impacted was the inclusion of a larger panel of paediatric tissue, which is very difficult to gain access to for research. Comparison of BA to a cohort of adult end-stage liver diseases is not an accurate way to observe alterations in protein expression in paediatric disease. At different stages of development, the adult and paediatric liver will inevitably react differently to identical insults. Thus, in order to better understand how expression of fibrocystin is altered in paediatric liver diseases such as BA a larger cohort of paediatric liver tissue should have also been included in this study. Tissue from patients with diseases such as Wilson's disease, autoimmune hepatitis, cystic fibrosis liver disease, and Tyrosinaemia has been shown to retain fibrocystin expression (personal communication).

Although this does suggest fibrocystin is expressed in these conditions, and is not a general marker of bile duct damage, the samples were taken from livers that were not at such an advanced stage of liver damage compared to the BA cohort. Furthermore, the number of samples examined was extremely limited. Therefore the examination of fibrocystin in paediatric liver disease requires further investigation with expansion of sample numbers and aetiology.

Studies carried out in the *Pkhd1^{del2/del2}* mouse model of ARPKD were designed specifically for functional characterisation of fibrocystin in relation to tubular epithelial cell differentiation and injury. The ideal way to do this, in relation to liver disease, would be to use RNAi technology in human cell lines or primary cultures. Unfortunately, despite several attempts to set-up and optimise such a system this proved unfeasible for a number of reasons. Thus, the direction of the investigation was altered slightly to focus on the *Pkhd1* knockdown model, the *Pkhd1^{del2/del2}* mouse [Woollard et al., 2007]. However, by moving into the mouse the technical difficulties and high variability of yield when isolating murine BEC made working with primary BEC from this model impractical. It was more feasible to work with a cell type equally affected in the mouse model that was easier to obtain. As the isolation and culture of murine PTCs is published, and the proximal tubular segment of the nephron is the most significantly affected in the *Del2* model, primary PTCs were the most practical cells to use for the investigation. Although BEC and PTCs are derived from different embryonic origins, endoderm and mesoderm respectively, they are comparable as epithelial cells that are required to form and maintain a tubular structure that is vital to the function of the organ. Despite originating from different embryonic origins, both the endoderm and mesoderm give rise to

epithelial cells with similar characteristics, for example the multiciliated cells of the reproductive tract arise from the mesoderm, while the multiciliated cells of the respiratory tract originate from the endoderm, both of which are completely affected in disorders such as primary ciliary dyskinesia, or cystic fibrosis. Thus, the use of PTCs should be relatively comparable to BEC in terms of the basic functional roles of fibrocystin, in a monociliated tubular epithelial cell.

However, a major drawback of the *Del2* model is that the actual level of fibrocystin knockdown could not be assayed for at the protein level. As this is a mouse model the production of highly specific monoclonal antibodies raised against fibrocystin is extremely difficult, as those raised in mice would cross-react at an unacceptable level. Although monoclonal antibodies raised in rabbits are starting to become widely available, there are none readily available to murine fibrocystin. Attempts to detect fibrocystin in control samples using several polyclonal antibodies were unsuccessful [Woollard et al., 2007]. Therefore it is uncertain if fibrocystin is completely knocked out in this animal model. It is clear in this model that the removal of the first coding exon has resulted in altered expression of fibrocystin as the model displays the hepatic and renal cystic disease of ARPKD. However, the fact the renal disease remains limited to the proximal tubules, and does not evolve to include the collecting ducts, as is evident in patients with ARPKD [Torres and Harris, 2005], does suggest the effect of removing exon 2 from the murine transcript is different to the effects caused by the mutations affecting *PKHD1* in human ARPKD patients. However this does not make the *Del2* model any less valuable as a tool to help unravel the mechanisms

underlying abnormal tubular morphology. Indeed, this was another reason the *Del2* model was used for this study.

The results obtained from investigations carried out in the *Del2* mouse model demonstrated not only that centrosomal overduplication is one of the mechanisms involved in tubular dilatation, but also that this mechanism displays a sensitivity to E2. The methodology used to obtain these findings did have several limitations. One very obvious problem was that the basal level of centrosomal amplification observed in control samples from both wt and *Del2* animals were very high, much higher than normally accepted. However, because addition of E2 resulted in a statistically significant increase in the levels of centrosomal amplification in a large number of samples this can be taken as a true result. Clearly such a high level of basal centrosomal amplification is not desirable and would need to be improved upon to make the data much stronger. The high basal levels of centrosomal overduplication could also mask any subtle differences in the level of centrosomal amplification caused by other factors, especially the knockdown of *PKHDI*. A number of factors could have resulted in this raised basal level of cells displaying more than two centrosomes in control samples, such as 'culture shock' as previously discussed in chapter 6. There are a number of ways in which this could be addressed, and are currently under investigation by the Harris group. A way to avoid culture shock induced centrosomal amplification would be to introduce E2 *in vivo*. This method is already being trialled at the Mayo Clinic by Dr Ward. The numbers of centrosomes within epithelial cells from both the liver and kidneys could then be examined using electron microscopy of tissue sections, or fluorescence microscopy of isolated tubular units, removing the need to culture the cells at all. Such methods are of course expensive and time consuming,

and would require specific ethical approval. Another method would be to simply count a higher number of cells in each sample, and include a higher number of animals in the study. This would increase statistical power, decreasing the possibility of type I or type II errors, and would also increase the likelihood of more subtle differences becoming more significant. The use of cell lines or RNAi would not be a suitable solution to the effect of culture shock. Cell lines, as previously described, are derived by colonial expansion of cells that have dedifferentiated or become altered in order to survive *in vitro* culture, thus they often display genomic abnormalities, and may also have altered numbers of centrosomes. The use of RNAi to abrogate *Pkhd1* expression in either a murine cell line or primary cells would also introduce yet another traumatic factor to the experiment. Although any such detrimental effects could be controlled for, there is always the selective pressure of *in vitro* culture.

Despite these obvious drawbacks it is clear from this work, and many other studies looking at the role of centrosomal overduplication in cancer and other proliferative disorders, that centrosomal amplification is a complex pathologic mechanism. Not only does it appear to link cytogenesis and tumorigenesis, but it may also play a role in more subtle epithelial hyperproliferative pathologies, such as the ductular proliferation observed in a number of cholangiopathies, or the pseudotumors associated with long-standing BA patients [Liu et al., 2007]. Furthermore, the observation of renal cysts in the small subset of BA patients included in this project provides further support for a possible link to centrosomal amplification. What differentiates these pathologies and results in the differences in severity is most likely disease specific and also governed by the gene or genes mutated in the disorder. Before such

factors can be determined, the exact point at which centrosomal overduplication occurs in the disease process would need to be clarified.

The relevance of the *Del2* studies to BA can also be found in the slight female predominance of the disorder [Lipsett et al., 1997]. This preponderance has been attributed to a dysregulation in autoimmunity, however it could also be the result of the mitogenic effects of E2 on epithelial proliferation. Of course this would have to be further investigated in specific relation to BA. Although true mouse models of BA do not exist as yet, the effect of E2 on disease progression in even the infectious models of BA or the *inv* mouse could provide further insight into the possible mechanisms that result in the complex pathology of BA and its many sub-types.

Despite the difficulties of visualising primary cilia and centrosomes in tissue sections it is not impossible, but would require the use of electron microscopy. Difficulties in getting primary BEC to express primary cilia *in vitro* would not necessarily prevent the study of centrosome numbers and nuclear morphology in these cells. Comparison of age and gender grouped tissue may also uncover interesting morphological differences, all of which would unravel the complex aetiopathology of BA.

To summarise, mutational screening of *PKHD1* in a cohort of BA with renal cysts has revealed *PKHD1* is unlikely to be directly involved in the pathogenesis of BA. A genetic

susceptibility may be identified in all children with BA, although a specific genetic mutation is more likely in those with the embryonal type BA. Absence of fibrocystin in end-stage BA was determined to not be specific to BA, but a non-specific marker of bile duct damage in a cohort of adult end-stage liver diseases. This coupled with increased acetylation of α -tubulin indicates the biliary epithelium may respond to insults in a similar way across a spectrum of disorders. Finally, investigation of the mechanism that drives abnormal tubular epithelial proliferation in the ciliopathies indicates centrosomal amplification with ciliary involvement may play a role in abnormal tubular development.

In conclusion, the ciliary protein fibrocystin and its encoding gene *PKHD1* do not appear to be directly involved in the pathogenesis of BA with or without cysts. However, the novel hypothesis that primary cilia are implicated in the pathogenesis of BA will enable further exploration of those genes involved in ciliary development and laterality [Fliegauf et al., 2007].

CHAPTER 8 FUTURE DIRECTIONS

The individual investigations that make up this project all aim towards further understanding the pathogenesis of BA, looking at *PKHD1* and its encoding protein fibrocystin for clues. However, in doing so this work has raised more questions than it has answered. In terms of meeting the main aim of this project, it is clear *PKHD1* is associated with a variety of phenotypic features in both man and mouse, all of which appear to be related to primary ciliary function, cellular polarity, and cellular proliferation. However, many questions remain to be answered in order to gain a full understanding of the role of *PKHD1* and fibrocystin in hepatic and renal disease.

In terms of a genetic basis for BA, mutational analysis of *PKHD1* was unable to uncover categorical evidence of pathological mutations leaving a key question remaining: which or what gene(s) are mutated in cases of BA? Although this project has no evidence of a link between BA and *PKHD1*, it does not provide enough evidence to inevitably rule it out as a susceptibility gene, and so more work would be required to do this.

In order to expand further upon the findings of the mutational analysis carried out in this project. A number of approaches can be used. To increase the power of a case-control association study, mutation screening could be extended to a larger cohort of patients, carefully stratified on the basis of a number of criteria (principally, the disease classification, presence of associated congenital malformations, and histology of the biliary remnant). By

carefully subdividing a large cohort into smaller groups with shared features, it may increase the chances of finding a positive association. To further increase the chances of a positive association the whole *PKHD1* gene would need to be sequenced covering all splice alternatives, the promoter region, and the 3' untranslated region. As with the ARPKD cases described by Bergmann *et al* [Bergmann et al., 2005b], sequence variants associated with BA may be located within alternatively spliced or untranslated regions. Increasing the size of the cohort substantially would of course require multicentre co-operation in order to obtain a large number of samples. By increasing the number of cases in a single investigation unexpected patterns of association could arise, providing further support for a genetic link. Familial cases may become apparent as more case data is compiled, which may allow for the use of linkage analysis.

Once any sequence variants had been identified their exact impact on gene expression or protein function would help determine the significance of the variant. A large number of novel missense mutations and a significant level of polymorphisms have been found in *PKHD1* [Harris and Rossetti, 2004], differentiating pathogenic mutations from neutral changes can be difficult [Rossetti et al., 2003]. Variants described as mutations in one study can be described as polymorphisms in others [Furu et al., 2003; Onuchic et al., 2002; Rossetti et al., 2003]. Segregation analysis in larger (especially multiplex) families, the nature of the substitution (and conservation of the base in other species), plus prevalence in the normal population can be used to try to differentiate mutations and polymorphisms. However, these methods cannot prove the significance of a change, in recessive disease mutations will be found in the normal population, although given the number of different mutations and

prevalence of carriers (\sim 1:70 individuals [Zerres et al., 1998a]), each change would be expected to be rare. Indeed, it is possible that some rare “polymorphisms” may be mutagenic when found in combination with other sequence variants [Harris and Rossetti, 2004]. To further characterise how individual sequence variants alter protein expression, and/or localisation, techniques such as site-directed mutagenesis could be used to create mRNA containing the introduced changes, which could then be cloned into cells, and the expression patterns observed.

Another area that would need to be investigated to further the work carried out here would be to screen several other genes that encode cystoproteins involved in disorders that share features with BA. Suitable candidates would include *INVS*, *NPHP3*, and *JAG1*, genes mutated in nephronophthisis 2, nephronophthisis 3, and Alagille syndrome, respectively. To expand even further on this, as BA with anomalies of laterality may be a more suitable candidate for a major gene mutation than the nonsyndromic form [Carmi et al., 1993; D-Y. Zhang et al., 2004a], stringent categorisation of BA sub-types may allow for a comparative genome-wide scan, much like that carried out by Zhang et al [2004a], who performed a comparative genome-wide expression analysis comparing expression of regulatory genes in embryonic and perinatal forms of BA. A similar approach using a SNP chip may identify marker clusters in certain subgroups, providing clues to possible genotype-phenotype associations. If actual sequence variants could not be identified, haplotype association may provide a rudimentary screening protocol to aid early diagnosis of BA [Guay-Woodford et al., 1995; Sharp et al., 2008].

As the investigative field of primary human BEC is still very much in its infancy a lot of basic experimental techniques need to be established in order to address the many questions that need to be answered in terms of liver diseases such as BA. Especially as no suitable human cholangiocyte cell lines exist to perform such work in. The establishment of RNAi in primary BEC would be an invaluable tool in future investigations of BA and other liver diseases. There are however many areas that can be further investigated without the use of RNAi that could still provide a huge amount of valuable information about the pathological mechanisms that cause the phenotype observed. Unfortunately there are a number of other obstacles that would need to be overcome. One of the main factors affecting this area of study is the expression of primary cilia *in vitro*. If a culture system could be established in which isolated BEC expressed primary cilia there are a number of ways this could be exploited. At the most basic level cells could be isolated from a variety of liver diseases and their morphology directly compared to that of normal cells, to determine if any gross abnormalities in ciliary morphology or centrosome numbers could provide clues to the pathological mechanisms underlying the disease. Techniques such as the isolation of enriched ciliary fractions, as described by Huang et al [2006], could also be utilised to compare the proteomes of cilia isolated from BEC taken from normal and affected livers. Such a comparison may reveal dysregulation in the expression of proteins key to ciliary structure, development, and/or function, providing strong candidates for mutational screening.

Establishment of a 3D culture system using primary BEC would also be a valuable tool in the investigation of biliary tubulogenesis. Cells isolated from the livers of patients with BA and other liver diseases could be compared to BEC from normal livers to determine if the cells

from affected livers display altered growth characteristics, or if they are able to form tubules in culture. BEC would also be more likely to express primary cilia if grown in a 3D culture system, where they would be able to better maintain an apical-basolateral orientation more akin to the *in vivo* environment. This would provide another system in which the primary cilia of these cells could be characterised, to determine if they are abnormal in the different sub-groups of BA.

The effect of mechanical bending of BEC primary cilia should also be investigated, by subjecting isolated cells or isolated ductular units to fluid shear stress in a perfusion chamber. Measurement of changes to intracellular calcium levels would provide evidence of any response to mechanical stimulation. This system could be employed to compare the mechanosensory response of cilia from normal and affected livers. RNAi methodology could also be combined with this system to determine the effect knockdown of *PKHDI* might have on mechanosensation in primary cells.

Another basic experimental technique that would need to be established in primary BEC would be the introduction of inhibitory RNAs, and other molecules into the cells. As primary BEC are highly sensitive to culture conditions, and can easily dedifferentiate under stress, a method to transfect cells whilst causing minimal trauma would be of great value to future research in this area. Once such a method was established, the development of more reliable BEC cell lines for use in investigations such as this would be easier to establish. Current BEC

lines have lost some of the essential features of fully differentiated BEC (investigations carried out at BCLR).

The ability to assay BEC using fluorescent-activated cell sorting (FACS) is also limited. However if a protocol for BEC could be optimised, it would add another valuable tool to help unravel the pathophysiological mechanisms affecting BEC in diseases such as BA.

Once a suitable assortment of basic experimental techniques specific to BEC have been established research in terms of BA could progress more rapidly. As the dysregulation of epithelial cell growth appears to be a key feature in the process of cyst formation and ductular proliferation, with such experimental techniques in place it would be possible to test if the abrogation of fibrocystin expression can cause a defect in cell-cycle regulation. For example, the effect of *PKHDI* knockdown on cell cycle progression could be assayed using FACS analysis to determine if cells become arrested at certain phases of the cell cycle, or if they are able to by-pass any checkpoints that should be activated by the disease process.

The JAK-STAT signalling pathway has been implicated in the function of the polycystins [Boucher and Sandford, 2004], it could therefore be determined if this pathway also mediates signalling by fibrocystin. STATS are latent cytoplasmic transcription factors that translocate to the nucleus after activation by direct phosphorylation by receptor tyrosine kinases. To investigate the involvement of the STAT pathway in any putative signalling by fibrocystin,

decreased levels of tyrosyl- and serine-phosphorylated STATs in cells subjected to RNAi could be assayed. Since fibrocystin lacks a kinase domain, it would most likely be unable to phosphorylate STATs directly, but may do so indirectly by activation of a member of the Janus kinase family of tyrosine kinases (JAKs), thus activation of JAK family members (JAK 1 to 3 or TyK2) could also be tested for.

Progressive bile duct destruction and portal tract fibrosis are hallmark features of BA. This suggests that, in common with many other liver diseases, an inappropriate inflammatory response is perpetuated in BA that may exacerbate the tissue damage caused by the underlying defect. During inflammation it is thought that cholangiocytes can promote an inflammatory response and contribute to their own destruction in a number of ways including: i) promotion of apoptosis via autocrine and paracrine mechanisms; ii) increasing expression of chemokines and adhesion molecules which in turn regulate leukocyte infiltration and activation; iii) during fibrogenesis it is also possible that activated cholangiocytes could modulate fibroblast activity via similar mechanisms resulting in excessive fibrogenic responses that lead to fibrosis and cirrhosis [Adams and Afford, 2005; Ahmed-Choudhury et al., 2003]. The development of primary co-culture systems with cholangiocytes, fibroblasts, macrophages, and cytolytic T cells would provide insight into the exact role cholangiocytes play in this response. Furthermore, by combining RNAi with this system it could be determined whether fibrocystin plays any role in cholangiocyte fibroblast interactions including: i) fibroblast survival and activation modulated via TNF receptor p75 [Oakley et al., 2003]; ii) fibroblast activation including chemokine secretion, adhesion molecule expression and extracellular matrix synthesis; iii) the effects of fibrocystin expression on cholangiocyte survival; these

parameters could be assessed using enzyme-linked immunosorbent assays, cytokine multiplex arrays, and cell survival assays for proliferation and apoptosis.

The most obvious way to expand upon the immunohistochemical studies carried out in this project would be to increase the number of early and late-stage paediatric, and early stage BA samples included. The inclusion of more paediatric cases at various stages of disease would enable a more detailed study of the exact stage of the disease that fibrocystin expression begins to decrease. To fully characterise the exact state of the cholangiocytes throughout the disease process. To examine how the altered hepatic environment affects them, an expanded panel of markers could be used. Markers to determine if the cells maintain their epithelial phenotype or if they are dedifferentiated, such as the epithelial markers cytokeratins 18 and 19, the fibroblast markers smooth muscle actin and T-cell antigen (Thy1), and the endothelial marker platelet-endothelial cell adhesion molecule (CD31). Markers of apoptosis or proliferation would also help identify areas where cell death, or activation are present. By comparing staining between normal and various affected livers, an expression profile characterising the levels of marker expression for different disorders may reveal similarities between disorders thought to be very dissimilar in their aetiology, and provide clues to the disease mechanisms active in diverse disorders that are less well characterised. Utilisation of more sensitive and powerful visualisation techniques such as electron, and confocal microscopy would also enable further characterisation of cellular morphology within tissue from patients, including high-resolution characterisation of ciliary ultrastructure and centrosome numbers.

The mechanisms responsible for the increased levels of α -tubulin acetylation in the different liver diseases included in the cohort remains undetermined at this point. In order to determine what causes this increase a study of the proteins known to be involved in α -tubulin acetylation may shed light in the pathways involved in this increase, and how they relate to the disease process. The levels and localisation of proteins such as the histone deacetylase HDAC6 may provide an explanation of the observed increase in MT acetylation.

The *Del2* mouse model, despite displaying few of the phenotypic characteristics of BA, will remain a valuable resource for the functional study of *Pkhd1* and fibrocystin. Further work to determine the exact levels or domains of fibrocystin still translated, if at all, will enable a more accurate assessment of any genotype-phenotype correlations. Further primary epithelial culture of other cell types, such as BEC may provide a more relevant understanding of the pathological mechanisms underlying liver disease in relation to *Pkhd1* knockdown. Exploration of techniques such as air/liquid interface culture may promote the expression of multi-ciliate cells and enable a more accurate evaluation of the severity of centrosomal overduplication in relation to *Pkhd1* knockdown. By combining such techniques with more sensitive visualisation techniques, such as electron microscopy, would allow for a more comprehensive study of cilia and centrosomal abnormalities in non-cancerous proliferative epithelial disorders that effect tubular structures. Once a greater understanding of such abnormalities is gained this knowledge can be applied to similar disorders to help determine the underlying pathological mechanisms resulting in altered tubule formation.

As BA does appear to present with a slight female preponderance, more in-depth study of the roles of E2, and the oestrogen receptors in BEC under both normal physiological and pathological conditions may provide further understanding of the increased female susceptibility to certain liver disorders. While the addition of E2 to cells in culture was an option explored in the current project, the complication of high basal readings in control samples may have masked more subtle effects on centrosomal overduplication. Thus, the development of a system that introduces high levels of E2 to mice *in vivo* would provide a useful tool to aid understanding of how E2 acts in less obvious target organs.

The aetiology of BA remains an enigma. While this complex disorder provides many clues to the mechanisms underlying its certain characteristic features, there is still no unifying factor to draw upon. The multiple clinical subtypes, lack of any informative familial cases, and lack of any spontaneous or genetic animal models displaying all the clinical features of BA impedes the rate at which progress can be made. In this regard, the more research done to pick apart the mechanisms that cause the characteristics shared between BA and other disorders with known genetic causes may help shed light on the pathogenesis of BA.

In short, it is the very complex nature of this disorder that makes it so difficult to determine its exact cause, but if the approach used to tackle this formidable task broke the disorder down into more stringently categorised subgroups it may just be that the cause of this apparent complexity is because BA is being approached as a single disease entity, not an end-stage phenotype common to multiple disorders.

APPENDIX 1

TABLE 1.1 Disorders associated with the ductal plate malformation. Modified from [Knisely, 2003]

DISORDER	OMIM	GENE OR LOCUS (GENES OR LOCI)	HEPATIC FEATURES	OTHER SIGNIFICANT CLINICAL FEATURES
Jeune asphyxiating thoracic dystrophy	208500 611263	Unknown (15q13) <i>IFT80</i> (3q24-q26)	May have neonatal cholestasis; Caroli's disease; and congenital hepatic fibrosis	Short stature, narrow, long thorax with short ribs; micromelia; skeletal malformations; pulmonary hypoplasia; retinal degeneration; pancreatic cysts and insufficiency; cystic renal tubular dysplasia
Autosomal dominant polycystic kidney disease (ADPKD)	601313 173910 600666	<i>PKD1</i> (16p13.3- p13.12) <i>PKD2</i> (4q21-q23) <i>PKD3</i> (Unknown)	Biliary microhamartomas and cysts; preserved hepatic function; severe hepatic cystic disease with pregnancy and oestrogen therapy	Renal cysts; renal failure; cyst complications (mass effect, haemorrhage, infection, rupture); intracranial aneurysm; hypertension; cardiac abnormalities
Autosomal recessive polycystic kidney disease (ARPKD)	606702	<i>PKHD1</i> (6p21.1- p12)	Biliary microhamartomas and cysts; recurrent cholangitis; congenital hepatic fibrosis; Caroli's disease, and biliary dysgenesis; cirrhosis; portal hypertension	Renal cysts; renal fibrosis; glomerulosclerosis; renal failure; pulmonary hypoplasia
Autosomal dominant polycystic liver disease (ADPLD)	174050 (PCLD) 177060 608648	<i>PRKCSH</i> (19p13.2- p13.1) <i>SEC63</i> (6q21)	Biliary microhamartomas and cysts; severe hepatic cystic disease with pregnancy and oestrogen therapy; cyst complications (mass effect, haemorrhage, infection, rupture), preserved liver function; portal hypertension; portal vein thrombosis; jaundice	Pancreatic cysts; mitral valve prolapse and other mitral valve leaflet abnormalities; cachexia; abdominal distension; abdominal pain; early satiety; fatigue; anorexia/malnutrition; persistent nausea; vomiting; supine dyspnoea; severe ascites; lower body oedema; uterine prolapse due to displacement.

DISORDER	OMIM	GENE OR LOCUS (GENES OR LOCI)	HEPATIC FEATURES	OTHER SIGNIFICANT CLINICAL FEATURES
Caroli's syndrome	600643	Subsumed in <i>PKHD1</i>	Polycystic segmental dilatation of the intrahepatic bile ducts; cyst complications; recurrent cholangitis; liver abscess; hepatomegaly; portal hypertension; cholangiocarcinoma	Associated with polycystic kidney disease
Congenital hepatic fibrosis (CHF)	263200	Subsumed in <i>PKHD1</i> <i>MPI</i> (15q22-qter)	Biliary microhamartomas surrounded by a dense fibrous stroma; portal hypertension; recurrent cholangitis; cholangiocarcinoma;	
Biliary atresia (early severe, 10-20%)	210500	Unknown	Progressive obliteration of the extrahepatic and intrahepatic biliary system; biliary obstruction; cholestasis; conjugated progressive hyperbilirubinemia; hepatic failure	Renal, cardiac, and gastrointestinal malformations (ventricular hypertrophy, intestinal malrotation, preduodenal portal vein); laterality abnormalities

DISORDER	OMIM	GENE OR LOCUS (GENES OR LOCI)	HEPATIC FEATURES	OTHER SIGNIFICANT CLINICAL FEATURES
Bardet-Biedl syndrome	209901 (BBS1)	<i>BBS1</i> (11q13)	Congenital hepatic fibrosis;	Retinal dystrophy; retinitis pigmentosa; obesity; polydactyly; dysmorphic extremities; hypogenitalism; renal cystic dysplasia; renal structural abnormalities; mental retardation; cardiac abnormalities; anosmia; situs inversus
	606151 (BBS2)	<i>BBS2</i> (16q21)		
	608845 (BBS3)	<i>ARL6</i> (3p12-q13)		
	600374 (BBS4)	<i>BBS4</i> (15q22.3)		
	603650 (BBS5)	<i>BBS5</i> (2q31)		
	604896 (BBS6)	<i>MKKS</i> (20p12)		
	607590 (BBS7)	<i>BBS7</i> (4q27)		
	608132 (BBS8)	<i>TTC8</i> (14q32.11)		
	607968 (BBS9)	<i>PTHB1</i> (7p14)		
	610148 (BBS10)	<i>BBS10</i> (12q)		
	602290 (BBS11)	<i>TRIM32</i> (9q33.1)		
	610683 (BBS12)	<i>BBS12</i> (4q27)		
	609883 (BBS13)	<i>MKS1</i> (17q23)		
	610142 (BBS14)	<i>CEP290</i> (12q21.3)		
Joubert syndrome	213300 (JBTS1)	<i>JBTS1</i> (9q34)	Congenital hepatic fibrosis	Retinal dystrophy; renal anomalies (multicystic dysplastic kidneys); dysmorphic extremities; cerebellar vermis hypoplasia and associated neurologic anomalies (hypotonia, developmental delay, hyperpnoea/apnoea); cardiac malformations; dysmorphic facial features
	608091 (JBTS2)	<i>JBTS2</i> (11p12-q13)		
	608629 (JBTS3)	<i>AIH1</i> (6q23.3)		
	609583 (JBTS4)	<i>NPHP1</i> (2q13)		
	610188 (JBTS5)	<i>CEP290</i> (12q21.3)		
	610688 (JBTS6)	<i>MKS3</i> (8q21.13-q22.1)		
	611560 (JBTS7)	<i>RPGRIP1L</i> (16q12.2)		
	612291 (JBTS8)	<i>ARL13B</i> (3q11.2)		
	612285 (JBTS9)	<i>CC2D2A</i> (4p15.3)		

DISORDER	OMIM	GENE OR LOCUS (GENES OR LOCI)	HEPATIC FEATURES	OTHER SIGNIFICANT CLINICAL FEATURES
Meckel-Gruber syndrome	609883 (MKS1)	<i>MKS1</i> (17q23)	Reactive bile duct proliferation; bile duct dilatation; periportal fibrosis; portal vascular obliteration; biliary dysgenesis	Occipital encephalocele; central nervous system abnormalities (e.g. dandy-walker malformation); postaxial polydactyly; polycystic kidneys; gross renal enlargement; cardiac malformations
	603194 (MKS2)	<i>MKS2</i> (11q13)		
	607361 (MKS3)	<i>TMEM67</i> (8q21.13-q22.1)		
	611134 (MKS4)	<i>CEP290</i> (12q21.3)		
	611561 (MKS5)	<i>RPGRIP1L</i> (16q12.2)		
	612284 (MKS6)	<i>CC2D2A</i> (4p15.3)		
Nephronophthisis	256100 (NPHP1)	<i>NPHP1</i> (2q13)	Congenital hepatic fibrosis; cholestasis; portal fibrosis; hepatomegaly; ductal proliferation	Small kidneys; corticomedullary cystic disease; glomerulosclerosis; retinal degeneration and ocular complications; cortical microcysts; cone shaped epiphyses
	602088 (NPHP2)	<i>INVS</i> (9q31)		
	604387 (NPHP3)	<i>NPHP3</i> (3q22)		
	606966 (NPHP4)	<i>NPHP4</i> (1p36)		
	609237 (NPHP5)	<i>IQCB1</i> (3q21.1)		
	610142 (NPHP6)	<i>CEP290</i> (12q21.3)		
	611498 (NPHP7)	<i>GLIS2</i> (16p13.3)		
	610937 (NPHP8)	<i>RPGRIP1L</i> (16q12.2)		
	609799 (NPHP9)	<i>NEK8</i> (17q11.1)		

APPENDIX 2

TABLE 2.1 Raw data table. Fibrocystin staining in human liver tissue cohort.

Sample	Total positive ducts	Percentage of positive cells (%)	Intensity	Cysts	Comments
NL 1	21/33	63.6	++	N/A	Severe steatosis? VMb complex -, nerve bundles +++
NL 2	50/55	90.9	+	N/A	Nerve bundles +++
NL 3	12/34	35.3	++	N/A	
NL 4	16/32	50	++	N/A	
NL 5	45/50	90	++	N/A	
PCLD 1	1/50	2	+	Occ+	
PCLD 2	3/30	10	+	++	Moderate steatosis
PCLD 3	4/45	8.9	+	Occ+	
PCLD 4	10/40	25	+	Occ+	
PCLD 5	33/36	91.7	++	+	VMb complex -
PCLD 6	3/80	3.8	+	+	
PBC 1	3/38	7.9	+	N/A	Nerve bundles +++
PBC 2	1/30	3.3	+	N/A	Nerve bundles +++
PBC 3	1/19	5.3	+	N/A	
PBC 4	0/20	0	-	N/A	
PBC 5	5/23	21.7	+	N/A	
PSC 1	13/61	21.3	+	N/A	Nerve bundles +++
PSC 2	0/41	0	-	N/A	Nerve bundles +++
PSC 3	0/0	0	-	N/A	Very sclerotic ducts
PSC 4	0/38	0	-	N/A	
PSC 5	0/48	0	-	N/A	
AIH 1	3/32	9.4	+	N/A	Nerve bundles +++
AIH 2	8/40	20	+	N/A	Nerve bundles +++
AIH 3	10/36	27.8	+	N/A	
AIH 4	0/0	0	-	N/A	
AIH 5	0/0	0	-	N/A	
ALD 1	13/52	25	+	N/A	Nerve bundles +++
ALD 2	0/0	0	-	N/A	Moderate steatosis
ALD 3	0/0	0	-	N/A	
ALD 4	0/0	0	-	N/A	
ALD 5	0/0	0	-	N/A	
α_1 ATdef.1	0/0	0	-	N/A	Moderate steatosis
α_1 ATdef.2	0/0	0	-	N/A	
α_1 ATdef.3	20/60	33.3	+	N/A	
α_1 ATdef.4	0/0	0	-	N/A	
α_1 ATdef.5	0/0	0	-	N/A	
HCC 1	0/0	0	-	N/A	No positive structures
HCC 2	0/30	0	-	N/A	
HCC 3	0/25	0	-	N/A	Very strong inflammatory cells

Sample	Total positive ducts	Percentage of positive cells (%)	Intensity	Cysts	Comments
HCC 4	23/30	76.7	+ / ++	N/A	Very strong inflammatory cells
HCC 5	6/14	42.9	+	N/A	
HCV 1	5/20	25	+	N/A	Portal vessels very strong
HCV 2	1/50	2	+	N/A	Portal vessels very strong in places
HCV 3	1/100	1	+ / -	N/A	Portal vessels very strong in places
HCV 4	1/50	2	+	N/A	Strong inflammatory cells and vessels in places
HCV 5	0/50	0	-	N/A	Strong inflammatory cells and vessels in places
BA 1	0/50	0	-	N/A	Portal vessels strong on places
BA 2	0/50	0	-	N/A	Portal vessels strong on places
BA 3	0/50	0	-	N/A	Portal vessels strong on places
BA 4	0/50	0	-	N/A	Portal vessels strong on places
BA 5	0/50	0	-	N/A	Portal vessels strong on places
BA 6	0/47	0	-	N/A	
BA 7	0/50	0	-	N/A	
BA 8	0/50	0	-	N/A	
BA 9	0/16	0	-	N/A	
BA 10	0/5	0	-	N/A	
BA 11	0/0	0	-	N/A	

Key: -, no visible staining; +, faint staining on cells; ++, moderate staining on most cells; +++, intense staining on cells; NL, normal liver; PCLD, polycystic liver disease; PBC, primary biliary cirrhosis; PSC, primary sclerosing cholangitis; AIH, autoimmune hepatitis; ALD, alcoholic liver disease; α_1 ATdef, α_1 -antitrypsin deficiency; HCC, hepatocellular carcinoma; HCV, hepatitis C virus; BA, biliary atresia; VMb complex, von Meyenburg complex.

TABLE 2.2 Details of liver diseases included in cohort study

Disease	Disease characteristics and features	Treatment	Reasons for inclusion in the current cohort
Hepatitis C viral infection (HCV)	<ul style="list-style-type: none"> - Mechanisms by which HCV causes chronic and progressive liver disease are not fully understood - HCV-associated liver damage thought to be immune mediated - Disease severity ranges from asymptomatic chronic infection, to cirrhosis and HCC - Morphological features: steatosis, intraportal lymphoid aggregates or follicles, and bile duct lesions 	<ul style="list-style-type: none"> - Liver transplantation in patients with life threatening liver complications of portal hypertension, cirrhosis, HCC, and liver failure 	<ul style="list-style-type: none"> - Epithelial involvement characterised by; lymphocytic infiltration, and epithelial changes (vacuolisation, eosinophilia of the cytoplasm, nuclear hyperchromasia, multilayering, and loss of cellular polarity)
Hepatocellular carcinoma (HCC)	<ul style="list-style-type: none"> - Median survival after diagnosis: 6 to 9 months - Major risk factors: hepatitis B viral infection, chronic HCV infection, prolonged dietary aflatoxin exposure, and cirrhosis - Genetic predisposition underlies both familial and sporadic (acquired) cases - Histological variant forms: combined hepatocellular carcinoma, fibromellar carcinoma, and cholangiocellular carcinoma 	<ul style="list-style-type: none"> - Partial hepatic resection - Total hepatectomy with liver transplantation in patients with poor underlying liver function 	<ul style="list-style-type: none"> - Biliary tract involvement includes: tumour thrombi, hemobilia, tumour compression, diffuse tumour infiltration, jaundice, metastatic lymphadenopathy at the porta hepatis - Association with a number of inflammatory and fibrotic liver diseases - HCC arising from malignant transformation of biliary hamartomas, hepatic lesions related to DPM
Polycystic liver disease (PCLD)	<ul style="list-style-type: none"> - Cyst number and size is often greater in women than in men - An asymptomatic course is common - Liver pathology is indistinguishable between PCLD and ADPKD - Genetically heterogeneous, with only two identified causative loci - Characterised by progressive multiple diffuse cysts forming in the liver parenchyma - Cystic dilatation arises from cellular proliferation and fluid secretion into the cysts 	<ul style="list-style-type: none"> - Surgical intervention for symptomatic PCLD includes: cyst unroofing, extensive fenestration, and fenestration combined with resection - For highly symptomatic patients with diffuse involvement of the liver or those with significant co-morbid condition treatment is limited to transplantation 	<ul style="list-style-type: none"> - Classic cholangiopathy - Distinct form of liver disease without concomitant ADPKD - Histological display of von Meyenburg complexes, and bile duct proliferation - Cystic dilatations known as biliary microhamartomas or von Meyenburg complexes are caused by ductular overgrowth after embryogenesis
α1-antitrypsin deficiency (α₁AT Def.)	<ul style="list-style-type: none"> - Inherited metabolic disorder affecting about 1 in 2000 to 1 in 5000 individuals - Most common genetic cause of neonatal liver disease - α₁AT is a serine protease inhibitor produced in the liver - α₁AT protects lungs against proteolytic damage from neutrophil elastase - Mutations in the coding sequence of α₁AT prevent its export from hepatocytes, where it polymerises into large aggregates, resulting in cell injury and death 	<ul style="list-style-type: none"> - In infants there is no approved treatment for liver disease except transplantation - Rare indication for liver transplantation amongst adults 	<ul style="list-style-type: none"> - Inflammatory cholangiopathy characterised by biliary epithelia cell destruction, inflammatory cell infiltration, and periportal fibrosis - Severe biliary epithelial cell damage, and paucity of intrahepatic bile ducts detected in some infants - Cholestatic presentation is hard to distinguish from other neonatal liver diseases, especially biliary atresia

Disease	Disease characteristics and features	Treatment	Reasons for inclusion in the current cohort
Autoimmune hepatitis (AIH)	<ul style="list-style-type: none"> - Poorly defined necroinflammatory liver disease of unknown aetiology - Major pathological mechanism is thought to be loss of tolerance against host hepatic tissue - Histological hallmarks: dense portal mononuclear cell infiltrate, emperipolesis, piecemeal necrosis, bridging necrosis, panlobular and multilobular necrosis, and cirrhosis 	<ul style="list-style-type: none"> - Immunosuppressive therapy - For cases that progress to cirrhosis and end-stage liver disease, treatment is liver transplantation with concurrent immunosuppression 	<ul style="list-style-type: none"> - Inflammatory biliary involvement found in 30-40% of cases - Biliary lesions consist of, epithelial necrosis, nuclear pyknosis and infiltration by lymphocytes
Alcoholic liver disease (ALD)	<ul style="list-style-type: none"> - Well known aetiology, exact pathogenesis remains unclear - Hepatic injury thought to be immune mediated, combined with free radical hepatic injury - Three recognised forms of ALD: alcoholic fatty liver disease (steatosis), acute alcoholic hepatitis, and alcoholic cirrhosis - Histological features: steatosis, fibrosis, cirrhosis, micronodular cirrhosis, cholestasis, Mallory's hyaline bodies, hepatocellular necrosis, macroregenerative nodules, chronic inflammation, bile duct proliferation, liver cell dysplasia, and HCC 	<ul style="list-style-type: none"> - Liver transplantation for end-stage ALD 	<ul style="list-style-type: none"> - Inflammatory liver disease with ductular involvement - Characterised by well established cirrhosis with abundant ductular proliferation
Primary biliary cirrhosis (PBC)	<ul style="list-style-type: none"> - Organ-specific autoimmune disease of unknown aetiology - Predominantly affects women - Characterised by slow progressive destruction of small intrahepatic bile ducts with portal inflammation, and fibrosis, leading to liver failure - Triad of diagnosis: elevated alkaline phosphatase, antimitochondrial antibodies, and characteristic histological changes - Characteristic histological features are granulomatous cholangitis, or nonsuppurative destructive cholangitis that progresses to cirrhosis 	<ul style="list-style-type: none"> - End-stage liver disease: liver transplantation 	<ul style="list-style-type: none"> - Established immune-mediated cholangiopathy - Characterised by: inflammatory destruction of the intrahepatic bile ducts, lymphocytic portal infiltration, periportal inflammation, ductular proliferation, ductopenia, biliary cirrhosis, and cholestasis
Primary sclerosing cholangitis (PSC)	<ul style="list-style-type: none"> - Rare cholestatic liver disease - Characteristics: chronic inflammation and fibrotic obliteration of the hepatic biliary tree, bile stasis, hepatic fibrosis - Aetiology and pathogenesis is little understood, although immune dysregulation thought to play a key role - Nonspecific histopathology, rarely diagnostic 	<ul style="list-style-type: none"> - No effective pharmacotherapy - End-stage liver disease: resection or transplantation 	<ul style="list-style-type: none"> - Histological involvement of the intrahepatic and extrahepatic bile ducts - Characteristic periductular fibrosis with concentric fibrosis of intrahepatic bile ducts, with stricturing and dilation of the biliary tree

Key: DPM – ductal plate malformation; ADPKD – autosomal dominant polycystic kidney disease.

APPENDIX 3

ONE MONTH OLD WILDTYPE B6 MICE: RAW DATA

TABLE 3.1 Centrosomal count data analysis for one-month-old wt males

Sample: E2 (pg/ml)	% cells with >2 centrosomes: animal 1	% cells with >2 centrosomes: animal 2	% cells with >2 centrosomes: animal 3	% cells with >2 centrosomes: animal 4	Mean % of cells with >2 centrosomes	Standard deviation	p-value*
0	12	17	8	22	15	5.749	
25	33	46	19	29	32	11.488	0.026
75	26	33	21	30	28	5.382	0.008
500	40	35	13	26	29	11.847	0.047

*p-values relative to control (0pg/ml E2). t-test: 1-sided, unequal variance assumed, p<0.05 significance.

TABLE 3.2 Centrosomal count data analysis for one-month-old wt females

Sample: E2 (pg/ml)	% cells with >2 centrosomes: animal 1	% cells with >2 centrosomes: animal 2	% cells with >2 centrosomes: animal 3	% cells with >2 centrosomes: animal 4	Mean % of cells with >2 centrosomes	Standard deviation	p-value*
0	22	9	23	19	18	6.295	
25	14	33	20	22	22	7.956	0.241
75	35	29	33	23	30	4.884	0.014
500	31	34	46	39	38	6.800	0.003

*p-values relative to control (0pg/ml E2). t-test: 1-sided, unequal variance assumed, p<0.05 significance.

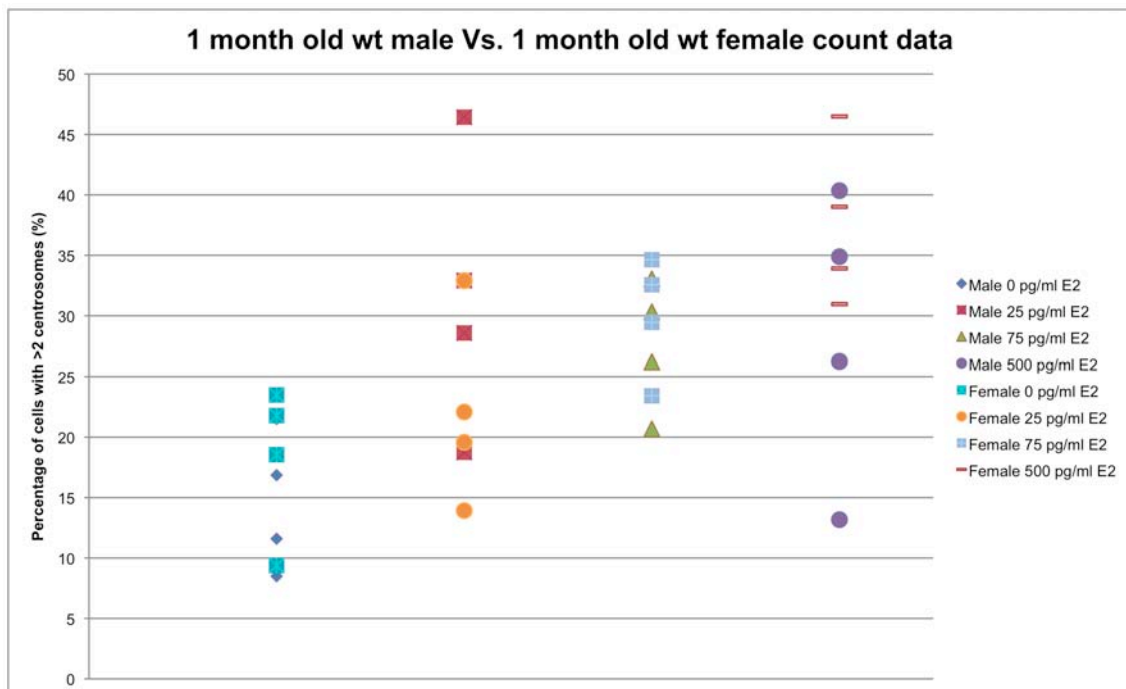


FIGURE 3.1 One-month-old wt: Scatter plot of mean percentage of cells with >2 centrosomes. Chart representation of the lack of significance between centrosomal overduplication between the sexes when treated with the same level of E2. This is illustrated by the fact the points representing each gender overlap at more than one data point at a single level of E2.

TABLE 3.4 Centrosomal count data analysis for one-month-old *Del2* males

Sample: E2 (pg/ml)	% cells with >2 centrosomes: animal 1	% cells with >2 centrosomes: animal 2	% cells with >2 centrosomes: animal 3	% cells with >2 centrosomes: animal 4	Mean % of cells with >2 centrosomes	Standard deviation	p-value*
0	28	18	8	8	14.7	7.986	
25	18	29	18	34	25.6	8.121	0.068
75	20	36	22	24	25.5	7.398	0.048
500	23	26	33	19	25.3	5.752	0.040

*p-values relative to control (0pg/ml E2). t-test: 1-sided, unequal variance assumed, p<0.05 significance.

TABLE 3.5 Centrosomal count data analysis for one-month-old *Del2* females

Sample: E2 (pg/ml)	% cells with >2 centrosomes: animal 1	% cells with >2 centrosomes: animal 2	% cells with >2 centrosomes: animal 3	% cells with >2 centrosomes: animal 4	Mean % of cells with >2 centrosomes	Standard deviation	p-value*
0	4	18	19	12	13	7.054	
25	5	36	16	23	20	13.095	0.199
75	20	25	33	36	28	7.233	0.011
500	20	35	44	31	33	9.703	0.010

*p-values relative to control (0pg/ml E2). t-test: 1-sided, unequal variance assumed, p<0.05 significance.

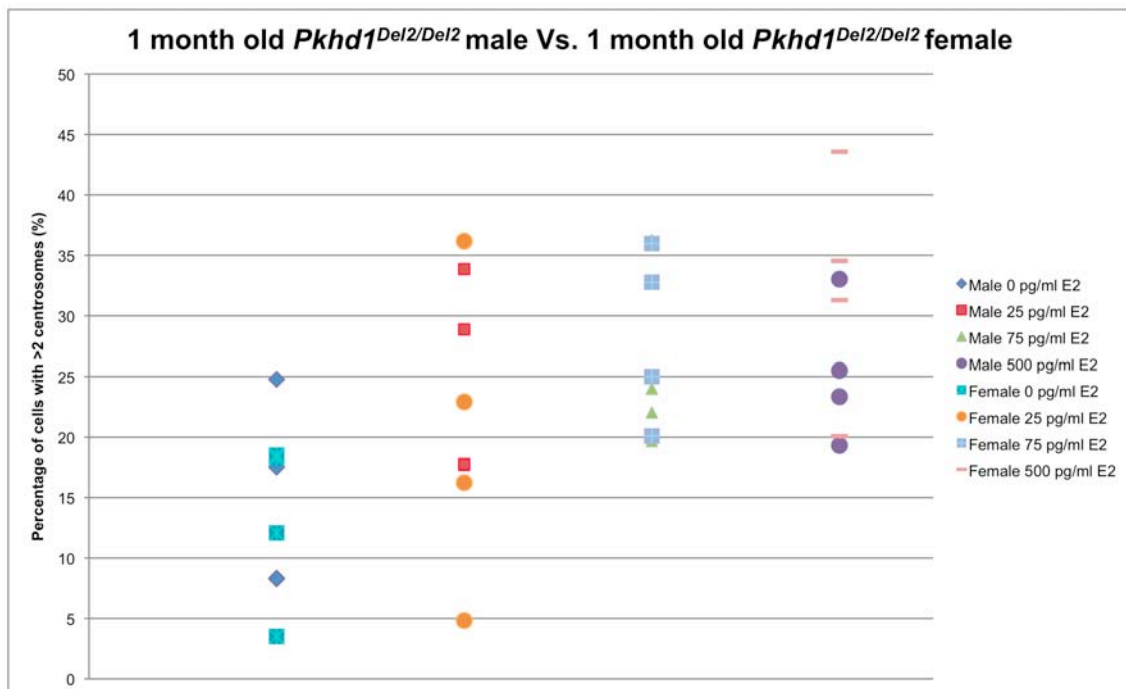


FIGURE 3.2 One-month-old *Del2*: Scatter plot of mean percentage of cells with >2 centrosomes. Chart representation of the lack of significance between centrosomal overduplication between the sexes when treated with the same level of E2. This is illustrated by the fact the points representing each gender overlap at more than one data point at any given level of E2.

THREE MONTH OLD WILDTYPE B6 MICE: RAW DATA

TABLE 3.7 Centrosomal count data analysis for three-month-old wt males

Sample: E2 (pg/ml)	% cells with >2 centrosomes: animal 1	% cells with >2 centrosomes: animal 2	% cells with >2 centrosomes: animal 3	Mean % of cells with >2 centrosomes	Standard deviation	p-value*
0	12	29	13	18.2	9.543	
25	39	49	20	36.1	14.938	0.084
75	44	57	37	46.1	5.823	0.013
500	46	53	35	43.3	5.296	0.015

*p-values relative to control (0pg/ml E2). t-test: 1-sided, unequal variance assumed, p<0.05 significance.

TABLE 3.8 Centrosomal count data analysis for three-month-old wt females

Sample: E2 (pg/ml)	% cells with >2 centrosomes: animal 1	% cells with >2 centrosomes: animal 2	% cells with >2 centrosomes: animal 3	Mean % of cells with >2 centrosomes	Standard deviation	p-value*
0	14	29	17	20.2	8.133	
25	23	22	26	23.6	2.043	0.276
75	32	34	38	34.6	3.444	0.038
500	48	49	36	44.2	7.092	0.010

*p-values relative to control (0pg/ml E2). t-test: 1-sided, unequal variance assumed, p<0.05 significance.

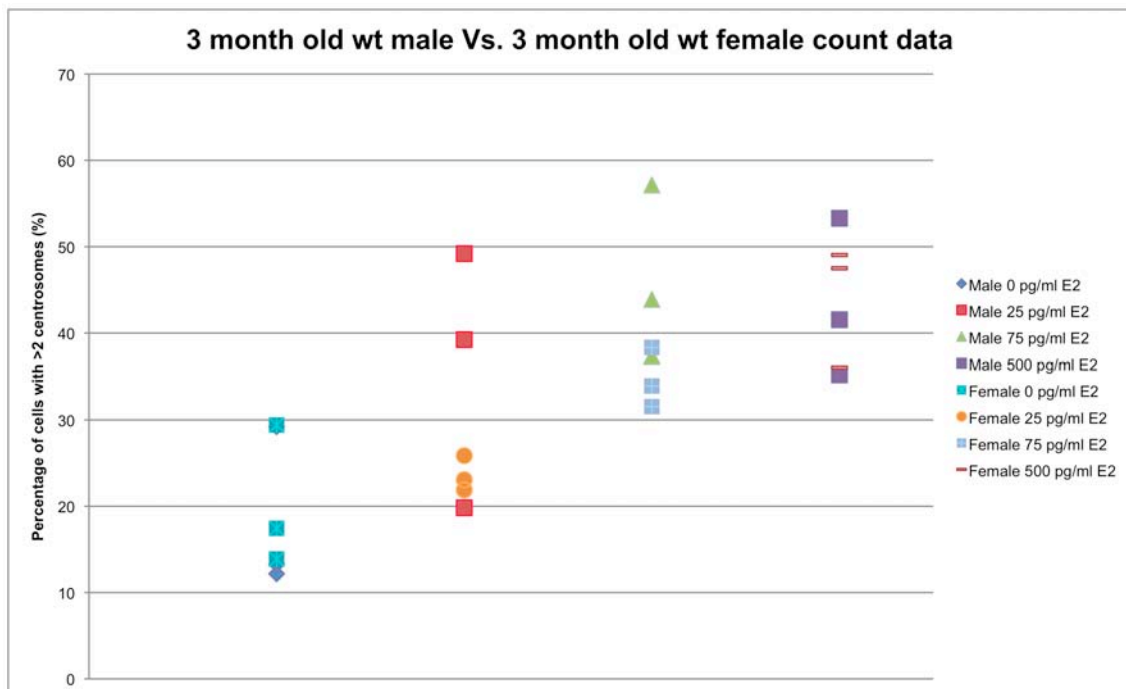


FIGURE 3.3 Three-month-old wt: Scatter plot of mean percentage of cells with >2 centrosomes. Chart representation of the lack of significance between centrosomal overduplication between the sexes when treated with the same level of E2. This is illustrated by the fact the points representing each gender overlap at more than one data point at a single level of E2.

THREE MONTH OLD *DEL2* B6 MICE: RAW DATA

TABLE 3.10 Centrosomal count data analysis for three-month-old *Del2* males

Sample: E2 (pg/ml)	% cells with >2 centrosomes: animal 1	% cells with >2 centrosomes: animal 2	% cells with >2 centrosomes: animal 3	Mean % of cells with >2 centrosomes	Standard deviation	p-value*
0	25	13	17	18.3	5.755	
25	42	40	31	37.9	5.858	0.007
75	56	45	24	41.5	16.232	0.060
500	38	39	35	37.3	1.778	0.010

*p-values relative to control (0pg/ml E2). t-test: 1-sided, unequal variance assumed, p<0.05 significance.

TABLE 3.11 Centrosomal count data analysis for three-month-old *Del2* females

Sample: E2 (pg/ml)	% cells with >2 centrosomes: animal 1	% cells with >2 centrosomes: animal 2	% cells with >2 centrosomes: animal 3	Mean % of cells with >2 centrosomes	Standard deviation	p-value*
0	12	22	12	15.5	5.818	
25	37	30	26	31.2	5.824	0.015
75	42	29	20	30.3	10.795	0.063
500	47	44	25	38.7	12.225	0.031

*p-values relative to control (0pg/ml E2). t-test: 1-sided, unequal variance assumed, p<0.05 significance.

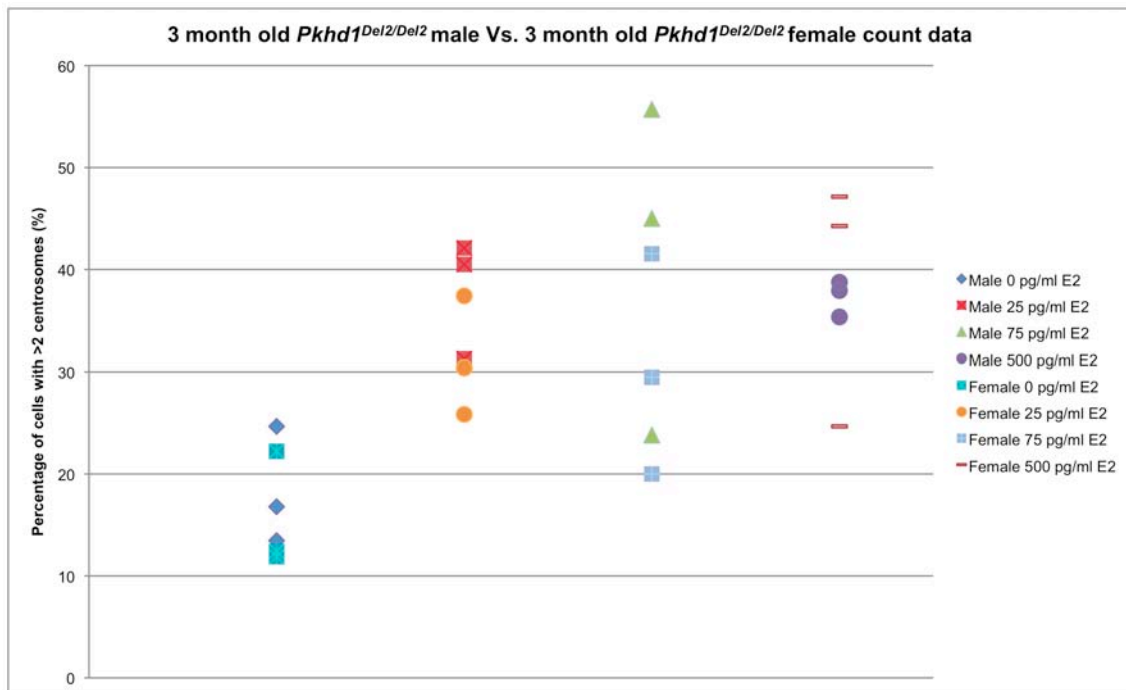


FIGURE 3.4 Three-month-old *Del2*: Scatter plot of mean percentage of cells with >2 centrosomes. Chart representation of the lack of significance between centrosomal overduplication between the sexes when treated with the same level of E2. This is illustrated by the fact the points representing each gender overlap at more than one data point at any given concentration of E2

SIX MONTH OLD WILDTYPE B6 MICE: RAW DATA

TABLE 3.13 Centrosomal count data analysis for six-month-old wt males

Sample: E2 (pg/ml)	% cells with >2 centrosomes: animal 1	% cells with >2 centrosomes: animal 2	% cells with >2 centrosomes: animal 3	Mean % of cells with >2 centrosomes	Standard deviation	p-value*
0	43	26	38	35.8	8.539	
25	40	39	38	38.8	0.742	0.301
75	39	42	39	39.8	1.599	0.253
500	44	38	48	43.5	4.932	0.132

*p-values relative to control (0pg/ml E2). t-test: 1-sided, unequal variance assumed, p<0.05 significance.

TABLE 3.14 Centrosomal count data analysis for six-month-old wt females

Sample: E2 (pg/ml)	% cells with >2 centrosomes: animal 1	% cells with >2 centrosomes: animal 2	% cells with >2 centrosomes: animal 3	Mean % of cells with >2 centrosomes	Standard deviation	p-value*
0	17	15	22	18.1	3.729	
25	26	19	31	25.2	6.121	0.088
75	38	14	41	31.1	15.224	0.136
500	36	29	43	36.1	7.213	0.016

*p-values relative to control (0pg/ml E2). t-test: 1-sided, unequal variance assumed, p<0.05 significance.

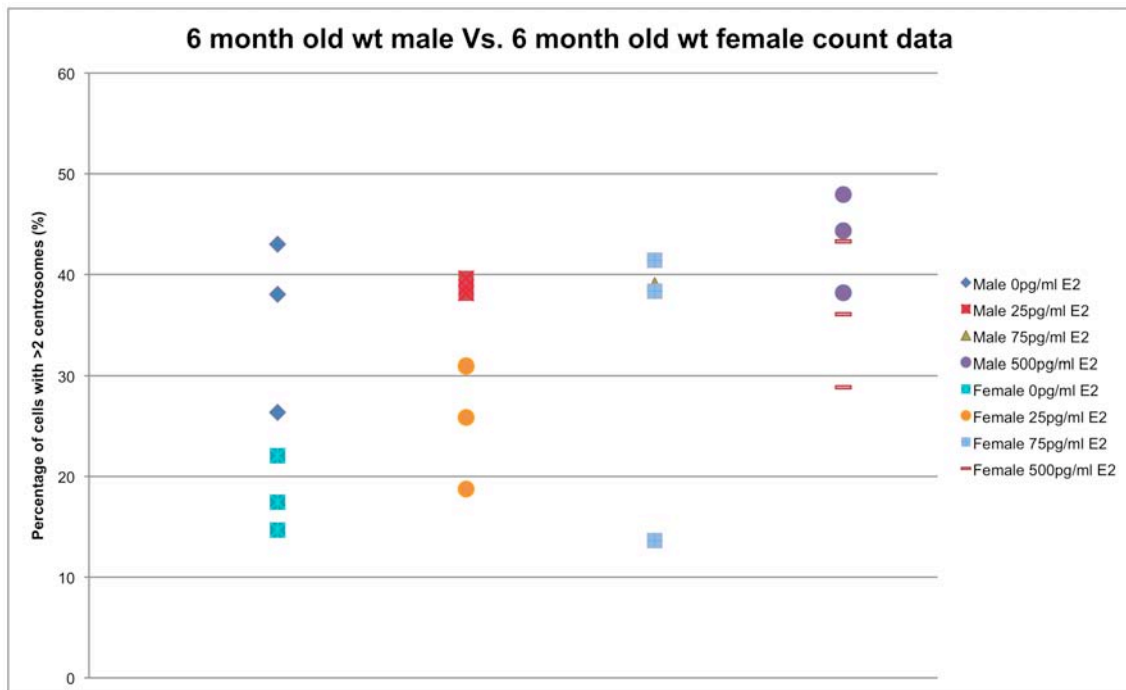


FIGURE 3.5 Six-month-old wt: Scatter plot of mean percentage of cells with >2 centrosomes. The significant difference between the mean percentage of cells with centrosomal overduplication between male and female mice at 0pg/ml and 25pg/ml is represented by no overlap between the data points representing each set. The lack of a significant difference at 75pg/ml and 500pg/ml is illustrated by the fact the data points representing each gender overlap at more than one data point.

SIX MONTH OLD *DEL2* B6 MICE: RAW DATA

TABLE 3.16 Centrosomal count data analysis for six-month-old *Del2* males

Sample: E2 (pg/ml)	% cells with >2 centrosomes: animal 1	% cells with >2 centrosomes: animal 2	% cells with >2 centrosomes: animal 3	Mean % of cells with >2 centrosomes	Standard deviation	p-value*
0	12	14	16	14.0	1.706	
25	28	34	31	30.7	3.211	0.002
75	34	36	32	34.0	2.224	0.0002
500	42	47	32	40.1	7.217	0.010

*p-values relative to control (0pg/ml E2). t-test: 1-sided, unequal variance assumed, p<0.05 significance.

TABLE 3.17 Centrosomal count data analysis for six-month-old *Del2* females

Sample: E2 (pg/ml)	% cells with >2 centrosomes: animal 1	% cells with >2 centrosomes: animal 2	% cells with >2 centrosomes: animal 3	Mean % of cells with >2 centrosomes	Standard deviation	p-value*
0	4	9	6	6.3	2.517	
25	22	12	21	18.3	5.508	0.023
75	25	24	24	24.3	0.577	0.002
500	39	21	29	29.7	9.018	0.019

*p-values relative to control (0pg/ml E2). t-test: 1-sided, unequal variance assumed, p<0.05 significance.

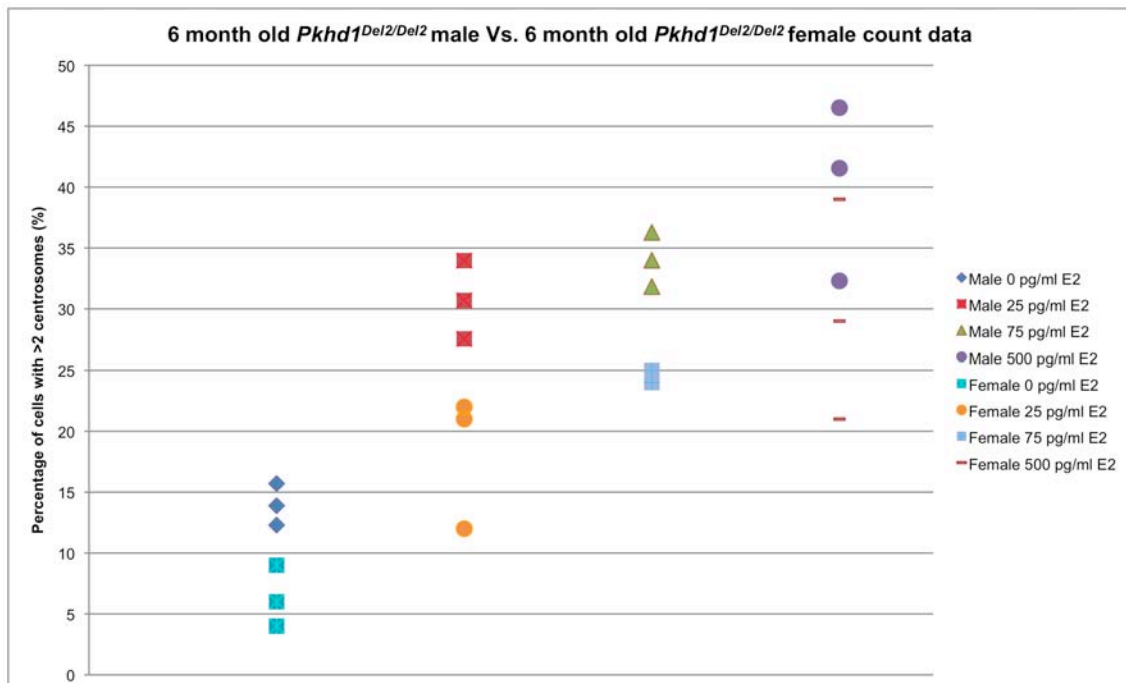


FIGURE 3.6 Six-month-old *Del2*: Scatter plot of mean percentage of cells with >2 centrosomes. The significant difference between the mean percentage of cells with centrosomal overduplication between male and female mice at 0pg/ml, 25pg/ml, and 75pg/ml is represented by no overlap between the data points representing each level of E2. The lack of a significant difference at 500pg/ml is illustrated by the fact the data points representing each gender overlap.

NINE MONTH OLD WILDTYPE B6 MICE: RAW DATA

TABLE 3.19 Centrosomal count data analysis for nine-month-old wt males

Sample: E2 (pg/ml)	% cells with >2 centrosomes: animal 1	% cells with >2 centrosomes: animal 2	% cells with >2 centrosomes: animal 3	Mean % of cells with >2 centrosomes	Standard deviation	p-value*
0	38	22	19	26.5	10.079	
25	55	27	30	37.3	15.035	0.183
75	52	30	25	35.7	14.145	0.208
500	56	39	40	45.0	9.612	0.041

*p-values relative to control (0pg/ml E2). t-test: 1-sided, unequal variance assumed, p<0.05 significance.

TABLE 3.20 Centrosomal count data analysis for nine-month-old wt females

Sample: E2 (pg/ml)	% cells with >2 centrosomes: animal 1	% cells with >2 centrosomes: animal 2	% cells with >2 centrosomes: animal 3	Mean % of cells with >2 centrosomes	Standard deviation	p-value*
0	43	28	11	27.4	15.618	
25	56	49	10	38.5	24.679	0.276
75	43	27	29	33.2	8.878	0.308
500	50	57	32	46.4	12.963	0.092

*p-values relative to control (0pg/ml E2). t-test: 1-sided, unequal variance assumed, p<0.05 significance.

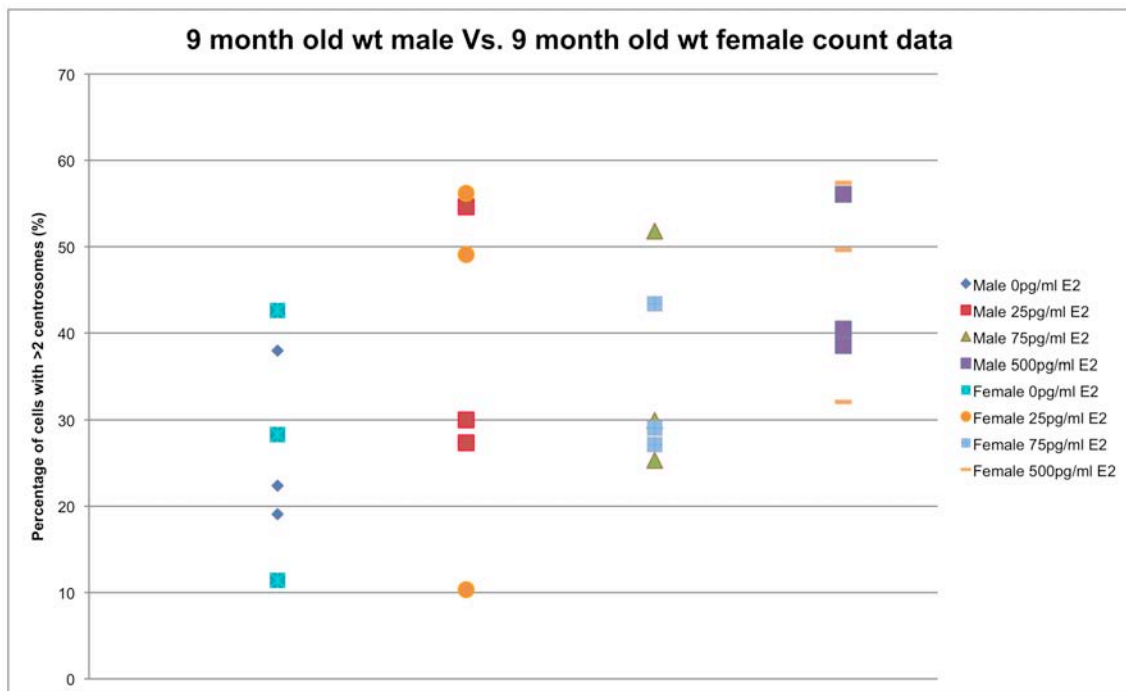


FIGURE 3.7 Nine-month-old wt: Scatter plot of mean percentage of cells with >2 centrosomes. Chart representation of the lack of significance between centrosomal overduplication between the sexes when treated with the same level of E2. This is illustrated by the fact the points representing each gender overlap at more than one data point at a single level of E2.

NINE MONTH OLD *DEL2* B6 MICE: RAW DATA

TABLE 3.22 Centrosomal count data analysis for nine-month-old *Del2* males

Sample: E2 (pg/ml)	% cells with >2 centrosomes: animal 1	% cells with >2 centrosomes: animal 2	% cells with >2 centrosomes: animal 3	Mean % of cells with >2 centrosomes	Standard deviation	p-value*
0	40	39	49	42.7	5.367	
25	37	30	44	36.9	6.860	0.155
75	50	46	45	46.8	2.533	0.163
500	49	45	58	50.5	6.753	0.099

*p-values relative to control (0pg/ml E2). t-test: 1-sided, unequal variance assumed, p<0.05 significance.

TABLE 3.23 Centrosomal count data analysis for nine-month-old *Del2* females

Sample: E2 (pg/ml)	% cells with >2 centrosomes: animal 1	% cells with >2 centrosomes: animal 2	% cells with >2 centrosomes: animal 3	Mean % of cells with >2 centrosomes	Standard deviation	p-value*
0	28	21	36	28.3	7.546	
25	33	31	49	37.7	9.970	0.135
75	39	45	47	43.6	4.320	0.026
500	47	38	65	49.8	13.722	0.047

*p-values relative to control (0pg/ml E2). t-test: 1-sided, unequal variance assumed, p<0.05 significance.

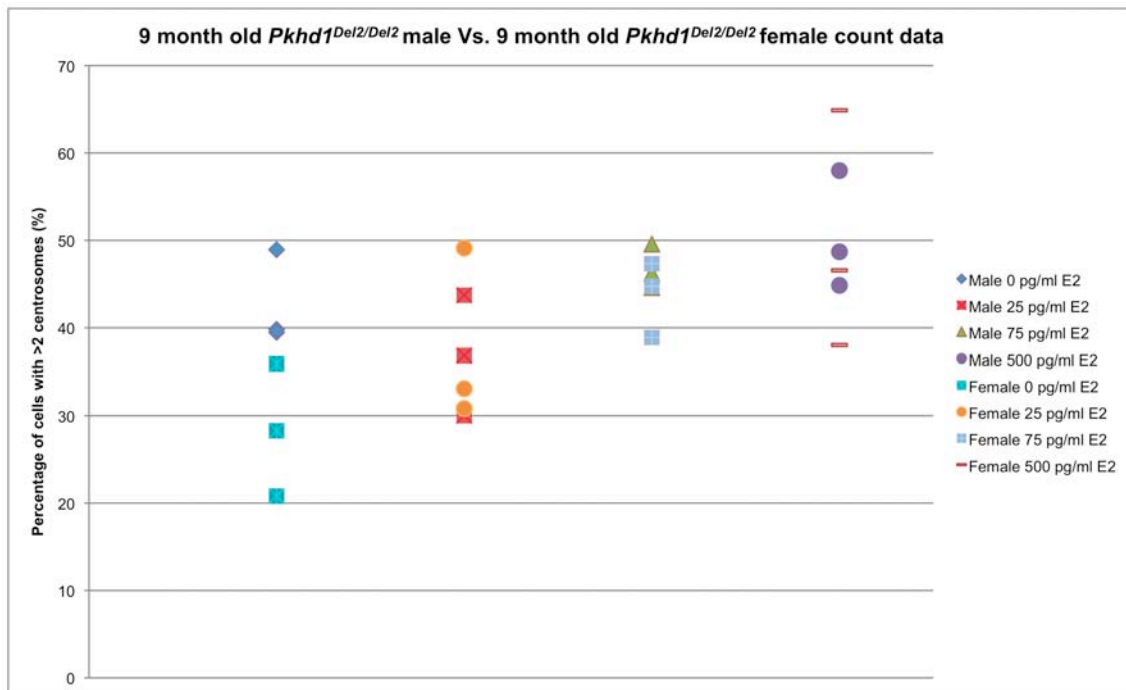


FIGURE 3.8 Nine-month-old *Del2*: Scatter plot of mean percentage of cells with >2 centrosomes. The significant difference between the mean percentage of cells with centrosomal overduplication between control cells from male and female mice represented by no overlap between the data points representing 0pg/ml of E2. The lack of a significant difference at 25pg/ml, 75pg/ml, and 500pg/ml is illustrated by the fact the data points representing each gender overlap.

PUBLICATIONS

Journal articles:

Dawe, H.R., Smith, U.M., Cullinane, A.R., Gerrelli, D., Cox, P., Badano, J.L., **Blair-Reid, S.**, Sriram, N., Katsanis, N., Attie-Bitach, T., Afford, S.C., Copp, A.J., Kelly, D.A., Gull, K., Johnson, C.A. (2007) The Meckel-Gruber syndrome proteins MKS1 and mecklin interact and are required for primary cilium formation. **Human Molecular Genetics**, 16: (2): 173-186.

Abstracts, and conference posters:

Blair-Reid, S., Reynolds, G., Hartley, J., Kelly, D., Hubscher, S., Harris, P., Johnson, C.A., Ward, C., Afford, S. (2007) Increased Acetylation of Alpha-Tubulin and Decreased Expression of Fibrocystin are Sensitive Markers of Cellular Damage and Activation in Inflammatory Liver Disease. **American Association for the study of Liver Diseases**, 1038.

Blair-Reid, S., Reynolds, G., Hartley, J., Kelly, D., Hubscher, S., Harris, P., Johnson, C.A., Ward, C., Afford, S. (2007) Increased Acetylation of Alpha-Tubulin and Decreased Expression of Fibrocystin are Sensitive Markers of Cellular Damage and Activation in Inflammatory Liver Disease. **British Association for Study of the Liver**, London, 117.

Hartley, J.L., Ward, C., Harris, P., Reynolds, G. M., Afford, S., Johnson, C., **Blair-Reid, S.**, Kelly, D. A. (2007) Biliary atresia associated with renal cyst formation: evidence of a ciliopathy? **British Association for Study of the Liver**, London, 107.

LIST OF REFERENCES

- Adams, D.H. and Afford, S.C. (2005) Effector mechanisms of nonsuppurative destructive cholangitis in graft-versus-host disease and allograft rejection. **Seminars in Liver Disease**, 25: (3): 281-297.
- Adelman, S. (1978) Prognosis of uncorrectable biliary atresia: an update. **Journal of Pediatric Surgery**, 13: (4): 389-391.
- Adeva, M., El-Youssef, M., Rossetti, S., et al. (2006) Clinical and molecular characterization defines a broadened spectrum of autosomal recessive polycystic kidney disease (ARPKD). **Medicine**, 85: (1): 1-21.
- Afford, S.C., Ahmed-Choudhury, J., Randhawa, S., et al. (2001) CD40 activation-induced, Fas-dependent apoptosis and NF- κ B/AP-1 signaling in human intrahepatic biliary epithelial cells. **The FASEB Journal**, 15: (13): 2345-2354.
- Afzelius, B.A. (2004) Cilia-related diseases. **Journal of Pathology**, 204: 470-477.
- Ahmed-Choudhury, J., Russell, C.L., Randhawa, S., et al. (2003) Differential induction of nuclear factor- κ B and activator protein-1 activity after CD40 ligation is associated with primary human hepatocyte apoptosis or intrahepatic endothelial cell proliferation. **Molecular Biology of the Cell**, 14: (4): 1334-1345.
- Alagille, D., Estrada, A., Hadchouel, M., et al. (1987) Syndromic paucity of interlobular bile ducts (Alagille syndrome or arteriohepatic dysplasia): Review of 80 cases. **The Journal of Pediatrics**, 110: 195-200.
- Alberts, B., Bray, D., Lewis, J., et al. (1994) **Molecular Biology of the Cell**. New York and London: Garland.
- Alpini, G., Glaser, S., Alvaro, D., et al. (2002a) Bile acid depletion and repletion regulate cholangiocyte growth and secretion by a phosphatidylinositol 3-kinase-dependent pathway in rats. **Gastroenterology**, 123: (4): 1226-1237.
- Alpini, G., Glaser, S., Robertson, W., et al. (1997) Bile acids stimulate proliferative and secretory events in large but not small cholangiocytes. **American Journal of Physiology - Gastroenterology and Liver Physiology**, 273: 518-529.
- Alpini, G., Glaser, S.S., Ueno, Y., et al. (1998) Heterogeneity of the proliferative capacity of rat cholangiocytes after bile duct ligation. **American Journal of Physiology - Gastroenterology and Liver Physiology**, 274: G767-G775.
- Alpini, G., Lenzi, R., Sarkozi, L., et al. (1988) Biliary physiology in rats with bile ductular cell hyperplasia. Evidence for a secretory function of proliferated bile ductules. **Journal of Clinical Investigation**, 81: 569-578.
- Alpini, G., McGill, J.M. and LaRusso, N.F. (2002b) The pathobiology of biliary epithelia. **Hepatology**, 35: 1256-1268.
- Alpini, G., Prall, R.T. and LaRusso, N.F. (2001) **The Liver; Biology & Pathobiology**, 4th ed. Philadelphia, PA: Lippincott Williams & Wilkins.
- Alvaro, D., Alpini, G., Onori, P., et al. (2002a) Alfa and Beta estrogen receptors and the biliary tree. **Molecular and Cellular Endocrinology**, 193: (1-2): 105-108.
- Alvaro, D., Alpini, G., Onori, P., et al. (2000a) Estrogens stimulate proliferation of intrahepatic biliary epithelium in rats. **Gastroenterology**, 119: 1681-1691.

- Alvaro, D., Gigliozzi, A. and Attili, A.F. (2000b) Regulation and deregulation of cholangiocyte proliferation. **Journal of Hepatology**, 33: 333-340.
- Alvaro, D., Onori, P., Metalli, V.D., et al. (2002b) Intracellular pathways mediating estrogen-induced cholangiocyte proliferation in the rat. **Hepatology**, 36: 297-304.
- Anderson, J.S., Wilkinson, C.J., Mayor, T., et al. (2003) Proteomic characterization of the human centrosome by protein correlation profiling. **Nature**, 426: (6966): 570-574.
- Artavanis-Tsakonas, S., Rand, M.D. and Lake, R.J. (1999) Notch signaling: cell fate control and signal integration in development. **Science**, 284: 770-776.
- Auth, M.K., Joplin, R., Okamoto, M., et al. (2001) Morphogenesis of primary human biliary epithelial cells: induction in high-density culture or by coculture with autologous human hepatocytes. **Hepatology**, 33: (3): 519-529.
- Avidor-Reiss, T., Maer, A.M., Koundakijian, E., et al. (2004) Decoding cilia function: Defining specialized genes required for compartmentalized cilia biogenesis. **Cell**, 117: 527-539.
- Axelrod, J.D. and McNeill, H. (2002) Coupling planar cell polarity signaling to morphogenesis. **The Scientific World**, 2: 434-454.
- Ayres, R.C., Neuberger, J.M., Shaw, J., et al. (1993) Intercellular adhesion molecule-1 and MHC antigens on human intrahepatic bile duct cells: effect of pro-inflammatory cytokines. **Gut**, 34: 1245-1249.
- Badano, J.L., Mitsuma, N., Beales, P.L., et al. (2006) The ciliopathies: an emerging class of human genetic disorders. **The Annual Review of Genomics and Human Genetics**, 7: 125-148.
- Badano, J.L., Teslovich, T.M. and Katsanis, N. (2005) The centrosome in human genetic disease. **Nature Reviews in Genetics**, 6: 194-205.
- Balistreri, W.F. (1985) Neonatal cholestasis - medical progress. **Journal of Pediatrics**, 106: 171-184.
- Balistreri, W.F., Grand, R., Hoofnagle, J.H., et al. (1996) Biliary atresia: current concepts and research directions. **Hepatology**, 23: (6): 1682-1692.
- Bamford, R.N., Roessler, E., Burdine, R.D., et al. (2000) Loss-of-function mutations in the EGF-CFC gene CFC1 are associated with human left-right laterality defects. **Nature Genetics**, 26: 365-369.
- Bangaru, B., Morecki, R., Glaser, J.H., et al. (1980) Comparative studies of biliary atresia in the human newborn and reovirus-induced cholangitis in weanling mice. **Laboratory Investigations**, 43: (5): 456-462.
- Barone, M., Maiorano, E., Ladisa, R., et al. (2004) Ursodeoxycholate further increases bile-duct cell proliferative response induced by partial bile-duct ligation in rats. **Virchows Archive**, 444: 554-560.
- Bassett, M.D. and Murray, K.F. (2008) Biliary Atresia. **Journal of Clinical Gastroenterology**, 42: (6): 720-729.
- Battini, L., Fedorova, E., Macip, S., et al. (2006) Stable knockdown of polycystin-1 confers integrin- $\alpha 2\beta 1$ -mediated anoikis resistance. **Journal of the American Society of Nephrology**, 17: 3049-3058.
- Battini, L., Macip, S., Fedorova, E., et al. (2008) Loss of polycystin-1 causes centrosome amplification and genomic instability. **Human Molecular Genetics**, 17: 2819-2833.
- BDBiosciences (Unknown) "BD BioCoat™ Cellware". In Biosciences, B. (Ed.) **On-line**. Canada, Becton, Dickinson and Company.

- Beales, P.L. (2005) Lifting the lid on Pandora's box: the Bardet-Biedl syndrome. **Current Opinion in Genetics & Development**, 15: 315-323.
- Benzing, T. and Walz, G. (2006) Cilium-generated signaling: a cellular GPS? **Current Opinion in Nephrology and Hypertension**, 15: 245-249.
- Bergmann, C., Kupper, F., Dornia, C., et al. (2005a) Algorithm for efficient PKHD1 mutation screening in autosomal recessive polycystic kidney disease (ARPKD). **Human Mutation**, 25: 225-231.
- Bergmann, C., Senderek, J., Küpper, F., et al. (2004) *PKHD1* mutations in autosomal recessive polycystic kidney disease (ARPKD). **Human Mutation**, 23: 453-463.
- Bergmann, C., Senderek, J., Sedlacek, B., et al. (2003) Spectrum of mutations in the gene for autosomal recessive polycystic kidney disease (ARPKD/PKHD1). **Journal of the American Society of Nephrology**, 14: 76-89.
- Bergmann, C., Senderek, J., Windelen, E., et al. (2005b) Clinical consequences of *PKHD1* mutations in 164 patients with autosomal-recessive polycystic kidney disease (ARPKD). **Kidney International**, 67: 829-848.
- Berthois, Y., Katzenellenbogen, J.A. and Katzenellenbogen, B.S. (1986) Phenol red in tissue culture media is a weak estrogen: Implications concerning the study of estrogen-responsive cells in culture. **Proceedings of the National Academy of Sciences of the United States of America**, 83: 2496-2500.
- Bezerra, J.A. (2006) Biliary atresia - translational research on key molecular processes regulating biliary injury and obstruction. **Chang Gung Medical Journal**, 29: (3): 222-230.
- Bhathal, P.S. and Gall, J.A.M. (1985) Deletion of hyperplastic biliary epithelial cells by apoptosis following removal of the proliferative stimulus. **Liver**, 5: (6): 311-325.
- Bhavsar, P., Ahmad, T. and Adcock, I.M. (2008) The role of histone deacetylases in asthma and allergic diseases. **The Journal of Allergy and Clinical Immunology**, 121: 580-584.
- Bhunja, A.K., Piontek, K., Boletta, A., et al. (2002) *PKD1* induces p21^{waf1} and regulation of the cell cycle via direct activation of the JAK-STAT signaling pathway in a process requiring *PKD2*. **Cell**, 109: 157-168.
- Blanchard, F., Kinzie, E., Wang, Y., et al. (2002) FR901228, an inhibitor of histone deacetylases, increases the cellular responsiveness to IL-6 type cytokines by enhancing the expression of receptor proteins. **Oncogene**, 21: 6264-6277.
- Blum, A. and Cannon, R.O. (1998) Effects of oestrogens and selective oestrogen receptor modulators on serum lipoproteins and vascular function. **Current Opinion in Lipidology**, 9: 575-586.
- Blyth, H. and Ockenden, B.G. (1971) Polycystic disease of kidney and liver presenting in childhood. **Journal of Medical Genetics**, 8: (3): 257-284.
- Bogert, P.T. and LaRusso, N.F. (2007) Cholangiocyte Biology. **Current Opinion in Gastroenterology**, 23: 299-305.
- Boichis, H., Passwell, J., David, R., et al. (1973) Congenital hepatic fibrosis and nephronophthisis. A family study. **The Quarterly Journal of Medicine**, 42: 221-233.
- Boucher, C. and Sandford, R. (2004) Autosomal dominant polycystic kidney disease (ADPKD, MIM173900, *PKD1* and *PKD2* genes, protein products known as polycystin-1 and polycystin-2. **European Journal of Human Genetics**, 12: 347-354.

- Boyault, C., Sadoul, K., Pabion, M., et al. (2007) HDAC6, at the crossroads between cytoskeleton and cell signaling by acetylation and ubiquitination. **Oncogene**, 26: (37): 5468-5476.
- Brasier, J.L. and Henske, E.P. (1997) Loss of the polycystic kidney disease (PKD1) region of chromosome 16p13 in cyst cells supports a loss-of-function model for cyst pathogenesis. **The Journal of Clinical Investigation**, 99: 194-199.
- Burtey, S., Riera, M., Ribe, E., et al. (2008) Centrosome overduplication and mitotic instability in *PKD2* transgenic lines. **Cell Biology International**, 32: 1193-1198.
- Calvet, J.P. (1993) Polycystic kidney disease: Primary extracellular matrix abnormality or defective cellular differentiation? **Kidney International**, 43: 101-108.
- Calvet, J.P. (1994) Injury and development in polycystic kidney disease. **Current Opinion in Nephrology and Hypertension**, 3: 340-348.
- Calvo-Garcia, M.A., Campbell, K.M., O'Hara, S.M., et al. (2008) Acquired renal cysts after pediatric liver transplantation: association with cyclosporine and renal dysfunction. **Pediatric Transplantation**, 12: (3): 666-671.
- Cano, D.A., Murcia, N.S., Pazour, G.J., et al. (2004) Orpk mouse model of polycystic kidney disease reveals essential role of primary cilia in pancreatic tissue organization. **Development**, 131: 3457-3467.
- Cardon, L.R. and Palmer, L.J. (2003) Population stratification and spurious allelic association. **The Lancet**, 361: 598-604.
- Carmi, R., Magee, C.A., Neill, C.A., et al. (1993) Extrahepatic biliary atresia and associated anomalies: etiologic heterogeneity suggested by distinctive patterns of associations. **American Journal of Medical Genetics**, 45: 683-693.
- Celli, A. and Que, F.G. (1998) Dysregulation of apoptosis in the cholangiopathies and cholangiocarcinoma. **Seminars in Liver Disease**, 18: (2): 177-185.
- Chang, K.T. and Min, K.T. (2002) Regulation of lifespan by histone deacetylase. **Ageing Research Review**, 3: 313-326.
- Chapman, A.B. (2003) Cystic disease in women: clinical characteristics and medical management. **Advances in Renal Replacement Therapy**, 10: (1): 24-30.
- Chardot, C., Carton, M., Spire-Bendelac, N., et al. (1999) Prognosis of biliary atresia in the era of liver transplantation: French national study from 1986 to 1996. **Hepatology**, 30: 606-611.
- Charlton, J.A. and Simmons, N.L. (1993) Established human renal cell lines: Phenotypic characteristics define suitability for use in in vitro models for predictive toxicology. **Toxicology in vitro**, 7: 129-136.
- Chauvet, V., Tian, X., Husson, H., et al. (2004) Mechanical stimuli induce cleavage and nuclear translocation of the polycystin-1 C terminus. **The Journal of Clinical Investigation**, 114: (10): 1433-1443.
- Cho, W.K., Mennone, A. and Boyer, J.L. (2001) Isolation of functional polarized bile duct units from mouse liver. **American Journal of Physiology. Gastroenterology and Liver Physiology**, 280: G241-G246.
- Clotman, F., Lannoy, V.J., Reber, M., et al. (2002) The onecut transcription factor HNF6 is required for normal development of the biliary tract. **Development**, 129: 1819-1828.

- Clotman, F., Libbrecht, L., Gresh, L., et al. (2003) Hepatic artery malformations associated with a primary defect in intrahepatic bile duct development. **Journal of Hepatology**, 39: 686-692.
- Coffinier, C., Gresh, L., Fiette, L., et al. (2002) Bile system morphogenesis defects and liver dysfunction upon targeted deletion of HNF1 β . **Development**, 129: 1829-1838.
- Cooper, S. and Gonzalez-Hernandez, M. (2009) Experimental reconsideration of the utility of serum starvation as a method for synchronizing mammalian cells. **Cell Biology International**, 33: (1): 71-77.
- Cunningham, M.L. and Sybert, V.P. (1988) Idiopathic extrahepatic biliary atresia: recurrence in sibs in two families. **American Journal of Medical Genetics**, 31: (2): 421-426.
- Czaja, A.J. and Donaldson, P.T. (2000) Genetic susceptibilities for immune expression and liver cell injury in autoimmune hepatitis. **Immunological review**, 174: 250-259.
- Czech-Schmidt, G., Verhagen, W., Szavay, P., et al. (2001) Immunological gap in the infectious animal model for biliary atresia. **The Journal of Surgical Research**, 101: (1): 62-67.
- D'Agata, I.D., Jonas, M.M., Perez-Atayde, A.R., et al. (1994) Combined cystic disease of the liver and kidney. **Seminars in Liver Disease**, 14: (3): 215-228.
- D'Assoro, A.B., Lingle, W.L. and Salisbury, J.L. (2002) Centrosome amplification and the development of cancer. **Oncogene**, 21: 6146-6153.
- Danks, D. and Bodian, M. (1963) A genetic study of neonatal obstructive jaundice. **Archives of Disease in Childhood**, 38: 378-390.
- Davenport, J.R. and Yoder, B.K. (2005) An incredible decade for the primary cilium: a look at a once-forgotten organelle. **American Journal of Physiology - Renal Physiology**, 289: F1159-1169.
- Davenport, M., Savage, M., Mowat, A.P., et al. (1993) Biliary atresia splenic malformation syndrome: an etiologic and prognostic subgroup. **Surgery**, 113: (6): 662-668.
- Davenport, M., Tizzard, S.A., Underhill, J., et al. (2006) The biliary atresia splenic malformation syndrome: A 28-year single-center retrospective study. **Journal of Pediatrics**, 149: 393-400.
- Davit-Spraul, A., Baussan, C., Hermeziu, B., et al. (2008) CFC1 gene involvement in biliary atresia with polysplenia syndrome. **Journal of Pediatric Gastroenterology and Nutrition**, 46: (1): 111-112.
- Day, C.P. (2003) **Host genetic factors and the progression of liver diseases**. Barcelona: Medicina STM.
- de Groot, P.W. and Klis, F.M. (2008) The conserved PA14 domain of cell wall-associated fungal adhesins governs their glycan-binding specificity. **Molecular Microbiology**, 68: (3): 535-537.
- De Vries, J.R., Ludes, J.H. and Fanestil, D. (1972) Estradiol renal receptor molecules and estradiol-dependent antinatriuresis. **Kidney International**, 2: 95-100.
- Deckert, J. and Struhl, K. (2001) Histone acetylation at promoters is differentially affected by specific activators and repressors. **Molecular and Cellular Biology**, 21: 2726-2735.
- Delladetsima, J.K., Rassidakis, G., Tassopoulos, N.C., et al. (1996) Histopathology of chronic hepatitis C in relation to epidemiological factors. **Journal of Hepatology**, 24: (1): 27-32.
- Desmet, V.J. (1992a) Congenital diseases of intrahepatic bile ducts: variations on the theme "Ductal plate malformation." **Hepatology**, 16: 1069-1083.

- Desmet, V.J. (1992b) What is congenital hepatic fibrosis? **Histopathology**, 20: 465-477.
- Desmet, V.J. (1998) Ludwig symposium on biliary disorders - part I. Pathogenesis of ductal plate abnormalities. **Mayo Clinic Proceedings**, 73: 80-89.
- Desmet, V.J., Roskams, T. and Van Eyken, P. (1995) Ductular reaction in the liver. **Pathology, Research, and Practice**, 191: (6): 513-524.
- Desmet, V.J., Roskams, T. and Van Eyken, P. (1998) Histopathology of vanishing bile duct diseases. **Advances in Clinical Pathology**, 2: 87-99.
- Deutsch, G.H., Sokol, R.J., Stathos, T.H., et al. (2001) Proliferation to paucity: evolution of bile duct abnormalities in a case of Alagille syndrome. **Pediatric and Developmental Pathology**, 4: (6): 559-563.
- Dillon, P., Belchis, D., Tracy, T., et al. (1994) Increased expression of intercellular adhesion molecules in biliary atresia. **The American Journal of Pathology**, 145: (2): 263-267.
- Domati-Saad, R., Dawson, D.B., Margraf, L.F., et al. (2000) Cytomegalovirus and human herpesvirus 6, but not human papillomavirus, and present in neonatal giant cell hepatitis and extrahepatic biliary atresia. **Pediatric and Developmental Pathology**, 3: (4): 367-373.
- Donaldson, P.T. (2004) Genetics of autoimmune and viral liver diseases; understanding the issues. **Journal of Hepatology**, 41: 327-332.
- Doxsey, S. (2001) Re-evaluating centrosome function. **Nature Reviews Molecular Cell Biology**, 2: 688-698.
- Drubin, D.G. and Nelson, W.J. (1996) Origins of cell polarity. **Cell**, 84: (3): 335-344.
- Drut, R., Drut, R.M., Gómez, M.A., et al. (1998) Presence of human papillomavirus in extrahepatic biliary atresia. **Journal of Pediatric Gastroenterology and Nutrition**, 27: (5): 530-535.
- Dubal, D.B., Zhu, H., Yu, J., et al. (2001) Estrogen receptor α , not β , is a critical link in estradiol-mediated protection against brain injury. **Proceedings of the National Academy of Sciences of the United States of America**, 98: (4): 1952-1957.
- Duensing, S. (2005) A tentative classification of centrosome abnormalities in cancer. **Cell Biology International**, 29: 352-359.
- Duensing, S. and Munger, K. (2002a) Human papillomaviruses and centrosome duplication errors: modeling the origins of genomic instability. **Oncogene**, 21: 6241-6248.
- Duensing, S. and Munger, K. (2002b) The human papillomavirus type 16 E6 and E7 oncoproteins independently induce numerical and structural chromosome instability. **Cancer Research**, 62: 7075-7082.
- Duensing, S. and Munger, K. (2003) Human papillomavirus type 16 E7 oncoprotein can induce abnormal centrosome duplication through a mechanism independent of inactivation of retinoblastoma protein family members. **Journal of Virology**, 77: 12331-12335.
- Eagar, T., Tompkins, S. and Miller, S. (2001) **Clinical Immunology Principles and Practice**. London: Mosby.
- Eagon, P.K., Elm, M.S., Epley, M.J., et al. (1996) Sex steroid metabolism and receptor status in hepatic hyperplasia and cancer in rats. **Gastroenterology**, 110: 1199-1207.
- Eagon, P.K., Porter, L.E., Francavilla, A., et al. (1985) Estrogen and androgen receptors in liver: their role in liver disease and regeneration. **Seminars in Liver Disease**, 5: 59-69.

- Eley, L., Yates, L.M. and Goodship, J.A. (2005) Cilia and disease. **Current Opinion in Genetics & Development**, 15: 308-314.
- Emerick, K.M., Rand, E.B., Goldmuntz, E., et al. (1999) Features of Alagille syndrome in 92 patients frequency and relation to prognosis. **Hepatology**, 29: 822-829.
- Everson, G.T., Taylor, M.R. and Doctor, R.B. (2004) Polycystic disease of the liver. **Hepatology**, 40: 774-782.
- Feng, P., Park, J., Lee, B., et al. (2002) Kaposi'sarcoma-associated herpesvirus mitochondrial K7 protein targets a cellular calcium-modulating cyclophilin ligand to modulate intracellular calcium concentration and inhibit apoptosis. **Journal of Virology**, 76: 11491-11504.
- Fickert, P., Fuchsbichler, A., Wagner, M., et al. (2004) Regurgitation of bile acids from leaky bile ducts causes sclerosing cholangitis in *Mdr2 (Abcb4)* knockout Mice. **Gastroenterology**, 127: 261-274.
- Fischer, E., Legue, E., Doyen, A., et al. (2006) Defective planar cell polarity in polycystic kidney disease. **Nature Genetics**, 38: 21-23.
- Fischler, B., Ehrnst, A., Forsgren, M., et al. (1998) The viral association of neonatal cholestasis in sweden: a possible link between cytomegalovirus infection and extrahepatic biliary atresia. **Journal of Pediatric Gastroenterology and Nutrition**, 27: (1): 57-64.
- Fischler, B., Haglund, B. and Hjern, A. (2002) A population-based study on the incidence and possible pre- and perinatal etiologic risk factors of biliary atresia. **Journal of Pediatrics**, 141: (2): 217-222.
- Fjaer, R.B., Bruu, A.L. and Nordbo, S.A. (2005) Extrahepatic bile duct atresia and viral involvement. **Pediatric Transplantation**, 9: 68-73.
- Fliegauf, M., Benzing, T. and Omran, H. (2007) When cilia go bad: cilia defects and ciliopathies. **Nature Reviews Molecular Cell Biology**, 8: 880-895.
- Fliegauf, M. and Omran, H. (2006) Novel tools to unravel molecular mechanisms in cilia-related disorders. **Trends in Genetics**, 22: (5): 241-245.
- Flynn, D.M., Nijjar, S., Hubscher, S.G., et al. (2004) The role of Notch receptor expression in bile duct development and disease. **Journal of Pathology**, 204: 55-64.
- Fowkes, M.E. and Mitchell, D.R. (1998) The role of preassembled cytoplasmic complexes in assembly of flagellar dynein subunits. **Molecular Biology of the Cell**, 9: (9): 2337-2347.
- Franchi-Abella, S., Mourier, O., Pariente, D., et al. (2007) Acquired renal cystic disease after liver transplantation in children. **Transplantation Proceedings**, 39: 2601-2602.
- Friedman, S.L. (1999) Cytokines and fibrogenesis. **Seminars in Liver Disease**, 19: (2): 129-140.
- Fukasawa, K. (2005) Centrosome amplification, chromosome instability and cancer development. **Cancer Letters**, 230: 6-19.
- Furu, L., Onuchic, L.F., Gharavi, A.G., et al. (2003) Milder presentation of recessive polycystic kidney disease requires presence of amino acid substitution mutations. **Journal of the American Society of Nephrology**, 14: 2004-2014.
- Gabow, P.A., Johnson, A.M., Kaehny, W.D., et al. (1990) Risk factors for the development of hepatic cysts in autosomal dominant polycystic kidney disease. **Hepatology**, 11: 1033-1037.

- Gaertig, J., Cruz, M.A., Bowen, J., et al. (1995) Acetylation of lysine 40 in alpha-tubulin is not essential in *Tetrahymena thermophila*. **The Journal of Cell Biology**, 129: (5): 1301-1310.
- Germino, G.G. (2005) Linking cilia to Wnts. **Nature Genetics**, 37: (5): 455-457.
- Ghadimi, B.M., Sackett, D.L., Difilippantonio, M.J., et al. (2000) Centrosome amplification and instability occurs exclusively in aneuploid, but not in diploid cancer cell lines, and correlates with numerical chromosomal aberrations. **Genes, Chromosomes, and Cancer**, 27: (2): 183-190.
- Gogusev, J., Murakami, I., Doussau, M., et al. (2003) Molecular cytogenetic aberrations in autosomal dominant polycystic kidney disease tissue. **Journal of the American Society of Nephrology**, 14: 359-366.
- Goldin, R.D., Patel, N.K. and Thomas, H.C. (1996) Hepatitis C and bile duct loss. **Journal of Clinical Pathology**, 49: 836-838.
- Gong, M., Wilson, M., Kelly, T., et al. (2003) HDL-associated estradiol stimulates endothelial NO synthase and vasodilation in an SR-BI-dependent manner. **Journal of Clinical Investigation**, 111: 1579-1587.
- Grantham, J.J. (1993) Fluid secretion, cellular proliferation, and the pathogenesis of renal epithelial cysts. **Journal of the American Society of Nephrology**, 3: 1843-1857.
- Grantham, J.J. (2001) Polycystic kidney disease: From the bedside to the gene and back. **Current Opinion in Nephrology and Hypertension**, 10: 533-542.
- Grantham, R. (1974) Amino acid difference formula to help explain protein evolution. **Science**, 185: (4151): 862-864.
- Gridley, T. (1997) Notch signaling in vertebrate development and disease. **Molecular and Cellular Neurosciences**, 9: 103-108.
- Guay-Woodford, L.M. (1996) **Autosomal recessive polycystic kidney disease: clinical and genetic profiles**. New York: Oxford University Press.
- Guay-Woodford, L.M. and Desmond, R.A. (2003) Autosomal polycystic kidney disease: the clinical experience in North America. **Pediatrics**, 111: 1072-1080.
- Guay-Woodford, L.M., Muecher, G., Hopkins, S.D., et al. (1995) The severe perinatal form of autosomal recessive polycystic kidney disease maps to chromosome 6p21.1-p12: implications for genetic counseling. **American Journal of Human Genetics**, 56: (5): 1101-1107.
- Gunasekaran, T.S., Hassall, E.G., Steinbrecher, U.P., et al. (1992) Recurrence of extrahepatic biliary atresia in two half sibs. **American Journal of Genetics**, 43: 592-594.
- Guo, N., Hawkins, C. and Nathans, J. (2004) Frizzled6 controls hair patterning in mice. **Proceedings of the National Academy of Sciences of the United States of America**, 101: 9277-9281.
- Hadchouel, M. (1992) Paucity of interlobular bile ducts. **Seminars in Diagnostic Pathology**, 9: 24-30.
- Haggarty, S.J., Koeller, K.M., Wong, J.C., et al. (2003) Domain-selective small-molecule inhibitor of histone deacetylase 6 (HDAC6)-mediated tubulin deacetylation. **Proceedings of the National Academy of Sciences of the United States of America**, 100: (8): 4389-4394.
- Haines, J.L. and Pericak-Vance, M.A. (1998) **Overview of mapping common and genetically complex disease genes**. New York: John Wiley and Sons.

- Han, H.J., Jung, J.C. and Taub, M. (1999) Response of primary rabbit kidney proximal tubule cells to estrogens. **Journal of Cell Physiology**, 178: 35-43.
- Hanaoka, K., Qian, F., Boletta, A., et al. (2008) Co-assembly of polycystin-1 and polycystin-2 produces unique cation-permeable currents. **Nature**, 408: 990-994.
- Hansen, L. (2001) **HLS [Liver, Gall Bladder, and Pncreas, Liver; portal triad]** [online]. <http://www.bu.edu/histology/p/152030oa.htm> Histology Learning System [Accessed April 2009]
- Harris, P.C. and Rossetti, S. (2004) Molecular genetics of autosomal recessive polycystic kidney disease. **Molecular Genetics and Metabolism**, 81: 75-85.
- Harris, P.C. and Watson, M.L. (1997) Autosomal dominant polycystic kidney disease: neoplasia in disguise? **Nephrology, Dialysis, Transplantation**, 12: 1089-1090.
- Haycraft, C.J., Swoboda, P., Taulman, P.D., et al. (2001) The *C. elegans* homolog of the murine cystic kidney disease gene Tg737 functions in a ciliogenic pathway and is disrupted in *osm-5* mutant worms. **Development**, 128: 1493-1505.
- Hays, D.M. and Kimura, K. (1980) **Biliary atresia, the Japanese experience**. Cambridge London: Harvard University Press.
- Hays, D.M. and Synder, W.H.J. (1963) Life-span in untreated biliary atresia. **Surgery**, 54: 373-375.
- Heald, R., Regis, T., Habermann, A., et al. (1997) Spindle assembly in *Xenopus* egg extracts: respective roles of centrosomes and microtubule self-organization. **The Journal of Cell Biology**, 138: 615-628.
- Hernandez, H.M., Kovarik, P., Whittington, P.F., et al. (2001) Autoimmune hepatitis as a late complication of liver transplantation. **Journal of Pediatric Gastroenterology and Nutrition**, 32: 131-136.
- Hiesberger, T., Gourley, E., Erickson, A., et al. (2006) Proteolytic cleavage and nuclear translocation of fibrocystin is regulated by intracellular Ca²⁺ and activation of protein kinase c. **The Journal of Biological Chemistry**, 281: (45): 34357-34364.
- Hildebrandt, F. and Otto, E.A. (2005) Cilia and centrosomes: A unifying pathogenesis concept for cystic kidney disease? **Nature Reviews in Genetics**, 6: 928-940.
- Hildebrandt, F. and Zhou, W. (2007) Nephronophthisis - Associated ciliopathies. **Journal of the American Society of Nephrology**, 18: 1855-1871.
- Hinchcliffe, E.H., Li, C., Thopmson, E.A., et al. (1999) Requirement of Cdk-2-cyclin E activity for repeated centrosome reproduction in *Xenopus* egg extracts. **Science**, 283: (5403): 851-854.
- Hinchcliffe, E.H. and Sluder, G. (2001) 'It takes two to tango': understanding how centrosome duplication is regulated throughout cell cycle. **Genes and Development**, 15: 1167-1181.
- Hirschhorn, J.N. and Daly, M.J. (2005) Genome-wide association studies for common diseases and complex traits. **Nature Reviews Genetics**, 6: 95-108.
- Ho, C.W., Shioda, K., Shirasaki, K., et al. (1993) The pathogenesis of biliary atresia: a morphological study of the hepatobiliary system and the hepatic artery. **Journal of Pediatric Gastroenterology and Nutrition**, 13: (1): 53-60.
- Ho, P.T.C. and Tucker, R.W. (1989) Centriole ciliation and cell cycle variability during G1 phase of BALB/c 3T3 cells. **Journal of Cell Physiology**, 139: 398-406.

- Hogan, M.C., Griffin, M.D., Rossetti, S., et al. (2003) *PKHDLI*, a homolog of the autosomal recessive polycystic kidney disease gene, encodes a receptor with inducible T lymphocyte expression. **Human Molecular Genetics**, 12: (6): 685-698.
- Hogan, M.C., Manganelli, L., Woollard, J.R., et al. (2009) Characterization of PKD protein-positive exosome-like vesicles. **Journal of the American Society of Nephrology**, 20: 278-288.
- Hogg, R.J., Furth, S., Lemley, K.V., et al. (2003) National kidney foundation's kidney disease outcomes quality initiative clinical practice guidelines for chronic kidney disease in children and adolescents: evaluation, classification, and stratification. **Pediatrics**, 111: (6(1)): 1416-1421.
- Hou, X., Mrug, M., Yoder, B.K., et al. (2002) Cystin, a novel cilia-associated protein, is disrupted in the *cpk* mouse model of polycystic kidney disease. **Journal of Clinical Investigation**, 109: 533-543.
- Howard, E.R. (1983) Extrahepatic biliary atresia - a review of current management. **The British Journal of Surgery**, 70: 193-197.
- Huang, B.Q., Masyuk, T.V., Muff, M.A., et al. (2006) Isolation and characterization of cholangiocyte primary cilia. **American Journal of Physiology - Gastroenterology and Liver Physiology**, 291: 500-509.
- Hyams, J.S., Glaser, J.H., Leichtner, A.M., et al. (1985) Discordance for biliary atresia in two sets of monozygotic twins. **Journal of Pediatrics**, 107: (3): 420-422.
- Igarashi, P. and Somlo, S. (2003) Genetics and pathogenesis of polycystin kidney disease. **Journal of the American Society of Nephrology**, 13: 2384-2398.
- Infante, A.S., Stein, M.S., Zhai, Y., et al. (2000) Detyrosinated (Glu) microtubules and stabilised by a ATP-sensitive plus-end cap. **Journal of Cell Science**, 113: (22): 3907-3919.
- Inglis, P.N., Borojevich, K.A. and Leroux, M.R. (2006) Piecing together a ciliome. **Trends in Genetics**, 22: (9): 491-500.
- Invernizzi, P. and Mackay, I.R. (2008) Aetiopathogenesis of autoimmune hepatitis. **World Journal of Gastroenterology**, 14: (21): 3306-3312.
- Ioannidis, J.P., Ntzani, E.E., Trikalinos, T.A., et al. (2001) Replication validity of genetic association studies. **Nature Genetics**, 29: (3): 306-309.
- Ito, K., Lim, S., Caramori, G., et al. (2002) A molecular mechanism of action of theophylline: induction of histone deacetylase activity to decrease inflammatory gene expression. **Proceedings of the National Academy of Sciences of the United States of America**, 99: 8921-8926.
- Jacquemin, E., Cresteil, D., Raynaud, N., et al. (2002) *CFC1* gene mutation and biliary atresia with polysplenia syndrome. **Journal of Pediatric Gastroenterology and Nutrition**, 34: (3): 326-327.
- Johnson, C.A., Gissen, P. and Sergi, C. (2003) Molecular pathology and genetics of congenital hepatorenal fibrocystic syndromes. **Journal of Medical Genetics**, 40: 311-319.
- Johnson, J.A., Davis, J.O., Baumber, J.S., et al. (1970) Effects of estrogen and progesterone on electrolyte balances in normal dogs. **American Journal of Physiology**, 219: 1691-1697.
- Johnson, K.A. and Rosenbaum, J.L. (1992) Polarity of flagellar assembly in *Chlamydomonas*. **The Journal of Cell Biology**, 119: 1605-1611.
- Joplin, R. (1994) Isolation and culture of biliary epithelial cells. **Gut**, 35: (7): 875-878.

- Joplin, R., Strain, A.J. and Neuberger, J.M. (1989) Immune-Isolation and culture of biliary epithelial cells from normal human liver. **In Vitro Cellular and Development Biology**, 25: (12): 1189-11952.
- Kaimori, J.-Y., Nagasawa, Y., Menezes, L.F., et al. (2007) Polyductin undergoes notch-like processing and regulated release from primary cilia. **Human Molecular Genetics**, 16: (8): 942-956.
- Kannarket, G.T., Tuma, D.J. and Tuma, P.L. (2006) Microtubules are more stable and more highly acetylated in ethanol-treated hepatic cells. **Journal of Hepatology**, 44: (5): 963-970.
- Kanno, N., LeSage, G., Glaser, S., et al. (2001) Regulation of cholangiocyte bicarbonate secretion. **American Journal of Physiology - Gastroenterology and Liver Physiology**, 281: G612-G625.
- Kaplan, B.S., Kaplan, P., de Chadarevian, J.P., et al. (1988) Variable expression of autosomal recessive polycystic kidney disease and congenital hepatic fibrosis within a family. **American Journal of Medical Genetics**, 29: (3): 639-647.
- Karrer, F.M. and Bensard, D.D. (2000) Neonatal cholestasis. **Seminars in Pediatric Surgery**, 9: 166-169.
- Karrer, F.M., Hall, R.J. and Lilly, J.R. (1991) Biliary atresia and the polysplenia syndrome. **Journal of Pediatric Surgery**, 26: 524-527.
- Karrer, F.M., Lilly, J.R. and Stewart, B.A. (1990) Biliary atresia registry. **Journal of Pediatric Surgery**, 25: 1076-1080.
- Karrer, F.M., Price, M.R., Bensard, D.D., et al. (1996) Long-term results with the Kasai operation for biliary atresia. **Archives of Surgery**, 131: 493-496.
- Kastner, S., Soose, M. and Stolte, H. (1993) **Human kidney cells in in vitro pharma-toxicology**. Brussels: VUB Press.
- Keller, R. (2002) Shaping the vertebrate body plan by polarized embryonic cell movements. **Science**, 298: (5600): 1950-1954.
- Kelly, D.A. and Davenport, M. (2007) Current management of biliary atresia. **Archives of Disease in Childhood**, 92: 1132-1135.
- Kerker, N., Hadzic, N., Davies, E.T., et al. (1998) *De-novo* autoimmune hepatitis after liver transplantation. **Lancet**, 351: 409-413.
- Khodjakov, A., Cole, R.W., Oakley, B.R., et al. (2000) Centrosome-independent mitotic spindle formation in vertebrates. **Current Biology**, 10: 59-67.
- Kim, I., Fu, Y., Hui, K., et al. (2008) Fibrocystin/polycystin modulates renal tubular formation by regulating polycystin-2 expression and function. **Journal of the American Society of Nephrology**, 19: 455-468.
- Klein, T.J. and Mlodzik, M. (2005) Planar cell polarization: An emerging model points in the right direction. **Annual Review of Cell Development and Biology**, 21: 155-176.
- Kleinman, H.K., Luckenbill-Edds, L., Cannon, F.W., et al. (1987) use of extracellular matrix components for cell culture. **Analytical Biochemistry**, 166: (1): 1-13.
- Knisely, A.S. (2003) Biliary Tract Malformations. **American Journal of Medical Genetics**, 122A: 343-350.
- Kobayashi, H. and Stringer, M.D. (2003) Biliary atresia. **Seminars in Neonatology**, 8: 383-391.

- Kochakian, C.D. (1947) Effect of estrogens on the body and organ weights and the arginase alkaline and acid phosphatases of the liver and kidney of castrated male mice. **American Journal of Physiology**, 151: 126-129.
- Kodama, Y., Hijikata, M., Kageyama, R., et al. (2004) The role of notch signaling in the development of intrahepatic bile ducts. **Gastroenterology**, 127: 1775-1786.
- Kohsaka, T., Yuan, Z.R., Guo, S.X., et al. (2002) The significance of human jagged 1 mutations detected in severe cases of extrahepatic biliary atresia. **Hepatology**, 36: (4): 904-912.
- Korach, K.S. and Wintermantel, T. (2007) **Tissue-Specific Estrogen Action: Novel Mechanisms, Novel Ligands, Novel Therapies**. First.Springer.
- Kouzarides, T. (2000) Acetylation: A regularity modification to rival phosphorylation? **The EMBO Journal**, 19: (6): 1176-1179.
- Krantz, I.D., Piccoli, D.A. and Spinner, N.B. (1997) Alagille syndrome. **Journal of Medical Genetics**, 34: 152-157.
- Krauss, A.N. (1964) Familial extrahepatic biliary atresia. **The Journal of Pediatrics**, 65: 933-937.
- Lager, D.A., Qian, Q., Bengal, R.J., et al. (2001) The pck rat: A new model that resembles human autosomal dominant polycystic kidney and liver disease. **Kidney International**, 59: 126-136.
- Landing, B.H. (1974) Consideration of the pathogenesis of neonatal hepatitis, biliary atresia and choledochal cyst - the concept of infantile obstructive cholangiopathy. **Progress in Pediatric Surgery**, 6: 113-139.
- Landman, N. and Kim, T.W. (2004) Got RIP? Presenilin-dependent intramembrane proteolysis in growth factor receptor signaling. **Cytokine Growth Factor Reviews**, 15: (5): 337-351.
- Lazaridis, K.N., Strazzabosco, M. and LaRusso, N.F. (2004) The cholangiopathies: Disorders of biliary epithelia. **Gastroenterology**, 127: 1565-1577.
- LeDizet, M. and Piperno, G. (1986) Cytoplasmic microtubules containing acetylated alpha-tubulin in *Chlamydomonas reinhardtii*: spatial arrangement and properties. **The Journal of Cell Biology**, 103: (1): 13-22.
- Leifeld, L., Ramaker, J., Schneiders, A.M., et al. (2001) Intrahepatic MxA expression is correlated with interferon-alpha expression in chronic and fulminant hepatitis. **Journal of Pathology**, 194: (4): 478-483.
- Lemaigre, F.P. (2003) Development of the biliary tract. **Mechanisms of Development**, 120: 81-87.
- Leng, X.-H., Zhang, W., Nieswandt, B., et al. (2005) Effects of estrogen replacement therapies on mouse platelet function and glycoprotein VI levels. **Circulation Resrahc**, 97: 415-417.
- Li, J.J. and Li, S.A. (1987) Estrogen carcinogenesis in Syrian hamster tissues: role of metabolism. **Federation Proceedings**, 46: (5): 1858-1863.
- Li, J.J., Talley, D.J., Li, S.A., et al. (1974) An estrogen binding protein in the renal cytosol of intact, castrated and estrogenized golden hamsters. **Endocrinology**, 95: (4): 1134-1141.
- Li, J.J., Weroha, S.J., Lingle, W.L., et al. (2004) Estrogen mediates Aurora-A overexpression centrosome amplification, chromosomal instability and breast cancer in female ACI rats. **Proceedings of the National Academy of Sciences of the United States of America**, 101: (52): 18123-18128.
- Li, X., Luo, Y., Starremans, P.G., et al. (2005) Polycystin-1 and polycystin-2 regulate the cell cyce through the helix-hoop-helix inhibitor Id2. **Nature Cell Biology**, 7: (12): 1202-1212.

- Lin, F. and Satlin, L.M. (2004) Polycystic kidney disease: the cilium as a common pathway in cystogenesis. **Current Opinion in Pediatrics**, 16: 171-176.
- Lipsett, P.A., Segev, D.L. and Colombani, P.M. (1997) Biliary atresia and biliary cysts. **Baillière's Clinical Gastroenterology**, 11: (4): 619-642.
- Liu, Y.-W., Concejero, A.M., Chen, C.-L., et al. (2007) Hepatic pseudotumor in long-standing biliary atresia patients undergoing liver transplantation. **Liver Transplantation**, 13: 1545-1551.
- Logan, C.Y. and Nusse, R. (2004) The Wnt signaling pathway in development and disease. **Annual Review of Cell Development and Biology**, 20: 781-810.
- Lorent, K., Yeo, S.Y., Oda, T., et al. (2004) Inhibition of Jagged-mediated Notch signaling disrupts zebrafish biliary development and generates multi-organ defects compatible with an Alagille syndrome phenocopy. **Development**, 131: 5753-5766.
- Lothschütz, D., Jennewein, M., Paahl, S., et al. (2002) Polyploidization and centrosome hyperamplification in inflammatory bronchi. **Inflammatory Research**, 51: 416-422.
- Low, Y., Vijayan, V. and Tan, C.E.L. (2001) The prognostic value of ductal plate malformation and other histologic parameters in biliary atresia: An immunohistochemical study. **Journal of Pediatrics**, 139: 320-322.
- Lu, W., Peissel, B., Babakhanlou, H., et al. (1997) Perinatal lethality with kidney and pancreas defects in mice with a targeted Pkd1 mutation. **Nature Genetics**, 17: (2): 179-181.
- Ludwig, J., Kim, C.H., Wiesner, R.H., et al. (1989) Floxuridine-induced sclerosing cholangitis: an ischemic cholangiopathy? **Hepatology**, 9: (2): 215-218.
- Ludwig, J., Wiesner, R.H., Batts, K.P., et al. (1987) The acute vanishing bile duct syndrome (acute irreversible rejection) after orthotopic liver transplantation. **Hepatology**, 7: 476-483.
- Mack, C.L. and Sokol, R.J. (2005) Unraveling the pathogenesis and etiology of biliary atresia. **Pediatric Research**, 57: (5): 87-94.
- MacRae Dell, K.M. and Avner, E.D. (2001) "Autosomal recessive polycystic kidney disease". **GeneReviews; Genetic Disease Online Reviews at GeneTests-GeneClinics**. University of Washington, Seattle.
- Mai, W., Chen, D., Ding, T., et al. (2005) Inhibition of *Pkhd1* impairs tubulomorphogenesis of cultured IMCD cells. **Molecular Biology of the Cell**, 16: 4398-4409.
- Marra, F. (2002) Chemokines in liver inflammation and fibrosis. **Frontiers in Biosciences**, 1: d1899-d1914.
- Marshall, W.F. and Nonaka, S. (2006) Cilia: tuning in to the cell's antenna. **Current Biology**, 16: R604-R614.
- Marshall, W.F. and Rosenbaum, J.L. (2001) Intraflagellar transport balances continuous turnover of outer doublet microtubules: implications for flagellar length control. **The Journal of Cell Biology**, 155: (3): 405-414.
- Martin-Subero, J.I., Knippschild, U., Harder, L., et al. (2003) Segmental chromosomal aberrations and centrosome amplifications: pathogenetic mechanisms in Hodgkin and Reed-Sternberg cells of classical Hodgkin's lymphoma? **Leukemia**, 17: (11): 2214-2219.
- Maruta, H., Greer, K. and Rosenbaum, J.L. (1986) The acetylation of alpha-tubulin and its relationship to the assembly and disassembly of microtubules. **The Journal of Cell Biology**, 103: (2): 571-579.
- Marx, J. (2001) Do centrosome abnormalities lead to cancer? **Science**, 292: 426-429.

- Masyuk, A.I., Masyuk, T.V., Splinter, P.L., et al. (2006) Cholangiocyte cilia detect changes in luminal fluid flow and transmit them into intracellular Ca^{2+} and cAMP signaling. **Gastroenterology**, 131: 911-920.
- Masyuk, T.V., Huang, B.Q., Masyuk, A.I., et al. (2004a) Biliary dysgenesis in the PCK rat, an orthologous model of autosomal recessive polycystic kidney disease. **American Journal of Pathology**, 165: 1719-1730.
- Masyuk, T.V., Huang, B.Q., Ward, C.J., et al. (2003) Defects in cholangiocyte fibrocystin expression and ciliary structure in the PCK rat. **Gastroenterology**, 125: 1303-1310.
- Masyuk, T.V., Huang, B.Q., Ward, C.J., et al. (2004b) Expression of fibrocystin during ciliogenesis (abstract). **Hepatology**, 40: 365A.
- Matsumoto, K., Fujii, H., Michalopoulos, G., et al. (1994) Human biliary epithelial cells secrete and respond to cytokines and hepatocyte growth factors in vitro: Interleukin-6, hepatocyte growth factor and epidermal growth factor promote DNA synthesis in vitro. **Hepatology**, 20: (2): 376-382.
- Mazziotti, M.V., Willis, L.K., Heuckeroth, R.O., et al. (1999) Anomalous development of the hepatobiliary system in the *Inv* mouse. **Hepatology**, 30: 372-378.
- McCright, B., Gao, X., Shen, L., et al. (2001) Defects in development of the kidney, heart and eye vasculature in mice homozygous for a hypomorphic *Notch2* mutation. **Development**, 128: 491-502.
- McCright, B., Lozier, J. and Gridley, T. (2002) A mouse model of Alagille syndrome: *Notch2* as a genetic modifier of *Jag1* haploinsufficiency. **Development**, 129: 1075-1082.
- McGrath, J., Somlo, S., Makova, S., et al. (2003) Two populations of node monocilia initiate left-right asymmetry in the mouse. **Cell**, 114: 61-73.
- McKiernan, P.J., Baker, A.J. and Kelly, D.A. (2000) The frequency and outcome of biliary atresia in the UK and Ireland. **Lancet**, 355: 25-29.
- Melero, S., Spirli, C., Zsembery, Á., et al. (2002) Defective regulation of cholangiocyte $\text{Cl}^-/\text{HCO}_3^-$ and Na^+/H^+ exchanger activities in primary biliary cirrhosis. **Hepatology**, 35: 1513-1521.
- Menezes, L.F., Cai, Y., Nagasawa, Y., et al. (2004) Polyductin, the PKHD1 gene product, comprises isoforms expressed in plasma membrane, primary cilium, and cytoplasm. **Kidney International**, 66: 1345-1355.
- Menezes, L.F. and Onuchic, L.F. (2006) Molecular and cellular pathogenesis of autosomal recessive polycystic kidney disease. **Brazilian Journal of Medical and Biological Research**, 39: 1537-1548.
- Mihm, S., Fayyazi, A., Hartmann, H., et al. (1997) Analysis of histopathological manifestations of chronic hepatitis c virus infection with respect to virus genotype. **Hepatology**, 25: 735-739.
- Mir, S., Rapola, J. and Koskimies, O. (1983) Renal cysts in pediatric autopsy material. **Nephron**, 33: (3): 189-195.
- Mizuno, M. and Singer, S.J. (1994) A possible role for stable microtubules in intracellular transport from the endoplasmic reticulum to the Golgi apparatus. **Journal of Cell Science**, 107: (5): 1321-1331.
- Mollet, G., Silbermann, F., Delous, M., et al. (2005) Characterization of the nephrocystin/nephrocystin-4 complex and subcellular localization of nephrocystin-4 to primary cilia and centrosomes. **Human Molecular Genetics**, 14: (5): 645-656.
- Moser, M., Matthiesen, S., Kirfel, J., et al. (2005) A mouse model for cystic biliary dysgenesis in autosomal recessive polycystic kidney disease (ARPKD). **Hepatology**, 41: 1113-1121.

- Müller, H.A. (2000) Genetic control of epithelial cell polarity: lessons from *Drosophila*. **Developmental Dynamics**, 218: (1): 52-67.
- Murcia, N.S., Sweeney, W.E.J. and Avner, E.D. (1999) New insights into the molecular pathophysiology of polycystic kidney disease. **Kidney International**, 55: 1187-1197.
- Nagano, J., Kitamura, K., Hujer, K.M., et al. (2005) Fibrocystin interacts with CAML, a protein involved in Ca²⁺ signaling. **Biochemical and Biophysical Research Communications**, 338: 880-889.
- Nagasawa, Y., Matthiesen, S., Onuchic, L.F., et al. (2002) Identification and characterization of *Pkhd1*, the mouse orthologue of the human ARPKD gene. **Journal of the American Society of Nephrology**, 13: (9): 2246-2258.
- Nakanishi, K., Sweeney, W.E.J., Zerres, K., et al. (2000) Proximal tubular cysts in fetal human autosomal recessive polycystic kidney disease. **Journal of the American Society of Nephrology**, 11: (4): 760-763.
- Nakanuma, Y., Hosono, M., Sanzen, T., et al. (1997) Microstructure and development of the normal and pathologic biliary tract in humans, including blood supply. **Microscopy Research and Technique**, 38: 552-570.
- Nakanuma, Y., Tsuneyama, K. and Harada, K. (2001) Pathology and pathogenesis of intrahepatic bile duct loss. **Journal of Hepato-biliary-pancreatic Surgery**.
- Nathanson, M.H. and Boyer, J.L. (1991) Mechanisms and regulation of bile secretion. **Hepatology**, 14: (3): 551-556.
- Nauli, S.M., Alenghat, F.J., Luo, Y., et al. (2003) Polycystins 1 and 2 mediate mechanosensation in the primary cilium of kidney cells. **Nature Genetics**, 33: 129-137.
- Nauli, S.M. and Zhou, J. (2004) Polycystins and mechanosensation in renal and nodal cilia. **BioEssays**, 26: 844-856.
- Nickel, C., Benzing, T., Sellin, L., et al. (2002) The polycystin-1 C-terminal fragment triggers branching morphogenesis and migration of tubular kidney epithelial cells. **The Journal of Clinical Investigation**, 109: (4): 481-489.
- Nigg, E.A. (2002) Centrosome aberrations: cause or consequence of cancer progression? **Nature Reviews Cancer**, 2: 1-11.
- Nijjar, S.S., Crosby, H.A., Wallace, L., et al. (2001) Notch receptor expression in adult human liver: a possible role in bile duct formation and hepatic neovascularization. **Hepatology**, 34: 1184-1192.
- Nishikawa, Y., Doi, Y., Watanabe, H., et al. (2005) Transdifferentiation of mature rat hepatocytes into bile duct-like cells in vitro. **American Journal of Pathology**, 166: 1077-1088.
- Nonaka, S., Shiratori, H., Saijoh, Y., et al. (2002) Determination of left-right patterning of the mouse embryo by artificial nodal flow. **Nature**, 418: (6893): 96-99.
- Nonaka, S., Tanaka, K., Okada, Y., et al. (1998) Randomization of left-right asymmetry due to loss of nodal cilia generating leftward flow of extraembryonic fluid in mice lacking KIF3B motor protein. **Cell**, 95: (6): 829-837.
- Nurnberger, J., Bacallao, R.L. and L., P.C. (2002) Inversin forms a complex with catenins and N-cadherin in polarized epithelial cells. **Molecular Biology of the Cell**, 13: 3096-3106.

- Oakley, F., Trim, N., Constandinou, C.M., et al. (2003) Hepatocytes express nerve growth factor during liver injury: evidence for paracrine regulation of hepatic stellate cell apoptosis. **American Journal of Pathology**, 163: (5): 1849-1858.
- Oberley, T.D., Lauchner, L.J., Pugh, T.D., et al. (1989) Specific estrogen-induced cell proliferation of cultured Syrian hamster renal proximal tubular cells in serum-free chemically defined media. **Proceedings of the National Academy of Sciences of the United States of America**, 86: 2107-2111.
- Ohi, R. (2000) Biliary atresia. A surgical perspective. **Clinics in Liver Disease**, 4: 779-804.
- Okada, Y., Nonaka, S., Tanaka, Y., et al. (1999) Abnormal nodal flow precedes situs inversus in *iv* and *inv* mice. **Molecular Cell**, 4: 459-468.
- Ong, A.C. and Harris, P.C. (2005) Molecular pathogenesis of ADPKD: the polycystic complex gets complex. **Kidney International**, 67: (4): 1234-1247.
- Ong, A.C.M. and Wheatley, D.N. (2003) Polycystic kidney disease - the ciliary connection. **The Lancet**, 361: 774-776.
- Onuchic, L.F., Furu, L., Nagasawa, Y., et al. (2002) *PKHD1*, the polycystic kidney and hepatic disease 1 gene, encodes a novel large protein containing multiple immunoglobulin-like plexin-transcription factor domains and parallel beta-helix 1 repeats. **American Journal of Human Genetics**, 70: 1305-1317.
- Otto, E.A., Schermer, B., Obara, T., et al. (2003) Mutations in *INVS* encoding inversin cause nephronophthisis type 2, linking renal cystic disease to the function of primary cilia and left-right axis determination. **Nature Genetics**, 34: (4): 413-420.
- Pagon, R.A., Haas, J.E., Bunt, A.H., et al. (1982) Hepatic involvement in the Bardet-Biedl syndrome. **American Journal of Medical Genetics**, 13: (4): 373-381.
- Palazzo, A., Ackerman, B. and Gundersen, G.G. (2003) Tubulin acetylation and cell motility. **Nature**, 421: 230.
- Pameijer, C.R., Hubbard, A.M., Coleman, B., et al. (2000) Combined pure esophageal atresia, duodenal atresia, biliary atresia, and pancreatic ductal atresia: prenatal diagnostic features and review of the literature. **Journal of Pediatric Surgery**, 35: 745-747.
- Pan, J. and Snell, W.J. (2007) The primary cilium: keeper of the key to cell division. **Cell**, 129: (7): 1255-1257.
- Pan, J., Wang, Q. and Snell, W.J. (2005) Cilium-generated signaling and cilia-related disorders. **Laboratory Investigations**, 85: (4): 452-463.
- Papadimitriou, J.M. (1968) The biliary tract in acute murine reovirus 3 infection. **American Journal of Pathology**, 52: (3): 595-611.
- Parashar, K., Tarlow, M.J. and McCrae, M.A. (1992) Experimental reovirus type 3-induced murine biliary tract disease. **Journal of Pediatric Surgery**, 27: 843-847.
- Park, W.H., Kim, S.P., Park, K.K., et al. (1996) Electron microscope study of the liver with biliary atresia and neonatal hepatitis. **Journal of Pediatric Surgery**, 31: (3): 367-374.
- Parkening, T.A., Lau, I.-F., Saksena, S.K., et al. (1978) Circulating plasma levels of pregnenolone, progesterone, estrogen, luteinizing hormone, and follicle stimulating hormone in young and aged C57BL/6 mice during various stages of pregnancy. **Journal of Gerontology**, 33: (2): 191-196.

- Pazour, G.J. (2004) Intraflagellar transport and cilia-dependent renal disease: The ciliary hypothesis of polycystic kidney disease. **Journal of the American Society of Nephrology**, 15: 2528-2536.
- Pazour, G.J., Dickert, B.L., Vucica, Y., et al. (2000) *Chlamydomonas IFT88* and its mouse homologue, polycystic kidney disease gene *Tg747*, are required for assembly of cilia and flagella. **The Journal of Cell Biology**, 151: (3): 709-718.
- Pazour, G.J. and Witman, G.B. (2003) The vertebrate primary cilium is a sensory organelle. **Current Opinion in Cell Biology**, 15: 105-110.
- Perantoni, A.O. (2003) Renal development: perspectives on a Wnt-dependent process. **Seminars in Cellular Development and Biology**, 14: 201-208.
- Perlmutter, D.H. and Shepherd, R.W. (2002) Extrahepatic biliary atresia: a disease or a phenotype? **Hepatology**, 35: (6): 1297-1304.
- Petersen, C., Biermanns, D., Kuske, M., et al. (1997a) New aspects in a murine model for extrahepatic biliary atresia. **Journal of Pediatric Surgery**, 32: (8): 1190-1195.
- Petersen, C., Bruns, E., Kuske, M., et al. (1997b) Treatment of extrahepatic biliary atresia with interferon-alpha in a murine infectious model. **Pediatric Research**, 42: (5): 623-628.
- Phillips, M.J., Latham, P.S. and Poucell-Hatton, S. (1989) **Electron microscopy of human liver disease**. Philadelphia: JB Lippincott Co.
- Phillips, P.A., Keast, D., Papadimitriou, J.M., et al. (1969) Chronic obstructive jaundice induced by reovirus type 3 in weanling mice. **Pathology**, 1: 193-203.
- Pihan, G.A., Purohit, A., Wallace, J., et al. (1998) Centrosome defects and genetic instability in malignant tumors. **Cancer Research**, 58: (17): 3974-3985.
- Pihan, G.A., Purohit, A., Wallace, J., et al. (2001) Centrosome defects can account for cellular and genetic changes that characterize prostate cancer progression. **Cancer Research**, 61: (5): 2212-2219.
- Pinzani, M., Marra, F. and Carloni, V. (1998) Signal transduction in hepatic stellate cells. **Liver**, 18: (1): 2-13.
- Piperno, G. and Fuller, M.T. (1985) Monoclonal antibodies specific for an acetylated form of alpha-tubulin recognize the antigen in cilia and flagella from a variety of organisms. **The Journal of Cell Biology**, 101: (6): 2085-2094.
- Piperno, G., LeDizet, M. and Chang, X.J. (1987) Microtubules containing acetylated α -tubulin in mammalian cells in culture. **The Journal of Cell Biology**, 104: 289-302.
- Polevoda, B. and Sherman, F. (2002) The diversity of acetylated proteins. **Genome Biology**, 3: (5): reviews0006.0001-0006.
- Poole, C.A., Flint, M.H. and Beaumont, B.W. (1985) Analysis of the morphology and function of primary cilia in connective tissues: a cellular cybernetic probe? **Cell Motility**, 5: 175-193.
- Praetorius, H.A. and Spring, K.R. (2001) Bending the MDCK cell primary cilium increases intracellular calcium. **The Journal of Membrane Biology**, 184: 71-79.
- Praetorius, H.A. and Spring, K.R. (2002) Removal of the MDCK cell primary cilium abolishes flow sensing. **The Journal of Membrane Biology**, 191: 69-76.

- Praetorius, H.A. and Spring, K.R. (2005) A physiological view of the primary cilium. **Annual Review of Physiology**, 67: 515-529.
- Prozialeck, W.C., Lamar, P.C. and Appelt, D.M. (2004) Differential expression of e-cadherin, n-cadherin and beta-catenin in proximal and distal segments of the rat nephron. **BioMed Central Physiology**, 4: (10).
- Quarumby, L.M. and Parker, D.K. (2005) Cilia and the cell cycle? **The Journal of Cell Biology**, 169: (5): 707-710.
- Rahman, I. (2002) Oxidative stress, transcription factors and chromatin remodelling in lung inflammation. **Biochemical Pharmacology**, 64: 935-942.
- Rauschenfels, S., Krassmann, M., Al-Masri, A.N., et al. (2009) Incidence of hepatotropic viruses in biliary atresia. **The European Journal of Pediatrics**, 168: (4): 469-476.
- Reynolds, G.M., Billingham, L.J., Gray, L.J., et al. (2002) Interleukin 6 expression by Hodgkin/Reed-Sternberg cells is associated with the presence of 'B' symptoms and failure to achieve complete remission in patients with advanced Hodgkin's disease. **British Journal of Haematology**, 118: (1): 195-201.
- Richards, W.G., Yoder, B.K., Isfort, R.J., et al. (1997) Isolation and characterization of liver epithelial cell lines from wild-type and mutant *TgN737Rpw* mice. **American Journal of Pathology**, 150: (4): 1189-1197.
- Rieder, C.L., Faruki, S. and Khodjakov, A. (2001) The centrosome in vertebrates: more than a microtubule-organizing center. **Trends in Cell Biology**, 11: (10): 413-419.
- Riepenhoff-Talty, M., Gouvea, V., Evans, M.J., et al. (1996) Detection of group C rotavirus in infants with extrahepatic biliary atresia. **The Journal of Infectious Diseases**, 174: (1): 8-15.
- Riepenhoff-Talty, M., Schaekel, K., Clark, H.F., et al. (1993) Group A rotavirus produce extrahepatic biliary obstruction in orally inoculated newborn mice. **Pediatric Research**, 33: (4 Pt. 1): 394-399.
- Rigden, D.J., Mello, L.V. and Galperin, M.Y. (2004) The PA14 domain, a conserved all-beta domain in bacterial toxins, enzymes, adhesins and signaling molecules. **Trends in Biochemical Science**, 29: (7): 335-339.
- Roberts, S.K., Ludwig, J. and LaRusso, N.F. (1997) The pathobiology of biliary epithelia. **Gastroenterology**, 112: 269-279.
- Roitbak, T., Ward, C.J., Harris, P.C., et al. (2004) A polycystin-1 multiprotein complex is disrupted in polycystic kidney disease cells. **Molecular Biology of the Cell**, 15: 1334-1346.
- Rolleston, H.D. and Hayne, L.B. (1901) A case of congenital hepatic cirrhosis with obliterative cholangitis (congenital obliteration of the bile ducts). **British Medical Journal**, 1: 758-760.
- Rosenbaum, J.L. and Child, F.M. (1967) Flagellar regeneration in protozoan flagellates. **The Journal of Cell Biology**, 34: 345-364.
- Rosenbaum, J.L. and Witman, G.B. (2002) Intraflagellar transport. **Nature Reviews Molecular Cell Biology**, 3: 813-825.
- Ross, A.J., May-Simera, H., Eichers, E.R., et al. (2005) Disruption of Bardet-Biedl syndrome ciliary proteins perturbs planar cell polarity in vertebrates. **Nature Genetics**, 37: (10): 1135-1140.
- Rossetti, S., Torra, R., Coto, E., et al. (2003) A complete mutation screen of PKHD1 in autosomal-recessive polycystic kidney disease (ARPKD) pedigrees. **Kidney International**, 64: (2): 391-403.

- Roy, S., Dillon, M.J., Trompeter, R.S., et al. (1997) Autosomal recessive polycystic kidney disease: long-term outcomes or neonatal survivors. **Pediatric Nephrology**, 11: 302-306.
- Ruemmele, P., Hofstaedter, F. and Gelbmann, C.M. (2009) Secondary sclerosing cholangitis. **Nature Reviews Gastroenterology and Hepatology**, 6: 287-295.
- Sakamoto, T., Liu, Z., Murase, N., et al. (1999) Mitosis and apoptosis in the liver in interleukin-6-deficient mice after partial hepatectomy. **Hepatology**, 29: (2): 403-411.
- Salisbury, J.L., Whitehead, C.M., Lingle, W.L., et al. (1999) Centrosomes and cancer. **Biology of the Cell**, 91: 451-460.
- Satir, P. and Christensen, S.T. (2007) Overview of structure and function of mammalian cilia. **Annual Review of Physiology**, 69: 377-400.
- Schinzel, A., Schmid, W., Fraccaro, M., et al. (1981) The "Cat Eye Syndrome": Dicentric small marker chromosome probably derived from a No. 22 (Tetrasomy 22pter→q11) associated with a characteristic phenotype. Report of 11 patients and delineation of the clinical picture. **Human Genetics**, (57): 148-158.
- Schmeling, D.J., Oldham, K.T., Guice, K.S., et al. (1991) Experimental obliterative cholangitis. A model for the study of biliary atresia. **Annals of Surgery**, 213: (4): 350-355.
- Schön, P., Tsuchiya, K., Lenoir, D., et al. (2002) Identification, genomic organization, chromosomal mapping and mutation analysis of the human INV gene, the ortholog of a murine gene implicated in left-right axis development and biliary atresia. **Human Genetics**, 110: 157-165.
- Schreiber, R.A. and Kleinman, R.E. (1993) Genetics, immunology, and biliary atresia: an opening or a diversion? **Journal of Pediatric Gastroenterology and Nutrition**, 16: (2): 111-113.
- Schwartz, E.A., Leonard, M.L., Bizios, R., et al. (1997) Analysis and modeling of the primary cilium bending response to fluid shear. **American Journal of Physiology - Renal Physiology**, 272: F132-F138.
- Schwarz-Romond, T., Asbrand, T., Bakkens, J., et al. (2002) The ankyrin repeat protein Diversin recruits Casein kinase Iε to the beta-catenin degradation complex and acts in both canonical Wnt and Wnt/JNK signaling. **Genes and Development**, 16: (16): 2073-2084.
- Schweizer, P. (1986) Treatment of extrahepatic bile duct atresia: results and long-term prognosis after hepatic portoenterostomy. **Pediatric Surgery International**, 1: 30-36.
- Seidman, S.L., Duquesnoy, R.J., Zeevi, A., et al. (1991) Recognition of major histocompatibility complex antigens on cultured human biliary epithelial cells by alloreactive lymphocytes. **Hepatology**, 13: (2): 239-246.
- Sergi, C., Adam, S., Kahl, P., et al. (2000) The remodeling of the primitive human biliary system. **Early Human Development**, 58: 167-178.
- Sharp, A.M., Messiaen, L.M., Page, G., et al. (2008) Comprehensive genomic analysis of PKHD1 mutations in ARPKD cohorts. **Journal of Medical Genetics**, 42: 336-349.
- Sherlock, S. and Dooley, J. (1997) **Cysts and congenital biliary abnormalities**. 10. Oxford: Blackwell Scientific Publications.
- Sherstha, R., McKinley, C., Russ, P., et al. (1997) Postmenopausal estrogen therapy selectively stimulates hepatic enlargement with autosomal dominant polycystic kidney disease. **Hepatology**, 26: 1282-1286.

- Shimadera, S., Iwai, N., Deguchi, E., et al. (2007) The *inv* mouse as an experimental model of biliary atresia. **Journal of Pediatric Surgery**, 42: 1555-1560.
- Shneider, B.L. and Magid, M.S. (2005) Liver disease in autosomal recessive polycystic kidney disease. **Pediatric Transplantation**, 9: 634-639.
- Shulman, J.M., Perrimon, N. and Axelrod, J.D. (1998) Frizzled signaling and the development control of cell polarity. **Trends in Genetics**, 14: 452-458.
- Shulman, J.M. and St Johnston, D. (1999) Pattern formation in single cells. **Trends in Genetics**, 9: (12): M60-M64.
- Silveira, T.R., Salzano, F.M., Howard, E.R., et al. (1991) Congenital structural abnormalities in biliary atresia: evidence for etiopathogenic heterogeneity and therapeutic implications. **Acta Paediatrica Scandinavica**, 80: 1192-1199.
- Simons, M., Gloy, J., Ganner, A., et al. (2005) Inversin, the gene product mutated in nephronophthisis type II, functions as a molecular switch between Wnt signaling pathways. **Nature Genetics**, 37: (5): 537-543.
- Simons, M. and Walz, G. (2006) Polycystic kidney disease: Cell division without a clue? **Kidney International**, 70: 854-864.
- Sloboda, R.D. (2005) Intraflagellar transport and the flagellar tip complex. **Journal of Cellular Biochemistry**, 94: 266-272.
- Smith, B.M., Laberge, J.M., Schreiber, R., et al. (1991) Familial biliary atresia in three siblings including twins. **Journal of Pediatric Surgery**, 26: 1331-1333.
- Sokol, R.J. and Mack, C. (2001) Etiopathogenesis of biliary atresia. **Seminars in Liver Disease**, 21: 517-524.
- Sokol, R.J., Mack, C., Narkewicz, M.R., et al. (2003) Pathogenesis and outcome of biliary atresia: current concepts. **Journal of Pediatric Gastroenterology and Nutrition**, 37: 4-21.
- Sokol, R.J. and Stall, C. (1990) Anthropometric evaluation of children with chronic liver disease. **The American Journal of Clinical Nutrition**, 52: 203-208.
- Sorokin, S. (1962) Centrioles and the formation of rudimentary cilia by fibroblasts and smooth muscle cells. **The Journal of Cell Biology**, 15: 363-377.
- Spirli, C., Fabris, L., Duner, E., et al. (2003) Cytokine-stimulated nitric oxide production inhibits adenylate cyclase and cAMP-dependent secretion in cholangiocytes. **Gastroenterology**, 124: 737-753.
- Spitz, L. (1980) Ligation of the common bile duct in the fetal lamb: an experimental model for the study of biliary atresia. **Pediatric Research**, 14: (5): 740-748.
- Steele, M.I., Marshall, C.M., Lloyd, R.E., et al. (1995) Reovirus 3 not detected by reverse transcriptase-mediated polymerase chain reaction analysis of preserved tissue from infants with cholestatic liver disease. **Hepatology**, 21: 697-702.
- Stephens, R.E. (1997) Synthesis and turnover of embryonic sea urchin ciliary proteins during selective inhibition of tubulin synthesis and assembly. **Molecular Biology of the Cell**, 8: 2187-2198.
- Stickel, F. and Osterreicher, C.H. (2006) The role of genetic polymorphisms in alcoholic liver disease. **Alcohol and Alcoholism**, 41: (3): 209-224.

- Strazzabosco, M. (1997) New insights into cholangiocyte physiology. **Journal of Hepatology**, 27: 945-952.
- Strazzabosco, M., Fabris, L. and Spirli, C. (2005) Pathophysiology of cholangiocytes. **Journal of Clinical Gastroenterology**, 39: (S2): S90-S102.
- Strazzabosco, M., Spirli, C. and Okolicsanyi, L. (2000) Pathophysiology of the intrahepatic biliary epithelium. **Journal of Gastroenterology and Hepatology**, 15: 244-253.
- Strickland, A.D. and Shannon, K. (1982) Studies in the etiology of extrahepatic biliary atresia: time-space clustering. **Journal of Pediatrics**, 100: 749-753.
- Strickland, A.D., Shannon, K. and Coln, C.D. (1985) Biliary atresia in two sets of twins. **The Journal of Pediatrics**, 107: (3): 418-420.
- Svegliati-Baroni, G., Ghiselli, R., Marziona, M., et al. (2006) Estrogens maintain bile duct mass and reduce apoptosis after biliodigestive anastomosis in bile duct ligated rats. **Journal of Hepatology**, 44: 1158-1166.
- Tabin, C.J. and Vogan, K.J. (2003) A two-cilia model for vertebrate left-right axis specification. **Genes and Development**, 17: (1): 1-6.
- Tahvanainen, E., Tahvanainen, P., Kaariainen, H., et al. (2005) Polycystic liver and kidney diseases. **Annals of Medicine**, 37: 546-555.
- Takeda, S., Yonekawa, Y., Tanaka, Y., et al. (1999) Left-right asymmetry and kinesin superfamily protein KIF3A: New insights in determination of laterality and mesoderm induction by *kif3A*^{-/-} mice analysis. **The Journal of Cell Biology**, 145: 825-836.
- Tan, C.E., Davenport, M., Driver, M., et al. (1994a) Does the morphology of the extrahepatic biliary remnants in biliary atresia influence survival? A review of 205 cases. **Journal of Pediatric Surgery**, 29: (11): 1459-1464.
- Tan, C.E., Driver, M., Howard, E.R., et al. (1994b) Extrahepatic biliary atresia: a first-trimester event? Clues from light microscopy and immunohistochemistry. **Journal of Pediatric Surgery**, 29: (6): 808-814.
- Tan, C.E. and Moscoso, G.J. (1994a) The developing human biliary system at the porta hepatis level between 11 and 25 weeks of gestation: a way to understanding biliary atresia. Part 2. **Pathology International**, 44: 600-610.
- Tan, C.E.L. and Moscoso, C.J. (1994b) The developing human intrahepatic biliary system at the porta hepatis level between 29 days and 8 weeks of gestation: A way to understanding biliary atresia. Part 1. **Pathology International**, 44: 587-599.
- Tanaka, Y., Okada, Y. and Hirokawa, N. (2005) FGF-induced vesicular release of Sonic hedgehog and retinoic acid in leftward nodal flow is critical for left-right determination. **Nature**, 435: 172-177.
- Tanano, H., Hasegawa, T., Kawahara, H., et al. (1999) Biliary atresia associated with congenital structural anomalies. **Journal of Pediatric Surgery**, 34: (11): 1687-1690.
- Tanimizu, N. and Miyajima, A. (2004) Notch signaling controls hepatoblast differentiation by altering the expression of liver-enriched transcription factors. **Journal of Cell Science**, 117: 3165-3174.
- Terada, T. and Nakanuma, Y. (1994) Profiles of expression of carbohydrate chain structure during human intrahepatic bile duct development and maturation. **Hepatology**, 20: 388-397.
- Terry, S., Jouret, F., Vandenabeele, F., et al. (2007) A primary culture of mouse proximal tubular cells, established on collagen-coated membranes. **American Journal of Physiology. Renal physiology**, 293: F476-F485.

- Thomsen, H.S., Levine, E., Meilstrup, J.W., et al. (1997) Renal cystic diseases. **European Radiology**, 7: (8): 1267-1275.
- Thung, S.N. (1990) The development of proliferating ductular structures in liver disease - an immunohistochemical study. **Archives of Pathology and Laboratory Medicine**, 114: 407-411.
- Timmermann, S., Lehrmann, H., Polesskaya, A., et al. (2001) Histone acetylation and disease. **Cellular and Molecular Life Sciences: CMLS**, 58: 728-736.
- Torres, V.E. and Harris, P.C. (2005) Mechanisms of Disease: autosomal dominant and recessive polycystic kidney diseases. **Nature Clinical Practice. Nephrology**, 2: (1): 40-55.
- Tovey, S.C., Bootman, M.D., Lipp, P., et al. (2000) Calcium-modulating cyclophilin ligand desensitizes hormone-evoked calcium release. **Biochemical and Biophysical Research Communications**, 276: 97-100.
- Trauner, M., Meier, P.J. and Boyer, J.L. (1998) Molecular pathogenesis of cholestasis. **New England Journal of Medicine**, 339: (17): 1217-1227.
- Tucker, R.W., Pardee, A.B. and Fujiwara, K. (1979a) Centriole ciliation is related to quiescence and DNA synthesis in 3T3 cells. **Cell**, 17: (3): 527-535.
- Tucker, R.W., Scher, C.D. and Stiles, C.D. (1979b) Centriole deciliation associated with the early response to 3T3 cells to growth factors but not to SV40. **Cell**, 18: (4): 1065-1072.
- Tyler, K.L., Sokol, R.J., Oberhaus, S.M., et al. (1998) Detection of reovirus RNA in hepatobiliary tissues from patients with extrahepatic biliary atresia and choledochal cysts. **Hepatology**, 27: (6): 1475-1483.
- Veeman, M.T., Axelrod, J.D. and Moon, R.T. (2003) A second canon. Functions and mechanisms of beta-catenin-independent Wnt signaling. **Developmental Cell**, 5: (3): 367-377.
- Vogel, G. (2005) News focus: betting on cilia. **Science**, 310: 216-218.
- Vos, T.A., Gouw, A.S., Klok, P.A., et al. (1997) Differential effects of nitric oxide synthase inhibitors on endotoxin-induced liver damage in rats. **Gastroenterology**, 113: (4): 1323-1333.
- Wagner, K.U., McAllister, K., Ward, T., et al. (2001) Spatial and temporal expression of the Cre gene under the control of the MMTV-LTR in different lines of transgenic mice. **Transgenic Research**, 10: (6): 545-553.
- Wang, S., Luo, Y., Wilson, P.D., et al. (2004) The autosomal recessive polycystic kidney disease protein is localized to primary cilia, with concentration in the basal body area. **Journal of the American Society of Nephrology**, 15: 592-602.
- Wang, S., Zhang, J., Nauli, S.M., et al. (2007) Fibrocystin/polyductin, found in the same protein complex with polycystin-2, regulates calcium responses in kidney epithelia. **Molecular and Cellular Biology**, 27: (8): 3241-3252.
- Ward, C.J., Hogan, M.C., Rossetti, S., et al. (2002) The gene mutated in autosomal recessive polycystic kidney disease encodes a large, receptor-like protein. **Nature Genetics**, 30: 259-269.
- Ward, C.J., Yuan, D., Masyuk, T.V., et al. (2003) Cellular and subcellular localization of the ARPKD protein; fibrocystin is expressed on primary cilia. **Human Molecular Genetics**, 12: 2703-2710.
- Ware, S.W., Peng, J., Zhu, L., et al. (2004) Identification and functional analysis of ZIC3 mutations in heterotaxy and related congenital heart defects. **American Journal of Human Genetics**, 74: 93-105.

- Watnick, T. and Germino, G. (2003) From cilia to cyst. **Nature Genetics**, 34: (4): 355-356.
- Webster, D.R. and Borisy, G.G. (1989) Microtubules are acetylated in domains that turn over slowly. **Journal of Cell Science**, 92: (1): 57-65.
- Wheatley, D.N. (1995) Primary cilia in normal and pathological tissues. **Pathobiology**, 63: (4): 222-238.
- Wheatley, D.N., Wang, A.M. and Strugnell, G.E. (1996) Expression of primary cilia in mammalian cells. **Cell Biology International**, 20: 73-81.
- Whittington, P.F. and Balistreri, W.F. (1991) Liver transplantation in pediatrics: indication, contraindications, and pre-transplant management. **Journal of Pediatrics**, 118: 169-177.
- Wilson, G.A., Morrison, L.A. and Fields, B.N. (1994) Association of the reovirus S1 gene with serotype 3-induced biliary atresia in mice. **Journal of Virology**, 68: (10): 6458-6465.
- Wilson, P.D. (1997) Epithelial cell polarity and disease. **American Journal of Physiology**, 272: F434-F442.
- Wistuba, I.I. and Gazdar, A.F. (2004) Gallbladder cancer: lessons from a rare tumour. **Nature Reviews Cancer**, 4: (9): 695-706.
- Woollard, J.R., Punyashthi, R., Richardson, S., et al. (2007) A mouse model of autosomal recessive polycystic kidney disease with biliary duct and proximal tubule dilatation. **Kidney International**, 72: 328-336.
- Wu, G., D'Agati, V., Cai, Y., et al. (1998) Somatic inactivation of Pkd2 results in polycystic kidney disease. **Cell**, 93: (2): 177-188.
- Xiong, H., Chen, Y., Yi, Y., et al. (2002) A novel gene encoding a TIG multiple domain protein is a positional candidate for autosomal recessive polycystic kidney disease. **Genomics**, 80: (1): 96-104.
- Yokomuro, S., Tsuji, H., Lunz, J.G.r., et al. (2000) Growth control of human biliary epithelial cells by interleukin 6, hepatocyte growth factor, transforming growth factor β 1, and activin A: comparison of a cholangiocarcinoma cell line with primary cultures of non-neoplastic biliary epithelial cells. **Hepatology**, 32: (1): 26-35.
- Yokoyama, T., Copeland, N.G., Jenkins, N.A., et al. (1993) Reversal of left-right asymmetry: a situs inversus mutation. **Science**, 260: 679-682.
- Yoon, P.W., Bresee, J.S., Olney, R.S., et al. (1997) Epidemiology of biliary atresia: a population-based study. **Pediatrics**, 99: (3): 376-382.
- Zaghloul, N.A. and Katsanis, N. (2009) Mechanistic insights into Bardet-Biedl syndrome, a model ciliopathy. **The Journal of Clinical Investigation**, 119: (3): 428-437.
- Zegers, M.M.P., O'Brian, L.E., Yu, W., et al. (2003) Epithelial polarity and tubulogenesis *in vitro*. **Trends in Cell Biology**, 13: (4): 169-176.
- Zen, Y., Harada, K., Sasaki, M., et al. (2005) Are bile duct lesions of primary biliary cirrhosis distinguishable from those of autoimmune hepatitis and chronic viral hepatitis? Interobserver histological agreement on trimmed bile ducts. **Journal of Gastroenterology**, 40: 164-170.
- Zerres, K., Mücher, G., Becker, J., et al. (1998a) Prenatal diagnosis of autosomal recessive polycystic kidney disease (ARPKD): molecular genetics, clinical experience, and fetal morphology. **American Journal of Medical Genetics**, 76: (2): 137-144.

Zerres, K., Rudnik-Schöneborn, S., Deget, F., et al. (1996) Autosomal recessive polycystic kidney disease in 115 children: Clinical presentation, course and influence of gender. *Acta Paediatrica*, 85: 437-445.

Zerres, K., Rudnik-Schöneborn, S., Steinkamm, C., et al. (1998b) Autosomal recessive polycystic kidney disease. *Journal of Molecular Medicine*, 76: 303-309.

Zhang, D.-Y., Sabla, G., Shivakumar, P., et al. (2004a) Coordinate expression of regulatory genes differentiates embryonic and perinatal forms of biliary atresia. *Hepatology*, 39: 954-962.

Zhang, M.-Z., Mai, W., Li, C., et al. (2004b) PKHD1 protein encoded by the gene for autosomal recessive polycystic kidney disease associates with basal bodies and primary cilia in renal epithelial cells. *Proceedings of the National Academy of Sciences of the United States of America*, 101: (8): 2311-2316.

Zhang, Q., Davenport, J.R., Croyle, M.J., et al. (2005) Disruption of IFT results in both exocrine and endocrine abnormalities in the pancreas of Tg737 (orpk) mutant mice. *Laboratory Investigations*, 85: 45-64.

Zimmerman, K.W. (1898) Beiträge zur Kenntniss einiger drüsen und epithelien [English translation: Contribution to knowledge of some glands and epithelium]. *Arch. Mikr. Anat.*, 52: 552-707.